A COUPLED UPLAND-EROSION, INSTREAM HYDRODYNAMIC-SEDIMENT

TRANSPORT MODEL FOR ASSESSING PRIMARY IMPACTS OF FOREST

MANAGEMENT PRACTICES ON SEDIMENT YIELD AND DELIVERY

By

WILLIAM JOHN CONROY

A dissertation submitted in partial fulfillment of
the requirements for the degree of

DOCTOR OF PHILOSOPHY IN CIVIL ENGINEERING

WASHINGTON STATE UNIVERSITY
Department of Civil and Environmental Engineering

MAY 2005

To the Faculty of Washington State University:

The members of the Committee appointed to examine the dissertation of
WILLIAM JOHN CONROY find it satisfactory and recommend that it be accepted.

_____
Chair

_____

_____

_____

ACKNOWLEDGEMENTS

A COUPLED UPLAND-EROSION, HYDRODYNAMIC-SEDIMENT TRANSPORT MODEL FOR ASSESSING PRIMARY IMPACTS OF FOREST MANAGEMENT PRACTICES ON SEDIMENT YIELD AND DELIVERY

Abstract

by William John Conroy, Ph.D.
Washington State University
May 2005

Chair: Rollin H. Hotchkiss

The purpose of this research was to develop a modeling system/framework for assessing forest management-related erosion at its sources and tracking sediment as it is transported from hillslopes to stream channels, and transported through a channel network to a watershed outlet. The ultimate goal was to develop a land management assessment tool capable of accurately assessing the primary impacts of spatiotemporally varied forest management practices on sediment yield and delivery at hillslope- and watershed-scales.

The modeling framework developed consists of four components: 1) the TOpographic ParameteriZation model for discretizing hillslope and channel elements, 2) the Water Erosion Prediction Project model for evaluating hillslope-scale surface erosion processes, 3) the National Center for Computational Hydrodynamics and Engineering One-Dimensional hydrodynamic-sediment transport model, and 4) an interface program to manage relational databases and data transfer between modules.

The coupled model was calibrated and validated with observed flow and sediment load data from Caspar Creek Experimental Watershed in coastal, northern California. The coupled model predicts peak flow rates, total flow volume, and sediment loads significantly better than the empirical methods used by the WEPP Watershed model. The coupled model predicted flow

rates that were not significantly different from observed values, and sediment loads that were within typical ranges for sediment transport equations.

The most significant finding of this research project was the limits of applicability of the WEPP Hillslope model. It was found that the results of WEPP Hillslope erosion simulations became more divergent from actual values as the critical source area for delineation of first order channels increases. Critical source areas (CSAs) between 5 and 10 ha yield runoff rates that are not significantly different from observed values. However, as the CSA is increased, runoff rates and sediment loads become exponentially divergent from observed values. It is concluded that the governing equations used to represent hillslope-scale erosion processes in the WEPP Hillslope model begin to break down for assessment areas greater than 10 ha; and that this area delineates a point where hillslope-scale runoff and erosion processes give way to more dominant watershed-scale open channel flow and sediment transport processes.

TABLE OF CONTENTS

CHAPTER ONE

GENERAL INTRODUCTION

CHAPTER TWO

LITERATURE REVIEW

CHAPTER THREE

MODEL DEVELOPMENT AND CALIBRATION, PART I: HYDRODYNAMICS

CHAPTER FOUR

MODEL DEVELOPMENT AND CALIBRATION, PART II: SEDIMENT TRANSPORT

CHAPTER FIVE

SENSITIVITY ANALYSIS OF INPUT VARIABLES AND RUN-TIME OPTIONS

CHAPTER SIX

SPATIAL SCALES FOR ASSESSING FOREST MANAGEMENT RELATED EROSION

CHAPTER SEVEN

SYNTHESIS AND GENERAL CONCLUSIONS

LIST OF TABLES

LIST OF FIGURES

CHAPTER ONE

GENERAL INTRODUCTION

The Environmental Protection Agency (EPA) waterbody impairment list, required by Section 303(d) of the Federal Clean Water Act (CWA), tabulates over 26,000 impaired waterbodies in the United States. These water-bodies comprise more than 300,000 miles of rivers and streams and more than five million acres of lakes (U.S.E.P.A., 2000). Excessive sediment is the third highest ranked category of impairment among pollutants listed by the EPA (Table 1-1). Sediment pollution, a type of non-point-source pollution, originates from diffuse land areas that intermittently contribute pollutants to surface water (Line et al., 1997). Sediment is one of the few pollutants that have both natural and anthropogenic causes. The CWA requires development of a management plan, called total maximum daily load (TMDL), to identify, assess, and reduce anthropogenic pollutants (U.S.E.P.A., 1999).

Table 1-1. Number of water-bodies in the United States reporting specific water quality impairments as of 1998 (U.S.E.P.A., 2005).

Impairment Name	Number Of Water-bodies Reporting Impairment (As Of 1998)	EPA Rank	Forest Management As A Possible Source
Pathogens	6,395	1	No
Metals	5,873	2	No
Sediment/Siltation	5,657	3	Yes
Nutrients	5,140	4	Yes
Organic Enrichment/Low DO	4,595	5	Yes
pH	2,586	6	No
Habitat Alterations	2,332	7	Yes
Thermal Modifications	1,970	8	Yes
Biological Criteria	1,860	9	No
Flow Alteration	1,672	10	Yes
Other	11,090	11 -- 41	Possible
Total	49,170		

Unlike most other pollutants, identification of sediment impaired watercourses is complicated a process since sediment in rivers has both natural and anthropogenic sources. In addition, sediment in rivers can be both necessary and detrimental to beneficial to beneficial uses. As such, determining the level of impairment, the level of effectiveness of alternative mitigation strategies, and the cumulative effect of multiple, spatiotemporally distributed management practices becomes much more complicated. These problems are difficult due to three of the most elusive problems for watershed hydrology: 1) the accurate prediction of runoff and sediment transport in ungaged watersheds (Sivapalan, 2003a); 2) the fate of transport of sediments as they are moved from their sources to and through watershed channel networks (Jetten, Govers, and Hessel, 2003); and 3) the determination of when the dominance of hillslope-scale processes (i.e., overland and rill flow) give way to the dominance of watershed-scale processes (i.e., open channel flow) (Sivapalan, 2003b).

To conduct these types of analyses, one must have the ability to evaluate explicitly the processes at a site-specific, hillslope-scale; and the ability to integrate a large collection of hillslopes into a single unit at the watershed-scale. These analyses are extremely difficult for several reasons: 1) hydrologic processes controlling the watershed response to forcing events operate at multiple spatial and temporal scales (Singh and Woolhiser, 2002); 2) physiographic data are generally limited in ungaged basins; and 3) where available, highly heterogeneous physiographic data are often represented by limited field measurements that may be temporally variant.

An example of this difficulty occurs where sediment impaired watercourses exist in forested landscapes subject to forest management practices (e.g., timber harvests, access roads, fuels management with fire). Analysis of sediment pollution due to forest management is particularly difficult because sediment in stream channels can result from both natural (e.g., landslides) and anthropogenic sources (Swanston, 1991). Many forest management practices are known to

alter significantly erosion rates from forested landscapes. However, these activities are rarely executed over large areas at one time. Forest management is typically fragmented and discontinuous spatially, due to the constraints placed on area (e.g., single managed areas rarely exceed 40 ha) that can be harvested at any one time. In addition, a single managed area is only entered periodically, with at least 5 to 25 years between entries. As such, the managed areas within a harvest cycle are dispersed over a large area, approximately 50 to 250 km^2. Therefore, it is important to evaluate both spatial and temporal aspects forest management practices on sediment erosion and delivery in TMDL analyses.

A goal of sediment TMDL analyses is to track the movement of sediment from multiple sources (forced at different times), to and through a channel network, to a watershed outlet. To accomplish this, most TMDL analyses make extensive use of computer models (U.S.E.P.A., 2002) because of the need to evaluate large areas with heterogeneous characteristics. The quality of modeled results is not only dependent on the quality of input data, but accuracy with which the model represents the physical processes being evaluated. If sufficient input data are available (e.g., climatic, physiographic), physics-based models have the potential to significantly improve the accuracy of modeled results over either conceptual or empirical models (Singh and Woolhiser, 2002).

The need for these types of models is well recognized (Singh and Woolhiser, 2002), the availability of high-quality, validated models that are universally applicable is still elusive. None of the existing upland erosion models currently available has the ability to evaluate hydrodynamics and sediment fate of transport with the most accurate, physical equations of motion (i.e., St. Venant and Exner equations). Likewise, none of the existing hydrodynamic or sediment transport models has a physically-based, distributed parameter upland erosion simulator to supply runoff and sediment load information. In both categories, however, there are examples of models that are potentially very useful for watershed-scale analyses.

The Water Erosion Prediction Project (WEPP) Model (Flanagan et al., 1995) is a physically-based, erosion simulation model commonly used to evaluate agricultural, forest management, and wildfire effects on surface sediment erosion processes. The WEPP model that has the ability to evaluate explicitly, spatiotemporally distributed climatic and physiographic variables, making it nearly ideal for use in sediment TMDL evaluations. The WEPP model is unique among erosion models in that it explicitly evaluates water balance and surface erosion processes from the ridge top to the channel bottom of a hillslope plane. Even though WEPP has many appropriate features for erosion simulations, it has one limitation that needs to be improved to allow the model to be used at the small watershed scale. For the purposes of this project, 'small watershed scale' includes watersheds up to 130 km^2 (U.S.E.P.A., 1999). The WEPP model does not explicitly include a flood flow routing (hydrodynamic) procedure. This inadequacy limits the accuracy of streamflow and sediment transport rates, especially as watershed size increases.

The National Center for Computational Hydrodynamics and Engineering One-Dimensional (CCHE1D) hydrodynamic-sediment transport model was designed to simulate unsteady flows and sedimentation processes in watershed-scale channel networks (Wu, Vieira, and Wang, 2004; Wu and Vieira, 2002). The CCHE1D model is unique among hydrodynamic models in that it explicitly evaluates the full equations of motion (i.e., St. Venant equations) and sediment continuity equation (i.e., Exner Equation) for large channel networks. The model simulates bed aggradation and degradation, bed material composition (hydraulic sorting and armoring), bank erosion, and the resulting channel morphologic changes under unsteady flow conditions. CCHE1D does not have an upland erosion model to generate sediment delivered to channels. Instead, it must be integrated with existing watershed processes (rainfall-runoff and field erosion) models to produce more accurate and reliable estimations of sediment loads and morphological changes in channel networks (Wu and Vieira, 2002).

OBJECTIVES

The purpose of this research project is to develop a modeling framework that can evaluate site-specific, forest management-related sediment erosion; and can determine the fate of transport of multiple sediment sources as eroded sediments are transported to and through a watershed-scale stream channel network. The resultant product would be an integrated upland erosion simulation and hydrodynamic-sediment transport model that would be a significant improvement over any modeling system currently available. This improvement is important in increasing the overall accuracy of surface runoff and erosion estimates associated with implementation of forest management erosion control measures, especially for ungaged watersheds with limited calibration data.

The goals of this project are to: 1) develop a modeling framework that couples an explicit, distributed, physically-based, hillslope-scale, upland-erosion simulation model (WEPP) with an appropriate watershed-scale, hydrodynamic-sediment transport model (CCHE1D); 2) calibrate and validate the modeling framework using data collected from Caspar Creek, California; a long-term experimental, paired watershed study conducted by the U.S. Forest Service (Henry, 1998); 3) demonstrate the utility of the modeling framework for comparing erosion simulations in managed and unmanaged forested watersheds; and 4) use the modeling framework to explore the spatial limitations of scaling hillslope-scale runoff and erosion processes to watershed-scale open channel flow and sediment transport processes.

DISSERTATION OUTLINE

This dissertation is presented in seven chapters, each detailing a distinct topic related to the project as a whole. Chapter Two presents a literature review of hillslope- and watershed-scale erosion process modeling, and watershed-scale hydrodynamic-sediment transport modeling theory and practice. This chapter presents the rationale for using the WEPP Hillslope erosion model and the CCHE1D hydrodynamic-sediment transport model. Chapter Three details the modeling framework linking WEPP with CCHE1D, and presents the results of the calibration of the hydrodynamic portion of the modeling framework. Chapter Four presents the calibration results of the sediment transport function of the modeling framework. Calibration details were separated into two chapters since each chapter was submitted separately for publication in a professional journal. Chapter Five contains the results of sensitivity analyses conducted on several key input variables to both WEPP and CCHE1D, and several run-time options available to CCHE1D. Chapter Six has two distinct features: 1) a validation of the modeling framework, using a series of management scenarios on a watershed adjacent to the watershed used for calibration and 2) a determination the upper limit to the areal extent that can be used for analyses with the WEPP model. Finally, in Chapter Seven, a synthesis of material is presented to provide the general conclusions of the research project and recommendations for work to extend the research presented here.

CHAPTER TWO

LITERATURE REVIEW

ABSTRACT

Five main topics are discussed in this literature review: 1) hydrodynamics and erosion processes in managed, forested watersheds, 2) modeling hillslope-scale erosion processes, 3) watershed-scale hydrodynamic theory, 4) instream sediment transport theory, and 5) current methods for modeling watershed-scale hydrodynamics, erosion, and instream sediment transport. The focus of this chapter is to demonstrate that the proposed research is a valuable contribution to the engineering field in that it is necessary and has not been previously accomplished. It will be demonstrated that none of the existing upland erosion models currently available has the ability to evaluate hydrodynamics and sediment fate of transport with the most accurate, physical equations of motion (i.e., St. Venant and Exner equations). Likewise, none of the existing hydrodynamic or sediment transport models has a physically-based, distributed parameter upland erosion simulator to supply runoff and sediment load information. As such, this chapter will detail the rationale for coupling the CCHE1D hydrodynamic-sediment transport model with the WEPP upland erosion model.

BACKGROUND

HYDRODYNAMIC PROCESSES IN FORESTED WATERSHEDS

Forested watersheds are markedly different from either urban or agricultural watersheds. Urbanized watersheds are typified by their amount of impervious surfaces, greatly simplifying rainfall-runoff analyses. Agricultural watersheds are usually in areas with gentle topography and nearly homogeneous vegetation and landuse practices. Forested watersheds, however, typically have heterogeneous physiographic, climatic, and landuse properties. As a result, prediction of outflow hydrographs (i.e., hydrodynamic process simulation) from forested watersheds is much more complex than either urban or agricultural watersheds.

Hydrodynamic processes govern how water moves between and within the atmosphere, biosphere, and lithosphere. Watershed physiography, climate, and analytical scale govern the rate of hydrodynamic processes. Important physiographic variables are soils, geology, relief, topography, drainage density, vegetation, and landuse (Dunne and Leopold, 1978). The most important climatic variables are temperature and the depth, duration, intensity, and type of precipitation. The importance of analytical scale relates to how hydrodynamic processes interact with each other. For very small scales (less than 2.6 km^2), where there are few surface channels, surface and subsurface movement of water on hillslopes dominates the hydrodynamic processes. However, for large scales (greater than 130 km^2), where there are extensive channel networks, surface water dominates the hydrodynamic processes (Beven, 2001).

SEDIMENT TRANSPORT PROCESSES IN FORESTED WATERSHEDS

Erosion processes govern how soil particles are detached, transported, deposited from upland hillslopes to lowland channels and floodplains. Sediment transport within a watershed often begins with the detachment of soil particles from upland areas, and ends with sediment

being transported out of the watershed with existing flow (Figure 2-1). Upland areas are often referred to as interrill (Stone et al., 1995) because water and sediment transport is accomplished without the aid of concentrated flow (i.e., within rills or channels). The mechanisms for initiating interrill sediment transport are gravitational (i.e., dry ravel rolling and/or sliding), mechanical (i.e., raindrop impact or particle-to-particle impact), and hydraulic (i.e., shear stress caused by flowing water). Once particles are detached and transport begins, particles are either deposited on the hillslope (where they can be transported further), or they are delivered to an area of concentrated flow.

Areas of concentrated flow include rills, gullies, stream channels, and rivers. Once sediment is delivered to these areas, it can either be deposited in the channel or continue to be transported. Whether a particle is deposited or transported is a function of several variables, including particle size and density, flow depth, and channel geometry. The residence time for any given particle depends on its size, the length of channel that it must travel, the flow characteristics, the bed material characteristics, and the channel geometry.

FOREST MANAGEMENT EFFECTS ON RAINFALL-RUNOFF AND EROSION PROCESSES

In undisturbed, forested watersheds, sediment transport from hillslopes to stream channels by surface erosion is generally low (Swanston, 1991); whereas, sporadic mass movements (e.g., creep, landslides, and debris torrents) are the major modes of sediment transport to channels (Swanston, 1991). In disturbed watersheds, forest management practices can significantly alter rainfall-runoff and erosion processes, resulting in excessive nonpoint source sediment pollution of water bodies (U.S.E.P.A., 1990). The major increases in sediment production are surface erosion and mass wasting associated with roads (Furniss, Roelofs, and Yee, 1991), and surface erosion associated with harvested and burned areas (Swanston, 1991).
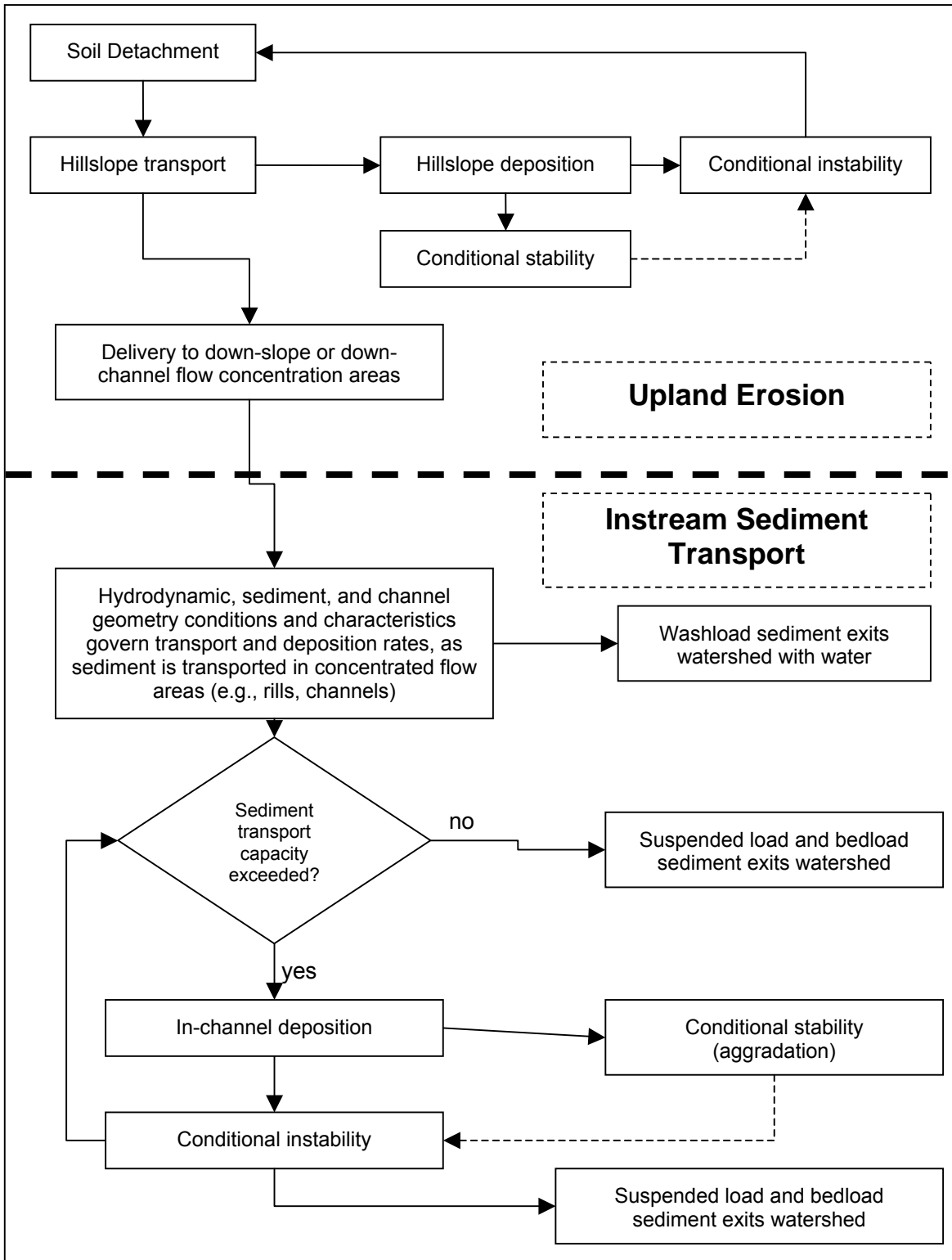
Figure 2-1. Schematic of watershed-scale erosion processes.

Forest management practices, unlike other agricultural operations, are highly varied spatiotemporally. In traditional agricultural operations, fields are plowed, planted, and harvested annually; vegetation is spatially homogeneous; entire watersheds are operated on in the same manner, all at the same time, annually; and physiographic characteristics rarely govern the type of practices used. Forest management rotations (i.e., harvest cycles) are typically between 20 and 100 years, instead of annual rotations. Entries into forests are irregular, often less than once every 10-20 years. National and State regulations prohibit harvesting entire watersheds in a single year, resulting in heterogeneous vegetation characteristics (e.g., height, age, canopy cover, stem density) within watersheds and even sub-watersheds. One of the most important differences between traditional agricultural and forest operations is physiography of where each are practiced. Traditional agriculture is practiced in areas of gentle topography and low relief. Forests are typically in areas that are rugged, irregular, and heterogeneous. As such, in forests, the physiographic characteristics often define the types of management practices for each area.

Forest management has two basic components: silviculture (Smith, 1986) and harvesting systems (Conway, 1976). Harvesting systems and silviculture, combined, have several attributes that alter water balance (Table 2-1) and erosion (Table 2-2) processes in forests. Of the silvicultural practices, the use of fire for regeneration or fuel management is the most significant erosion producing practice (Robichaud and Waldrop, 1994; Wilson, 1999). Harvesting systems, however, have many more opportunities to affect erosion processes. For example, logging equipment can compact the soil during vegetation removal, leading to decreased infiltration capacity (Croke, Hairsine, and Fogarty, 2001; Startsev and McNabb, 2000); vegetation removal creates areas of bare mineral soil, increasing the susceptibility of the soil particles to erosion (Edeso et al., 1999); and vegetation removal alters the patterns of snow accumulation and melt, resulting in altered runoff and erosion rates (Anderson, Hoover, and Reinhart, 1976).

Table 2-1. Impacts of forest management practices on water balance processes.

Water Balance Processes	Impact of Forest Management	Reference(s)
Precipitation	No effects on amount or timing of rain or snow; Altered rates of fog drip	(Chamberlin, Harr, and Everest, 1991; Harr, 1982; Keppeler, 1998)
Snow Accumulation and Melt	Increased accumulation in small openings; Decreased accumulation in large openings; Increased melt in openings	(Anderson, Hoover, and Reinhart, 1976; Chamberlin, Harr, and Everest, 1991; Swanston, 1991)
Evapo-transpiration	Reduced by total vegetation removal; Increased or unchanged in partial vegetation removal	(Douglass, 1966; Murakami et al., 2000; Pereira et al., 1999; Wu, Liu, and Jelinski, 2000; Ziemer, 1979)
Interception	Reduced by vegetation removal	(Rutter and Morton, 1977; Swanston, 1991; Wallace, 1997; Ziemer, 1979)
Infiltration	Reduced by compaction due to heavy equipment; Reduced by hydrophobicity induced by fire	(Croke, Hairsine, and Fogarty, 2001; Johnson and Beschta, 1980; Luce, 1997; Robichaud and Waldrop, 1994)
Water storage	Increased by reduced plant uptake of water; Decreased by increased evaporation of exposed soil	(Beven, 2001; Messina et al., 1997; Nisbet, 2001; Wigmosta and Lettenmaier, 1999)
Movement of soil water	Decreased by soil compaction or collapse of preferential flow paths; Increased by interception and redirection of subsurface flow	(Cafferata, 1983; Huang, Lacey, and Ryan, 1996; Laffan, Jordan, and Duhig, 2001; Megahan, 1972; Sidle and Drlica, 1981; Startsev and McNabb, 2000)
Runoff Volume	Total volume is typically unchanged (out=in); Rates altered by changes in snow accumulation and melt, evapotranspiration, infiltration, water storage, and soil water movement	(Chamberlin, Harr, and Everest, 1991; Montgomery, 1994; Rashin et al., 1999; Thomas and Megahan, 1998; Wilson, 1999; Wright et al., 1990)
Channel flow	Peak and recession duration altered by changes in rates of runoff volume	(Harr, Levno, and Mersereau, 1982; Hicks, Beschta, and Harr, 1991; Jones and Grant, 1996; Storck et al., 1998; Swanston, 1991; Thomas and Megahan, 1998; Wright et al., 1990)

Table 2-2. Impact of forest management practices on erosion processes.

Erosion Processes	Impact of Forest Management	Reference(s)
Detachment (splash erosion)	Increased by reduced cover following fire; Increased by reduced cover on roads or skid trails; Decreased by increased litter (slash) volume	(Ciampalini and Torri, 1998; Cullen, Montagne, and Ferguson, 1991; Huang, Lacey, and Ryan, 1996; Robichaud and Waldrop, 1994; Startsev and McNabb, 2000; Wilson, 1999)
Detachment (rill-hydraulic erosion)	Increased by increased runoff volume; Decreased by compaction in clayey soils	(Bryan, 2000; Furniss, Roelofs, and Yee, 1991; Nearing et al., 1997)
Transport (overland flow)	Increased by increased runoff volume; Decreased by increased hydraulic roughness (increased slash deposition)	(Angermann et al., 2002; Chamberlin, Harr, and Everest, 1991; Wright et al., 1990)
Transport (rill flow)	Increased by increased area of compacted surfaces and exposed mineral soil	(Bryan, 2000; Chamberlin, Harr, and Everest, 1991; Lane and Sheridan, 2002; Megahan and Ketcheson, 1996; Montgomery, 1994)
Transport (channel flow)	Increased by increases in detachment and hillslope (rill and overland flow) transport; Increased channel erosion increased channel flow	(Binkley and Brown, 1993; Cornish, 2001; Green et al., 1999; Jackson, Sturm, and Ward, 2001; Lyons and Beschta, 1983)
Deposition (hillslope)	Increased by increased hydraulic roughness (increased slash deposition); Decreased by compaction; Decreased by increased overland flow	(Edeso et al., 1999; Keim and Shoenholtz, 1999; Lane, Shirley, and Singh, 1988; N.C.A.S.I., 1992; N.C.A.S.I., 1994; N.C.A.S.I., 1999; Rashin et al., 1999)
Deposition (channel)	Increased by increased sediment delivery from hillslopes; Increased by decreased low flows (altered channel flow volume/rate)	(Anderson, Hoover, and Reinhart, 1976; Chikita, Kemnitz, and Kumai, 2002; Green et al., 1999)

Best management practices (BMPs) systems are designed to minimize the amount of sediment that is generated and ultimately delivered to watercourses, at levels sufficient to meet the goals of the Clean Water Act TMDL plans (N.C.A.S.I., 1999; U.S.E.P.A., 1999). The problem, however, is that BMPs are frequently implemented in watersheds with sparse monitoring data (Bonta, 2002), without knowledge of the level of effectiveness of individual or suites of BMPs (N.C.A.S.I., 1994). Examples of typical forest management BMPs include, excluding heavy equipment from riparian areas, restricting equipment operation during rainstorms, minimizing soil disturbance, and retaining harvest residue *in situ*.

In general, it is assumed that implementing BMP systems will result in a reduction of sediment delivered to watercourses, thereby improving the water quality, hopefully to a level such that beneficial uses are restored (N.C.A.S.I., 2001; Rashin et al., 1999). Many studies exist regarding the effectiveness of individual, site-specific BMPs (Croke, Hairsine, and Fogarty, 2001; Luce, 1997; Robichaud and Waldrop, 1994; Wynn et al., 2000). What is lacking, however, is the quantitative determination of levels of effectiveness for BMPs at the hillslope level, and for BMP systems at the watershed-scale (N.C.A.S.I., 1999). This can be accomplished with expensive, detailed, long-term research projects, or with validated erosion simulation models. For a forest project manager, this is a very easy decision; use a model. The difficult decision becomes, choosing the 'best' erosion simulation model.

MODELING UPLAND RAINFALL-RUNOFF AND EROSION PROCESSES

A priori evaluation of sediment generation and transport requires consideration of land surface (i.e., erosion and runoff) and instream (i.e., suspension and deposition) processes (Merritt, Letcher, and Jakeman, 2003), under a wide range of conditions, and across multiple spatial and temporal scales. To assess watershed-scale hydrodynamic processes in forested watersheds, the model must account for the following likely scenarios: 1) widely varied channel configurations, including overbank flows on floodplains, 2) widely varied channel gradients, 3) widely varied flow regimes, including transcritical flows and downstream hydrograph attenuation, 4) backwater flows at tributary junctions, 5) minimal calibration data, 6) mixed climatic regimes within the same watershed, and, 7) spatiotemporally varied physiographic characteristics (i.e., vegetation and cover).

Models, both erosion and hydrodynamic, can be classified into three general categories: 1) empirical, statistical, or metric; 2) conceptual; and 3) physics-based (Merritt, Letcher, and Jakeman, 2003). Empirical models are generally the simplest models, and are often based on statistical analyses of catchment data (Merritt, Letcher, and Jakeman, 2003). Empirical models are aggregated spatially and temporally, such that heterogeneities are ignored, leading to unrealistic simplifying assumptions about the physical processes being modeled (Merritt, Letcher, and Jakeman, 2003). Examples of empirical, process simulation models are the Soil Conservation Service (SCS) curve number method (Soil Conservation Service, 1991) for evaluating the water balance, and the universal soil loss equation (USLE) (Wischmeier and Smith, 1978) or one of its variants (e.g., RUSLE (Renard et al., 1994), MUSLE (Neitsch et al., 2001)) for predicting sediment yield. These models are often inappropriate to adequately simulate the different hydrologic and erosion processes that occur across varied spatial and temporal scales (Merritt, Letcher, and Jakeman, 2003).

Conceptual models usually are based on a general description of watershed processes, but do not include specific details regarding the physics of individual processes or the interaction between processes (Merritt, Letcher, and Jakeman, 2003). Conceptual models are categorized between empirical and physics-based models because they tend to be spatially aggregated, but reflect the processes that govern the behavior of the system (Beck, 1987). An example of a conceptual erosion simulation model is the Agricultural Nonpoint Source (AGNPS) model (Young et al., 1989). Conceptual models can provide an indication of qualitative effects of land management practices on erosion processes, but tend to lack predictive capability due to their extensive reliance on calibration data (Merritt, Letcher, and Jakeman, 2003).

Physics-based (a.k.a., physically-based) models are based on fundamental physical equations governing atmospheric, biologic, hydrologic, and lithospheric processes. Physics-based models have several distinct advantages over empirical and conceptual models: 1) they are based on physically significant process, and consequently are more accurate and can be extrapolated to areas without calibration data; 2) they more accurately represent the processes and the interaction between processes; 3) they are more accurate for single event storms, because they are not temporally aggregated; and, 4) they can evaluate more complex areas, because spatial heterogeneity is explicitly considered (Johnson et al., 2000).

Although physically-based, some of governing equations are still empirical (e.g., Green and Ampt's infiltration equation), or are subject to numerous assumptions that limit their applicability across spatial scales (Merritt, Letcher, and Jakeman, 2003). However, the most significant problem with physical models is the quantity of accurate, spatially distributed data (e.g., weather, soils, vegetation, and topography) required to run the model accurately (Merritt, Letcher, and Jakeman, 2003). These data are rarely complete (even in research settings), and woefully inadequate for most areas requiring TMDL evaluations. Assuming that the data are

available, physically-based erosion simulation models will yield more reliable results in ungaged areas than either empirical or conceptual models.

The problem then becomes, given the current level of understanding of erosion processes, which model or models are the best for evaluating TMDL erosion management scenarios. Although there are numerous erosion simulation models (Borah and Bera, 2003; Merritt, Letcher, and Jakeman, 2003), this review is limited to those that are publicly available (either commercial software or freeware), excluding those that are private research tools (i.e., unpublished, unverified, or unavailable). Several models are available through U.S. Government agencies, including: the Agricultural Non-Point Source Pollution Model [AGNPS-2001] (Young et al., 1989), the Hydrologic Simulation Program – FORTRAN [HSPF] (Bicknell et al., 1997), the Kinematic Runoff and Erosion Model [KINEROS-2] (Goodrich et al., 2002; Woolhiser, Smith, and Goodrich, 1990), the Precipitation-Runoff Modeling System [PRMS] (Leavesley et al., 1983), and the Water Erosion Prediction Project [WEPP] model (Flanagan et al., 1995). Other models are available from researchers at universities, including: the Areal Nonpoint Source Watershed Environment Response Simulation [ANSWERS-2000] (Bouraoui and Dillaha, 1996), the Cascade of planes in 2-Dimensions [CASC2D] (Downer et al., 2002; Johnson et al., 2000), the Limburg Soil Erosion Model [LISEM] (De Roo et al., 1994; Jetten, 2002), and the Soil Water Assessment Tool [SWAT] (Neitsch et al., 2001). Available commercially, from the Danish Hydrologic Institute, is the Systeme Hydrologique Europeen [MIKE-SHE-SHESED] (Wicks and Bathurst, 1996; Yan and Zhang, 2001). Although usually not used by itself, another erosion model, the Universal Soil Loss Equation [USLE] (Wischmeier and Smith, 1978) is evaluated because it is the core erosion equation of many erosion simulation models (e.g., AGNPS, CASC2D, and SWAT).

The purpose of the following model comparison is to illustrate that a) no model is perfect in its representation of all physical processes involved in modeling erosion, b) the majority of

erosion models rely on empirical relations to represent process and/or ignore processes altogether, and c) numerous processes must be considered to physically model erosion. For each process considered, each model is ranked according to whether 1) the process is modeled physically, 2) the process is modeled empirically, statistically, or conceptually, or 3) the process is not considered. In this evaluation, two main process categories are evaluated: water balance processes and erosion processes. Water balance processes include precipitation, snow accumulation and melt, precipitation interception, evapotranspiration, infiltration, soil water redistribution (i.e., percolation and lateral subsurface flow), and runoff volume and timing. Erosion processes considered are detachment (both mechanical and hydraulic), transport (by overland flow, rills, or channels), and deposition (both hillslope and channel).

As is illustrated in Tables 2-3 and 2-4, one erosion simulation model, the WEPP model, consistently uses physics instead of empirical relations to evaluate processes. As described by its authors, "the WEPP model is a physically-based, process-oriented erosion prediction model based on fundamentals of stochastic weather generation, infiltration theory, hydrology, soil physics, plant science, hydraulics, and erosion mechanics" (Flanagan et al., 1995). The most notable advantages of this model include the capabilities for estimating spatial and temporal distributions of soil loss, the ability to be extrapolated to a broad range of conditions that may not be practical or economical to field test, and the ability to be used at plot, field, and watershed scales (Flanagan et al., 1995).

Table 2-3. Water balance processes considered by selected erosion simulation models.

Model Name	Rain	Snow Melt	ET	INT	INF	Soil Physics	Runoff Volume	Runoff Timing
USLE	1	0	0	0	0	0	0	0
AGNPS-2001	2	0	1	0	1	1	1	2
ANSWERS-2000	2	0	2	2	2	2	2	2
CASC2D-SED	2	0	1	1	2	2	2	2
HSPF	2	2	1	1	1	1	1	1
KINEROS-2	2	0	0	0	2	2	2	2
LISEM EUROSEM	2	0	0	1	2	2	2	2
SHESED	2	2	2	2	2	2	2	2
PRMS	2	1	2	0	2	1	2	2
SWAT	2	1	2	2	2	1	1	1
WEPP	2	2	2	2	2	2	1	1

Key to Codes:

0 = Process not modeled

1 = Process modeled empirically, conceptually, or statistically

2 = Process modeled physically

ET = Evapotranspiration

INT = Interception of precipitation by vegetation

INF = Infiltration

Table 2-4. Erosion processes modeled by selected, current erosion simulation models.

Model	Detachment		Transport			Deposition	
	Mechanical (splash) Erosion	Hydraulic (rill) Erosion	Overland (sheet) Flow	Rill Flow	Channel Flow	Hill-slope	Channel
USLE	1	1	1	1	0	0	0
AGNPS-2001	1	1	1	1	2	0	2
ANSWERS-2000	1	1	2	2	2	0	0
CASC2D-SED	1	1	2	2	2	0	2
HSPF	1	1	1	1	2	1	1
KINEROS-2	1	2	2	2	2	2	2
LISEM EUROSEM	2	0	2	0	2	2	2
SHESED	1	0	1	0	2	0	2
PRMS	1	0	1	0	2	0	0
SWAT	1	0	1	0	1	0	1
WEPP	2	2	2	2	2	2	2

Key to Codes:
0 = Process not modeled
1 = Process modeled empirically, conceptually, or statistically
2 = Process modeled physically

The WEPP model, however, is not without its' limitations. The WEPP model does not explicitly include a flow routing procedure. Instead, WEPP provides two empirical methods for calculating the peak runoff rate at the channel (sub-watershed) or watershed outlet, 1) a modified version of the Rational Equation (Singh, 1995), or 2) a regression equation used in the CREAMS model (Ascough *et al.,* 1995). Using empirical relations to route flood flows conflicts with the authors' stated goal of having a physically-based model (Flanagan et al., 1995). Thus, to be used for watershed-scale erosion simulations, the WEPP model needs a physically-based flood flow routing (hydrodynamic) algorithm or to be coupled with an existing hydrodynamic model designed to assess watershed channel networks.

The WEPP model, like all models, has limits to its applicability. The WEPP model describes soil-water balance processes using either saturated or infiltration excess mechanisms. As such, the model is applicable to areas where these are the primary mechanisms for the generating stormflow runoff volume delivered to channels. Although WEPP includes lateral subsurface flow in its water balance calculations, subsurface erosion and sediment transport are not considered. In addition, the current version of WEPP is known to produce inaccurate lateral subsurface flow volumes (W. Elliot, U.S. Forest Service, Rocky Mountain Research Station, *personal communication*), and is currently being re-coded. Therefore, WEPP may not function properly in areas where lateral subsurface flow dominates stormflow generation. For example, the model may produce sediment loads that are too high if flow is calibrated first, and runoff volumes that are too low if sediment load is calibrated first.

The WEPP model is strictly limited to evaluating erosion processes of surface soils (i.e., sheet and rill erosion). It cannot be used in areas where gully erosion and mass wasting (e.g., landslides, debris torrents) dominate the sediment budget of a watershed (Foster et al., 1995). In addition, the WEPP model assumes that there is only one rill per meter width of hillslope area, and that the length of the rill can be up to the same length as the analytical hillslope plane. Therefore, the hillslope assessment area (i.e., the size of sub-areas within a watershed) cannot be set so large that watershed-scale drainage network is described primarily by rills (i.e., ignoring channel flow), or so small that the watershed-scale drainage network is described primarily by channels (i.e., ignoring rill flow).

WATERSHED CHANNEL-NETWORK HYDRODYNAMICS

Hydrodynamic modeling (a.k.a., channel-, flood flow-, storm-, runoff routing) is accomplished by solving a system of partial differential equations for unsteady flow in open channels. In watershed-scale rainfall-runoff modeling, one-dimensional flows are a convenient, reasonable approximation to the full three-dimensional flows (Beven, 2001). The one-dimensional case is solved with two equations, one for conservation of mass (Equation 2-1) and one for conservation of momentum (Equation 2-2), which are collectively called the St. Venant Equations (Beven, 2001).

Equation 2-1. $\qquad \dfrac{\partial}{\partial t}A + \dfrac{\partial}{\partial x}Q - q_L = 0$ $\qquad\qquad\qquad\qquad$ [L^{2}T^{-1}]

Equation 2-2. $\qquad \dfrac{\partial}{\partial t}Q + \dfrac{\partial}{\partial x}\dfrac{Q^2}{A} + g\dfrac{\partial}{\partial x}(yA) + gA(S_o - S_f) - q_L V_{Lx} = 0$ $\qquad$ [L^{2}T^{-1}]

In these formulas, Q is water discharge rate [L^{3}T^{-1}], A is channel area [L^2], q_L is lateral inflow rate per unit length of channel [L^{2}T^{-1}], y is the flow depth [L], V_{Lx} is the x-component velocity of lateral inflow [LT^{-1}], g is the gravitational constant [LT^{-2}], x is downstream channel distance [L], t is time [T], S_o is the bed slope [LL^{-1}], and S_f is the friction slope [LL^{-1}].

Historically, due to the mathematical complexity of the Saint-Venant equations, simplifications were necessary to obtain feasible solutions (Fread, 2003). Approximations to the St. Venant (dynamic wave) equations are created by combining the mass conservation equation (i.e., water continuity equation) with various simplifications of the momentum equation (U.S.A.C.E., 1994). These approximations have three main categories: 1) empirical, 2) hydrologic, and 3) hydraulic (Fread, 2003; U.S.A.C.E., 1994). Hydraulic routing has four sub-categories, based on the level of simplification to the momentum equation: 1) full dynamic wave, 2) quasi-steady dynamic wave, 3) non-inertia wave, and 4) kinematic wave.

The empirical and hydrologic methods typically use a conceptual or systems approach, whereas the hydraulic methods use a physical approach. The hydrologic and hydraulic methods can usually be used in any channel or watershed configuration; however, the empirical methods are limited to areas or conditions for which they were developed (Dunne and Leopold, 1978). The hydrologic and empirical methods are, in general, simpler than hydraulic methods but may not be satisfactory in complex problems (Singh, 1988). The hydraulic methods are generally more accurate and versatile (Singh, 1988), but require complex calculations and numerical solutions to differential equations. Each of these methods is discussed below, such that it is clear which method is most appropriate for use in watershed scale modeling.

METHODS OF CHANNEL NETWORK HYDRODYNAMIC MODELING

Simplified Flood- Runoff Analyses

Although not technically hydrodynamic modeling, several simplified rainfall-runoff analysis techniques are commonly used to determine the peak runoff and/or volume (U.S.A.C.E., 1994). The Rational Method (Dunne and Leopold, 1978), Soil Conservation Service Curve Number method (Soil Conservation Service, 1991), regional regression equations, and unit hydrographs (Dunne and Leopold, 1978) are all examples of simplified runoff analysis methods. These methods, combined with GIS data, are used to estimate total flow volume or peak flow rate for a combined group of distributed sources. These approaches are useful for an approximate answer with a minimum of effort, and are often used in ungaged drainage areas (U.S.A.C.E., 1994), but are not appropriate for use in a physically-based watershed-scale hydrologic model.

Hydrologic Routing Methods

Hydrologic methods are based on the spatially lumped, finite difference form of the continuity equation. An empirical equation relating storage to inflow and outflow is required to obtain a unique solution of the continuity equation (Singh, 1988). Several of these methods

have their basis in regulated flow from reservoirs or dams, where water levels are constant with location (at a given time) and the storage and outflow are assumed unique functions of the depth of water behind the dam (Singh, 1988). Generally, these models are not suitable for situations with backwater effects from tides, significant tributary inflow, and dams or bridges (Fread, 2003; U.S.A.C.E., 1994), nor are they well-suited for rapidly changing unsteady flows such as dam-break flood waves, reservoir power releases, or hurricane storm surges (Fread, 2003). However, the hydrologic routing models are simple, easy to use, computationally efficient, and normally well within the range of acceptable values of accuracy (U.S.A.C.E., 1994). Examples of this method include the lag model, Muskingum routing, and modified Puls routing. These methods are crude approximations of flow routing, and are not appropriate for use in a physically-based watershed-scale hydrologic model.

Kinematic Wave Routing

The simplest type of distributed hydraulic routing is the kinematic wave model. Kinematic flow occurs when gravitational and frictional forces achieve a balance (U.S.A.C.E., 1994), or are assumed to be in balance; thus implying that the last three terms in the momentum equation (i.e., pressure differential, convective acceleration, local acceleration) are negligible. With this reduction, the momentum of the flow can be approximated with a steady, uniform flow assumption (U.S.A.C.E., 1994), such that flow velocity can be approximated with an empirical, uniform flow equation such as Manning's or Chezy's equation.

The kinematic wave equation has a limited set of situations where it is applicable due to numerous simplifying assumptions (U.S.A.C.E., 1994). First, the steady uniform flow assumption does not allow for hydrograph attenuation downstream, just simple translation of the hydrograph (U.S.A.C.E., 1994). This limits its usage to relatively short, steep (gradient greater than 0.2%, but less than 10%), well-defined channels, where the flood wave is gradually varied. Flow with a kinematic wave can only propagate in the downstream direction because the

diffusion and inertial terms were excluded as negligible. Therefore, reverse (negative) or backwater flows cannot be predicted. The method does not explicitly allow for separation of the main channel and the overbanks. No lateral, secondary circulations may be present. The channel is stable with no lateral migration, degradation, and aggradation. Finally, the reach has a simple stage-discharge relation (i.e., no hysteresis effects for rising vs. falling hydrograph limbs).

The kinematic wave approximation is considered reasonable to describe overland flow, and flows in most steep natural channel slopes, and flows over smooth urban surfaces (e.g., storm sewers) (Singh and Woolhiser, 2002). The kinematic wave model has been applied in numerous overland flow models (e.g., DHSVM (Wigmosta and Lettenmaier, 1999), KINEROS2 (Goodrich et al., 2002), SHE (Abbott et al., 1986), WEPP), and hydraulic models (e.g., HEC-HMS (U.S.A.C.E., 2000)). However, as discussed above, this method is inappropriate for two conditions common in larger watersheds: tributary backwater and shallow gradient floodplains.

Non-Inertia Wave Routing

The non-inertia wave (a.k.a., diffusion or diffusive (Yen and Tsai, 2001)) model is based on the continuity equation and an approximation of the momentum equation that retains the first two terms, friction slope and pressure differential, and neglecting the two inertia terms. The non-inertia wave model is a significant improvement over the kinematic wave model because of the inclusion of the pressure differential term. This term allows the non-inertia model to describe the attenuation (diffusion effect) of the flood wave (U.S.A.C.E., 1994) as it moves downstream. It also allows for the specification of a boundary condition at the downstream routing reach to account for backwater effects (Beven, 2001).

Because the non-inertia wave model is applicable to a wide range of channel and flow conditions, it is appropriate for watershed-scale hydrodynamic modeling. Use of the non-inertia wave for unsteady flow routing has been increasing in recent years because it is the simplest

among the approximations that can account for the downstream backwater effect and still yields reasonably good results (Yen and Tsai, 2001). This type of flood routing has been incorporated into hydraulic models (e.g., CCHE1D (Wu and Vieira, 2002)) and hydrologic models (e.g., CASC2D (Downer et al., 2002)).

Due to its applicability, some current research in hydrodynamic modeling has focusing on numerical methods to apply the non-inertia routing method. For example, Wang et al. (2003a) use a mixing cell method, which discretizes the nonlinear convection-diffusion equation into a first-order nonlinear ordinary differential equation. Moussa and Bocquillon (2001) present a method that converts the diffusive wave problem into two single problems by utilizing separate equations for convection and diffusion, thus providing an efficient and accurate resolution of the diffusive wave equation under some conditions on space and time steps and on spatial and temporal distribution of lateral inflow (Moussa and Bocquillon, 2001). Other areas of research using non-inertia waves have focused on improving accuracy of Muskingum-Cunge routing, an analytical solution to the non-inertia equation.

Muskingum-Cunge Routing

The Muskingum-Cunge (M-C) channel routing technique is a nonlinear coefficient method that simulates hydrograph diffusion based on physical channel properties and the inflowing hydrograph (U.S.A.C.E., 1994). The M-C method is a hybrid model that is between the hydrologic and hydraulic routing methods. The basis of the M-C method is to control the spatial step to induce numerical diffusion in the finite difference solution to the kinematic wave equation (Bajracharya and Barry, 1997), thus simulating diffusion by equating the convective diffusion to the numerical diffusion produced by the analytical technique (U.S.A.C.E., 1994).

This method has several advantages of over hydrologic techniques: 1) the model parameters are more physically-based; 2) the method compares well against the dynamic wave equations over a wide range of flow situations; 3) the solution is independent of the user-

specified computation interval, 4) it can account for flood wave attenuation (U.S.A.C.E., 1994), and 5) it is applicable in situations where observed hydrographs were not available (Fread, 2003). The major limitations of the M-C technique are: 1) backwater effects cannot be modeled because it is essentially a kinematic wave routing method (Ponce and Lugo, 2001), and 2) rapidly rising hydrographs (i.e., less than 2 hours) cannot be routed through flat channel sections (i.e., slopes less than 0.020%) (U.S.A.C.E., 1994), 3) stage-discharge rating curves cannot not have significant hysteresis loops (Fread, 2003).

This routing technique can be used in many of the situations commonly encountered in watershed-scale hydrologic modeling, and is used in some erosion models (e.g., SWAT (Neitsch et al., 2001)). Although this method originally had limited applicability to physically-based watershed modeling, there may be cases where the M-C method can be used as a reasonable approximation to the non-inertia wave (Wang et al., 2003). Since the M-C equations are computationally efficient and they approximate solutions to the convective-diffusion equation, current research in hydrodynamic modeling with the non-inertia wave has also included improving limitations of the M-C method. For example, Ponce and Lugo (2001) developed a method where the M-C method can be applied to reaches that have hydrographs with looped ratings (i.e., hysteresis) (Ponce and Lugo, 2001).

Quasi-steady Dynamic Wave

The quasi-steady dynamic wave approximation combines the continuity equation and a simplification of the momentum equation that excludes only the last term (local acceleration) (U.S.A.C.E., 1994). This equation is typically used to compute steady flow, water surface profiles, where local acceleration is assumed zero, but convective acceleration (changes in velocity with respect to distance) is important. This equation is most commonly used in conjunction with unsteady sediment transport models, and is not used in flood routing (U.S.A.C.E., 1994).

Dynamic Wave (Full St. Venant Equations)

The full St. Venant, dynamic wave equations are considered to be the most accurate and comprehensive solution to the 1-D unsteady flow problems in open channels (U.S.A.C.E., 1994), and are generally the standard to which other routing methods are compared. Dynamic routing allows for a higher degree of accuracy when modeling flood situations because it includes all of the parameters that other methods neglect (e.g., diffusion, local acceleration). Dynamic routing, when compared to other modeling techniques, relies less on calibration data and more on the physical properties of the stream (Beven, 2001), and provides more hydraulic information about flow events (Beven, 2001), which can be used to determine sediment transport rates. For full channel networks, where the flow divides and possibly changes direction during the event, only the full unsteady flow equations can be applied (U.S.A.C.E., 1994; U.S.A.C.E., 2000). As such, if a computationally efficient numerical solution were available (or can be developed), dynamic wave routing would yield the most physically-based hydrodynamic solution. The remainder of this section focuses on numerical methods and models that solve the full dynamic wave equations.

CHANNEL NETWORK HYDRODYNAMIC MODELS

There are three main categories of numerical solutions currently used to solve the St. Venant equations (Chaudhry, 1993): 1) characteristic methods, 2) finite-difference methods, and 3) finite element methods. Of these, only the characteristic and finite-difference methods are used extensively in open channel flow (Chaudhry, 1993). In the method of characteristics, a characteristic variable, wave celerity (Chaudhry, 1993; Cunge, Holly, and Verwey, 1980), is used to eliminate the space variable from the governing equations, thus converting the equations into ordinary differential equations of one variable, time. Recent applications of the method of characteristics have used the Froude number rather than the celerity to develop an analytical (Moramarco, Fan, and Bras, 1999) and semi-analytical (Wang, Chen, and Boll, 2003)

unsteady flood routing solutions. Moramarco et al. (1999) developed a linearized solution to the full St. Venant equations and included a term for uniform lateral inflow in each reach of a channel network, whereas, Wang et al., (2003b) converted the St. Venant equation into a nonlinear diffusion analogy equation.

The finite difference methods are further divided into explicit and implicit categories. For the explicit solutions, flow conditions are computed for each spatial location separately for each time step (Chaudhry, 1993). For the implicit solutions, the initial conditions are known for each spatial step, and the flow conditions are computed for each time step based on previous time-steps and adjacent spatial locations (Chaudhry, 1993). Chaudhry (1993) and Cunge et al. (1980) present several schemes for solving both explicit and implicit finite difference equations, and the reader is referred to those texts for derivations.

In recent literature, much attention has been given to weighted four-point-implicit finite-difference schemes, also known as Preissmann's schemes (e.g., (DeLong, Thompson, and Lee, 1997; Jha, Herath, and Musiake, 2000; Ping and Xiaofang, 1999; Sen and Garg, 2002; Venutelli, 2002), which has been proved to be highly efficient in the numerical simulation of unsteady flows. However, their work has focused more on matrix-solvers and computational algorithms rather than the general solution. For example, Ping and Xiaofang (1999) developed a flood routing model of a multi-branch river system by using the double-sweeping method to solve the irregular sparse matrix produced from the coefficients of the sets of equations developed for each channel reach (Ping and Xiaofang, 1999). In addition, DeLong et al., (1997) use a Gaussian elimination procedure to accomplish the same task.

Several publicly and commercially available models have implemented the full dynamic wave equations for routing water through a network of channels. For example, the U.S. Geological Survey has three separate models, the Branch-Network Dynamic Flow Model—BRANCH (Schaffranek, Baltzer, and Goldberg, 1981), the Full Equations Model—FEQ (Franz

and Melching, 1997), and FourPt (DeLong, Thompson, and Lee, 1997). In addition, the Danish Hydrological Institute has developed MIKE-11 hydrodynamic model as a component for its SHE modeling system (Yan and Zhang, 2001) and the National Center for Computational Hydroscience and Engineering, in conjunction with the U.S.D.A. Agricultural Research Service, has developed the CCHE1D model (Wu and Vieira, 2002).

None of the available erosion simulation models discussed in this chapter have incorporated algorithms to use the dynamic wave equations for channel networks, although reasonably accurate numerical solutions to the St. Venant equations have been available for some time (Chaudhry, 1993). Instead of rewriting their model to incorporate hydrodynamic models, AGNPS and SWAT have been coupled with CCHE1D to improve flood routing capabilities (Wang et al., 2002). The reasons most often given for not solving the full dynamic wave equations are 1) excessive computational time, and 2) excessive input data requirements (e.g., (Sen and Garg, 2002)). Recent improvements in computer processors have made the first point all but moot, and as more watershed data are collected, the second limitation may be eliminated as well.

WATERSHED CHANNEL NETWORK SEDIMENT TRANSPORT

Between the time when the sediment exits the upland areas and when it exits a watershed, sediments are transported in a network of channels. The solution to modeling this problem is the key to determining the fate of transport of management-related erosion, the sedimentation effects on individual reaches in a channel network, and the cumulative effect of multiple, spatiotemporally distributed management practices. Approaches to watershed-scale sediment transport are discussed, with particular attention given to methods used in available hydrodynamic-sediment transport models. It will be shown that none of the available watershed-scale models completely represents the physical processes of both upland erosion and hydrodynamic-sediment transport.

MODELING INSTREAM SEDIMENT TRANSPORT

Modeling instream sediment transport requires the simultaneous solution of five equations: 1) conservation of water mass (Equation 2-1), 2) conservation of fluid mixture momentum (Equation 2-2), 3) conservation of sediment mass, 4) an empirical relation to evaluate friction losses or flow resistance, and 5) an empirical relation to evaluate sediment transport capacity or incipient motion. The first two equations, described in previous sections, are the St. Venant equations. The third equation is often referred to as the Exner equation or the sediment continuity equation (Lyn and Altinakar, 2002), and will be discussed further below. Friction losses are described by empirical resistance formulas (e.g., Darcy-Weisbach, Chezy, Manning) (Yang, 1996) or boundary shear stress relations based on the von Karmon-Prandtl equation (Aberle and Smart, 2003). Sediment transport capacity relations are also empirical formulae developed to describe bedload, suspended load, or total load transport (Yang, 1996), as will also be discussed further below.

The Exner, or sediment continuity equation, (Equation 2-3) describes the mass balance of sediment moving with the fluid and the exchange of sediment with the fluid and the bed (Parker, Paola, and Leclair, 2000). In this formulation, λ is the bed material porosity [unitless], A_{bed} is the area of the channel bed [L^2], A_w is the cross-sectional area of flow [L^2], C_{sed} is the concentration of sediment [unitless], Q_{sed} is the sediment discharge rate [L^3T^{-1}], and q_{sed} is the lateral inflow of sediment [L^2T^{-1}]. With the Exner equation, it is possible to track the non-uniform transport of sediment through a network of channels. That is, aggradation, degradation, and exchange of material between the fluid and the bed are determined explicitly as a function of flow and sediment characteristics. This is necessary because, with the exception of washload, sediment travels through a channel network much slower than the propagation of flood waves (Knighton, 1984).

Equation 2-3.
$$(1-\lambda)\frac{\partial A_{bed}}{\partial t} + \frac{\partial(A_W C_{SED})}{\partial t} + \frac{\partial Q_{SED}}{\partial x} = q_{SED_{Lat}} \qquad [L^2T^{-1}]$$

There are likely as many sediment transport equations as there are sediment transport researchers. Of the large number of equations available, all contain some empirical component and no single equation yields good results for all river and sediment conditions; principally because each equation was developed for specific sediment sizes or flow conditions. Shen (1971) and Yang (1996) both describe numerous sediment transport equations; separating them into three main categories: bedload, suspended load, and total load (the integration of bedload and suspended load).

Washload is defined as the portion of sediment load governed by the upslope supply rate and is considerably less than the sediment transport capacity of a river (Shen, 1971). Washload sediment particles do not typically deposit on the channel bed because the particles are so small that their fall velocities are significantly smaller than the turbulent eddies produced under natural flow conditions (Knighton, 1984). As such, washload is generally ignored in sediment

transport equations; and is assumed wholly transported by the flow. Washload particle sizes are usually assumed less than 0.0625 mm (i.e., the division between sand and silt) (Shen, 1971; Yang, 1996), but are sometimes assumed less than 0.01 mm (Garbrecht, Kuhnle, and Alonso, 1995).

Bedload transport equations are of four general categories (as described by Yang (1996)): 1) excess methods; 2) probabilistic methods (e.g., Einstein or Vanoni and Brooks); 3) stream power (e.g., Bagnold), and 4) statistical regressions (e.g., Rottner). The excess methods have four main sub-categories: shear stress (e.g., Shields, Yalin, or Parker), velocity (e.g., DuBoys), discharge (e.g., Schoklitsch), and energy slope (e.g., Meyer-Peter and Muller). None of the above equations is universally applicable to all sediment transport and flow conditions. For example, the Meyer-Peter and Muller, and Parker equations strictly apply to gravel bed rivers (Yang, 1996), and the Bagnold equation applies only to wide sand-bed channels (Yang, 1996). As such, sediment transport models like SEDTRA (Garbrecht, Kuhnle, and Alonso, 1995) and CCHE1D (Wu and Vieira, 2002) incorporate several bedload transport equations to evaluate varied sediment and flow conditions.

Suspended sediment transport equations are generally based on diffusion theory or the turbulent exchange of particles in the fluid (Yang, 1996). The concentration gradient of suspended sediment in the flow is assumed to have a semi-logarithmic profile. The Rouse equation (Yang, 1996), based on the von Karmon-Prandtl logarithmic velocity profile, describes the theoretical sediment concentration profile. Since this equation cannot be solved analytically, several researchers have developed approximate solutions that are commonly used in suspended sediment transport models (e.g., Lane and Kalinske, or Einstein) (Yang, 1996).

Total load transport functions have two general categories (as detailed by Yang (1996)): 1) methods that compute bedload and suspended load separately, then add them together (e.g., Colby and Hembree, or Toffaleti), and 2) methods that compute total load without partitioning

bedload or suspended load (e.g.,(Ackers and White, 1973) or (Engelund and Hansen, 1967)). Yang (1996) provides a summary of several studies that have compared applicability of sediment transport equations. From tests with experimental data, the Ackers-White (1973) and the Engelund-Hansen (1967) total load equations have emerged among the more generally applicable; and the Yang (1973) equation yields acceptable results for sand-bed streams (Yang, 1996). As such, each of these equations has been incorporated into commercially available sediment transport models like SEDTRA (Garbrecht, Kuhnle, and Alonso, 1995), CCHE1D (Wu and Vieira, 2002), and SHE-SED (Wicks and Bathurst, 1996).

COUPLING UPLAND EROSION AND INSTREAM SEDIMENT TRANSPORT

The instream sediment-transport equations described above are not complete watershed process, sediment transport models. These equations ignore the processes of sediment generation and delivery to channels. Even when a sediment transport model incorporates a complete hydrodynamic model, sediment supply from upland erosion must be supplied from an appropriate watershed process model. The examples below describe recent attempts at linking upland erosion models with hydrodynamic-sediment transport models.

The WEPP model is an upland erosion model that has been extended for use in small watersheds by incorporating a simplified flood-runoff analysis method and a sediment transport equation into its watershed model (Ascough et al., 1995). The WEPP model uses a modified form of Yalin's bedload equation (Yalin, 1963) to compute sediment transport capacity in rills, interrill areas, and channels. Yalin's equation has been successfully applied to overland flow sediment transport in interrill areas by several authors (Alonso, Neibling, and Foster, 1981; Ferro, 1998; Finkner et al., 1989; Wicks and Bathurst, 1996), but has been demonstrated as inadequate for bedload transport in rivers (Bravo-Espinosa, Osterkamp, and Lopes, 2003). Although the WEPP model is one of the better upland erosion models, its' lack of a physically-based hydrodynamic model and its use of a suspect bedload transport equation make it less than ideal for use in watersheds greater than 2.6 km^2.

Bdour (2004) developed a framework for coupling macro-scale (upland erosion) and micro-scale (instream sediment transport) processes to simulate watershed scale erosion and sediment transport. He coupled the output from the WEPP model with SEDZL, a reach-scale, two-dimensional, hydrodynamic-sediment transport model developed at the University of California at Santa Barbara (Ziegler and Lick, 1986). His effort, however, was not a true coupling of upland erosion and instream sediment transport processes. Bdour modeled the

sediment and water discharge at the outlet of a 228-km^2 watershed using the WEPP model (Bdour, 2004). Taking those output as input for the SEDZL model, Bdour modeled the bed elevation changes of a 325-m study reach. This procedure ignored the sediment transport processes for the entire watershed upstream of the study reach, and therefore was not a true coupling of an upland erosion model with an instream hydrodynamic-sediment transport model.

Wicks and Bathurst (1996) developed SHESED, a "physically-based, spatially distributed erosion and sediment yield component for the SHE hydrological modeling system". SHESED simulates detachment of soil by raindrop impact, leaf drip, and overland flow, and the transport of eroded material by overland flow (Wicks and Bathurst, 1996). The empirical erosion equation is similar to Wischmeier's equation used in the USLE (Wischmeier and Smith, 1978). Because SHE is a grid-based model that cannot separate the sub-grid processes of rill and sheet erosion, the SHESED upland erosion model only evaluates overland flow, ignoring rill flow and erosion (Wicks and Bathurst, 1996). This limitation makes SHESED an incomplete, physically-based upland erosion model. Despite its limitations as an upland erosion model, SHESED has an exceptional hydrodynamic-sediment transport model. This model uses an implicit, four-point, finite difference scheme to solve simultaneously the St. Venant and Exner equations (Wicks and Bathurst, 1996) to route both water and sediment through a channel network. The model also uses the Engelund-Hansen (1967) and Ackers-White (1973) total load equations to determine sediment transport rates for particles greater than 0.062 mm; particles smaller than 0.062 mm are considered washload.

The CCHE1D modeling system was designed to simulate unsteady flows and sedimentation processes in channel networks (Wu, Vieira, and Wang, 2004; Wu and Vieira, 2002) by solving the complete, dynamic St. Venant and Exner equations. The model simulates bed aggradation and degradation, bed material composition (hydraulic sorting and armoring), bank erosion, and the resulting channel morphologic changes under unsteady flow conditions. CCHE1D does not

have an upland erosion model to generate sediment delivered to channels. Instead, it must be integrated with existing watershed processes (rainfall-runoff and field erosion) models to produce more accurate and reliable estimations of sediment loads and morphological changes in channel networks (Wu and Vieira, 2002). As such, the CCHE1D hydrodynamic-sediment transport model has been coupled with AGNPS and SWAT (Wang et al., 2002) to produce an integrated watershed-scale erosion model. Although CCHE1D is an exceptional hydrodynamic-sediment transport model, neither AGNPS nor SWAT is a physically-based upland erosion model. Both AGNPS (Young et al., 1989) and SWAT (Neitsch et al., 2001) are grid-based, empirical erosion models that are based on modifications to the USLE. As such, coupling either of these erosion models with CCHE1D does not produce a physically-based, watershed-scale erosion and sediment transport model.

CONCLUSION

It is clear that a complete, physically-based erosion model should explicitly consider the physical processes in each of the erosion phases, detachment, transport, and deposition. Erosion models that rely on empirical relations (e.g., AGNPS, SHESED, SWAT) to simulate erosion processes cannot accomplish this goal. The best model available that can accomplish this goal is the WEPP model. Since it was designed for use on hillslopes and small watersheds, WEPP must be coupled with a hydrodynamic-sediment transport model to be useful for simulations in watersheds larger than 2.6 km^2.

It is also clear that for a watershed-scale hydrodynamic model to be physically-based, it should not rely on empirical relations. Therefore, the empirical models (i.e., Rational Method, SCS Curve Number, regional regression equations, and unit hydrographs) and the purely hydrologic models (i.e., lag, Muskingum, and modified Puls) are inappropriate to use in physically-based hydrodynamic models. Only the full dynamic St. Venant equations can simulate all of these conditions completely.

Modeling instream sediment transport within a network of channels requires use of appropriate sediment transport equations and a method for computing sediment continuity. Of the available instream hydrodynamic models, only CCHE1D and MIKE-11 (a component of SHESED) are also physically-based instream sediment transport models. Either of which could be used satisfactorily for this research project.

As stated in the introduction, the goal of this research is to develop a fully, physically-based, coupled upland erosion and instream hydrodynamic-sediment transport model. Although several attempts have been made, this goal has not been accomplished by previous research. Available hydrodynamic-sediment transport models do not include physically-based upland erosion components. Likewise, available upland erosion models do not adequately model

instream hydrodynamic-sediment transport processes. Thus, there is a need to develop a procedure to couple an upland erosion model with a watershed-scale instream hydrodynamic-sediment transport model. Therefore, the proposed research will couple the most physically-based upland erosion model, WEPP, with the most physically-based instream hydrodynamic-sediment transport model, CCHE1D. It is expected that the results of this project will demonstrate a proof-of-concept for coupling the two models, and that those results will inspire the owners of the models will allow access to their proprietary code to explore the most efficient means for coupling the two models.

CHAPTER THREE

MODEL DEVELOPMENT AND CALIBRATION, PART I: HYDRODYNAMICS

ABSTRACT

Accurate assessment of current and projected impacts of forest management practices on sediment yield and delivery requires physically-based simulation models. Upland erosion rates are reasonably simulated with the Water Erosion Prediction Project (WEPP) model. Since WEPP does not simulate hydrodynamics or sediment transport in channels, it was linked via an interface program with CCHE1D, a one-dimensional, channel network, hydrodynamic-sediment transport model. The linked model was run with data from Caspar Creek Experimental Watershed, California. A 13-day test simulation resulted in predicted runoff volume that was less than 1% different from observed runoff volume. However, due to limitations of the output data from the WEPP model, only daily, rectangular hydrographs could be generated. After routing the flows, daily peak discharge rates had an average relative error (RE%) of 97% and a Nash-Sutcliffe (NS) coefficient of 0.41. These results are a marked improvement over the current method that WEPP uses for routing flow (RE%=1,110%, NS=-70.1). Hydrographs were generated for a three year period based on WEPP generated runoff volume and shape parameters of observed hydrographs, and re-routed with CCHE1D. The hypothetical hydrographs showed further improvement in model efficiency (RE%=66%, NS=0.62). These results suggest that by using an appropriate hydrodynamic model to route flood-flows, the accuracy of peak flow estimates can be increased by over two orders of magnitude.

INTRODUCTION

Most total maximum daily load (TMDL) analyses make extensive use of computer models (U.S.E.P.A., 2002) because of the need to evaluate large areas with heterogeneous characteristics. The Water Erosion Prediction Project (WEPP) Model (Flanagan et al., 1995) is a physically-based, erosion simulation model commonly used to assess management-related surface erosion in agricultural (Zhang et al., 2003) and forest (Foltz and Elliot, 1999) settings. Its ability to evaluate spatiotemporally distributed climatic and physiographic variables make it nearly ideal for use in site-specific, sediment TMDL evaluations. Although developed primarily for fields and small watersheds (area less than 2.6 km^2), the WEPP model has been extended for use in larger watersheds (area up to 130 km^2 (U.S.E.P.A., 1999)). As an upland erosion model, it has two limitations that need to be improved before the model can be used for simulations in larger watersheds: network hydrodynamics and sediment transport.

The WEPP Watershed model simulates hydrodynamics and sediment transport by using a simplified hydrologic model and a single sediment transport capacity equation (Ascough et al., 1995). To simulate hydrodynamic transport from hillslopes, to and through a channel network, WEPP applies modifications to the Rational (McCuen, 1998) and Soil Conservation Service Curve Number (Soil Conservation Service, 1991) methods. These methods are not hydrodynamic modeling, since they are only capable of determining the peak runoff and/or volume (U.S.A.C.E., 1994), and they ignore the physical processes governing open channel flow. The accuracy of runoff simulations in larger watersheds is severely limited by not including a hydrodynamic procedure. This inadequacy also limits the accuracy of sediment transport, which is highly dependent on discharge rates.

The WEPP model uses a modified form of Yalin's bedload equation (Yalin, 1963) to compute sediment transport capacity in rills, interrill areas, and channels. Yalin's equation has

41

been successfully applied to overland flow sediment transport in interrill areas by several authors (Alonso, Neibling, and Foster, 1981; Ferro, 1998; Finkner et al., 1989; Wicks and Bathurst, 1996), but has been demonstrated as inadequate for bedload transport in rivers (Bravo-Espinosa, Osterkamp, and Lopes, 2003). The purpose of this research project is to develop and implement a procedure to link the WEPP upland erosion model with an appropriate hydrodynamic and sediment transport model, significantly reducing the current limitations of the WEPP model.

The full St. Venant dynamic wave equations are considered to be the most accurate and comprehensive solution to the 1-D unsteady flow problems in open channels (U.S.A.C.E., 1994), and are generally the standard to which other flow routing methods are compared. Several publicly and commercially available models have implemented the full dynamic wave equations for routing water through a network of channels. For example, the U.S. Geological Survey has three separate models: the Branch-Network Dynamic Flow Model—BRANCH (Schaffranek, Baltzer, and Goldberg, 1981), the Full Equations Model—FEQ (Franz and Melching, 1997), and FourPt (DeLong, Thompson, and Lee, 1997). In addition, the Danish Hydrological Institute has developed the MIKE-11 hydrodynamic model as a component for its SHE modeling system (Yan and Zhang, 2001) and the National Center for Computational Hydroscience and Engineering, in conjunction with the USDA Agricultural Research Service, has developed the CCHE1D model (Wu, Vieira, and Wang, 2004; Wu and Vieira, 2002).

Of the above models, only the CCHE1D modeling system was designed to simulate both unsteady flows and sedimentation processes in channel networks (Wu and Vieira, 2002). The model simulates bed aggradation and degradation, bed material composition (hydraulic sorting and armoring), bank erosion, and the resulting channel morphologic changes under unsteady flow conditions. CCHE1D was designed to be integrated with existing watershed process (rainfall-runoff and field erosion) models to produce more accurate and reliable estimations of

sediment loads and morphological changes in channel networks(Wu, Vieira, and Wang, 2004; Wu and Vieira, 2002). As such, the CCHE1D hydrodynamic-sediment transport model has been coupled with AGNPS (Young et al., 1989) and SWAT (Neitsch et al., 2001) to produce an integrated watershed-scale erosion model (Wang et al., 2002).

Both AGNPS and SWAT are grid-based, empirical erosion models that are based on modifications to the Universal Soil Loss Equation (USLE) (McCuen, 1998) and are not physically-based upland erosion models. As such, coupling either of these erosion models with CCHE1D does not produce a physically-based, watershed-scale erosion and sediment transport model. The research project described here was designed to resolve this limitation, by coupling WEPP and CCHE1D. Both models are used as is (without modifications to the model code), with an interface program to control the flow of data between WEPP and CCHE1D. The hydrodynamic and sediment transport capabilities of CCHE1D were evaluated separately, with only results from hydrodynamic calibration presented here.

METHODS

STUDY AREA

The Caspar Creek Experimental Watershed (CCEW) is located on the Jackson Demonstration State Forest in northwestern coastal California, approximately 15 km southeast of Fort Bragg (Figure 3-1). The CCEW consists of the 424-ha South Fork (SFCC) and the 473-ha North Fork (NFCC) sub-watersheds (Henry, 1998). These two tributary basins are located in the headwaters of the 2,167-ha Caspar Creek watershed, which discharges into the Pacific Ocean near the community of Caspar.

The CCEW was chosen for this research primarily due to the availability of extensive datasets that had been continuously collected over 35 years for a paired watershed study. Physiographic, climatic, and hydrologic data (Table 3-1) were collected to study the effects of forest management on streamflow, sedimentation, fish, fish habitat, timber, and other vegetative growth (Henry, 1998). This watershed was also chosen because there was only one climatic regime, one forest cover type, and spatially similar soil properties; all of which reduced the analytical complexity of simulations. For this research, the SFCC was used for calibration of the models, and the NFCC was used for model evaluation and example scenarios.

The primary land-use/land-cover is coniferous forest, consisting mainly of dense stands of second-growth Douglas-fir (*Pseudotsuga menziesii*) and coast redwood (*Sequoia sempervirens*) (Henry, 1998). The SFCC sub-watershed was last harvested between 1971 and 1973, and the NFCC sub-watershed between 1985 and 1990 (Henry, 1998). The elevation of the watershed ranges from 37 to 320 m.a.m.s.l. (meters above mean sea level). Hillslope gradients are generally less than 70 percent, but are frequently over 70 percent adjacent to deeply incised streams (Henry, 1998). The soils in the study area are well-drained clay-loams 1 to 2 m in depth (Henry, 1998). Soils typically have high hydraulic conductivity (50-100 mm/hr), producing

saturated areas of only limited extent and duration, and rapid subsurface stormflow (Henry, 1998).
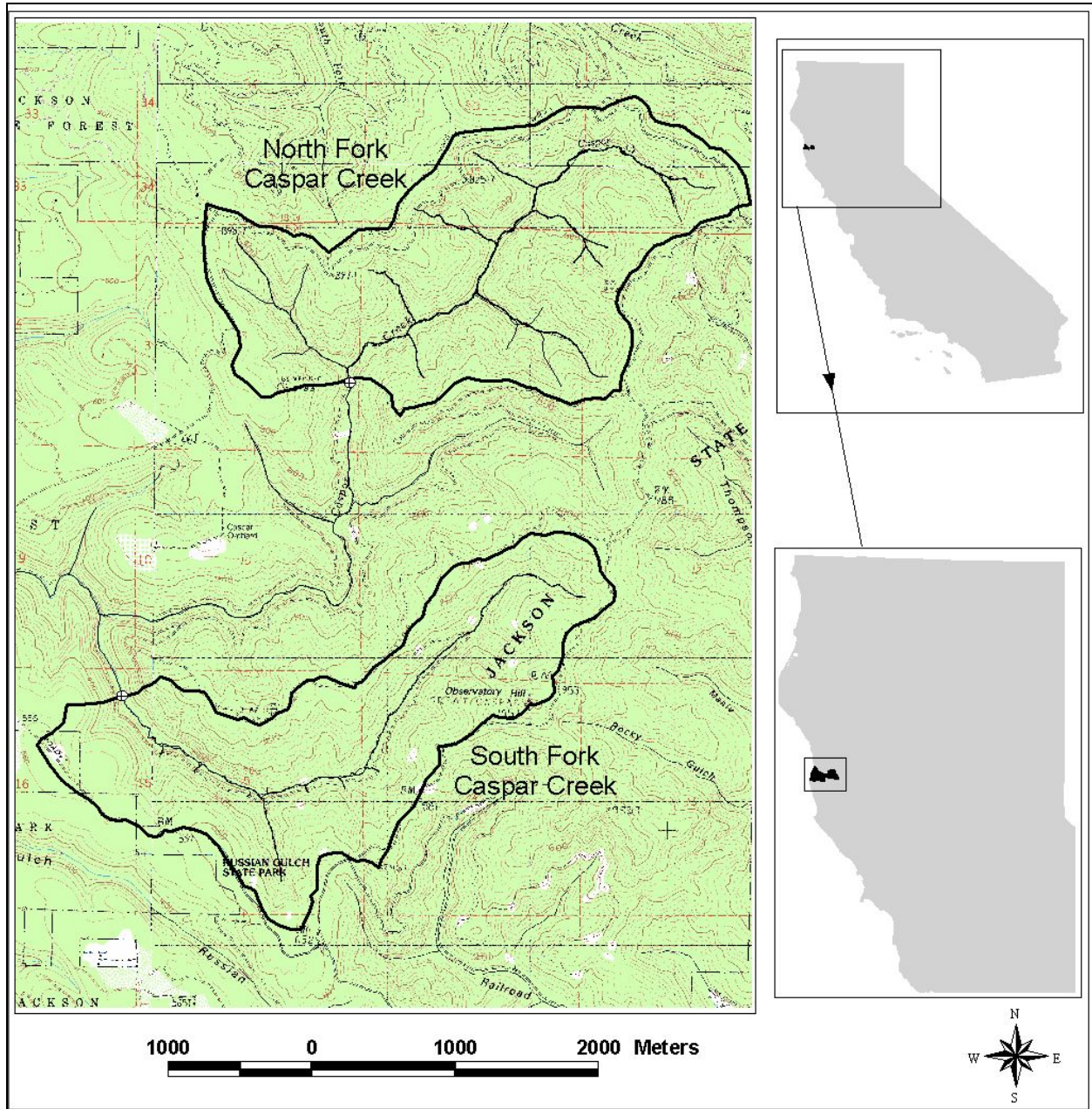
Figure 3-1. North and South Fork Caspar Creek Watersheds in the Caspar Creek Experimental Watershed, coastal, northern California. Watershed outlets are coincident with stream and sediment gauging stations, indicated by crossed circles.

Table 3-1. Spatiotemporal data available for the Caspar Creek Experimental Watershed, CA.

Data Category Sub-category	Spatial Resolution or Data Type	Temporal Resolution	Range (Time Span)
Physiography			
Topography	10 m DEM	n/a	n/a
Vegetation	Dominant Canopy Herbaceous Sub-layer	Harvest Schedule	n/a
Hydrography	DLG Derived from field surveys	n/a	n/a
Channel Cross-sections	NF Main Stem	Annual Measurements	1986-1997
Roads	DLG Derived from field surveys	Date Built	n/a
Climate			
Precipitation	n/a	Instantaneous; Daily Totals	1986-2000
Temperature	n/a	30-60 minute; Daily Max-Min-Ave	1988-2000
Solar Radiation	n/a	5-minute, Daily Ave.	1988-1996
Soils			
Particle Size Distribution	%Sand, Silt, Clay Rock, OM	n/a	n/a
Ksat--Infiltration	Percolation, Effective KSAT	n/a	n/a
Depth	Horizons	n/a	n/a
Soil Water	Piezometers	15-minute	1990-1998
Hydrology			
Stream Stage/Discharge	Various Meters Rating Curves	10-minute Daily Total	1963-2001
Suspended Sediment	ISCO Pumped Samples DH-48 DI Hand Samples Turbidity Controlled SALT	Storm Intervals 10-Minute Regression	1986-2001 1963-2001 1986-2001
Bedload	Outlet Settling Pond	Annual Total	1964-2001
Landuse Management	Timber Harvest, Road Building, Herbicide Application, Broadcast Burning, Natural Fire	Management/Incident Timing	1963-2001

CCEW experiences a Mediterranean climate, which is typical of low-elevation watersheds on the central North American Pacific coast (Henry, 1998). Mean annual precipitation is 1,190 mm, ranging between 305 to 2,007 mm, over the period 1962-1997 (Henry, 1998). High intensity, short duration thunderstorms in the summer, and winter snowfall are both very rare for this coastal, low elevation region. Summers are relatively dry, with cool coastal fog that contributes a small portion of the annual precipitation and reduces evapotranspiration losses (Keppeler, 1998). Temperatures are mild with muted annual extremes and narrow diurnal fluctuations due to the moderating effect of the Pacific Ocean (Henry, 1998).

In Caspar Creek, streamflow follows the precipitation pattern; with winter maximum flows three orders of magnitude larger than summer minimum flows. Highest streamflows generally occur in November through February, resulting from low-intensity, long-duration rainfall events. The bankfull discharge rate for both sub-watersheds is approximately 3.0 m^3/s (Lisle, 1995). Since the soils have typically high saturated hydraulic conductivity, the dominant mechanism for generating stormflow is lateral subsurface flow (Keppeler and Brown, 1998). Saturated overland flow occurs from limited areas for a limited duration (Henry, 1998), and is limited to areas adjacent to stream channels and areas that have low saturated hydraulic conductivity (e.g., roads and landings).

The sediment transport regime is primarily sediments smaller than large gravels, including a significant sand and silt component (Lisle, 1995). As with streamflow, sediment transport exhibits strong seasonality, with minimal or no sediment transport during low-flow periods, and very high sediment loads during winter rainstorms.

MODELING COMPONENTS

The modeling framework developed for this research project uses an aggregated, distributed parameter approach to modeling hillslope-scale runoff and erosion processes and watershed-scale hydrodynamic and sediment transport processes. The TOpographic

PArameteriZation-TOPAZ (Garbrecht and Martz, 1995) digital landscape evaluation tool was used to delineate channel networks (i.e., channel elements) and discretize sub-watershed boundaries (i.e., hillslope elements) from 10-m digital elevation models (DEMs). The WEPP model was used to determine the water runoff volume and sediment load for each hillslope element separately. Data from the TOPAZ and WEPP output files were processed with a FORTRAN relational-database management program written specifically for this research project. The data files generated from the interface program were used to run the CCHE1D simulations. Finally, output data from WEPP and CCHE1D were post-processed with Microsoft EXCEL for comparison with observed data.

The TOPAZ model, as used here, is directly linked to both WEPP (Renschler, 2003) and CCHE1D (Wu and Vieira, 2002) for watershed discretization. TOPAZ requires the user to define the minimum allowable area above the head of a first order channel (Garbrecht and Martz, 1995). This area, called the critical source area (CSA), is the basis for defining limits on the analytical scale (i.e., the length and width of hillslope elements). In practice, the CSA is set equal to the size of management units (or mapped sub-watersheds), or the CSA is changed until the derived channel network visually matches the observed channel network (Cochrane and Flanagan, 1999). Since both WEPP and CCHE1D use the TOPAZ program to discretize and define the structure of watersheds, it was necessary to choose a consistent definition for the minimum source area and channel length that defines each hillslope area. For this research, the minimum source area was fixed at 25 ha and the minimum channel length was fixed at 100 m. These values were chosen to limit the size of hillslopes simulated by WEPP-H (which, as discussed previously, should only be used on small hillslopes or sub-watersheds); and to match the derived channel network and sub-watershed boundaries with those mapped.

The WEPP model (version 2004.610, released June 2004) requires four input data files to run: 1) climate, 2) slope (landscape geometry), 3) soil, and 4) plant-management. The climate

data required by the WEPP model were extracted from the CCEW databases, including daily values for temperature (max/min), solar radiation, and wind speed, and instantaneous values for precipitation. Landscape geometry data are automatically generated with TOPAZ from the 10 m DEM. All soil property data were extracted from the CCEW databases, including, depth, particle size gradation, organic matter content, and cation exchange capacity. The forest management files from the WEPP databases were used to describe plant/management conditions. These files were modified to adjust plant spacing, tree height, and leaf-area index based on typical growth and yield conditions for the region (Lindquist and Palley, 1967; McArdle, Meyer, and Bruce, 1961).

The WEPP model has two distinct components: WEPP Hillslope (WEPP-H) and WEPP Watershed (WEPP-W), both of which were used in this research. WEPP-H is the main component used to simulate erosion separately for each hillslope in a watershed. The results of individual hillslope simulations are passed to the WEPP-W simulator via text output files. The watershed simulator uses the flow and sediment load information, combined with physiographic information generated by TOPAZ to compute daily flow volume, peak flow rate, and total sediment load at the watershed outlet for each event simulated. WEPP-W does not simulate routing of flows or sediment load, but uses empirical relations to provide an event-by-event summary. In the present study, the results from WEPP-H are passed to CCHE1D to simulate routing of water and sediment.

The CCHE1D channel network model computes unsteady flows using either the dynamic or non-inertia wave approaches (Wu and Vieira, 2002). For all simulations discussed in this project, the dynamic wave simulation mode was used. The CCHE1D model provides several well-known equations for the determination of sediment transport capacity, which were temporarily disabled for this project to focus on calibration of the hydrodynamic portion of the

model. Otherwise, CCHE1D was used 'as is' for all flow simulations, in accordance with instructions provided by the model developers (Wu and Vieira, 2002).

To facilitate data transfer between WEPP-H and CCHE1D, a FORTRAN interface module was written specific to this research project. The purpose of this module is to ensure that the data necessary to run CCHE1D are provided with the correct units and formatting. The interface program has the following functions: 1) Create a relational database to uniquely organize watershed structure; 2) extract rainfall, runoff, baseflow, and sediment load data from WEPP hillslope input and output files; 3) convert the data into consistent units (e.g., depth to volume, seconds to hours); 4) generate time-series hydrographs for each channel segment in the watershed network; 5) generate, where necessary, cross-sectional geometry at channel nodes; and, 6) create properly formatted text files necessary to run the CCHE1D simulations.

CCHE1D can operate at time steps as small as one second and as large as 24 hours. The computational time step is controlled by the Courant condition and the wave celerity (Vieira and Wu, 2002b), and is determined internally (exclusive of the user) by the model. Input time steps are typically in the 1 minute to 1 hour range (Vieira and Wu, 2002b; Wang et al., 2002). However, the user is required to supply a maximum computational time step. For this research, the maximum computational time step was set at 5-minutes, since this would provide adequate resolution for the hourly summaries that were desired for comparison with observed data.

CCHE1D needs physiographic, flow boundary conditions, and sediment data to operate. Daily streamflow volume and sediment load information obtained from WEPP-H were converted to continuous, time-series hydrographs for purposes of routing the flow and sediment load with CCHE1D. For this research, it was assumed that daily runoff events were continuous as long as there were less than four (4) days separating daily rainfall events. This cutoff was selected based on the observed time from peak discharge to return to baseflow conditions of historic hydrographs.

Physiographic data include channel network geometry, channel cross-sections at each source and junction node, and channel roughness (Manning's n) for each reach. Channel network geometry data were automatically generated with TOPAZ, requiring only a relational table to maintain the spatial properties between WEPP-H and CCHE1D. Since it is rare to have cross-section data for every reach in a watershed, even for extensively studied areas, it was necessary to develop a method for generating these data automatically.

The method developed for this research has five basic steps: 1) determine the location of channel network computational nodes where cross-sections are needed using TOPAZ; 2) compute the drainage area above each cross-section location with TOPAZ; 3) calculate hydraulic geometry parameters for each cross-section using regional hydraulic geometry relations; 4) calculate the spatial coordinates of the cross-section features using TOPAZ elevation data and the calculated hydraulic geometry parameters; and 5) prepare the data in a format usable by CCHE1D.

For this research, these cross-sectional data were generated using unpublished regional hydraulic geometry relations (Conroy, 2001) developed for coastal northern California rivers and streams north of Caspar Creek. These equations were applied to Caspar Creek because it is in the same geographic region, in a similar geologic setting (Snyder et al., 2003), with similar climatic conditions, but were adjusted for locality based on measured cross-sections in North Fork Caspar Creek (Lisle and Napolitano, 1988). The methods used for developing the regional hydraulic geometry relations are described in many journal articles and hydrology texts (e.g., (Castro and Jackson, 2001; Dunne and Leopold, 1978)).

Channel parameters were defined as a function of the drainage area (in km^2) above the location of the cross-section, including: maximum bankfull width [m] (Equation 3-1), valley width [m] (Equation 3-2), average bankfull depth [m] (Equation 3-3), and maximum bankfull depth [m] (Equation 3-4). The equations inside the parentheses are adjusted for units from those reported

in Conroy (2001). The coefficients outside the parentheses are locality adjustments specific to CCEW, based on measured hydraulic parameters of 42 observed cross-sections that span the length of the mainstem of NFCC.

Equation 3-1. $\quad W_{BF} = 1.1728 * (6.443 * AREA^{0.5495})$ $\qquad$ [m]

Equation 3-2. $\quad W_{VAL} = 0.8717 * (14.183 * AREA^{0.4814})$ $\qquad$ [m]

Equation 3-3. $\quad D_{AVE} = 0.9065 * (0.628 * AREA^{0.2756})$ $\qquad$ [m]

Equation 3-4. $\quad D_{MAX} = 1.0779 * (0.785 * AREA^{0.3002})$ $\qquad$ [m]

Measured values of bankfull channel geometry from NFCC were regressed against predicted values to adjustment the Conroy (2001) predictive equations to apply in CCEW. Equations 3-1, 3-3, and 3-4 predict bankfull width and average and maximum bankfull depth reasonably well (r^2 = 0.72, 0.55, and 0.69, respectively (Figures 3-2 and 3-3)). Valley width, however, was not predicted as accurately, but as with all other parameters, was predicted within a factor of 2 of measured values. This is consistent with the relations developed by Conroy (2001), where the relations have reasonable r-squared values (i.e., ranging between 0.79 and 0.92). However, the 95% prediction limits for each equation indicate that the actual value of the parameter are within a factor of two of the predicted value (Conroy, 2001). As such, when using these equations, the predicted values for width and depth may be in error by a factor of two.

Bankfull Width

Valley Width

Bankfull Width
Measured = 1.1728*Predicted
$r^2 = 0.72$

Valley Width
Measured = 0.8717*Predicted
$r^2 = 0.18$

Measured Width (m)
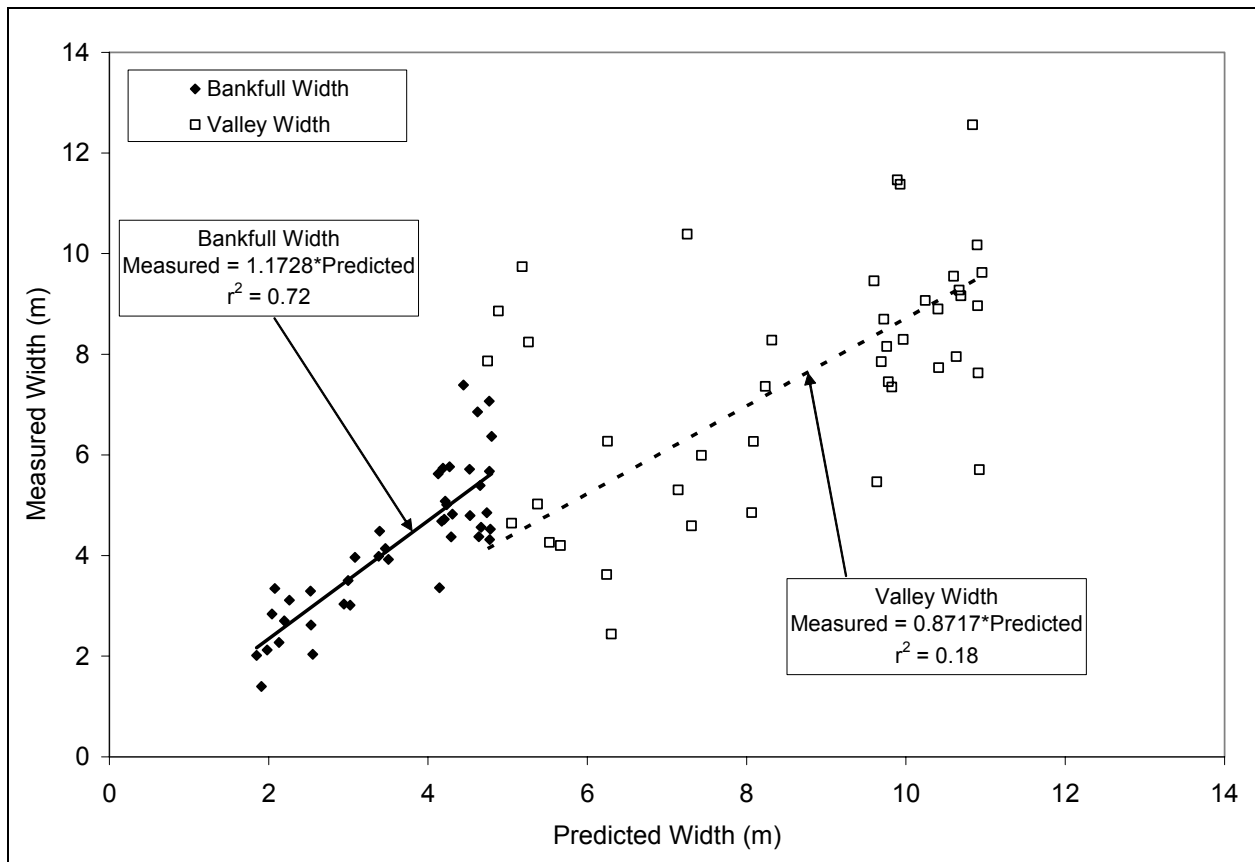
Predicted Width (m)

Figure 3-2. Measured vs. predicted bankfull and valley width for 42 stream channel cross-sections in North Fork Caspar Creek, CA. Predicted values were computed with Equations 1 and 2, respectively.
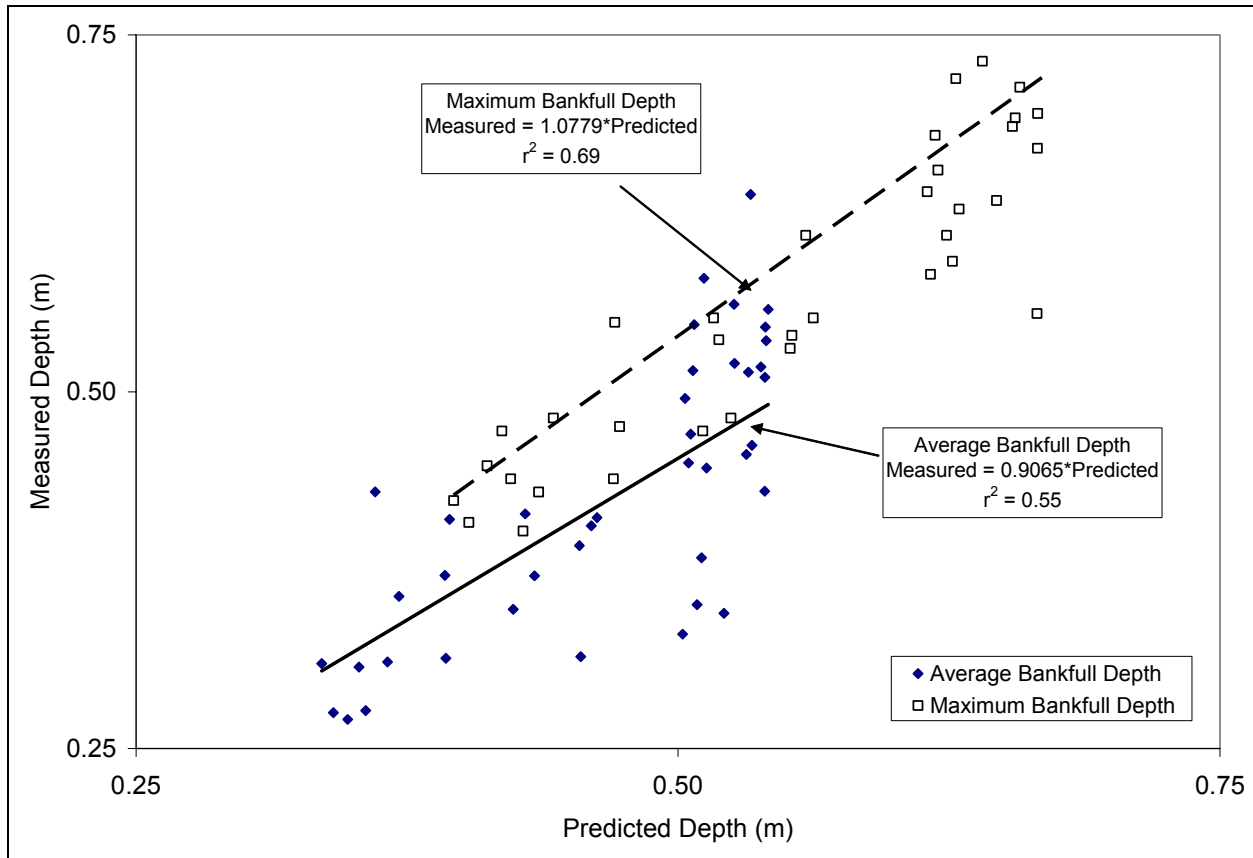
Figure 3-3. Measured vs. predicted average and maximum bankfull depth for 42 stream channel cross-sections in North Fork Caspar Creek, CA. Predicted values were computed with Equations 3 and 4.

Equations 3-1, 3-2, and 3-4 are used to create a trapezoidal main channel that is inset symmetrically into another trapezoid (representing the overbank area) (Figure 3-4).   To determine the side-slope shape of each trapezoid, a shape factor [m/m] (Equation 3-5) was calculated as the ratio of average to maximum bankfull depth (Western et al., 1997). A shape factor of 1.0 produces a rectangular channel, and a shape factor of 0.5 produces a triangular channel. Shape factor values cannot exceed 1.0 or be less than 0.5. The shape factor is then used to compute the bottom width of the overbank valley [m] (Equation 3-6) and the bottom width of the main channel [m] (Equation 3-7). In the case that the calculated valley bottom width is less than the bankfull width, the valley bottom width is set equal to the bankfull width.
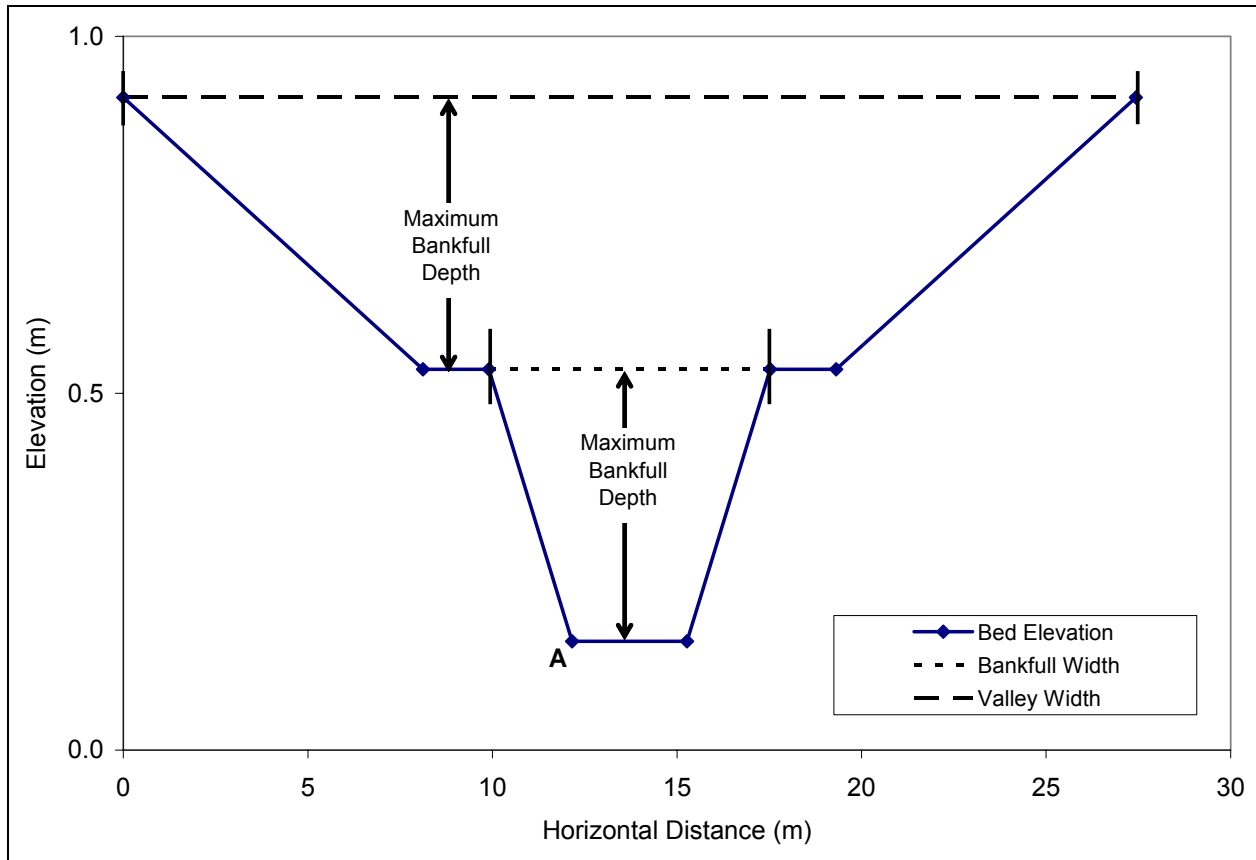
Figure 3-4. Schematic diagram of generated channel geometry.

Equation 3-5. $\quad \Psi = D_{AVE} / D_{MAX}$ $\qquad$ [no units]

Equation 3-6. $\quad W_{VB} = W_{VAL} * (2 * \Psi - 1)$ $\qquad$ [m]

Equation 3-7. $\quad W_{CB} = W_{BF} * (2 * \Psi - 1)$ $\qquad$ [m]

With the width and depth dimensions computed, the x-y coordinates of the cross-section points are calculated using two reference points. The horizontal reference point is the upper-left point of the cross-section (the outer valley width point on the left bank looking down stream), which is arbitrarily set to 0.0 m. The vertical reference point is the lower left bed elevation point of the main channel (point A on Figure 3-4), which is set equal to the bed elevation generated by TOPAZ for the given cross-section.

PROOF-OF-CONCEPT MODELING

From the initial simulations, it was readily apparent that the WEPP-H output data were inadequate to predict accurate outflow hydrographs. These data produce a rectangular, step-function shaped hydrograph that always has a duration time of 24 hours or less (Figure 3-5). Since the objective of this research was to link the WEPP model with a hydrodynamic-sediment transport model, adjusted hydrographs were generated and routed with CCHE1D to demonstrate a 'proof-of-concept' for linking the two models.
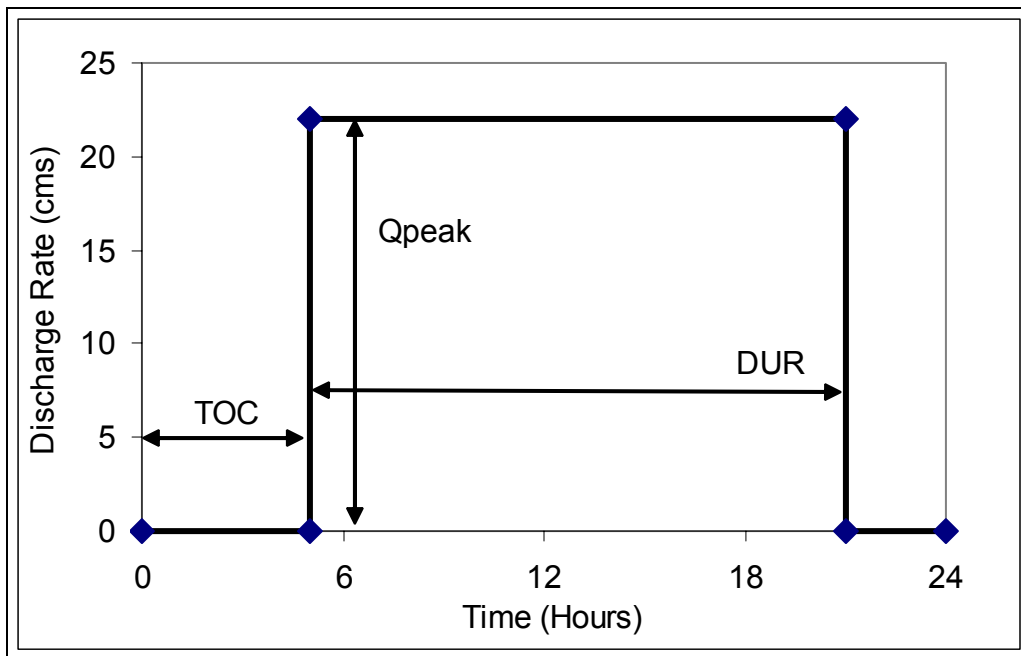
Figure 3-5. Example hydrograph created using data from WEPP Hillslope output pass file. TOC is time-of-concentration, DUR is runoff duration, and Qpeak is peak flow rate.

As is apparent in Figure 3-6, three parameters are necessary to define the shape of the hydrograph: the time duration that the hydrograph is rising, the peak flow rate, and the time duration that the hydrograph is falling. It is also necessary to have a function to determine the ordinates of the hydrograph for both the rising and falling limbs. The adjusted hydrographs

were generated using the same input and output data that were used for and generated by the WEPP-H simulations. Runoff volume was held constant and hydrograph shape parameters were adjusted (e.g., end of direct runoff, recession decay rate) based on several, observed, single-storm, single-peak hydrographs. For this research, the WEPP-H model estimates of runoff volume and initiation of runoff (called time of concentration by the WEPP-H model) were used, but not peak flow rate or duration of runoff.
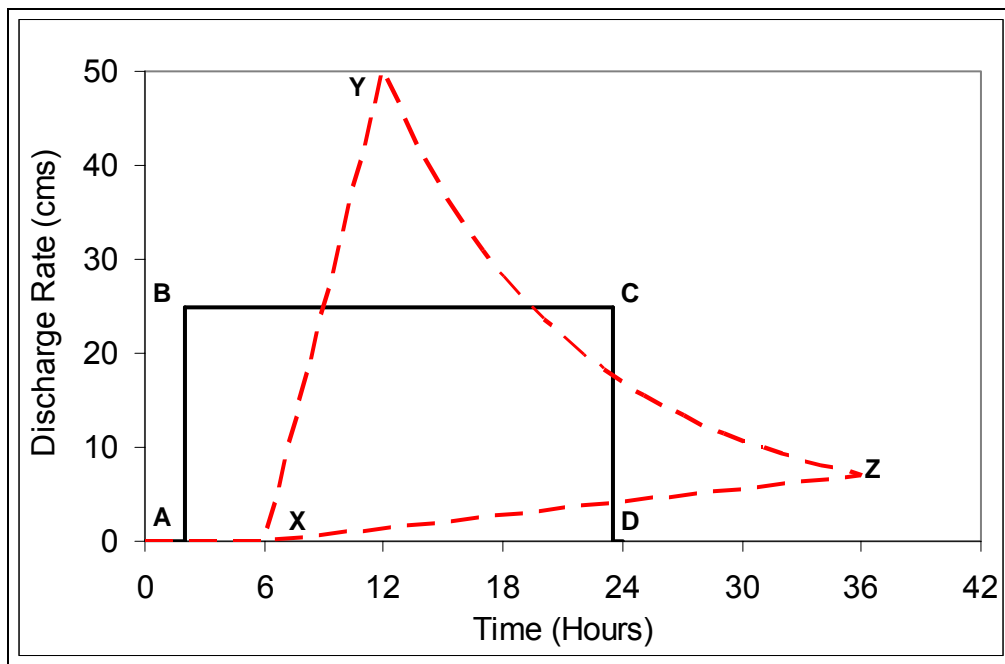
Figure 3-6. Adjusted hydrograph (dashed area X-Y-Z) with an equal volume to the rectangular hydrograph (solid area A-B-C-D).

The rising hydrograph limb was assumed to be a linear equation based on initial flow rate, peak flow rate, and rise time. Since all WEPP-H output events start at midnight on a given day, it was assumed that runoff begins at a time equal to the start time of precipitation (for a given day) plus the time of concentration given by WEPP-H. As used by WEPP-H, the time of concentration is the time that it takes for hillslope-generated overland flow to reach the nearest channel (Ascough et al., 1995). It was assumed that the difference between the start time of

precipitation and the time of maximum precipitation intensity can be added to the beginning time of runoff to obtain a peak runoff time.

The decay rate of the recession limb was computed using average values of decay rates of several, observed, single-storm, single-peak hydrographs. The end time of direct runoff was computed as the average of values computed from the same observed hydrographs. For this research, the point on the recession limb where direct runoff ends was assumed to be the inflection point; the point where the recession slope changes from greater than one to less than one (McCuen, 1998). The baseflow decay rate was also computed from observed hydrographs. The peak runoff rate was then established to preserve the continuity of runoff volume (Figure 3-6).

To obtain realistic hydrograph recession rates, 23 observed, single-storm, single-peak hydrographs were analyzed from the period of January 1, 1995 to December 31, 1997. Hydrographs that had multiple peaks, or had overlapping events (104 peaks in the period) were not used to eliminate the need for baseflow separation techniques (McCuen, 1998). All 23 hydrographs were used to determine the decay rate equations (Equations 3-8 and 3-9). In this formulation, discharge rate is a function of the discharge rate at the previous time step multiplied by a decay rate factor (always less than unity), where Q is the discharge rate [m^3/s], t is the time step [hours], and K_f is the decay factor [no units]. These equations were used to generate the both the recession limb discharge rates and baseflow recession discharge rates.

Equation 3-8. $\qquad Q_{t+1} = Q_t * K_f \qquad\qquad\qquad\qquad$ [$m^3\ s^{-1}$]

Equation 3-9. $\qquad K_f = 0.95 * (Q_{t-1})^{-0.015} \qquad\qquad$ [no units]

Only 15 of the 23 hydrographs had identifiable inflection points on the recession limbs. Of these 15 hydrographs, the average time to end of direct runoff (calculated from the peak time) was 22 hours (standard deviation = 5.5 hours). These values were added to the WEPP-H time-

of-concentration and the time to event maximum precipitation intensity to establish a duration time for each runoff event.

The only variable that could not be solved for directly was peak flow rate. To determine this value, an iterative solution was required. Since, the total flow volume is given, if a peak flow rate is assumed, the volume of the new hydrograph can be computed. The peak flow rate is then adjusted such that the new volume equals the original volume. The algorithm used to solve this problem is a binary search method (Burden and Faires, 2001). The algorithm searches for a peak flow rate that has an area under its curve equal to the original runoff volume. The minimum value that Qp can have is zero, this serves as the lower boundary. There is no upper limit that Qp can take, but there are realistic limits. Since I am converting rectangular hydrographs into irregularly-triangular hydrographs, if the time-base is equal, the peak of a triangular hydrograph is exactly twice that of a rectangular hydrograph. To insure that there was always an unapproachable upper bound, a factor of four was used instead of two. Therefore, the upper bound was calculated as four times the volume [given as the area of rectangle ABCDA in Figure 3-6] divided by the duration of the original hydrograph.

Computation of volume (area of irregular-triangle XYZ in Figure 3-6) uses a trapezoidal rule of numerical integration. Since the computation of points on the Y-Z limb of the triangle are equally spaced at 1-hour, the integration step is also set at 1-hour. The volume is computed in two stages. The first stage integrates the entire area under the curves X-Y and Y-Z. The second stage integrates the area under the X-Z curve. The second area is subtracted from the first area to obtain the area within the triangle. This area is compared to the area of rectangle ABCDA. If the two areas are not equal, the value at point-Y on the triangle is adjusted (using the iterative, Bisection method) until the volume is within the specified tolerance. The algorithm is finished its computations when the absolute error of original volume to computed volume is less than 0.0001. This value was chosen because the computational units are in cubic meters,

59

and I wanted to have output units of cubic feet to accuracy of 0.01. If this tolerance is not reached, the algorithm quits after 10,000 iterations and saves the current result.

CCHE1D requires a single, continuous hydrograph to simulate hydrographs that are closely spaced in time (i.e., where direct runoff from a new event occurs before baseflow from a preceding event has returned to zero). To produce a single, continuous hydrograph, it is often necessary to superimpose hydrographs that are closely spaced in time. To do this it was assumed that portions of hydrographs that overlap are additive. The newly generated hydrographs were then routed through the watershed channel network with CCHE1D using the same settings as previously described.

STATISTICAL ANALYSES

In this research, three routing procedures are compared to observed values for two variables (i.e., daily peak runoff rate and daily total runoff volume). The three routing procedures are: 1) WEPP Watershed (WEPP-W) model used as is, 2) unaltered WEPP Hillslope results routed with CCHE1D (hereafter referred to as WEPP/CCHE-1), and 3) WEPP Hillslope results altered with methods described as proof-of-concept, then routed with CCHE1D (hereafter referred to as WEPP-2-CCHE)

The Nash-Sutcliffe coefficient (NS) of model efficiency was used as a statistical criterion for evaluating hydrologic goodness of fit between measured and predicted values for each method (Nash and Sutcliffe, 1970). This statistic is recommended by the American Society of Civil Engineers Watershed Management Committee for evaluating the performance of models that simulate continuous runoff hydrographs (A.S.C.E., 1993). For this research, two output parameters were evaluated: daily streamflow volume and peak streamflow discharge rate. The Nash-Sutcliffe coefficient is calculated with Equation 3-10, where Q_{oi} are the observed values (e.g., volume or flow rate), Q_{mi} are model predicted values, and n is the number of data pairs. The NS coefficient ranges from $-\infty$ to 1.00, where an NS value of one indicates a perfect fit

between measured and predicted values, and would plot as a 1:1 line. A value of zero suggests that the fit is as good as using the average value of all the measured data for each event, indicating a poor model fit. Negative NS-values are generally considered meaningless (A.S.C.E., 1993), but indicate poor predictive value of the model, with more negative values indicating a poorer model fit.

Equation 3-10. $$NS = 1 - \frac{\sum\limits_{i=1}^{n}(Q_{o_i} - Q_{m_i})^2}{\sum\limits_{i=1}^{n}(Q_{o_i} - \overline{Q_o})^2}$$ [no units]

Since the Nash-Sutcliffe ratio is a composite of all observed-predicted pairs, the error associated with individual pairs was given as the relative error (Burden and Faires, 2001). The relative error, also described as the fractional uncertainty (Taylor, 1982), is the ratio of the difference between observed and predicted values to the observed value (Equation 3-11). In situations where it was desirable to know whether the relative error was positive or negative, the absolute values were removed from the equation and recomputed.

Equation 3-11. $$RE\% = 100 * \frac{|Q_o - Q_m|}{|Q_o|}$$ [no units]

RESULTS AND DISCUSSION

The TOPAZ-generated watershed structure contained 18 unique hillslopes and 7 channel segments for the SFCC sub-watershed. The erosion simulation was conducted using the WEPP Windows interface, for a 13-day simulation period from January 3, 1995 to January 15, 1995 (the first multi-peak event to occur during the observation period). Erosion simulations were conducted using input parameters developed from site-specific data (Tables 3-2 and 3-3). Since CCHE1D needs values for observed baseflow and WEPP did not directly produce a value for baseflow, it was assumed that baseflow was the sum of the percolation and lateral subsurface flow depths (given in the daily water balance output file).

Table 3-2. User-defined input Parameters Used for WEPP Hillslope Simulations.

Management File Parameters.		Soil Properties	
Plan	Twenty-year old forest (from Disturbed WEPP Database)	Depth (mm)	1525
Operations	None	Texture Class	Clay Loam
Crop Type	Perennial	Sand Content (%)	30.0
Growth Pattern	Continuous	Clay Content (%)	25.0
Stem Diameter (m)	0.30	Organic Matter Content (%)	3.0
Canopy Height (m)	30.0	Rock Content (%)	2.0
Spacing (m)	2.0	Initial Saturation (m/m)	0.70
Leaf Area Index	20.0	Effective Hydraulic Conductivity (mm/hr)	50.0

Table 3-3. Observed Monthly Average Climate Parameters for Caspar Creek, CA (1995-1997), used in WEPP Hillslope simulations.

Month	Maximum Temperature (C)	Minimum Temperature (C)	Solar Radiation (Langleys)	Total Rainfall (mm)
Jan	10.20	9.38	70	377
Feb	10.23	9.09	207	122
Mar	10.62	9.09	310	218
Apr	11.04	9.19	361	133
May	13.31	10.40	530	57
Jun	14.83	11.20	604	23
Jul	16.63	12.07	618	0.7
Aug	15.64	12.64	563	7.8
Sep	14.92	12.41	467	16
Oct	12.24	10.38	333	58
Nov	10.74	9.52	184	154
Dec	10.30	9.32	95	368

The observed daily runoff volume and peak rates were compared to those predicted by WEPP-W and WEPP/CCHE-1 (Tables 3-4 and 3-5). Both WEPP-W and WEPP/CCHE-1 adequately predicted the observed runoff volume (within 0.5 and 0.8%, respectively) for the 13-day period (Table 3-4). Visual inspection of Figure 3-7 indicates that rectangular hydrographs created by WEPP-H (and routed with CCHE1D) bear very little resemblance to the observed hydrographs. Also, when using CCHE1D to route WEPP-H hydrographs, small events (e.g., Jan. 4, Jan. 5, Jan. 6, Jan. 11, Jan. 14, Jan 15) have over-predicted peak rates, and that larger events (e.g., Jan. 8, Jan. 9, Jan. 10 Jan. 12, and Jan. 13) have under-predicted peak rates. This observation is confirmed with data in Table 3-4. WEPP-W does not produce output hydrographs, only daily values for runoff volume and peak flow rate. As such, there is no direct means to compare graphically these results with observed values.

Table 3-4. Observed Daily Runoff Volume at South Fork Caspar Creek, compared to

CCHE1D and WEPP Watershed predicted values.

Date	Observed Daily Runoff Volume (m^3)	WEPP/CCHE-1 Predicted		WEPP-W Predicted	
		Daily Runoff Volume (m^3)	Relative Error (%)	Daily Runoff Volume (m^3)	Relative Error (%)
1/3/1995	7,365	8,444	15	665	91
1/4/1995	8,729	29,322	236	18,298	110
1/5/1995	13,923	42,009	202	27,788	100
1/6/1995	16,318	55,142	238	74,907	359
1/7/1995	53,387	58,567	10	52,733	1
1/8/1995	114,029	182,690	60	271,054	138
1/9/1995	260,039	155,762	40	196,407	24
1/10/1995	91,222	55,700	39	21,130	77
1/11/1995	39,467	70,019	77	51,883	31
1/12/1995	109,167	90,884	17	79,960	27
1/13/1995	195,552	186,089	5	214,947	10
1/14/1995	99,610	58,769	41	16,002	84
1/15/1995	34,911	58,683	68	22,976	34
Sum (or Average for RE%)	1,043,718	1,052,080	81	1,048,749	84

Table 3-5. Observed Daily Peak Runoff Rate at South Fork Caspar Creek compared with CCHE1D (routing WEPP Hillslope data) and WEPP Watershed predicted values.

Date	Observed Peak Runoff Rate (m³/s)	WEPP/CCHE-1 Predicted		WEPP-W Predicted	
		Peak Runoff Rate (m³/s)	Relative Error (%)	Peak Runoff Rate (m³/s)	Relative Error (%)
1/3/1995	3.8	4.6	21	4.6	20
1/4/1995	3.6	14.6	302	103.5	2753
1/5/1995	7.0	19.0	172	152.3	2088
1/6/1995	8.9	40.0	350	380.7	4192
1/7/1995	28.3	24.4	14	275.3	873
1/8/1995	103.3	86.3	16	1249.3	1109
1/9/1995	180.7	67.3	63	927.7	413
1/10/1995	59.2	20.4	66	118.2	100
1/11/1995	20.0	31.9	60	271.2	1258
1/12/1995	69.2	40.9	41	404.4	484
1/13/1995	157.6	85.9	45	1008.3	540
1/14/1995	81.2	25.3	69	91.5	13
1/15/1995	18.9	26.8	42	127.8	576
Average	57.0	37.5	97	393.4	1109

When using WEPP/CCHE-1 routed hydrographs, peak rates were over-predicted by as much as 350% and under-predicted by as much as 69%, with a moderate model efficiency (NS=0.41). When using WEPP-W, the estimated daily peak flow rates were uniformly over-predicted by a minimum of 13% and a maximum of 4,200%, with an extremely low model efficiency (NS=-70.1). This indicates that using CCHE1D to route WEPP Hillslope hydrographs provides much improved estimates peak flow rates over the empirical methods used in the WEPP Watershed model.
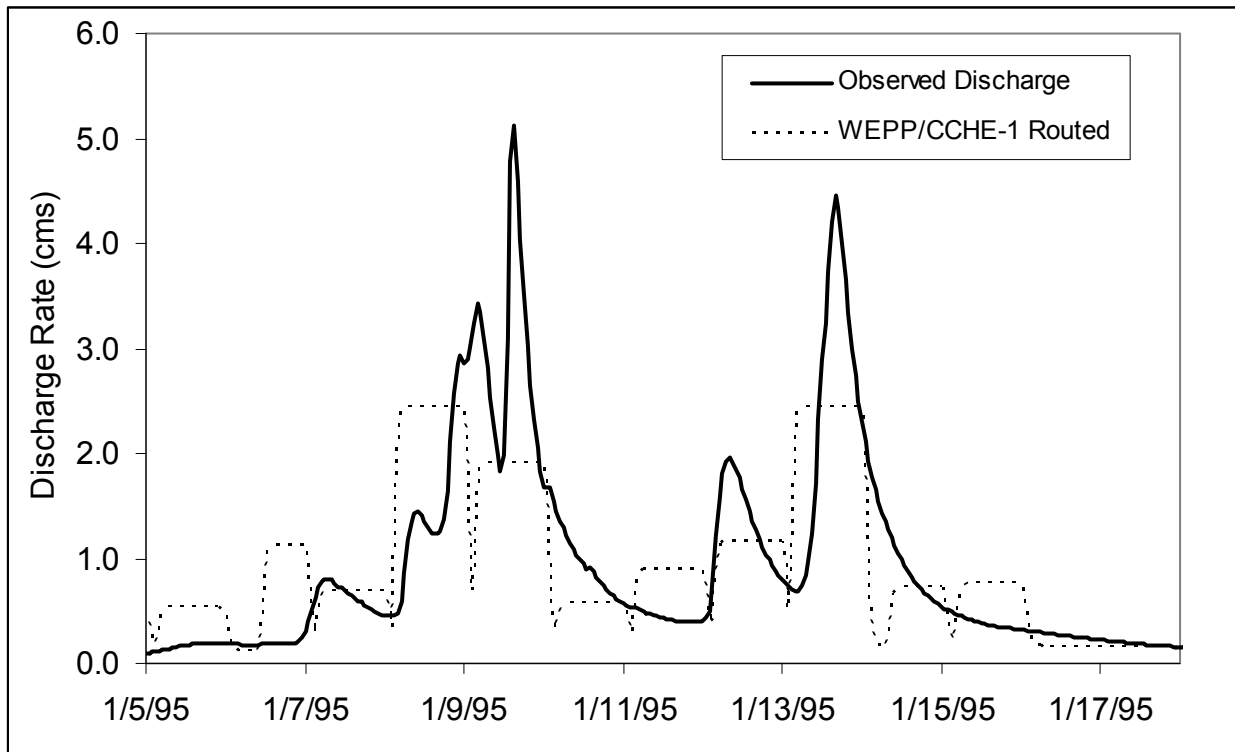
Figure 3-7. Observed discharge at South Fork Caspar Creek (January 3-18, 1995) vs.

Predicted discharge (simulated with WEPP/CCHE-1).

Based on the above results, it is clear that the current WEPP output data cannot be used to predict continuous runoff hydrographs that are representative of observed hydrographs. This is because the output data are daily summaries that provide inadequate sub-daily hydrograph information. When using only daily hydrograph information, several problems are apparent: 1) Trying to represent a continuous, single hydrograph produces discontinuities between daily events. Hydrograph ascension and recession limbs unrealistically rise and fall, respectively. 2) Daily events with multiple peaks cannot be evaluated. 3) Runoff events that span multiple days are not evaluated correctly. None of the flow generated on one day is carried over to the next day. 4) Closely spaced runoff events do not display auto-correlation and inter-dependence, as they should.

The WEPP model assumes for purposes of generating sediment loads from hillslopes, that the flow exiting the hillslope is constant at its peak rate for the entire duration of the storm event. Although this method may produce reasonable estimates of flow volume and sediment load, it does not produce hydrographs with shapes comparable to observed hydrographs. To generate a hydrograph that can be compared to observed data, the WEPP-H output files need to be modified in one of two ways. 1) Write the runoff volumes and rates for regular, sub-daily time intervals (hourly values would be adequate), such that the actual runoff hydrograph can be exported; or 2) include a value for time-to-peak, such that daily, triangular (SCS-type) hydrographs can be created to approximate the actual hydrograph. It was beyond the scope of this project to re-write the WEPP program code to accomplish either of these tasks.

PROOF-OF-CONCEPT FOR COUPLING WEPP AND CCHE1D

The WEPP-H model was re-run using the same input data as was used for the preliminary modeling step, except that the simulation was run from January 1, 1995 to December 31, 1997. The simulation period for the proof-of-concept modeling was longer than the initial modeling to demonstrate that the two models could work together for simulation periods lasting multiple years. For this three year period, the WEPP-H simulation generated 89 days with runoff. These flows were routed using the WEPP-Watershed model and the WEPP-2-CCHE modeling framework to produce continuous hydrographs.

The WEPP-2-CCHE model shows a noticeable improvement in predicted hydrograph shape (Figure 3-8) over those simulated by WEPP/CCHE-1 (Figure 3-7). However, there are a few noticeable limitations to using adjusted hydrographs to compare to observed hydrographs. For example, days with multiple peaks (as occurs on both January 8 and 9, 1995) cannot be predicted without input hydrographs that demonstrate multiple peaks. In addition, using the characteristics of precipitation events as surrogates for hydrograph characteristics produces differences between predicted and observed hydrographs. As is illustrated in Figure 3-8, the

majority of the peaks are shifted to the left (i.e., occurring before the observed peak), with the beginning of runoff occurring a few hours before the observed hydrographs. These differences are the result of two assumptions made when generating the hypothetical hydrographs. 1) The beginning of runoff can be approximated as the time of concentration (calculated by WEPP-H) added to the beginning time of precipitation. 2) The rise to peak has a linear rate of increase. Differences due to the first assumption are the result of assuming that precipitation excess occurs at the same time as the event starts. Although this is not a realistic assumption, methods to determine precipitation excess were not explored because only hypothetical hydrographs were needed to demonstrate a proof-of-concept.
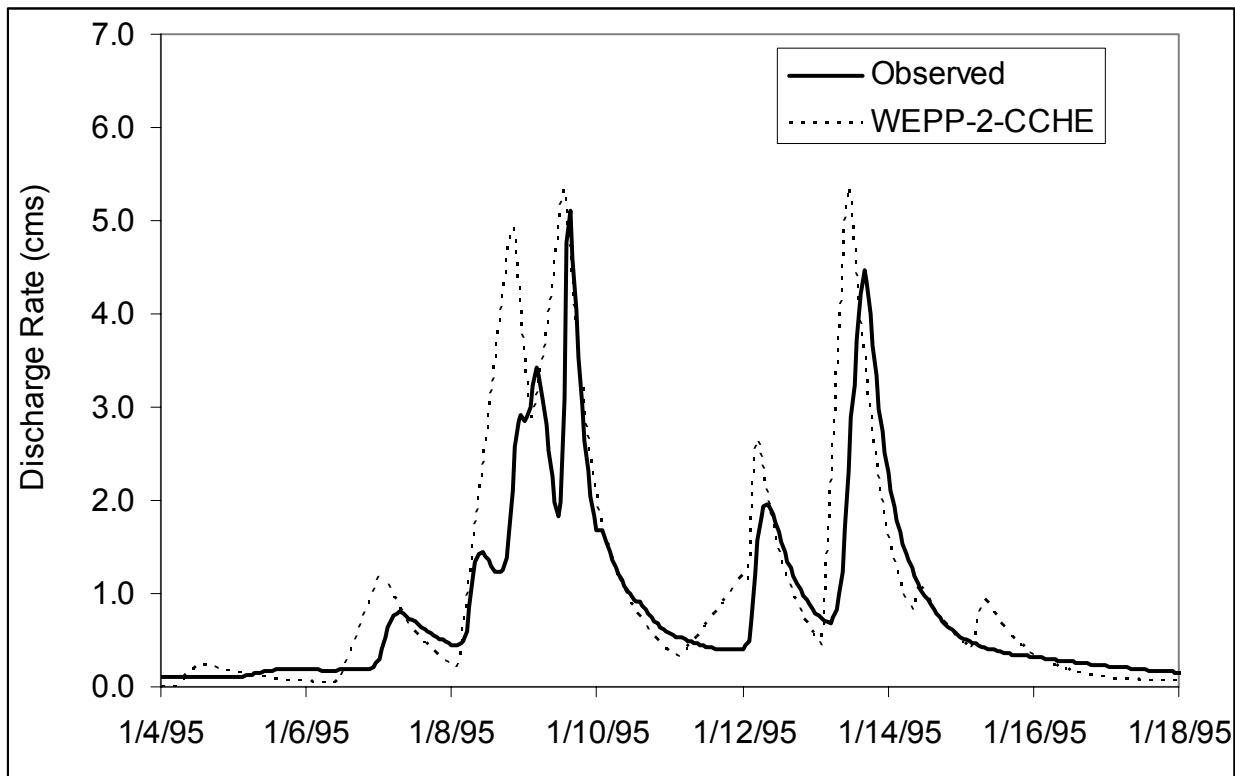
Figure 3-8. Observed discharge at South Fork Caspar Creek (January 3-18, 1995) vs.

Predicted discharge (simulated with WEPP-2-CCHE).

The observed daily runoff volumes were compared to those predicted by WEPP-W and WEPP-2-CCHE for the three years of simulation (Figure 3-9 and Table 3-6). Both WEPP-W and WEPP-2-CCHE predict total daily runoff volumes that are not statistically significantly different from observed values. The WEPP-2-CCHE modeling framework produces a total volume within 20% of observed (Table 3-6), compared to 6% for the WEPP-W model. For the 89 daily observations, the WEPP-2-CCHE modeling procedure had an average relative error of 87%, with a Nash-Sutcliffe coefficient of 0.75; whereas, for the same 89 observations, the WEPP-W modeled predictions had an average relative error of 127%, with a Nash-Sutcliffe coefficient of 0.45. On the average, the WEPP-W model under-predicted daily runoff volume by approximately 3.4%, with an r^2 of 0.36. While the WEPP-2-CCHE modeling procedure over-predicted daily runoff volume by approximately 3.4%, with an r^2 of 0.68. These results indicate a marked improvement in both prediction accuracy and model efficiency for runoff volume, by using simple assumptions about hydrograph shape.

Table 3-6. Observed and predicted daily runoff volume statistics for 89 daily runoff events at Caspar Creek Experimental Watershed, CA (January 1995 to December 1997).

	Daily Runoff Volume (m^3)			Relative Error (%)			Nash-Sutcliffe Coefficient
	Max	Min	Total	Max	Ave	Min	
Observed	268,864	1,550	5,518,742	--	--	--	--
WEPP-2-CCHE	318,289	3,248	6,602,724	1,857	87	1	0.75
WEPP-W	394,716	1	5,862,164	3,086	127	0	0.45

Although the WEPP-2-CCHE routing procedure shows marked improvement in predicting both total volume (all events) and daily runoff volume, these results are not surprising. It was assumed that WEPP-H produced reasonable estimates of daily runoff volume, but that the routing procedure used by WEPP-W was inadequate and that a sophisticated hydrodynamic

model would necessarily produce results that are more accurate. The resulting high NS coefficient supports this assumption. What are most notable are the differences in accuracy and model efficiency when comparing daily peak discharge rates.
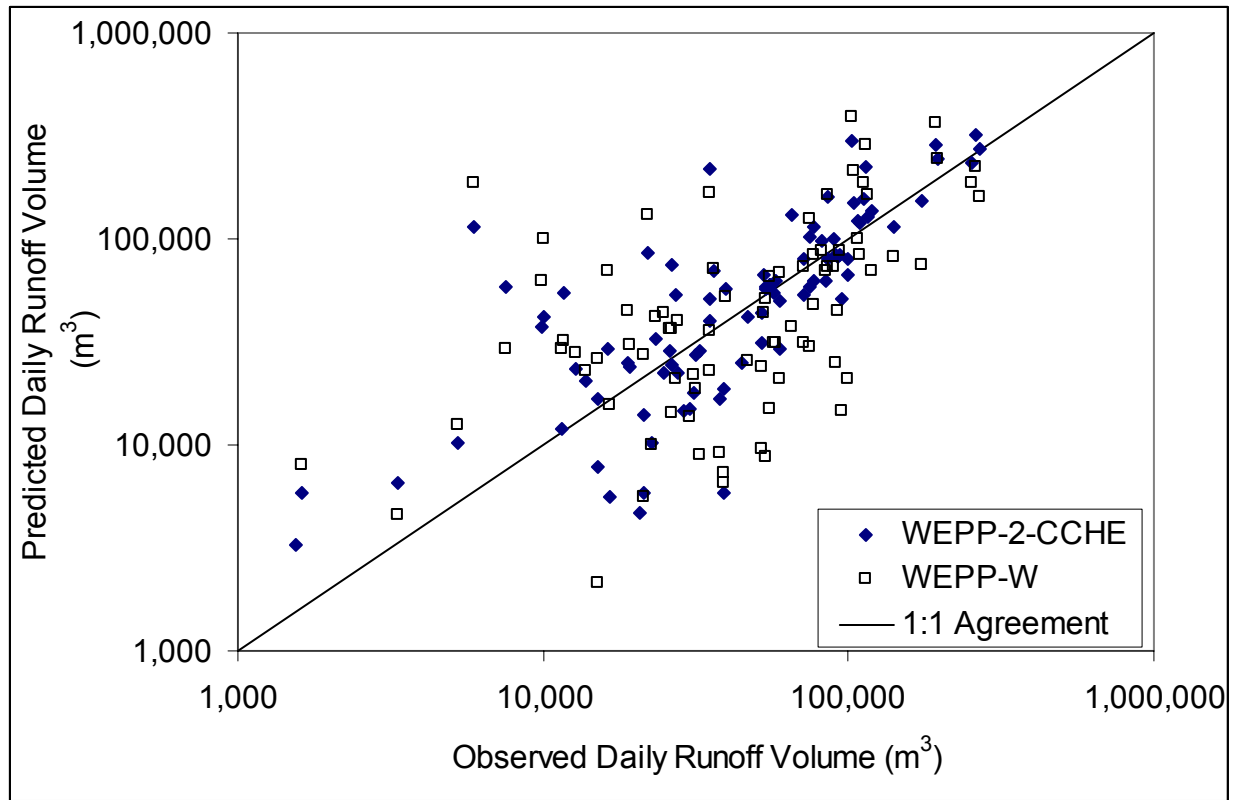
Figure 3-9. Observed vs. predicted daily runoff volume for 89 events at South Fork Caspar Creek Experimental Watershed, CA (1995-1997).

For the 89 daily runoff events evaluated in the three-year period, the WEPP-2-CCHE simulated peak flow rates show a remarkable improvement over the WEPP-W simulated peaks. The WEPP-W model predicts peak runoff rates that are statistically significantly different from observed values ($p<0.0001$, $\alpha=0.05$). The WEPP-2CCHE modeling framework, however, predicts peak flow rates that are not statistically significantly different from observed values ($p> 0.999$). The WEPP-2-CCHE routed flows have a much improved model efficiency (NS = 0.51), with an average relative error of 83%. The Nash-Sutcliffe coefficient for the WEPP-W simulated

peaks was even lower (NS=-86) than when using WEPP/CCHE-1 (NS=0.41). On the average,

the WEPP-2-CCHE predicted peaks are approximately 10% higher than the observed peaks,

with an r^2 of 0.66 (Figure 3-10). Whereas the WEPP-W predicted peaks are approximately

660% greater than observed peaks. Even though the relation between observed peaks and

those predicted by WEPP-W is reasonable, with an r^2 of 0.55, the predicted values are, on the

average, over-predicted by at least an order of magnitude and have an average relative error of

973% (Table 3-7).
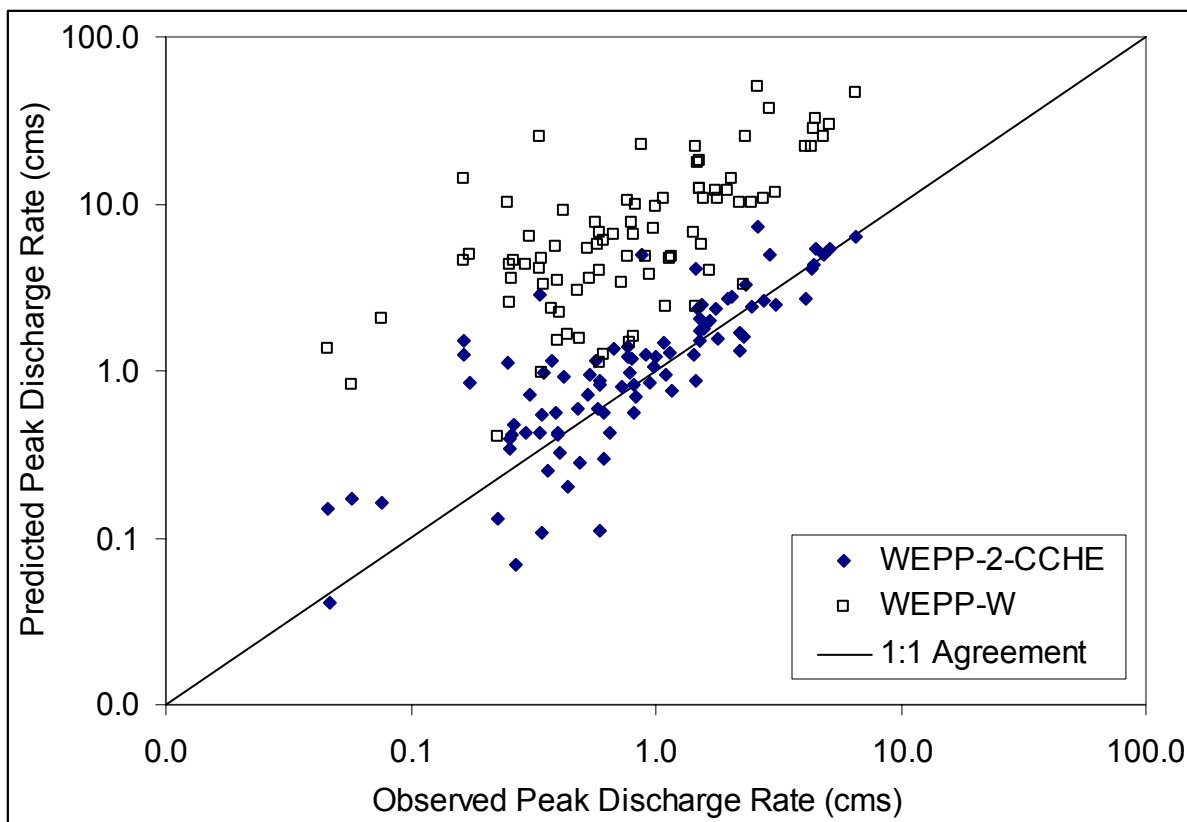
Figure 3-10. Observed vs. predicted daily peak runoff rate for 89 events at South Fork Caspar

Creek Experimental Watershed, CA (1995-1997).

Table 3-7. Observed and predicted daily peak runoff rate statistics for 89 daily runoff events at Caspar Creek Experimental Watershed, CA (January 1995 to December 1997).

	Peak Runoff Rate (m^3/s)		Relative Error (%)			Nash-Sutcliffe Coefficient
	Max	Min	Max	Ave	Min	
Observed	6.5	0.046	--	--	--	--
WEPP-2-CCHE	7.2	0.040	812	83	1	0.51
WEPP-W	50.1	0.000	8,361	973	43	-86

The above results suggest that the WEPP Hillslope model can successfully be linked with CCHE1D to simulate hydrodynamics in channel networks, and that the results can be significant improvement over the simplified hydrologic methods used in the current WEPP-W model. Even when using adjusted hydrographs, the WEPP-2-CCHE routing procedure increases model efficiency by a factor of two for daily runoff volume, and over two orders of magnitude for daily peak runoff rate. It is expected that if the WEPP Hillslope model were revised to allow access to sub-daily time step hydrodynamic data that can be computed by the model when modeling single-storm events, that the flow routing model efficiency would be further increased. This would create a very powerful, linked upland erosion and hydrodynamic model.

The interface developed for this study addressed two very important modeling issues: spatial discretization and time-step synchronization. Of the two, time step synchronization has a much more straight forward solution; simply making sure that the units of each variable are consistent. Because both WEPP and CCHE1D use the TOPAZ model to generate watershed structure, the spatial discretization problem was greatly simplified. The TOPAZ model creates a structure file for a watershed (with the outlet defined by the user), that uniquely relates each sub-watershed and channel segment in the watershed. The sub-watersheds are further sub-divided into source hillslopes, side-channel hillslopes, and channel segments. Taking advantage of this organizational feature, a relational database was constructed within the

interface program so that hillslope and channel-specific information could be passed easily from

WEPP to CCHE1D.

CONCLUSION

Physically-based modeling of upland erosion and open-channel flow and sediment transport requires, at this time, two separate models. The WEPP model was used to generate upland hydrographs. These hydrographs were then routed through a watershed-channel network with a CCHE1D, a hydrodynamic-sediment transport model. However, to couple these two models, an interface program was required. The interface program created for this project uses the TOPAZ data generated by the CCHE1D and WEPP interfaces as a relational key for managing the runoff and sediment load databases.

Linking an upland erosion model like WEPP with a hydrodynamic-sediment transport model like CCHE1D is certainly viable. Results of this study demonstrate that the accuracy of peak flow estimates is increased by over two orders of magnitude when flow volumes are routed with an appropriate hydrodynamic model. However, to produce a linked model that is useful, the WEPP model needs to be updated. Without access to the sub-daily computations, it is very difficult to calibrate the model with observed data. Future versions of WEPP should allow access to these data, either directly while the simulations are running, or indirectly through a series of output files that can be post-processed. WEPP evaluates erosion processes at small scales (e.g., hillslope and sub-watershed), and CCHE1D evaluates hydrodynamic-sediment transport processes at large (e.g., watershed network) scales. By linking these two types of models, we can take advantage of beneficial features of both models, such that large watersheds can be evaluated at a very fine resolution. The resultant product would be a comprehensive, integrated watershed-scale, erosion simulation, and hydrodynamic-sediment transport model.

The objective of this research was to develop procedures for coupling a physically-based upland erosion model (WEPP) with a fully dynamic, physically-based hydrodynamic-sediment

transport model (CCHE1D). Due to limitations of the current WEPP model, this objective was not fully realized. However, with modifications to the WEPP model, it is expected that this goal could be realized. This improvement is important for increasing the overall accuracy of surface runoff/erosion estimates associated with implementation of effective erosion control measures within ungaged watersheds.

CHAPTER FOUR

MODEL DEVELOPMENT AND CALIBRATION, PART II: SEDIMENT TRANSPORT

ABSTRACT

In the modeling system developed here, upland erosion was simulated with the Water Erosion Prediction Project (WEPP) Hillslope model; instream hydrodynamics and sediment transport were simulated with CCHE1D, a one-dimensional, channel network, hydrodynamic-sediment transport model; and both were linked via a spatiotemporal database management program. The linked model, WEPP-2-CCHE, was run with data from Caspar Creek Experimental Watershed, California. WEPP-2-CCHE predicted peak daily suspended sediment concentrations within the same range as those measured, but were an average of 30% lower than observed. Predicted total daily sediment loads were well correlated with observed loads (r^2=0.77), but were over-predicted by an average factor of two. Relative errors of predicted values (both peak concentration and total load) were comparable to those observed for sediment transport equations that used observed sediment loads instead of predicted sediment loads to compute estimated sediment loads and concentrations. The WEPP-2-CCHE model predicts both total daily sediment loads and peak daily suspended sediment concentrations that are at least an order of magnitude more accurate than the WEPP-W model. Although WEPP-H was developed for small agricultural watersheds, this research successfully demonstrated the models' applicability to forested watersheds in the rugged, Pacific Northwest Mountains. In addition, the integration of a small-scale erosion model with a large-scale hydrodynamic-sediment transport model provides a useful tool for watershed-scale non-point source sediment analyses; for evaluating individual and systems of erosion-control best management practices;

and for evaluating the cumulative watershed effects of spatially, temporally, and physically

disparate forest management practices.

INTRODUCTION

Most sediment total maximum daily load (TMDL) analyses make extensive use of computer models (U.S.E.P.A., 2002) because of the need to evaluate large areas with heterogeneous characteristics. The Water Erosion Prediction Project (WEPP) Model (Flanagan et al., 1995) is a physically-based, erosion simulation model commonly used to assess management-related surface erosion in agricultural (Zhang et al., 2003) and forest (Foltz and Elliot, 1999) settings. Its ability to evaluate spatiotemporally distributed climatic and physiographic variables make it a valuable tool for site-specific, sediment TMDL evaluations on hillslopes. However, the WEPP model lacks two features that are needed for simulations in larger watersheds (i.e., up to 130 km^2 (U.S.E.P.A., 1999)): network hydrodynamics and instream sediment transport.

The WEPP model has two distinct components: WEPP Hillslope (WEPP-H) and WEPP Watershed (WEPP-W). WEPP-H is the main component used to simulate erosion separately for each hillslope in a watershed. The results of individual hillslope simulations are passed to the WEPP-W simulator via text output files. The WEPP-W simulator uses the flow and sediment load information, combined with physiographic information (e.g., hillslope and channel lengths and widths) to compute daily flow volume, peak flow rate, and total sediment load at the watershed outlet for each event simulated.

WEPP-H was developed primarily for plots and fields, and WEPP-W was developed for small watersheds (area less than 2.6 km^2) (Flanagan et al., 1995). By using a GIS interface (Renschler, 2003), WEPP-W has been extended for use in watersheds with areas as large as 228 km^2 (Bdour, 2004). However, its reliance on the rational method for computing peak flow rates, make its use in larger watersheds questionable since the rational method is generally limited to watersheds smaller than 81 ha (Dunne and Leopold, 1978). WEPP-W does not simulate routing of flows through a channel network, but instead uses empirical relations to

provide a daily, event-by-event summary of total flow and peak flow rate. As such, WEPP-W provides only a coarse estimate of flow at one point in a watershed, the outlet, thereby ignoring the physical processes of open channel flow in the entire channel network.

A second major limitation of the WEPP-W model is that it uses a single sediment transport capacity equation, regardless of bed material composition, to compute the sediment transport rate at the watershed outlet. Both components of the WEPP model use a modified form of Yalin's bedload equation (Yalin, 1963) to compute sediment transport capacity in rills, interrill areas, and channels. Yalin's equation has been successfully applied to overland flow sediment transport in interrill areas by several authors (Alonso, Neibling, and Foster, 1981; Ferro, 1998; Finkner et al., 1989; Wicks and Bathurst, 1996), but has been demonstrated as inadequate for bedload transport in rivers (Bravo-Espinosa, Osterkamp, and Lopes, 2003). Therefore, to overcome the above limitations, the WEPP-W component should be replaced with a watershed network hydrodynamic, sediment-transport model.

The purpose of this research was to develop and implement a procedure to link the WEPP-H model with a watershed network, hydrodynamic and sediment-transport model. In the present study, the results from WEPP-H are passed to the CCHE1D (Center for Computational Hydroscience and Engineering, One-Dimensional) model (Wu and Vieira, 2002) to simulate routing of water and sediment. The CCHE1D modeling system was designed to simulate both unsteady flows and sedimentation processes in channel networks (Wu and Vieira, 2002). The model simulates bed aggradation and degradation, bed material composition (hydraulic sorting and armoring), bank erosion, and the resulting channel morphologic changes under unsteady flow conditions. CCHE1D was designed to be integrated with existing watershed process (rainfall-runoff and field erosion) models to produce more accurate and reliable estimations of sediment loads and morphological changes in channel networks (Wu and Vieira, 2002).

79

The CCHE1D hydrodynamic-sediment transport model has been coupled with Agricultural Non-Point Source Model (AGNPS) and Soil and Water Assessment Tool (SWAT) (Wang et al., 2002) to produce two separate, integrated watershed-scale erosion models. Both AGNPS (Young et al., 1989) and SWAT (Neitsch et al., 2001) are grid-based, empirical erosion models based on modifications to the Universal Soil Loss Equation (USLE) (McCuen, 1998) and are not physically-based upland erosion models. As such, coupling either of these erosion models with CCHE1D does not produce a physically-based, watershed-scale erosion and sediment transport model.

By coupling the WEPP-H model with CCHE1D, it was demonstrated in Chapter Three (of this dissertation) that a dynamic wave model produced significantly more accurate predictions of flow volume and peak flow rate for a 424 ha watershed over a three-year simulation period. In Chapter Three of this dissertation, the sediment transport capabilities of CCHE1D were temporarily disabled to evaluate the hydrodynamic capabilities of CCHE1D without the confounding issues of sediment transport. The research presented here details the sediment transport calibration results of simulations using a linked WEPP-H and CCHE1D model (WEPP-2-CCHE).

METHODS

STUDY AREA

The Caspar Creek Experimental Watershed (CCEW) is located on the Jackson Demonstration State Forest in northwestern coastal California, approximately 15 km southeast of Fort Bragg (Figure 3-1, in Chapter 3). The CCEW consists of the 424-ha South Fork (SFCC) and the 473-ha North Fork (NFCC) sub-watersheds (Henry, 1998). These two tributary basins are located in the headwaters of the 2,167-ha Caspar Creek watershed, which discharges into the Pacific Ocean near the community of Caspar.

The CCEW was chosen for this research primarily due to the availability of extensive datasets that had been continuously collected over 35 years for a paired watershed study. Physiographic, climatic, and hydrologic data (Table 3-1, in Chapter 3) were collected to study the effects of forest management on streamflow, sedimentation, fish, fish habitat, timber, and other vegetative growth (Henry, 1998). This watershed was also chosen because there was only one climatic regime (i.e., rain-dominated), one forest cover type, and spatially similar soil properties; all of which reduced the complexity of simulations. For this research, the SFCC was used for calibration of the models, and the NFCC was used for model evaluation and example scenarios. For a more detailed description of the study area, the reader is referred to the Methods section of Chapter Three.

MODELING COMPONENTS

The modeling system used for this research spatially integrates upland erosion estimates from the WEPP-H model for a watershed composed of multiple hillslope and channel elements by using the WEPP-H output as input to the CCHE1D hydrodynamic-sediment transport model. Watersheds are discretized into hillslope and channel elements using the TOPAZ (Garbrecht and Martz, 1995) GIS landscape analysis tool. Upland erosion simulations are conducted with

the WEPP-H model via the WEPP Windows interface program (Version 2004.610). The WEPP-H model, its usage, and input parameters (Table 3-2 in Chapter Three) are described in Chapter Three.

An interface program, specially written for this research creates a spatial database from the WEPP-H output and prepares properly formatted input files (e.g., time series hydrographs, sediment particle size distribution) for the CCHE1D model. Streamflow and sediment are transported through each segment of the watershed channel network with CCHE1D to produce outlet hydrographs and sediment graphs. The CCHE1D output is post-processed with Microsoft EXCEL.

For the sediment transport simulations, it was necessary to define 12 sediment size classes (Table 4-1). Classes 1 thru 5 are defined to have the same limits, representative diameters, and specific gravities as the five classes used by the WEPP-H model (Foster et al., 1995). Classes 6 thru 12 were defined using increasing powers of 2 as the lower and upper limits (Yang, 1996), up to 256 mm, such that all classes of observed bed material (Lisle, 1995) would be included. The representative diameter of classes 6 thru 12 are defined as the geometric mean of the upper and lower limits of the given class. Lacking measured density data for classes 6 thru 12, specific gravity for sediment in these classes was set at 2.65, the average value for sand particles (Brady, 1990).

Lisle (1995) measure the particle size distribution (PSD) at the outlet of the North Fork Caspar Creek sub-watershed. The observed bed material composition is largely gravel and cobble (Table 4-1), with a median particle diameter of 24 mm and less than 16% of the material being sands or finer (Lisle, 1995). It was assumed for the purposes of this research that PSD for the South Fork was identical to the North Fork, since there were no PSD data collected for the SFCC watershed. Since both watersheds have the same geology and soils, this assumption is deemed reasonable.

Table 4-1. Fraction of bed material, by size class (with upper and lower limits and representative diameter), for North Fork Caspar Creek (Lisle, 1995).

Sediment Size Class	Representative Diameter (mm)	Lower Limit of Class (mm)	Upper Limit of Class (mm)	Fraction of Bed Material in Class	Specific Gravity
1	0.002	0.001	0.004	0.010	2.60
2	0.010	0.004	0.016	0.010	2.65
3	0.030	0.016	0.062	0.020	1.80
4	0.200	0.062	0.250	0.040	2.65
5	0.500	0.250	2	0.075	1.60
6	2.83	2	4	0.077	2.65
7	5.66	4	8	0.125	2.65
8	11.3	8	16	0.163	2.65
9	22.6	16	32	0.200	2.65
10	45.3	32	64	0.175	2.65
11	90.5	64	128	0.095	2.65
12	181	128	256	0.010	2.65

Sediment transport options used in all CCHE1D simulations are summarized in Table 4-2. Where possible, the default model settings were used. The dynamic wave model was chosen over the diffusion wave model because the former can be applied to a much wider range of flow conditions. The computational time step was reduced from 15 to 5 minutes to ensure numerical stability throughout the simulation. The open boundary condition was used because time series stage measurements were unavailable (even though time series discharge data were available). The bank stability analysis option was disabled for two reasons: 1) bank stability information was unavailable, and 2) the research described here was designed to evaluate the transport of sediment from upland areas via surface erosion to and through a channel network. For the simulations described here, the erodible bed option was enabled, to allow resuspension of bed material that may be deposited on receding hydrographs.

Table 4-2. Sediment transport parameters and options used for Caspar Creek, CA hydrodynamic-sediment transport simulations.

Sediment Transport Option	Value	Default Value
Computational Time step (minutes)	5	15
Hydrograph Type	Time-series (1-hour time step)	None
Downstream Boundary Condition	Open	User Specified Stage Time Series
Baseflow Discharges	User Specified	User Specified
Flow Mode	Dynamic Wave	Diffusion Wave
Small Depth Algorithm	Enabled	Enabled
Sediment Transport Equation	(Wu, Wang, and Jia, 2000)	(Wu, Wang, and Jia, 2000)
Bank Stability Analysis	Disabled	Enabled
Computation of Bedload Adaptation Length	Function of Alternate Bar Length	Function of Alternate Bar Length
Computation of Suspended Load Adaptation Length	0.5	User Specified (but default value is 0.5)
Computation of Washload Adaptation Length	Infinite	Infinite
Computation of Washload Size Classes	Function of Rouse Parameter	Function of Rouse Parameter
Computation of Mixing Layer Thickness	Related to Grain Size	Related to Grain Size
Minimum Mixing Layer Thickness (m)	0.05	0.05
Computation of Bed Porosity	(Komura and Simons, 1967)	(Komura and Simons, 1967)
Initial Bed Porosity	0.30	None (User Specified)
Erodible Bed	Enabled	None (User Specified)
Maximum Erodible Depth of Bed (m)	0.00	None (User Specified)

The observed suspended sediment concentration values in Caspar Creek are from regression equations that relate discharge to point samples of suspended sediment (Lewis et al., 2001). Pumped sediment samples using an ISCO automatic sampler were adjusted by depth-integrated hand samples to produce a composite suspended sediment concentration for the entire channel cross-section (Lewis et al., 2001). In Caspar Creek, the suspended fraction of the total load only includes particles less than 2 mm (Lisle, 1995), in classes 1 thru 5 (Table 4-1). All of the bedload (classes 6 thru 12) and approximately 40 percent of the suspended load are trapped in weir ponds upstream of the sediment sampling stations (Lewis et al., 2001). To compare observed suspended sediment concentration values with predicted values, only sediment classes 1 thru 5 were included in the computations and the predicted sediment concentration was reduced by a constant factor of 40 percent.

STATISTICAL ANALYSES

In this research, two routing procedures are compared to observed values for two variables (i.e., daily peak suspended sediment concentration (in mg/L) and daily total sediment load (in kg)). The two routing procedures are: 1) WEPP Watershed (WEPP-W) model used as is, and 2) WEPP Hillslope results altered with methods described as proof-of-concept, then routed with CCHE1D (hereafter referred to as WEPP-2-CCHE).

The Nash-Sutcliffe coefficient (NS) of model efficiency was used as a statistical criterion for evaluating hydrologic goodness of fit between measured and predicted values for each method (Nash and Sutcliffe, 1970). Since the Nash-Sutcliffe ratio is a composite of all observed-predicted pairs, the error associated with individual pairs was given as the relative error (Burden and Faires, 2001). This equation is used to compare pairs of observed and predicted values for total daily sediment load (kg) and peak daily suspended sediment concentration (mg/L).

RESULTS AND DISCUSSION

All sediment transport simulations used the same TOPAZ-generated watershed structure created in Chapter Three for the South Fork Caspar Creek (SFCC) watershed. This generated structure contained 18 unique hillslopes and 7 channel segments. The WEPP input parameters were identical to those used for hydrodynamic simulations of Chapter Three (Table 3-2). The erosion simulation was conducted using the WEPP Windows interface, for a 3-year simulation period from January 1, 1995 to December 31, 1997. This simulation produced 96 days with water runoff and 89 days with sediment delivery. Due to technical difficulties at the SFCC gauging station (e.g., equipment malfunction, operator error), only 74 of the 89 days (in the 3-year period) that the WEPP-H model predicted measurable sediment load could be compared to observed sediment data.

The WEPP-W model only yields total daily sediment load, with no indication of either the peak load or duration of sediment transport. As such, only the WEPP-2-CCHE results are compared to observed peak sediment loads. The range of observed and predicted values of peak suspended sediment concentration spans three orders of magnitude (Table 4-3). The WEPP-2-CCHE model predicted peak suspended sediment concentrations that were on average in agreement with observed values (Figure 4-1), but were generally under-predicted (Figure 4-2). The predicted values are scattered ($r^2 = 0.37$), have a low model efficiency (NS = -0.12), and have an average relative error of 351 percent (Table 4-3). However, the predicted values were not significantly different from observed values when compared using either a paired t-test ($p > 0.92$, $\alpha = 0.05$), or a single-factor ANOVA ($p > 0.94$, $\alpha = 0.05$).

Table 4-3. Relative error and model efficiency of predicted vs. observed peak suspended sediment concentration values for South Fork Caspar Creek, CA simulations (1995-1997).

	Peak Sediment Concentration (mg/L)		Relative Error (%)			Nash-Sutcliffe Coefficient
	Max	Min	Max	Ave	Min	
Observed	3,117	3	--	--	--	--
WEPP-2-CCHE	1,565	4	7,040	351	1	-0.12
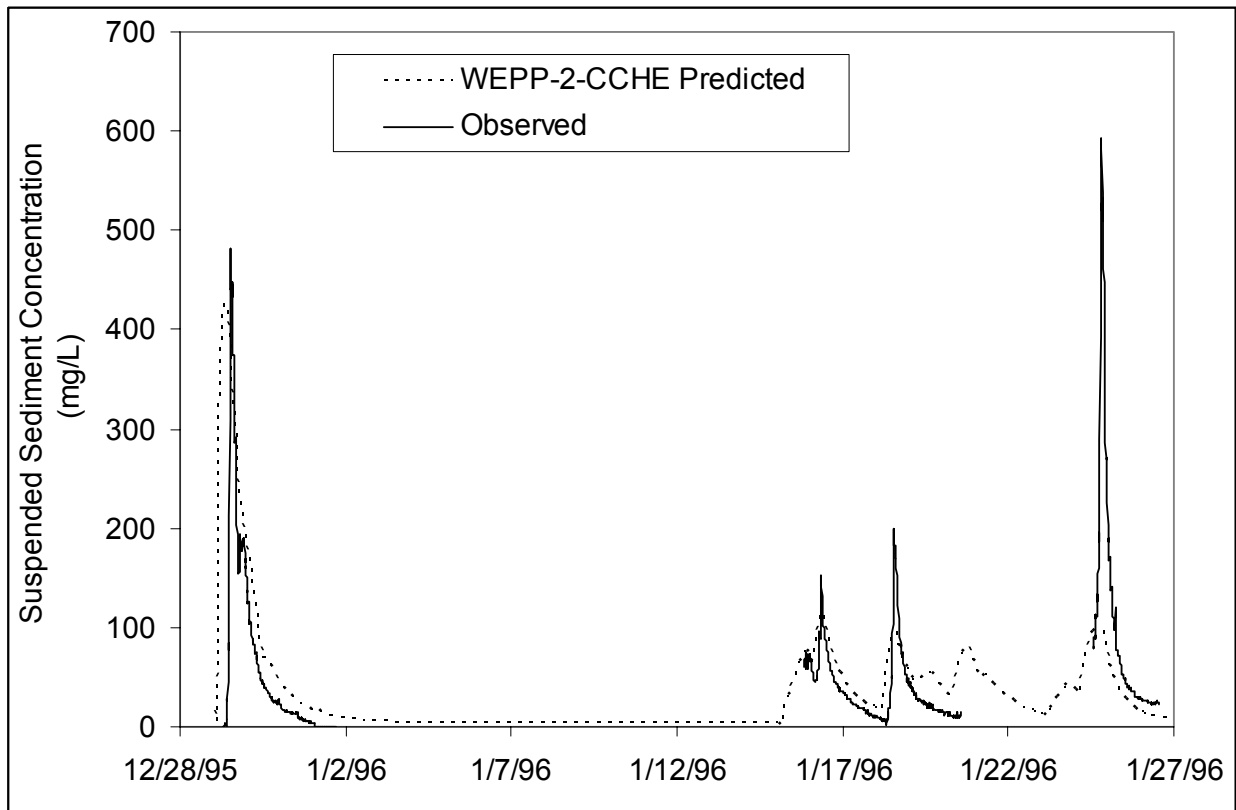
Figure 4-1. Observed and predicted suspended sediment concentration at South Fork Caspar Creek, CA, December 1995 thru January 1996.
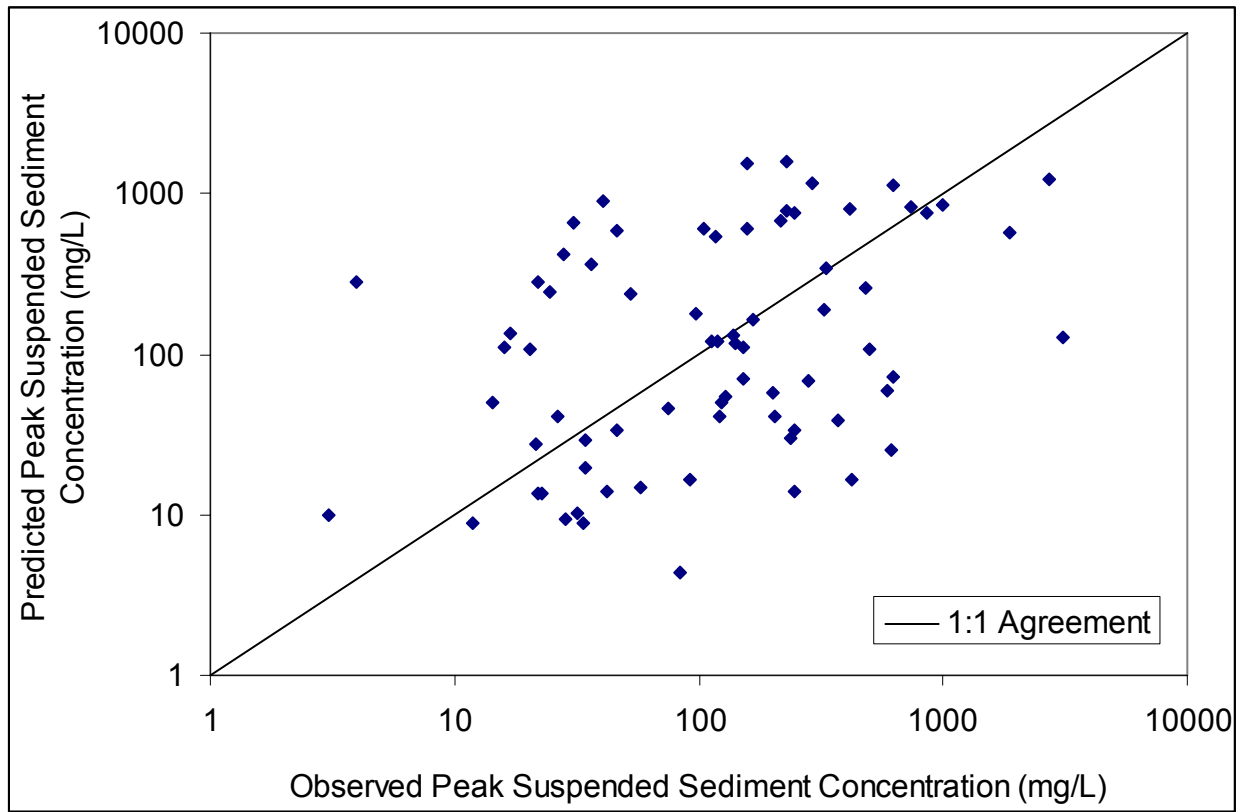
Figure 4-2. Predicted vs. observed peak daily suspended sediment concentration for South Fork Caspar Creek simulation (1995-1997).

Although the WEPP-2-CCHE model efficiency is relatively low and the average relative error is high, these results are typical of sediment transport models (Jetten, Govers, and Hessel, 2003; Yang, 1996), even when those models use observed instead of predicted sediment loads for upstream boundary conditions. Most of the WEPP-2-CCHE predicted peak suspended sediment concentrations are within an order of magnitude of the observed values. Of the 74 values compared, 30 (41%) were within a factor of two, 49 (674%) were within a factor of 4, and only 16 (30%) were greater than a factor of 10 (i.e., 'an order of magnitude'). The CCHE1D model developers (Wu and Vieira, 2002) reported similar results for the accuracy of the Wu et al. (2000) sediment transport capacity equation (also used for the current simulations) when they tested their model using sediment transport data collected by Toffaleti (1968) on the Rio

Grande, Middle Loup, Niobrara, and Mississippi Rivers. Toffaleti's data covered a wider range of flow rates than were simulated here (up to 21,600 m^3/s), but had similar sediment sizes (0.062 to 1.0 mm) (Toffaleti, 1968) as were simulated by the WEPP-H model (Table 4-1).

The range of observed and predicted values of total daily sediment load spans five orders of magnitude (Table 4-4), which is not uncommon for natural streams (Leopold, Wolman, and Miller, 1964). The WEPP-W model predicts total daily sediment loads that are significantly different that observed loads ($p<0.0001$ at $\alpha=0.05$). Loads are either dramatically over-predicted or under-predicted (note two disparate clusters of WEPP-W predicted data [closed diamonds] in Figure 4-3). WEPP-W predicts total daily sediment loads that are between one and two orders of magnitude different from observed loads, as is indicated by a Nash-Sutcliffe coefficient of -42 (Table 4-4).

Table 4-4. Relative error and model efficiency of predicted vs. observed total daily sediment load values for South Fork Caspar Creek, CA simulations (1995-1997).

	Daily Total Sediment Load (kg)				Average Relative Error (%)	Nash-Sutcliffe Coefficient
	Max	Min	Ave	Total		
Observed	168,916	2	16,069	1,173,053	--	--
WEPP-2-CCHE	241,421	50	30,767	2,245,996	2,523	0.05
WEPP-W	1,336,796	0	87,562	6,479,609	12,623	-42
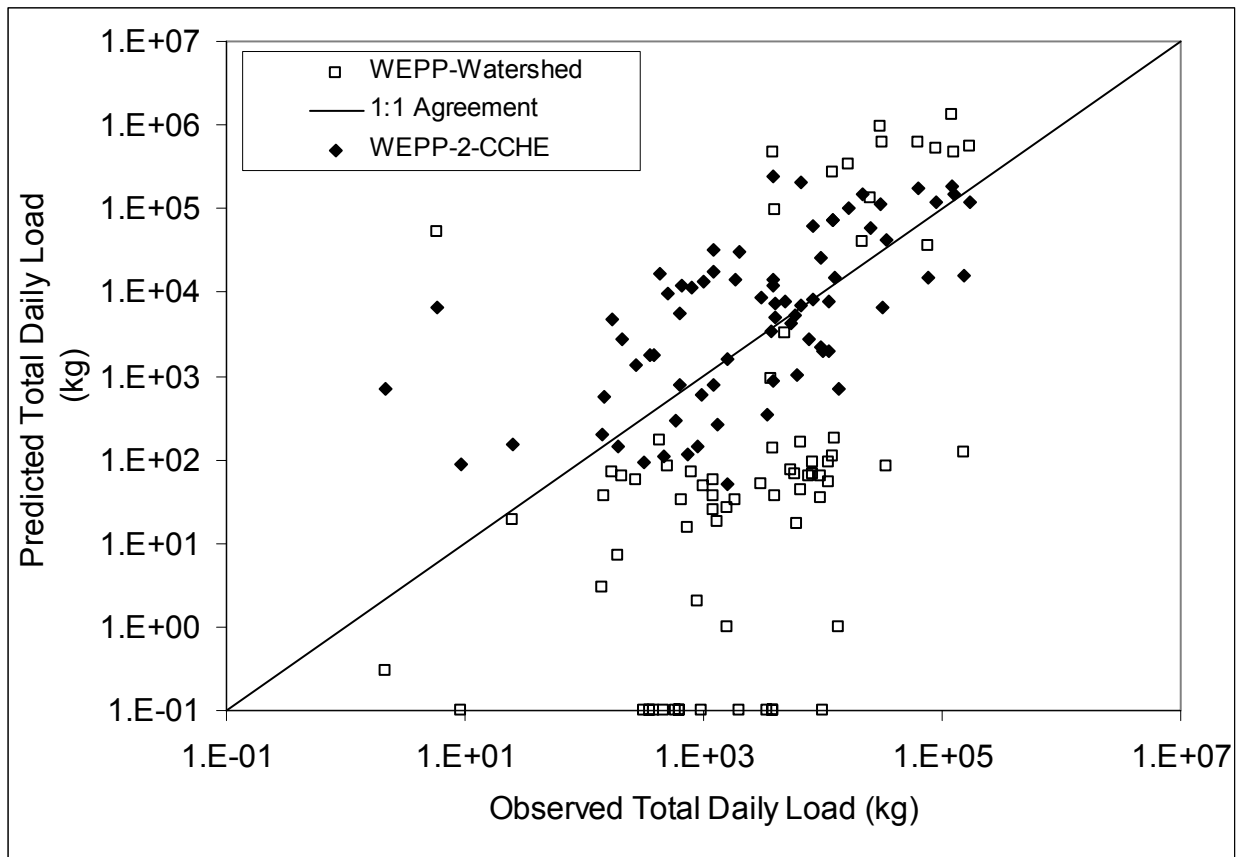
Figure 4-3. Predicted total daily sediment load (with WEPP-2-CCHE) vs. observed total daily

sediment load for South Fork Caspar Creek simulation (1995-1997).

The WEPP-2-CCHE model predicts total daily sediment loads that are not significantly different from observed values ($p < 0.08$, $\alpha = 0.05$), but with significant scatter ($r^2 = 0.34$). The predicted values have an average relative error of 2,523% and a Nash-Sutcliffe coefficient of 0.05; indicating that the model dramatically over-predicts and under-predicts total daily loads, but is not significantly different from observed on the average. Of the 74 values compared, 25 (34%) were within a factor of two, 41 (56%) were within a factor of four, and only 18 (25%) were greater than a factor of 10. These predictions are a significant improvement over WEPP-Watershed predictions.

Sediment discharge, both peak rate and total daily load, are not predicted nearly as well as water discharge reported in Chapter Three for the same period and simulation conditions. This result is consistent with the results of Jetten et al. (2003) for WEPP model simulations using data from a 40 ha catchment in the Netherlands. Their results, however, were not exclusive to the WEPP model since they evaluated seven erosion simulation models with the same data set (Jetten, Govers, and Hessel, 2003). Of the seven models evaluated, all models generally predicted total water discharge better than peak water discharge, and water discharge significantly better than sediment discharge (Jetten, Govers, and Hessel, 2003).

There are several reasons for the low predictive capability of erosion models in general, but for WEPP-H in particular. There is measurement uncertainty in the values of input parameters (e.g., saturated hydraulic conductivity is very difficult to measure on steep, heavily vegetated hillslopes (Brooks, Boll, and McDaniel, 2004)). In addition, with any measured variable, there may be significant operator or equipment induced errors that are difficult to predict. For the simulations in the present study, soil properties, vegetation characteristics, and climatic conditions were assumed to be uniform over the entire assessment area; all of which were based on discrete samples at relatively few locations (e.g., only one weather station was used for climatic input data). Any one of the above sources of uncertainty may not produce estimates that are over an order of magnitude different than observed values. However, in combination, any model can propagate the errors due to uncertainty of input parameters to produce results that do not compare well to observed values (Taylor, 1982).

In the present study, the errors in predicted values are attributed to two primary causes: inaccurate predictions of water and sediment discharge by the WEPP-H model, and incorrect assumptions in the interface program regarding the distribution of sediment load. Each of these sources or error is discussed with reference to how they might explain the differences between

observed and predicted sediment loads. Other sources of uncertainty (e.g., input variables, runt-time options) are discussed in detail in Chapter Five of this dissertation.

In Chapter Three, the WEPP-H model was found to produce peak runoff rates that were approximately one order of magnitude too high. Even after the peaks were corrected, there was still an average relative error of over 87%. Since the method of computing sediment discharge in WEPP-H relies on estimates of peak runoff rates (Foster et al., 1995), it is reasonable to assume that WEPP-H also predicts sediment discharge inaccurately. Although the inaccuracies in the magnitude of sediment discharge present a significant error, the inaccurate prediction of when sediment discharge occurs introduces another source of error. Jetten et al. (2003) found that the WEPP model predicted runoff and sediment discharge on the wrong days. Similar problems were discovered for several events in the current simulations (Figure 4-4). Sediment discharge is occasionally predicted when none occurred (e.g., 12/6/1996 on Figure 4-4). Sediment discharge is observed low on one day and high on the next day (or vice-versa), but is predicted in the opposite order (e.g., 12/9-10/1996 on Figure 4-4).

The WEPP-H model may also be over-predicting sediment loads due to an inaccurate representation of hillslope processes in South Fork Caspar Creek. The SFCC is known to have significant lateral subsurface flow and minimal saturated overland flow (Keppeler and Brown, 1998). To calibrate the modeled flow to observed runoff peak rates and volumes (in Chapter Three), the modeling domain CSA was set to 25 ha, because using CSA levels less than 25 ha produced peak runoff rates and flow volumes that were significantly less than observed. This CSA produced a channel network that matched the mapped network, but produced large hillslope areas drained by long rills. Under these conditions, the model produces greater surface runoff volumes because rill lengths are longer and the source area adjacent to rills is greater; thereby forcing stormflow to be generated by rill-flow instead of lateral subsurface flow. As such, it can be inferred that the lateral subsurface flow algorithm in WEPP is indeed not

working correctly, and that analytical scale is an important factor for accurately modeling hillslope-scale runoff and erosion processes.

The second source of errors in predicted sediment loads is likely due to procedures and assumptions used in the interface program that links WEPP-H to CCHE1D. To produce time series sediment discharges, the interface program used an algorithm that disaggregated the total daily sediment load produced by WEPP-H into hourly load rates. In the formulation of the algorithm, it was assumed that the sediment load was a direct function of the flow rate in a given interval. The reason for this was that the WEPP-H model yields sediment concentration values relative to the volumetric flow rate. Because of this limitation, all hysteresis effects are ignored, thereby producing continuous sediment discharge throughout the runoff event.
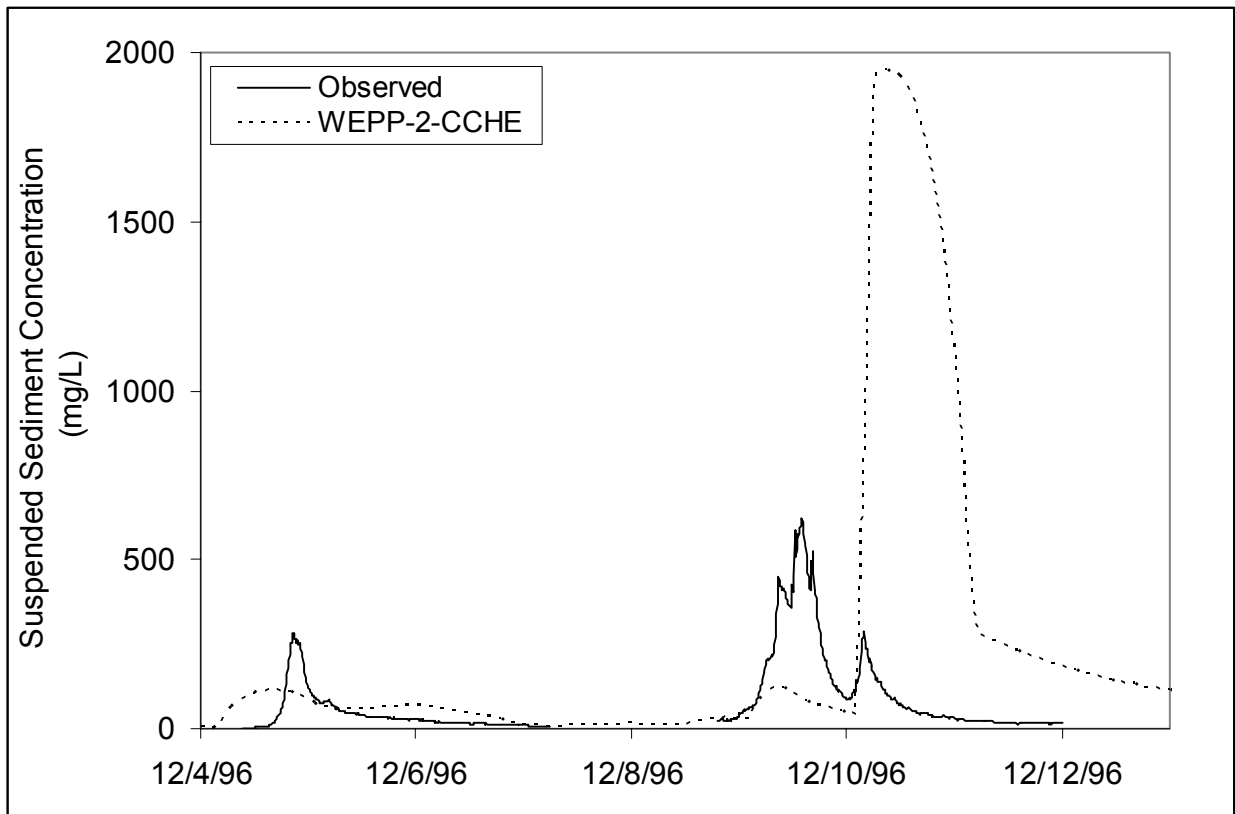
Figure 4-4. Predicted and observed hourly suspended sediment concentration for South Fork Caspar Creek simulation (04 December 1996 thru 05 January 1997).

CONCLUSION

The upland erosion and hydrodynamic-sediment transport modeling system used for this research spatially integrates upland erosion estimates from the WEPP-H model for a watershed composed of multiple hillslope and channel elements by using the WEPP-H output as input to the CCHE1D hydrodynamic-sediment transport model. The interface program created for this research provided an efficient means for managing the voluminous spatial and temporal data produced by WEPP-H. Although primarily a database management program, the interface program also transforms WEPP-H output into the format (spatial and temporal) required by CCHE1D. The modeling system (WEPP-2-CCHE) takes advantage of WEPP's abilities to simulate rainfall, runoff, and surface erosion at small scales (i.e., hillslopes), and CCHE1D's abilities to route water and sediment through a watershed-scale channel network. The interface program, TOPAZ, and CCHE1D are used in combination to integrate spatiotemporal rainfall, runoff, and sediment load data for entire watersheds.

WEPP-2-CCHE predicts peak daily suspended sediment concentrations within the same range as those measured, but are an average of 50% lower than observed, with significant scatter. Predicted total daily sediment loads are not significantly different from observed loads, but are over-predicted by an average of 42 percent. Predicted values (both peak concentration and total load) had relative errors comparable to those observed for sediment transport equations that used observed sediment loads instead of predicted sediment loads to compute estimated sediment loads and concentrations.

As was hypothesized when developing this research project, the WEPP-2-CCHE model predicts both total daily sediment loads and peak daily suspended sediment concentrations that are at least an order of magnitude more accurate than the WEPP-W model. This suggests that the empirical relations used to evaluate streamflow and sediment transport in the WEPP-W

94

model should be replaced with precise, theoretically sound hydrodynamic and sediment transport equations. Limitations that remains with WEPP-H are: 1) that the model only generates daily summary information even though it is possible to generate sub-daily hillslope runoff and sediment delivery information; and 2) the lateral subsurface flow algorithm is not working correctly. Access to sub-daily time series runoff and sediment load data would certainly improve the ability to compare predicted to observed values of discharge and sediment load. Correcting the lateral subsurface flow algorithm would yield more accurate water balance computations (which would yield more accurate surface erosion rates) for areas that have a combination of surface and subsurface stormflow generation mechanisms.

The model presented here provides a significant advancement in the development of physically-based, spatially distributed erosion simulation models. The integration of a small-scale erosion model with a large-scale hydrodynamic sediment transport model can be used for numerous watershed-scale non-point source sediment erosion analyses. By retaining the small-scale upland erosion model, individual, site-specific, erosion prevention best management practices can be evaluated. By using a large-scale hydrodynamic-sediment transport model, systems of best management practices that are spatially, temporally, and physically disparate can be evaluated. Although not explored in this research, this modeling system may be suitable for evaluating the cumulative watershed effects (e.g., aggradation or degradation of any reach in the channel network) due to forest management practices.

CHAPTER FIVE

SENSITIVITY ANALYSIS OF INPUT VARIABLES AND RUN-TIME OPTIONS

ABSTRACT

Sensitivity to changes in input variables and run-time options specific to CCHE1D and WEPP-H were explored in this chapter. For the CCHE1D model, channel geometry, Manning's roughness coefficient, bed material porosity, St. Venant equation solution, and sediment transport capacity equations were altered from values/options used in calibrating WEPP-2-CCHE. For the WEPP-H model, values of saturated hydraulic conductivity, soil depth, and ground surface cover were varied within the range of observed values in the Caspar Creek Experimental Watershed.

Peak discharge is relatively insensitive to changes in CCHE1D-specific variables since discharge is determined external to CCHE1D using WEPP-H, and would not be expected to change appreciably for a small, steep watershed. Sediment concentration is linearly sensitive to changes in CCHE1D-specific variables since sediment transport is sensitive to changes in flow depth and velocity (which may vary considerably for the same discharge rate). Both peak discharge rate and sediment concentration are sensitive to changes in WEPP H-specific variables; with sediment concentration being more sensitive than peak discharge rate. Changes in saturated hydraulic conductivity, soil depth, and soil cover produce exponential changes in sediment concentration. Peak discharge rates are changed exponentially only when rainfall intensity is greater than the saturated hydraulic conductivity; and when soil cover is below 25% (which only occurs on roads or severely burned forest lands).

The analyses completed in this chapter provided useful information for selecting run-time options to be used when modeling watershed hydrodynamics with CCHE1D. In addition, these analyses provide useful information for determining which variables are most important to determine more accurately with measured data. In general, peak discharge rates are much less sensitive to changes in variables and run-time options than sediment concentration; and both peak discharge rate and sediment concentration are more sensitive to changes in WEPP H-specific variables than CCHE1D-specific variables. As such, accurate determination of soil properties (i.e., KSAT, depth, cover) is more important than accurate determination of channel properties (i.e., depth, width, roughness, porosity) in achieving accurately modeled results.

INTRODUCTION

In the previous two chapters, the calibration of the coupled upland-erosion and instream hydrodynamic-sediment transport model, WEPP-2-CCHE, was completed using a controlled set of values for input variables and a single set of run-time options. Upland erosion simulations using the WEPP Hillslope model (WEPP-H) were conducted with single values for saturated hydraulic conductivity, soil depth, and ground surface cover (Table 3-2). In addition, hydrodynamic-sediment transport simulations using CCHE1D were conducted with single values for Manning's n and bed material porosity, using mostly default run-time settings (Table 4-2). Since each of these parameters has a range that occurs within and between watersheds, using a single value to represent each variable introduces additional errors that may significantly affect the model results. As such, the purpose of this chapter is to discuss the effects that variations in each variable produce on modeled results, and to present sensitivity to changes in variables and run-time options to the modeled results. The modeled results assessed in this analysis are the predicted peak discharge rate and peak total sediment concentration. The objectives of these analyses are to provide useful guidelines on selecting run-time options of the models, to determine which input variables are most sensitive to changes, and to recommend which input variables should be more accurately determined prior to modeling to assure accurate results.

METHODS

In these analyses, there are two categories of input variables and run-time options (i.e., those that are specified by the user) explored; those that are specific to 1) CCHE1D, and 2) WEPP-H. For the CCHE1D model, three variables (i.e., channel geometry, Manning's roughness coefficient, bed material porosity) and two run-time options are explored (i.e., St. Venant equation solution, and sediment transport capacity equation). For the WEPP-H model, three input variables (i.e., saturated hydraulic conductivity, soil depth, ground surface cover) are explored because these are the variables that have the greatest influence on soil water volume and surface erosion potential (Foster et al., 1995). For the WEPP-H model, there are no run-time options that affect the results of simulations, since the user can only alter the input data or choose the data reports generated by the model.

To perform the sensitivity analyses for CCHE1D-specific options/variables, a set of 15 runoff events were selected from the original analyses discussed in the previous chapters. These 15 events were from two distinct periods: 1) December 29, 1995 thru January 29, 1996, and 2) November 26, 1997 thru December 17, 1997. Although the total number of runoff events selected for analysis was arbitrary, the events themselves were selected for three reasons. First, the range of peak runoff rates of the selected events spans the range observed for the entire three-year period simulated (i.e., 1995-1997) in South Fork Caspar Creek. Second, two common runoff scenarios existed: 1) single day, single peak events, and 2) multi-day, multi-peak events. Finally, water discharge (Figures 5-1 and 5-2) and total sediment discharge (Figures 5-3 and 5-4) were predicted reasonably well compared to observed values for these events.
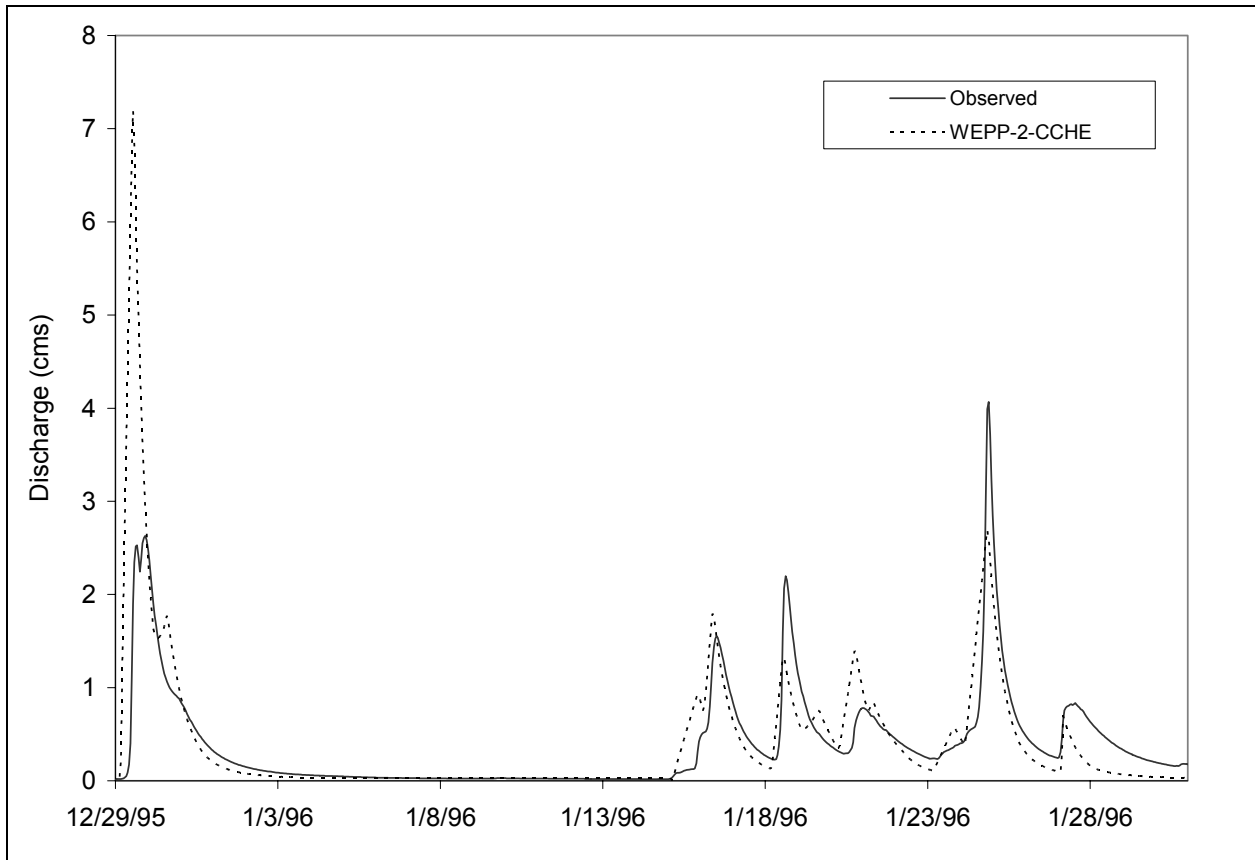
Figure 5-1. Observed and predicted discharge for South Fork Caspar Creek, CA, for the period

of December 29, 1995 thru January 31, 1996.
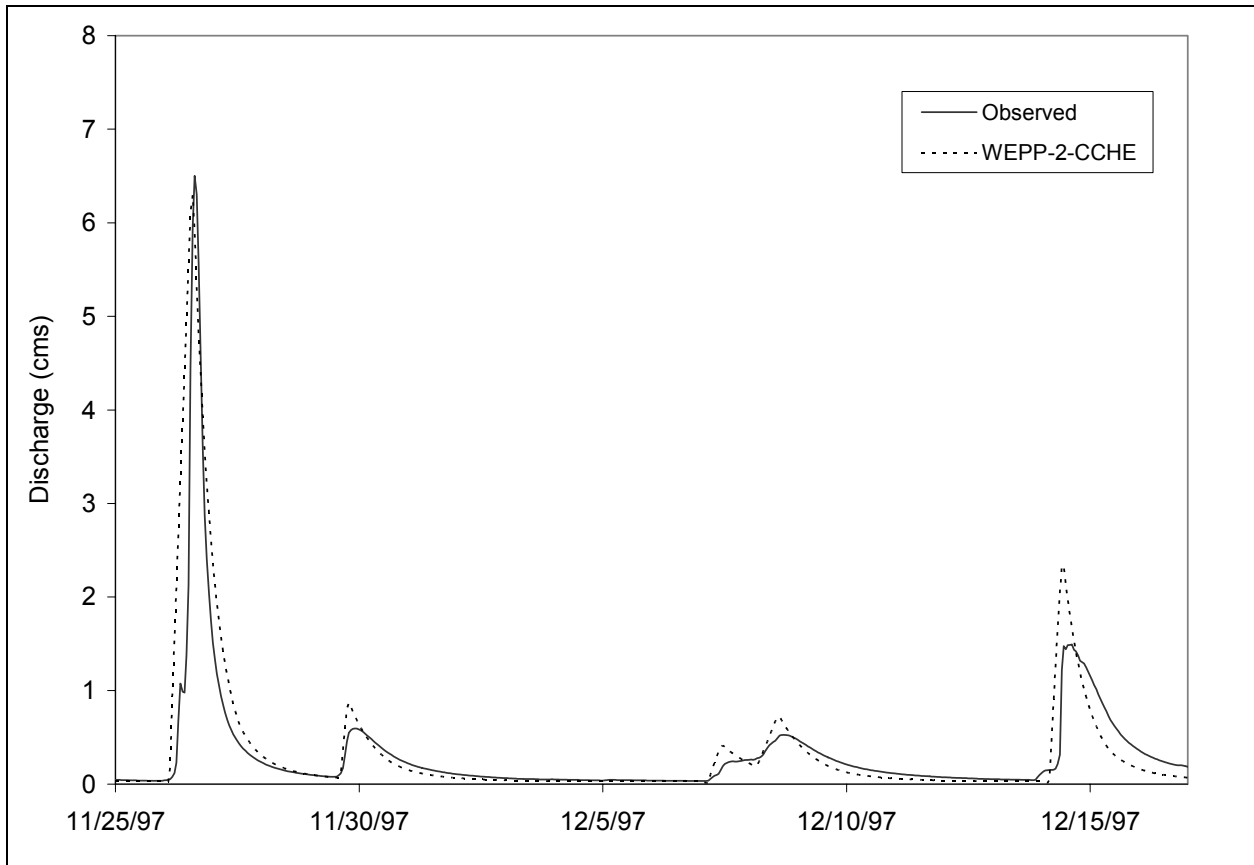
Figure 5-2. Observed and predicted discharge for South Fork Caspar Creek, CA, for the period

of November 26, 1997 thru December 17, 1997.
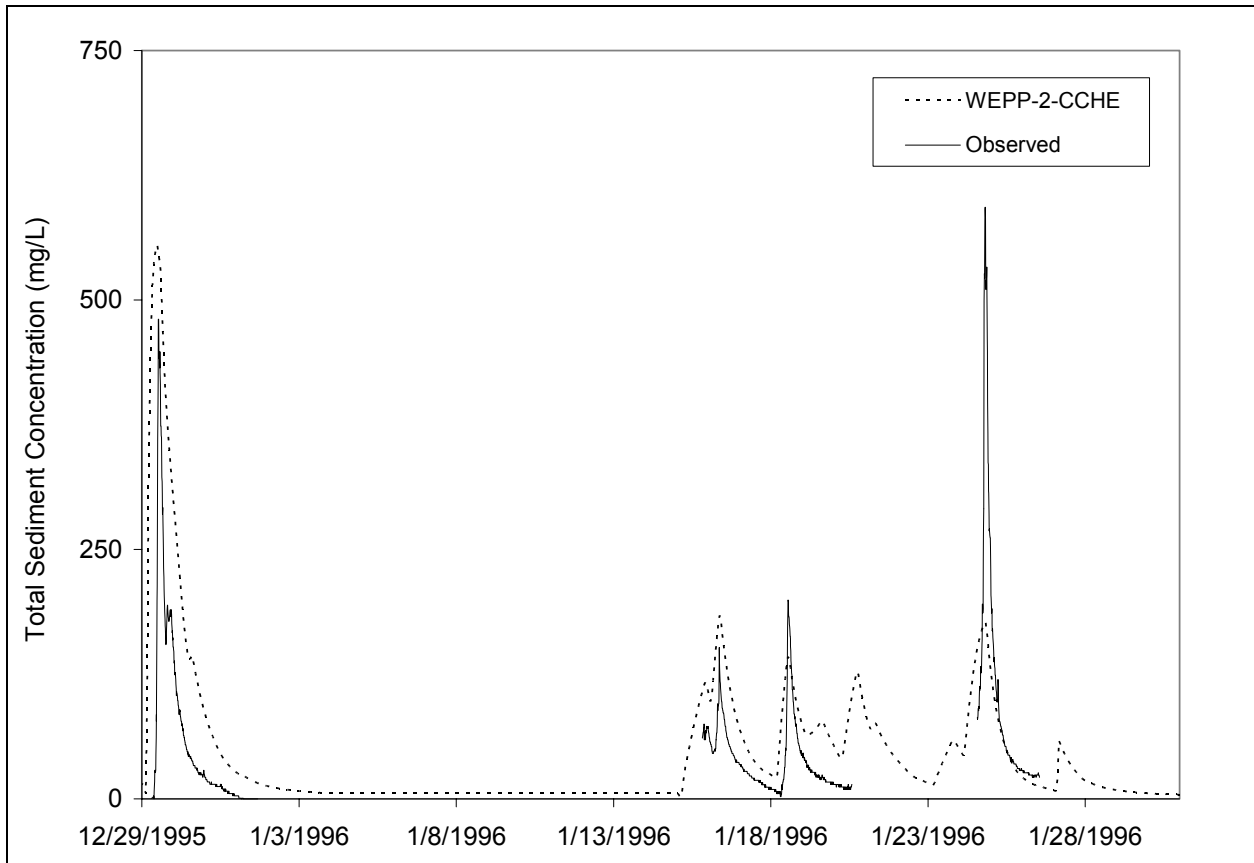
Figure 5-3. Observed and predicted total sediment concentration for South Fork Caspar Creek,

CA, for the period of December 29, 1995 thru January 29, 1996.
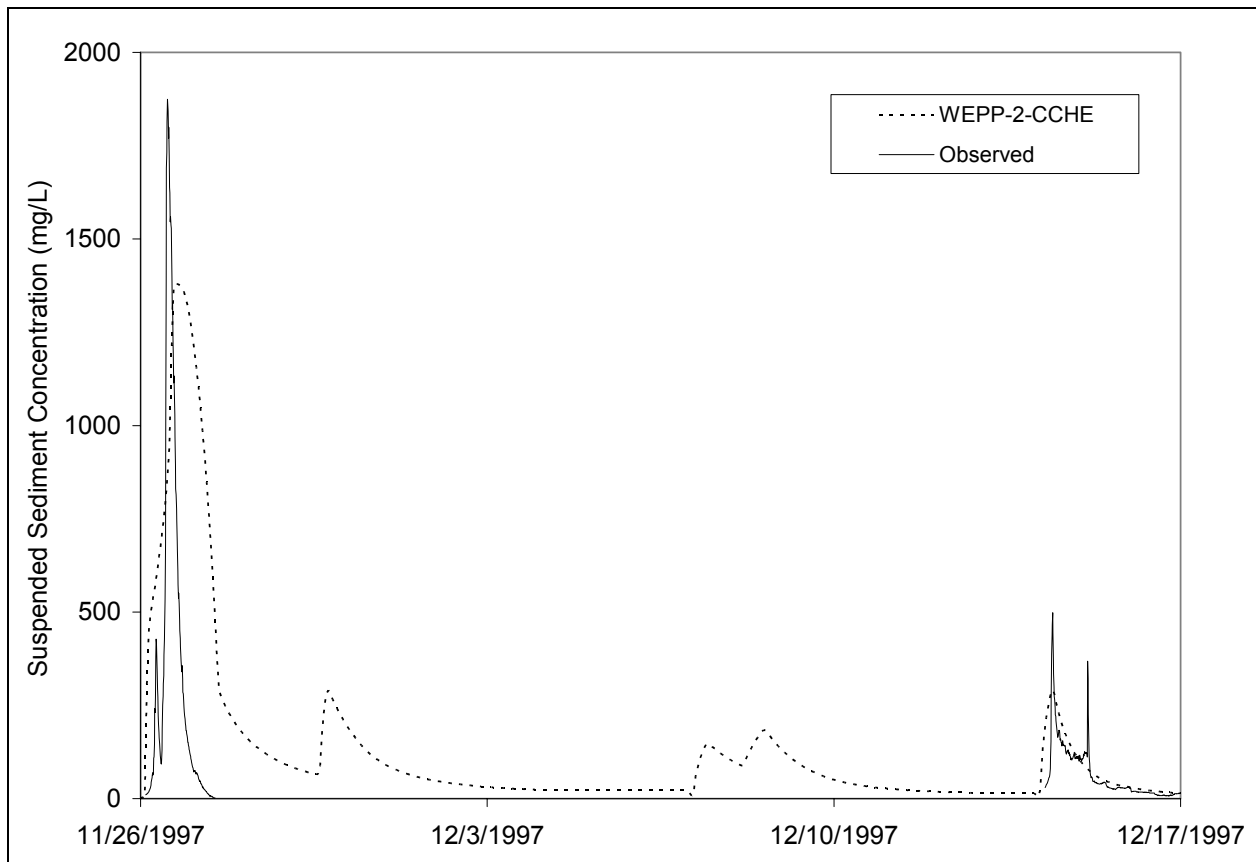
Figure 5-4 Observed and predicted total sediment concentration for South Fork Caspar Creek, CA, for the period of November 26, 1997 thru December 17, 1997.

To perform sensitivity analyses for WEPP-H-specific variables, all 89 runoff events in the hydrodynamic calibration period (January 1, 1995 thru December 31, 1997) were used (see Chapter Three for details). It was deemed necessary to use a greater number of events to assess WEPP-H sensitivities since it is expected that altering input variables will have greater variability and thus greater sensitivity to smaller changes.

For each sensitivity analysis, one variable or run-time option was selected and changed from the original (baseline) modeling scenario. The models were then re-run to produce a modified set of results. The modified results were compared to baseline results to determine

the percentage difference in modeled results that occurred as a direct result of changing the modeling scenario. To isolate the effects of each change, combinations of changes were not explored. By doing so, any synergistic or attenuating effects cannot be assessed. For all analyses in this chapter, peak discharge rate and total sediment concentration results using altered options and variables were compared to results from calibration model runs from Chapters Three and Four or to observed values.

CCHE1D-SPECIFIC ANALYSES

There are three user-supplied input variables that can alter the results of hydrodynamic-sediment transport simulations: channel cross-section geometry, channel roughness (in the form of Manning's N values), and bed material porosity. In addition, there are two run-time options selected by the user that also can potentially alter simulated results: the St. Venant equation solution used (i.e., dynamic wave vs. diffusive wave), and the sediment transport capacity equation used. The importance of each variable and run-time option and the ranges of values evaluated (Table 5-1) and discussed below.

Table 5-1. Ranges of values and options evaluated for selected parameters of the CCHE1D model.

Parameter	Range of Values or Options Evaluated
Channel Width	25 and 50 percent below baseline; 50 and 100 percent above baseline
Channel Depth	25 and 50 percent below baseline; 50 and 100 percent above baseline
Manning's n	100 percent above and 50 percent below baseline
Bed Material Porosity	Komura and Simons (1967) equation; Han (1981) equation; Constant values of 0.40, 0.30, 0.20, and 0.10
St. Venant Equation Solution	Dynamic wave; Diffusion Wave
Sediment Transport Capacity Equation	Engelund and Hansen (1967); Ackers and White (1973); SEDTRA (1995); Wu et al. (2000)

Channel Geometry

Stream channel geometry is a key variable in both hydrodynamics and sediment transport. The one-dimensional form of the St. Venant equations used in CCHE1D implicitly solves for cross-sectional flow area, a function of flow depth and channel width for each time step and computational node (Wu, Vieira, and Wang, 2004). It is unlikely that altering the channel geometry will significantly affect the discharge rate because discharge is a function of up and downstream boundary conditions and is generally independent of channel geometry (i.e., water continuity).

However, changes in channel geometry will alter the hydraulic radius for a given discharge rate (Figure 5-5). Altering hydraulic radius which will affect flow velocity (Jain, 2001) since

CCHE1D uses the hydraulic radius in the computation of friction slope (Equation 5-1) and in the momentum equation (Equation 5-2). As such, it is expected that altering channel geometry will only affect the flow velocity, thereby altering only the time of travel of the floodwave and not the discharge rate itself. In addition, it is expected that altering channel width and depth will significantly affect the simulated sediment transport rate, since all of the sediment transport capacity equations used by CCHE1D have either a bed shear stress term ($\tau = \gamma RS$) or a shear velocity term ($U_* = [gRS]^{0.5}$) (Wu and Vieira, 2002; Yang, 1996), where R is the hydraulic radius. Visual inspection of these two equations suggests that altering channel geometry will produce changes in sediment transport rate that are at least linear, but are likely nonlinear.
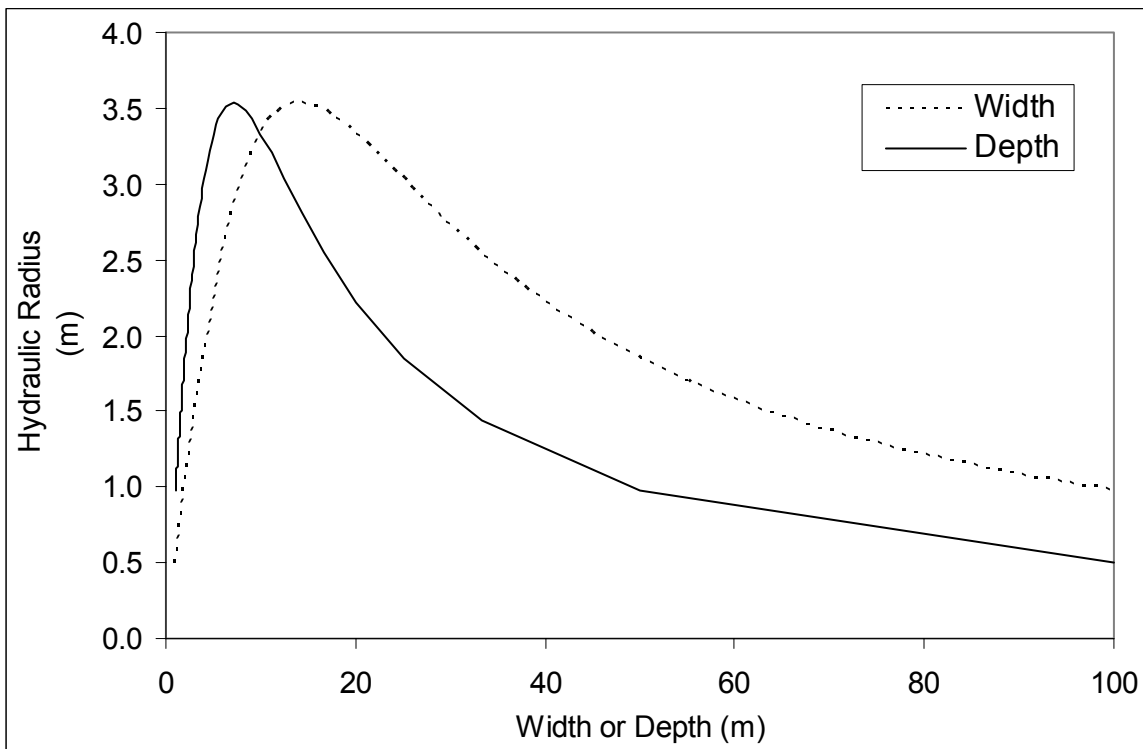
Figure 5-5. Changes in hydraulic radius of a hypothetical, rectangular channel (cross-sectional area = 100 m^2) when channel width and depth are changed but area is held constant.

Equation 5-1. $\qquad S_f = \dfrac{Q^2 n^2}{A^2 R^{4/3}}$ $\qquad\qquad\qquad\qquad$ [L L^{-1}]

Equation 5-2. $\qquad \dfrac{\partial}{\partial t}\left(\dfrac{Q}{A}\right) + \dfrac{\partial}{\partial x}\left(\dfrac{\beta Q^2}{2A^2}\right) + g\dfrac{\partial h}{\partial x} + g\left(S_f - S_o\right) = 0$ $\qquad$ [L T^{-2}]

Channel parameters were calculated as a function of the drainage area (in km^2) above the location of the cross-section, including: maximum bankfull width [m] (Equation 3-1), valley width [m] (Equation 3-2), average bankfull depth [m] (Equation 3-3), and maximum bankfull depth [m] (Equation 3-4). For these analyses, width and depth were evaluated separately by decreasing each value by 25 and 50 percent, and by increasing each value by 50 and 100% in successive simulations. This method produced values for each variable that are up to a factor of 2 different from the original values used in the original simulation.

Channel Roughness (Manning's n)

The CCHE1D model uses Manning's roughness formula to compute the friction slope (Equation 5-1) term of the momentum equation (Equation 5-2). The roughness coefficient, Manning's n, increases with increasing surface roughness, vegetation growth, and channel irregularity (Jain, 2001). Since Manning's formula is used for computing uniform flow velocity, changes in the roughness coefficient will change the flow velocity, thereby affecting the peak discharge rate and the timing of the peak discharge rate. It is expected that there will be no significant changes in discharge rates, by application of the water continuity equation, for given changes in Manning's n. However, altering flow velocity will significantly alter sediment transport rates nonlinearly, as is discussed above for channel geometry.

The CCHE1D user is required to supply a value for Manning's n for each cross-section (both main channel and overbank) in the computational network (Wu and Vieira, 2002). For the original simulation, roughness values for both main channel and overbank areas were unknown,

and therefore were calibrated using observed discharge hydrographs at the watershed outlet. As such, it is possible that the assumed values are in error by a factor of two. Therefore, to evaluate sensitivity of discharge and sediment transport rates to changes in Manning's n, the calibrated values of Manning's n were changed by plus 100 and minus 50 percent of baseline values.

Bed Material Porosity

The CCHE1D model computes the non-equilibrium transport of non-uniform sediment with a form of the Exner equation (Equation 5-3), also called the sediment continuity equation. The sediment continuity equation is used in sediment transport computations when the sediment transport rate is different than the sediment transport capacity (equilibrium sediment transport) (Wu, Vieira, and Wang, 2004). For example, when the incoming sediment load is lower than the sediment transport capacity, the channel bed can be scoured and degraded; or aggraded when the sediment load exceeds the transport capacity. The sediment continuity equation considers the exchange of material between the bed and the flow field, and multiple sources of sediment (e.g., bed, banks, tributaries, and lateral inflow). In this formulation, the bed material porosity (λ) is constant [no units], and regulates the rate of bed deformation in a linear manner. Therefore, the value of porosity can significantly affect the total sediment transport rate, and the rates of aggradation and degradation. However, the rate of change of sediment transport is expected to change only linearly with linear changes in bed material porosity.

Equation 5-3.
$$(1-\lambda)\frac{\partial A_{bed}}{\partial t} + \frac{\partial(A_W C_{SED})}{\partial t} + \frac{\partial Q_{SED}}{\partial x} = q_{SED_{Lat}} \qquad [L^2\,T^{-1}]$$

Bed material porosity can be determined by field measurements (e.g., bulk density or freeze cores), but is time consuming and rarely measured for more than one reach in a channel network, if at all (Bunte and Abt, 2001). Therefore, to solve the Exner equation, values for

porosity are either determined empirically or given an assumed value (possibly based on the porosity of the surface soils of the hillslopes adjacent to the channels (Wu and Vieira, 2002). For these analyses, changes in flow and sediment transport due to changes in channel bed material porosity were evaluated using six different options: the default empirical formula by Komura and Simons (1967) (cited in Wu and Vieira (2002)), a semi-empirical formula proposed by Han et al. (1981) (cited in Wu and Vieira (2002)), and four user-defined constant values (0.40, 0.30, 0.20, and 0.10).

St. Venant Equation Solution

The CCHE1D model has two methods for computing the unsteady movement of water waves in open channels: a dynamic wave model and a diffusive wave model (Wu and Vieira, 2002). The hydrodynamic simulations in previous chapters used the dynamic wave solution in CCHE1D exclusively. The difference between the two models is that the diffusive wave model ignores the inertia terms in the momentum equation (first two terms of Equation 5-2). The inertia terms can be important where channel confluences and instream hydraulic structures occur, or where flood waves move rapidly through a very shallow gradient reach (Jain, 2001; U.S.A.C.E., 1993). These situations can produce significant backwater effects due to rapid changes in channel geometry and flow conditions. For this analysis, the original modeling domain (as described in previous chapters) was used for both simulations, and only the wave solution was changed. for the modeling domain simulated, it is expected that there will be minimal differences in either discharge or sediment transport rate when selecting between dynamic or diffusion wave models. The Caspar Creek watershed has high gradient channels, a short travel distance (less than 5 km), and slowly rising floodwaves. Under these conditions, it is expected that the floodwave is primarily kinematic, with minimal inertial effects; resulting in only minimal differences between dynamic or diffusion wave solutions.

Sediment Transport Capacity Equations

The CCHE1D model has four methods for the determination of sediment transport capacity: Wu et al.'s (2000) formula, a modified form of Ackers and White's formula (Proffit and Sutherland, 1983), a modified form of Engelund and Hansen's formula with Wu et al.'s (2000) hiding and exposure correction factor (Wu and Vieira, 2002), and the SEDTRA module (Garbrecht, Kuhnle, and Alonso, 1995). The SEDTRA module uses three different formulas to calculate sediment transport capacities for different size ranges: Laursen's (1958) formula for size classes from 0.01 to 0.25 mm, Yang's (1973) formula for size classes from 0.25 to 2.0 mm, and Meyer-Peter and Mueller's (1948) formula for size classes from 2.0 to 50.0 mm.

All of these methods are based on stream power concepts (Yang, 1996), but are known to produce dramatically different results for the same flow conditions (Wu and Vieira, 2002; Yang, 1996). One potential limitation is with the Ackers and White equation. This equation was developed for bed material with particle sizes greater than 0.04 mm (Yang, 1996), and can produce erroneous results in transport rates of sediments smaller than 0.04 mm (D. Vieira, National Center for Computational Hydroscience and Engineering, *personal communication*, January 15, 2005). The WEPP-H model produces most of its sediment load in these categories, which are the lowest three size classes modeled (Table 4-2). Even with this limitation, the calibration scenario was run with each of the four sediment transport capacity options separately. It is expected that the differences in sediment transport rates would be nonlinear for the different sediment transport capacity equations, because all of the equations used are nonlinear equations.

WEPP Hillslope-specific Analyses

When using the WEPP Windows interfaces, the WEPP-H model runs transparent to the user, with no opportunities to change the run-time simulation options. Calibration of the model was accomplished only by altering parameters in the input files. Of the four main user-supplied

input files: 1) topography, 2) climate, 3) soil, and 4) management (vegetation composition), only soil and vegetation properties are changed to evaluate management-related erosion. Changes in vegetation density and biomass will affect the amount soil surface that is exposed to erosive forces (i.e., rainfall and overland flow). The Green-Ampt, Mein-Larsen (Mein and Larson, 1973) infiltration model used in WEPP-H is an infiltration capacity excess (Hortonian overland flow) model that is sensitive to the effective saturated hydraulic conductivity of the soil. This parameter determines the rate at which water can move into and through the soil profile. In soils with high saturated hydraulic conductivities, which are common in the forested environments evaluated here (Henry, 1998), the depth of soil can dramatically affect the volume of water moving into the water table, and the response to lateral subsurface flow. Since both of these parameters can affect the volume of water moving through the soil, both can alter the volume of water that is left as saturated overland flow. As such, changes in soil properties can elicit dramatic changes in runoff volume, which in turn can dramatically alter the surface erosion rates. The sensitivity analyses conducted here explore a wide range of saturated hydraulic conductivities that would be expected in forest environments, the full range of soil depths used in the WEPP-H model, and the full range of possible soil cover percentages (Table 5-2).

Table 5-2. Ranges of values and options evaluated for selected parameters of the WEPP Hillslope model.

Parameter	Range of Values or Options Evaluated
Saturated Hydraulic Conductivity	5, 10, 15, 20, 25, 50, 100, and 150 mm/hr
Soil Depth	500, 750, 1000, 1250, and 1525 mm
Soil Cover Percentage	5, 25, 50, 75, and 100 percent

Soil Saturated Hydraulic Conductivity

The saturated hydraulic conductivity (KSAT) of a soil represents the ease with which fluids pass through a bulk mass of soil (Brady, 1990). The Green-Ampt, Mein-Larsen (GAML) infiltration model (Mein and Larson, 1973) used by WEPP-H, is directly dependent upon the KSAT of the soil (Stone et al., 1995). The lower the KSAT of the surface soil, the more difficult it is for incoming precipitation to infiltrate into the soil, which results in greater saturated overland flow and surface erosion.

Since the GAML infiltration model is a function of several variables (e.g., KSAT, precipitation rate, soil water content), it is difficult to predict the precise changes that will occur for changes in only one of the variables. However, since the KSAT variable is used in both the numerator and denominator of the GAML equation (Stone et al., 1995), it is expected that the changes in discharge and sediment transport rates will be nonlinear. For example, for well-drained soils that have hydraulic conductivities that are greater than the incoming precipitation intensity, it is expected that there would be minimal changes in discharge and sediment delivery. However, for poorly drained or compacted soils with hydraulic conductivities that are less than or equal to the incoming precipitation intensity, it is expected that discharge and sediment delivery would be very sensitive to small changes in hydraulic conductivity.

For the Caspar Creek Experimental watershed, soil surveys indicate that soil permeability (i.e., the term used in soil surveys to measure saturated hydraulic conductivity (Brady, 1990)) ranges between 15 and 150 mm/hr. For this analysis, the KSAT values for soils on each hillslope were varied from 5 to 150 mm/hr to encompass the range of observed values. Two additional KSAT scenarios, with values of 5 and 10 mm/hr, were assessed to simulate soils that may have been mechanically compacted. The range assessed here includes the majority of KSAT values that are likely to be observed in a forested setting.

Soil Depth

The depth of the surface soil, combined with the bulk material properties of the soil (e.g., particle size distribution and saturated hydraulic conductivity), determines the total volume of water that can be stored in the soil profile and length of time required for a volume of water to move through the soil profile. For short-duration, low-intensity precipitation events that do not produce enough water volume to saturate the soil profile, soil depth would have a minimal effect on discharge and sediment delivery. However, for storms that produce large water volumes (e.g., high-intensity short-duration events; multiple events that are closely spaced in time) soil depth could have a significant effect on discharge and sediment delivery. As such, changes in discharge and sediment transport rates for changes in soil depth will be nonlinear, and affected more by rainfall rate and volume than soil depth.

For the Caspar Creek Experimental watershed, soil surveys indicate that depths to bedrock range between 500 and 1,525 mm, with the majority of the soil depths in the watershed greater than 1,000 mm (Henry, 1998). For these experiments, soil depths were varied in 500 mm increments through the observed range.

Soil Cover

Soil cover is any material that protects bare mineral soil from the erosive forces of rainfall impact. In forests, these materials include decaying organic matter, live vegetation, and rocks. As surface soil cover increases, splash erosion is reduced and rill erosion is impeded. This variable, of all variables discussed and evaluated here, is subject to the greatest changes resulting from forest management activities. Timber harvesting and herbicide use can remove a significant portion of the standing vegetation canopy, but can significantly increase the amount of decaying organic matter. Harvesting equipment can remove significant volumes of cover, and can compact the soil surface (affecting the effective saturated hydraulic conductivity, as discussed above). Where roads, landings, and skid trails are used, the soil surface is almost

113

completely bare (except for rocks and small amounts of organic matter), and is often highly compacted (Cafferata, 1983). The effects of fuel burning vary with fire intensity, but can result in complete removal of all surface organic matter and decreased effective saturated hydraulic conductivity due to heat-induced hydrophobicity (Robichaud and Waldrop, 1994).

In the Caspar Creek Experimental Watershed, there are several forest management activities that alter the soil surface cover, including timber harvesting, road building, and fuels reduction with herbicides and burning (Henry, 1998). In the WEPP-H model, making changes to the ground surface cover requires adjustments to several variables. Changes must be made to the initial ground cover conditions, the rate of biomass produced by the plants during the growing season, plant spacing, and the leaf-area index (a ratio of total leaf area to total ground surface). It is expected that changes in discharge and sediment transport rates for changes in soil cover would be nonlinear since evapotranspiration (Savabi and Williams, 1995) and surface erosion (Foster et al., 1995) equations used in the WEPP-H model are nonlinear.

Soil surface cover percent was varied from completely bare (5%) to completely covered (100%) in increments of 25% to evaluate the changes in surface erosion and runoff. The lower limit of 5% cover was used for two reasons. First, bare soil will likely include rocks and some organic matter on the surface that would act as cover from raindrop impact, even after a severe fire (Robichaud and Waldrop, 1994). Second, to calculate tree spacing, which is the inverse-square root of cover percentage, a number greater than zero was needed. To produce these ground cover percentages, the biomass conversion ratio (Arnold et al., 1995), leaf area index, and plant spacing were altered (Table 5-3).

Table 5-3. Rill cover, interrill cover, biomass conversion ratio, leaf area index, and plant spacing used in the WEPP-H model to produce selected ground cover percentages.

Ground Cover (%)	Initial Interrill Cover (%)	Initial Rill Cover (%)	Biomass Conversion Ratio	Maximum Leaf Area Index	Plant Spacing (m)
100	100	100	40	10	2.0
75	75	75	20	7.5	2.3
50	50	50	10	5	2.8
25	25	25	5	2.5	4.0
5	0	0	2.5	0.5	8.9

RESULTS AND DISCUSSION

CHANNEL GEOMETRY

Changes in the values for channel geometry, both width and depth, have an insignificant effect on the discharge rate and volume. There was less than one percent difference between peak rates for all changes in channel depth (Table 5-4) and channel width (Table 5-5). In fact, hydrograph peaks are indistinguishable even when the channel depths (Figure 5-6) or channel widths (Figure 5-7) are increased or decreased by a factor of two. This result is not too surprising since discharge is a function of input from the upland areas and not the channel dimensions. For a given discharge rate, if either the width or depth are changed, the continuity equation (Equation 2-1) requires a concomitant change in depth or width; resulting in equal cross-sectional areas.

Table 5-4. Average, minimum, and maximum percent difference in peak discharge rate for given percentage changes in channel depth (from original channel depth).

Change from Original Depth (%)	Average Difference (%)	Maximum Difference (%)	Minimum Difference (%)
-50	0.16	0.45	0.00
-25	0.11	0.43	0.01
50	0.12	0.51	0.01
100	0.15	0.65	0.00

Table 5-5. Average, minimum, and maximum percent difference in peak discharge rate for given percentage changes in channel width (from original channel width).

Change from Original Width (%)	Average Difference (%)	Maximum Difference (%)	Minimum Difference (%)
-50	0.20	0.74	0.01
-25	0.16	0.74	0.00
50	0.18	0.77	0.01
100	0.21	0.81	0.02
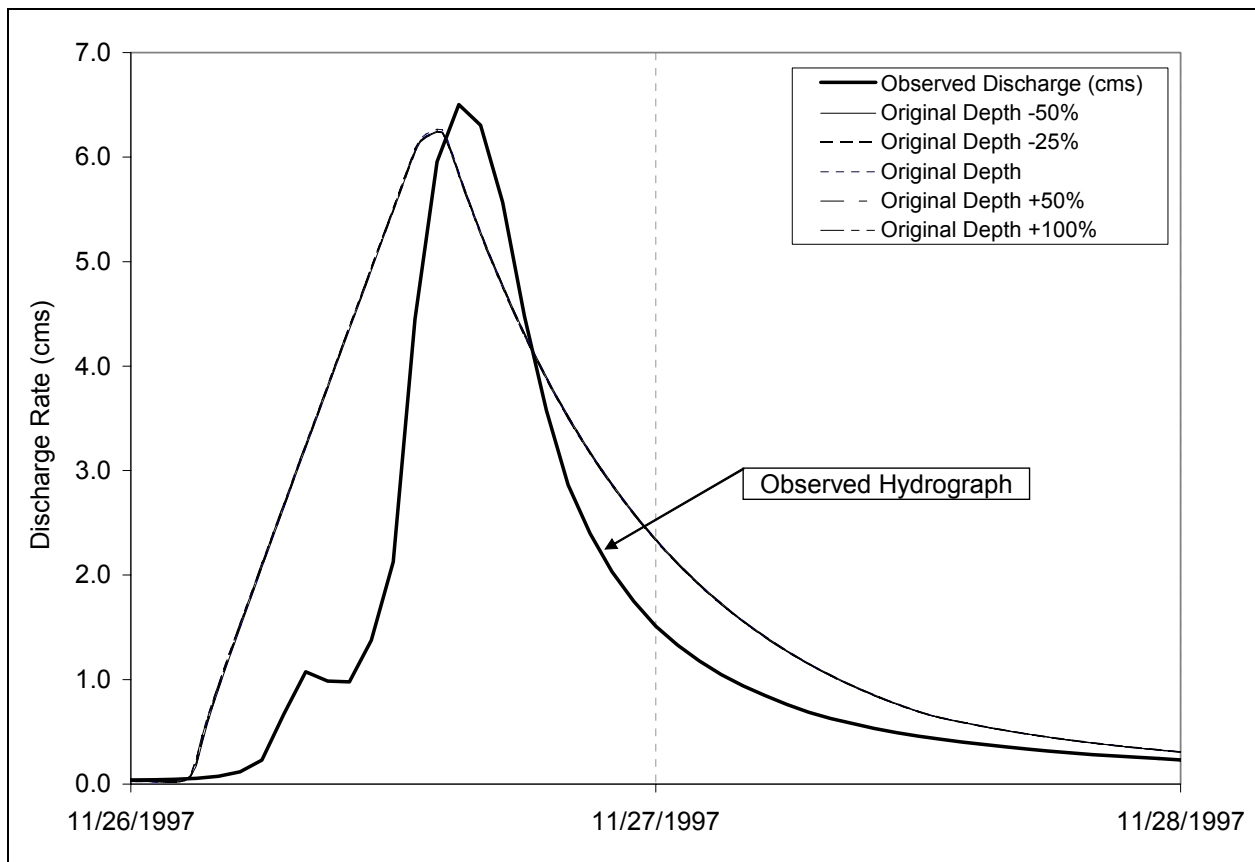
Figure 5-6. Example hydrographs for an event with channel cross-section depth changed from originally modeled value.
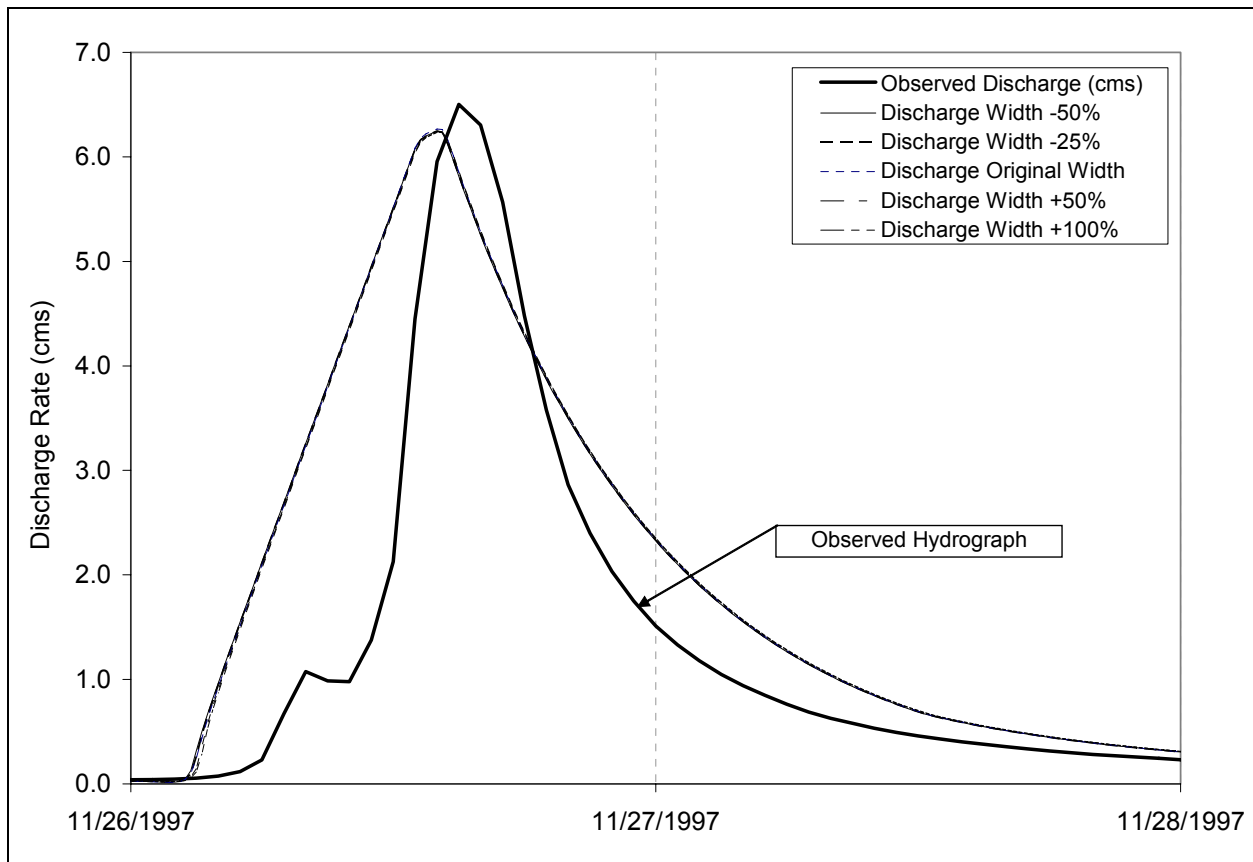
Figure 5-7. Example hydrographs for an event with channel cross-section width changed from originally modeled value.

For sediment transport, however, changes in channel geometry have a significant effect. For the same runoff events, there are significant differences in total sediment concentration for changes in channel depth (Figure 5-8, Table 5-6) and channel width (Figure 5-9, Table 5-7). This result is consistent with the stream power-based sediment transport capacity equation used in CCHE1D (Wu and Vieira, 2002), which is affected by changes in channel hydraulic radius. As expected, increasing channel depth increases sediment transport rates (Figure 5-8) due to increased shear stress and velocity as depth is increased. Likewise, increasing channel width decreases sediment transport rates (Figure 5-9) for the same reason.
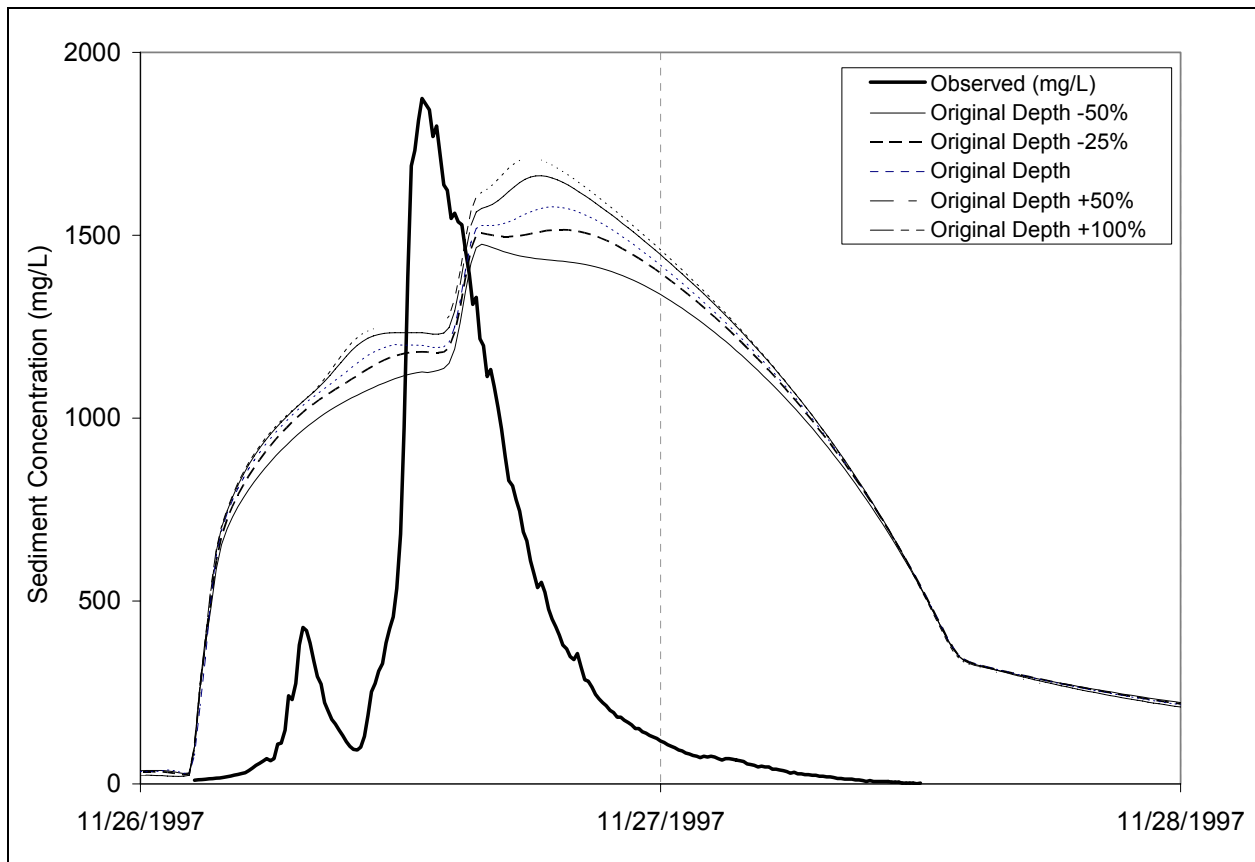
Figure 5-8. Example sediment graph for an event with channel cross-section depth changed

from originally modeled value.

Table 5-6. Average, minimum, and maximum percent difference in peak sediment

concentration for given percentage changes in channel depth (from original channel depth).

Change from Original Depth (%)	Average Difference (%)	Maximum Difference (%)	Minimum Difference (%)
-50	12	26	3.6
-25	5.2	10	2.0
50	7.3	13	2.2
100	12	21	1.6
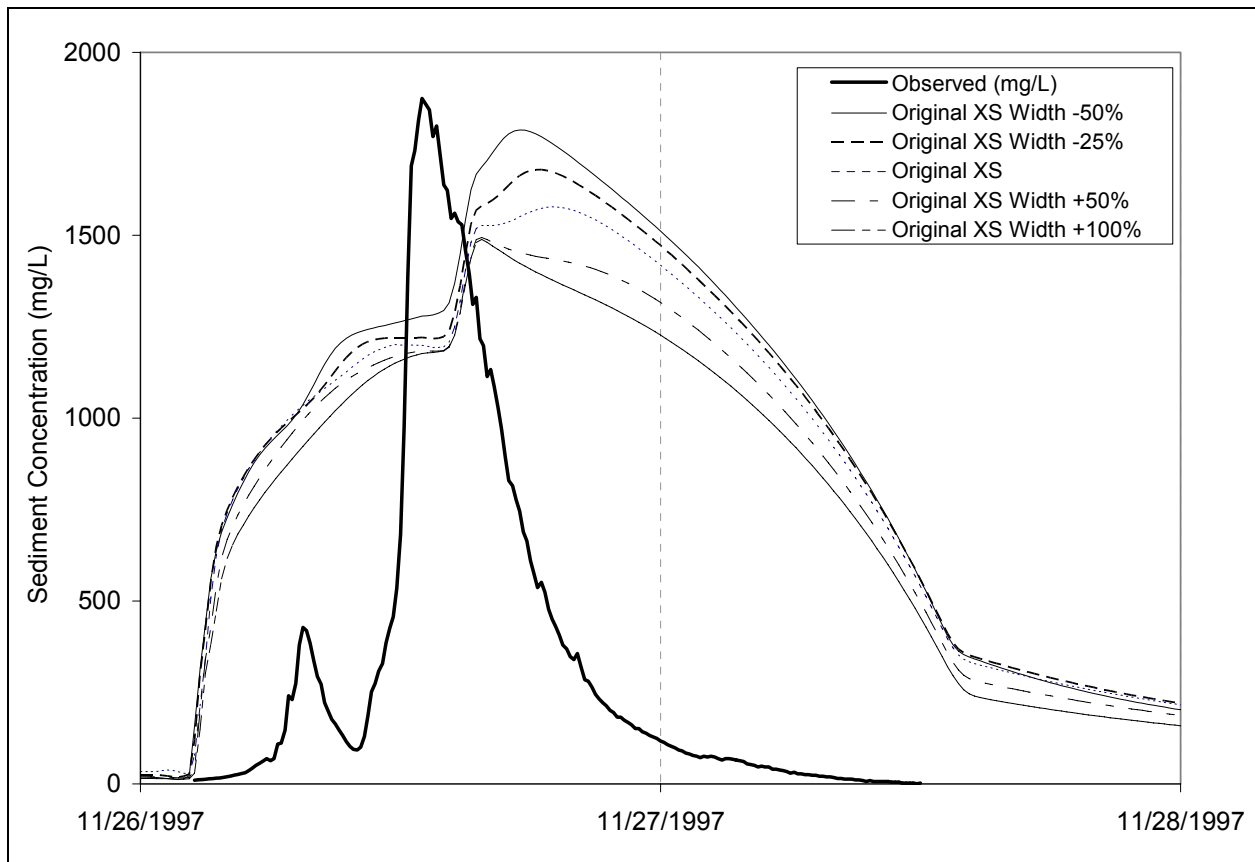
Figure 5-9. Example sediment graph for an event with channel cross-section width changed

from originally modeled value.

Table 5-7. Average, minimum, and maximum percent difference in peak sediment

concentration for given percentage changes in channel width (from original channel width).

Change from Original Width (%)	Average Difference (%)	Maximum Difference (%)	Minimum Difference (%)
-50	16	36	2.7
-25	6.9	12	1.1
50	6.8	18	0.2
100	11	33	1.6

Decreasing channel depth decreases peak total sediment concentration and increasing channel depth increases peak total sediment concentration (Table 5-6). Decreasing the main channel depth increases the incidence of overbank flows, resulting in a decrease in average flow depth (since the valley widths are approximately twice the bankfull widths). Increasing the main channel depth decreases the incidence of overbank flows, resulting in an increase in average flow depth (since more of the flow volume is contained in the main channel). Changes in sediment concentration for given changes in channel depth are approximately linear. The greater the error in channel depth prediction is, the greater the error in predicted sediment concentration; with an increase of depth of equal percentage to decrease in depth producing nearly identical changes in sediment concentration (Table 5-6).

Decreasing channel width increases peak total sediment concentration and increasing channel width decreases peak total sediment concentration (Table 5-7). Decreasing the main channel width increases the average flow depth, and increasing the main channel width decreases the average flow depth. Changes in sediment concentration for given changes in channel width are approximately linear, and are comparable to changes affected by depth. The greater the error in channel depth prediction is, the greater the error in predicted sediment concentration; with an increase of depth of equal percentage to decrease in depth producing nearly identical changes in sediment concentration (Table 5-7).

Since discharge is independent of channel geometry, changes in channel geometry have an insignificant influence on discharge. Therefore, for hydrodynamic simulations, it is not very important to have precise measurements of channel geometry. For hydrodynamic simulations, the only consideration necessary for determining appropriate channel geometry is that the channel should have sufficient cross-sectional area (main channel and overbank areas combined) to contain all of the flow to be simulated. As such, any reasonable estimate of channel geometry will produce satisfactory hydrodynamic simulation results.

For sediment transport simulations, however, inaccurate estimates of channel geometry can significantly affect the predictions of sediment concentration. For the simulations conducted here, changing channel width or depth by a factor of two produced changes in sediment concentration an average of 12 and 14 percent, respectively. However, there were changes of up to 27 and 37 percent, respectively. Therefore, it is reasonable to assume that errors in predicting channel geometry will produce errors in sediment transport predictions, and that the errors could be significant. As such, to produce accurate sediment transport estimates, regional hydraulic geometry relations should be adjusted for local conditions or precise channel cross-sections should be measured.

CHANNEL ROUGHNESS (MANNING'S N)

For these analyses, changes in channel roughness were evaluated by decreasing and increasing each value of Manning's n by 50 and 100 percent, respectively, in successive simulations (Table 5-8). Peak discharge rate, total daily flow volume, peak daily sediment concentration, and total daily sediment load values computed using the altered channel roughness values are compared to the same values computed using the original channel roughness values. Relative differences are used to compare the magnitude of changes in predicted runoff and load values.

Table 5-8. Manning's n values, by Strahler stream order, used for CCHE1D sensitivity simulations.

CCHE1D Simulation Scenario	Manning's n	
	Order 1	Order 2
Original	0.1250	0.0750
Original +100%	0.2500	0.1500
Original -50%	0.0625	0.0375

Changing the roughness coefficient produced two changes in outflow hydrographs: peak magnitude and peak timing. Decreasing Manning's n resulted in typically larger discharge peaks that occurred earlier. While increasing Manning's n resulted in smaller peaks that occurred later (Figure 5-10). Increasing Manning's n by 100 percent produced an average increase in the peak flow rate of the 15-simulated events of 0.7 percent (Table 5-9) with the peaks occurring an average of 17 minutes sooner (Table 5-10). Decreasing Manning's n by 50 percent produced an opposite but comparable effect.
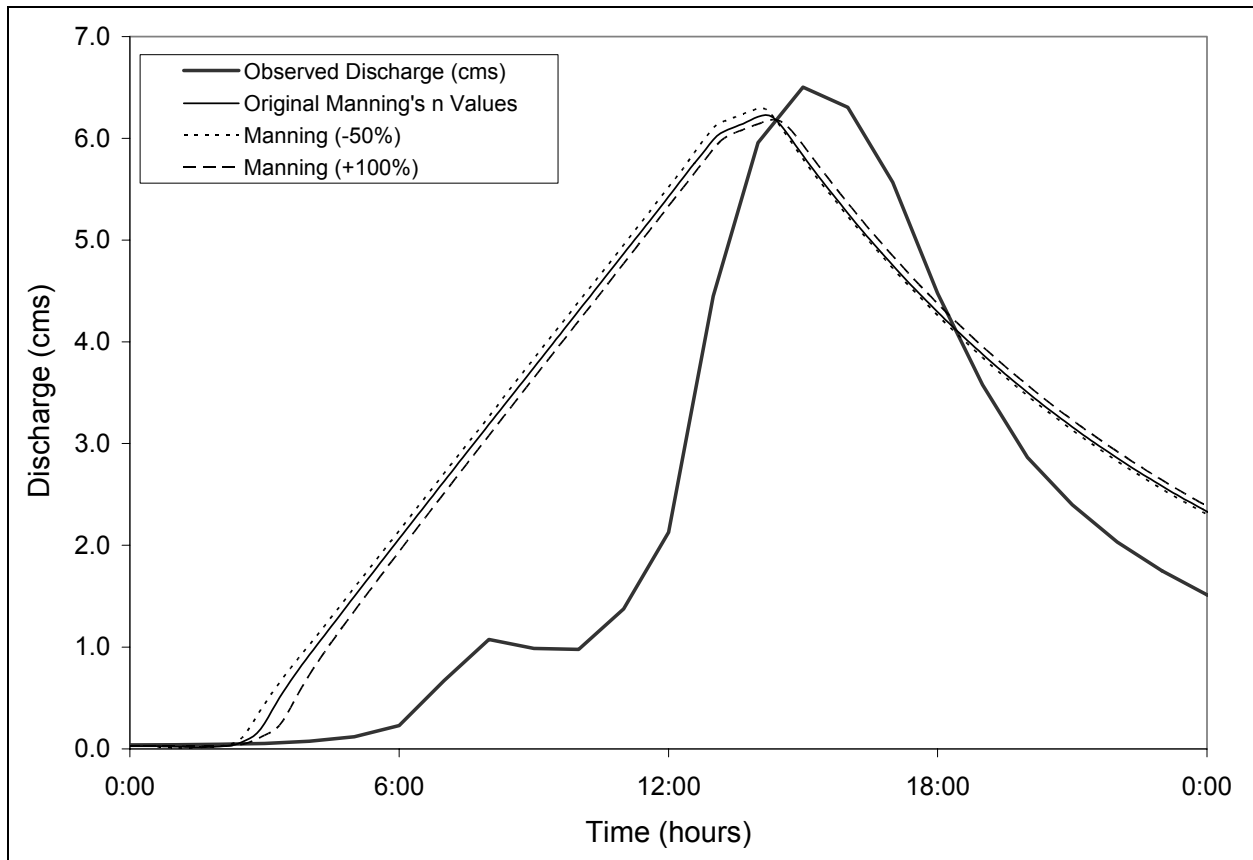
Figure 5-10. Example differences in hydrographs for increases and decreases of Manning's roughness coefficient of 100 and 50 (respectively) from originally used values for a selected runoff event in South Fork Caspar Creek, CA.

Table 5-9. Average, maximum, and minimum percent difference from original peak runoff rates for Manning's roughness coefficients increased and decreased 50% from originally used values, for 15 selected runoff events at South Fork Caspar Creek, CA.

Scenario	Percent Difference From Original Peak Runoff Rates		
	Average	Maximum	Minimum
Manning's N -50%	0.7	1.1	0.4
Manning's N +100%	0.6	1.5	0.2

Table 5-10. Average, maximum, and minimum time difference in occurrence of peak runoff rates from original peak runoff rates for Manning's roughness coefficients increased and decreased 50% from originally used values, for 15 selected runoff events at South Fork Caspar Creek, CA.

Scenario	Time Difference in Occurrence of Peak Runoff Rates (minutes)		
	Average	Maximum	Minimum
Manning's N -50%	10.7	20.0	5.0
Manning's N +100%	-16.7	-25.0	-10.0

These results suggest that even very large errors in estimating channel roughness results in minimal errors in peak discharge rate, but the timing of the peaks could be in error significantly. However, since these simulations were conducted on only one channel network, it is difficult to generalize about the sensitivity of hydrodynamics to changes in Manning's roughness coefficient. For CCEW, the main channel is approximately 4,000 meters long with an average slope of 0.045 m/m. The durations of the hydrographs simulated are between 24 and 72 hours long. Under these conditions, it is expected that the pressure differential and gravitational terms of the momentum equation will be substantially greater than the inertial terms; resulting in hydrograph peaks that are nearly translated with minimal attenuation. As such, changes in

Manning's roughness coefficient would only result in changes in wave velocity (i.e., peak timing) instead of wave magnitude. It is likely that for larger channel networks with shallower channel gradients, significant changes in Manning's n would produce substantial changes in both magnitude and timing of flood peaks (that were not observed here).

Although large changes in Manning's n produced small changes in peak discharge rates for the events simulated, the small changes in velocity and roughness produced large changes in total sediment concentration (Table 5-11, Figure 5-11). By decreasing Manning's n by 50 percent, discharge increased an average of one percent, which increased sediment transport by over 60 percent (Table 5-11). By increasing the Manning's n by 100 percent, discharge decreased approximately one percent (Table 5-11). Sediment concentration, however, changed minimally when Manning's n was increased (Table 5-11).

Table 5-11. Average, maximum, and minimum percent difference from original peak total sediment concentration for Manning's roughness coefficients increased and decreased 100 and 50% (respectively) from originally used values, for 15 selected runoff events at South Fork Caspar Creek, CA.

Scenario	Percent Difference From Original Peak Total Sediment Concentration		
	Average	Maximum	Minimum
Manning's N Minus 50%	62	127	-15
Manning's N Plus 100%	0	15	-20

This result is consistent with the expected behavior of the sediment transport capacity equation used in CCHE1D. The equation by Wu, Wang, and Jia (2000) is based on stream power theory (Wu, Vieira, and Wang, 2004), and is therefore sensitive changes in streamflow velocity. For example, given a hypothetical trapezoidal channel with a constant slope and

channel geometry, changes to Manning's n produce significant and nonlinear changes in velocity (Figure 5-12).

These results indicate that sediment transport is sensitive to changes in values of Manning's roughness coefficient, even when discharge rate is not very sensitive to equal changes in channel roughness. As such, when collecting data prior to modeling sediment transport, estimates of Manning's n should be made at each of the locations deemed necessary for channel geometric data. Since there is a natural range of roughness values, occurring with both spatial location and depth of flow, this variable presents itself as quite useful for calibrating sediment concentration, while not affecting the hydrodynamic results significantly.
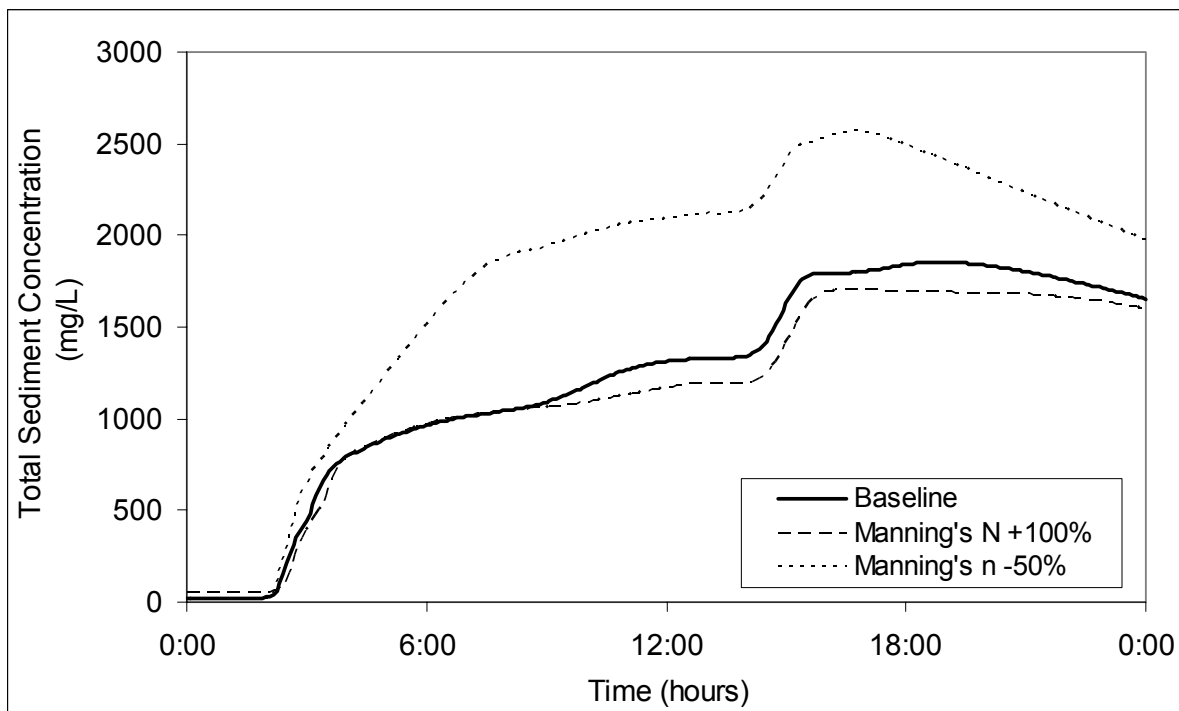
Figure 5-11. Example differences in hydrographs for increases and decreases of Manning's roughness coefficient of 50% from originally used values for a selected runoff event in South Fork Caspar Creek, CA.
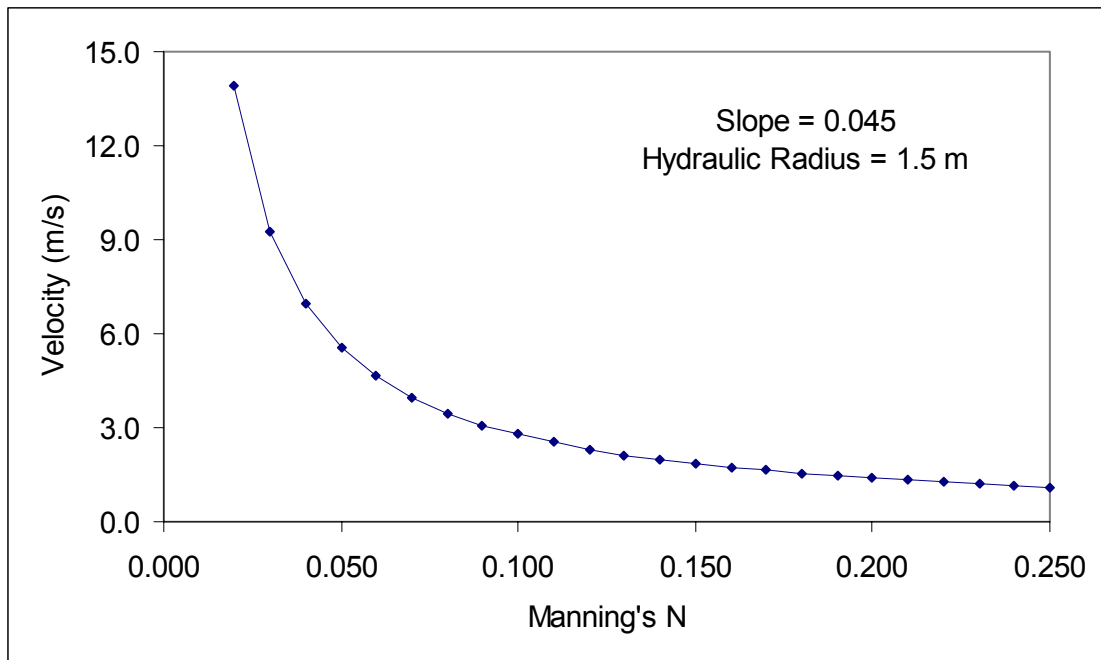
Figure 5-12. Variations in streamflow velocity for uniform flow in a trapezoidal channel with varying Manning's roughness coefficient.

BED MATERIAL POROSITY

For these analyses, changes flow and sediment transport due to changes in channel bed material porosity were evaluated using six different bed material porosity options: the empirical formula by Komura and Simons (1967) (cited in Wu and Vieira (2002)), a semi-empirical formula proposed by Han et al. (1981) (cited in Wu and Vieira (2002)), and four user-defined constant values (0.40, 0.30, 0.20, and 0.10). For all simulations, the Komura and Simons (1967) formula was used as the default option, as was suggested by the CCHE1D model developers (Vieira and Wu, 2002a).

For the 15 runoff events evaluated, the choice of bed material porosity significantly effected peak total sediment concentration (Table 5-12). The Komura and Simons formula produces bed

material porosities that are between all of the other methods used (λ ≈ 0.35), and as a result produces total sediment concentrations that are roughly between all of the other options evaluated. The greater the difference between the default value and the tested option was the greater the percent difference in sediment concentration (Table 5-12), as would be expected by observing Equation 5-3. Since the bed material porosity variable is linear in Equation 5-3, uniform differences in bed material porosity produce nearly linear changes in total sediment concentration (Figure 5-13).

Table 5-12. Average, maximum, and minimum percent difference from original peak total sediment concentration for bed material porosity options from originally used option (Komura and Simons, 1967), for 15 selected runoff events at South Fork Caspar Creek, CA.

Bed Porosity Option	Percent Difference From Original Peak Total Sediment Concentration		
	Average	Maximum	Minimum
Han and Wang (1981)	8.8	16.7	0.2
Constant at 0.40	5.1	9.4	0.5
Constant at 0.30	5.2	18.7	0.6
Constant at 0.20	9.4	20.0	0.4
Constant at 0.10	15.1	26.8	0.3
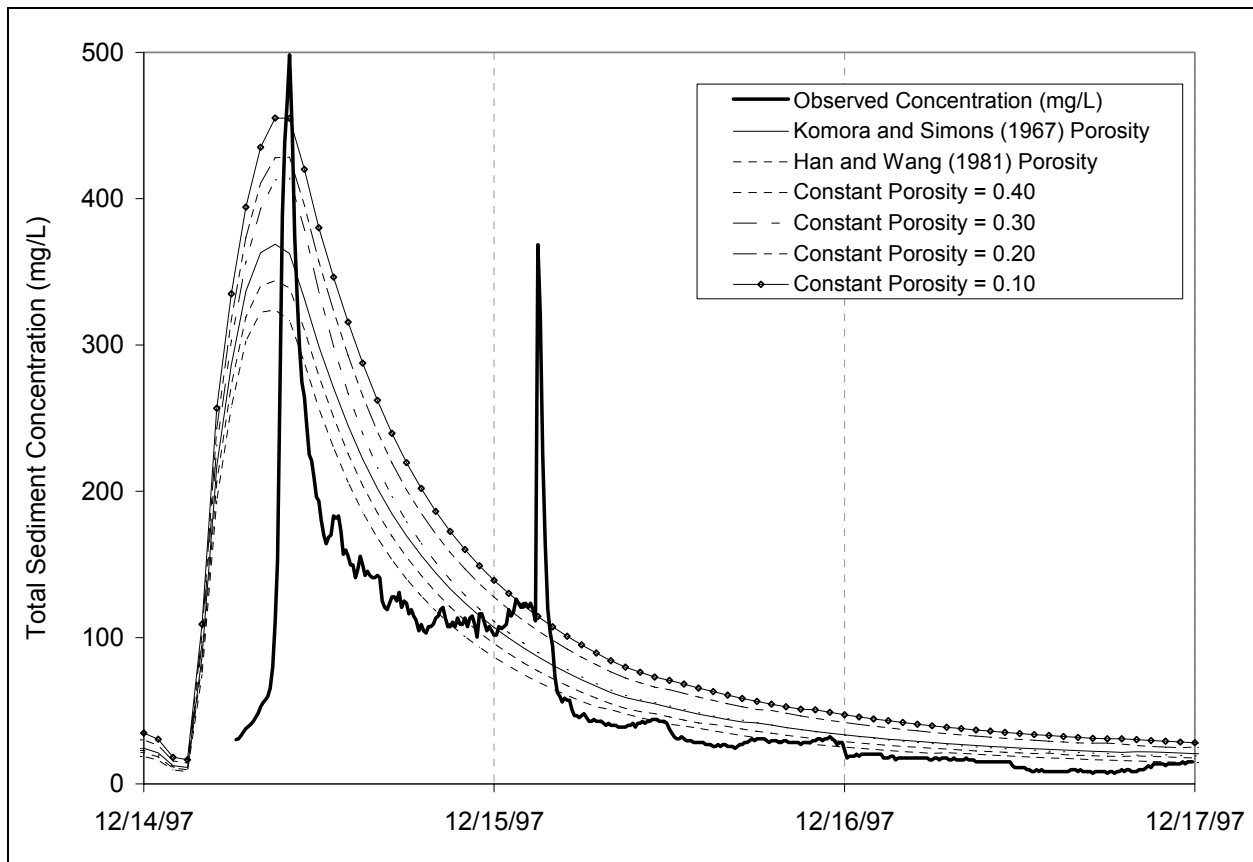
Figure 5-13. Example differences in hydrographs for changes in bed material porosity options from originally used option (Komura and Simons, 1967) for a selected runoff event in South Fork Caspar Creek, CA.

Total sediment concentration was very sensitive to changes in values of bed material porosity, but in a predictable (and linear) manner. Changing bed material porosity between 0.10 and 0.60 (the approximate value produced by the Han and Wang equation) resulted in differences of total sediment concentration between 0.2 and 27 percent. As such, this would be a good variable to obtain measured values for the channels being assessed. However, since this is a rather difficult parameter to measure *in situ* and is rarely measured (Bunte and Abt, 2001), a more reasonable approach would be to use the Komura and Simons equation for channels without porosity measurements; as is recommended by the CCHE1D model

developers (Wu and Vieira, 2002). Since using the Komura and Simons equation results in average values of total sediment concentration (Table 5-13) and the differences in results are linearly dependent (Figure 5-14), it is reasonable to use this equation exclusively and use other options (e.g., Han and Wang or $\lambda \approx 0.10$) as lower and upper (respectively) bounds on the sediment concentration estimates.

Table 5-13. Average, maximum, and minimum predicted peak total sediment concentration for bed material porosity options, for 15 selected runoff events at South Fork Caspar Creek, CA.

Bed Porosity Option	Predicted Peak Total Sediment Concentration (mg/L)		
	Average	Maximum	Minimum
Komura and Simons (1967)	515	1855	150
Han and Wang (1981)	489	1858	126
Constant at 0.40	500	1878	136
Constant at 0.30	533	1897	157
Constant at 0.20	543	1841	173
Constant at 0.10	558	1814	185
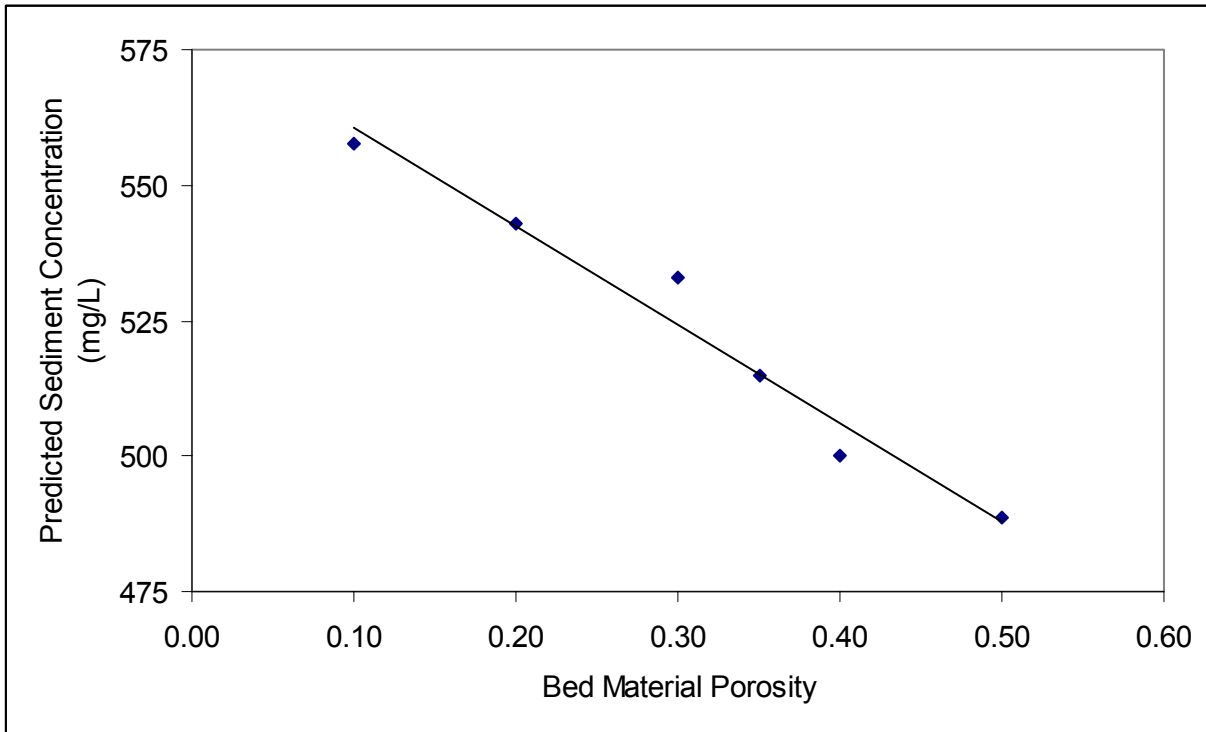
Figure 5-14. Predicted total sediment concentration for varying bed material porosity levels.

ST. VENANT EQUATION SOLUTION

For the 15 events simulated in this chapter, using the diffusive wave solution produced virtually indistinguishable peak discharge rates from those produced using the dynamic wave solution (Table 5-14). The maximum absolute difference between the two solutions was 0.00008 m^3/s for the largest event simulated (Figure 5-15), which was a 0.0049 percent difference between the two solutions. This event also had the largest difference in total sediment concentration between the two hydrodynamic solutions. This difference of 1.3 mg/L was a 0.29 percent difference in peak sediment concentration (Table 5-15).

Table 5-14. Average, maximum, and minimum percent difference from original peak discharge rate for the diffusive wave option vs. the originally used dynamic wave option, for 15 selected runoff events at South Fork Caspar Creek, CA.

Hydrodynamic Solution Option	Predicted Peak Discharge Rates (cms)		
	Average	Maximum	Minimum
Dynamic Wave	2.04196	7.25108	0.41565
Diffusive Wave	2.04194	7.25100	0.41564
Percentage Difference	0.0014	0.0049	0.0000

Table 5-15. Average, maximum, and minimum percent difference from original peak total sediment concentration for the diffusive wave option vs. the originally used dynamic wave option, for 15 selected runoff events at South Fork Caspar Creek, CA.

Hydrodynamic Solution Option	Predicted Total Sediment Concentration (mg/L)		
	Average	Maximum	Minimum
Dynamic Wave	329.77	1460.58	27.11
Diffusive Wave	329.83	1459.28	27.13
Percentage Difference	0.11	0.29	0.01
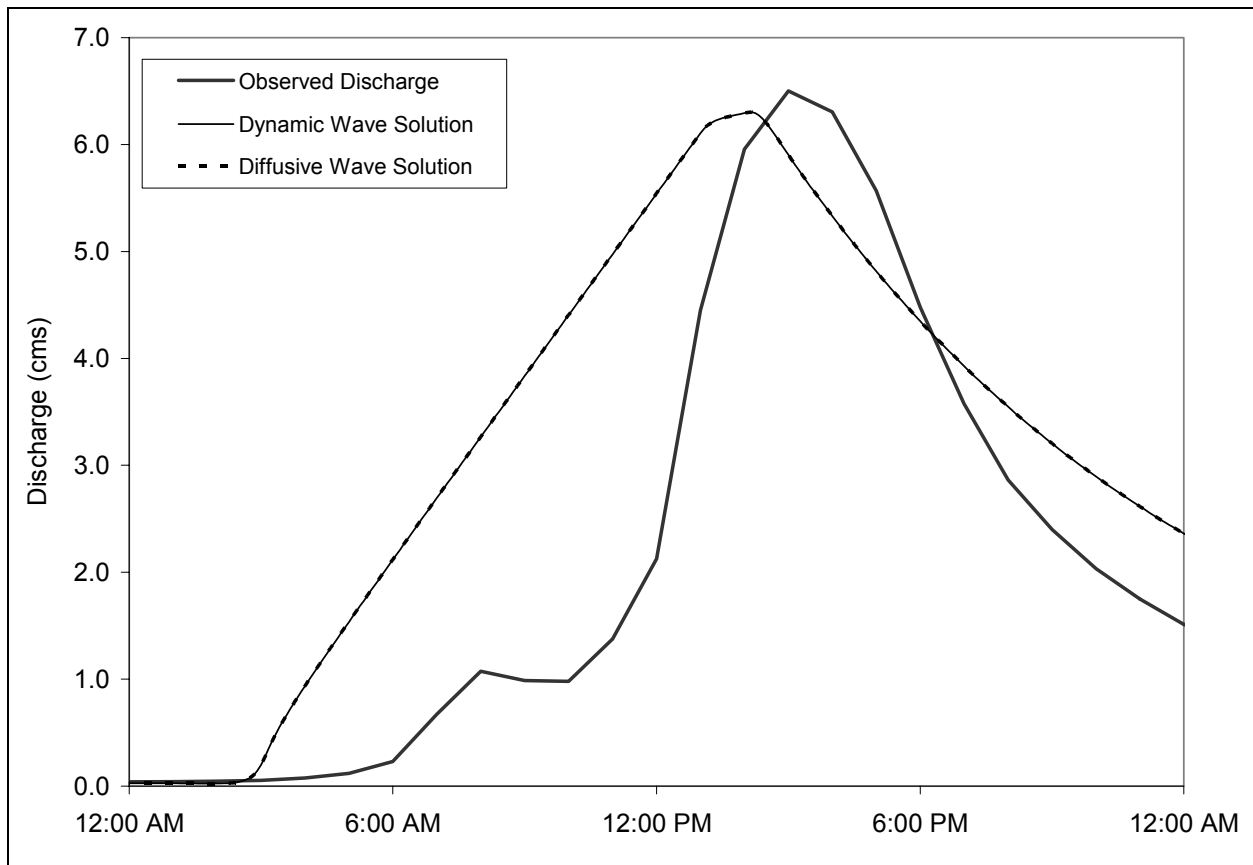
Figure 5-15. Example differences in hydrographs for dynamic and diffusive wave solutions for a selected runoff event in South Fork Caspar Creek, CA.

For the physiographic conditions in Caspar Creek (e.g., steep channel gradients, slowly rising floodwaves, short travel distances), it was expected that there would be minimal differences between the two St. Venant equation solutions. It was expected that these conditions would lead to flow regimes that were primarily kinematic, with negligible inertial effects. For watersheds with these conditions, these results suggest that the hydrodynamic equation solutions available in CCHE1D will produce nearly identical results, and that the only difference between the two solutions will be run time. However, for watersheds with shallow channel gradients, long travel distances, rapidly rising floodwaves, there may be significant

inertial effects and the choice of hydrodynamic equation would then become much more important.

SEDIMENT TRANSPORT CAPACITY EQUATIONS

The CCHE1D model has four options for sediment transport capacity: Wu, Wang, and Jia's (2000) formula, a modified form of Ackers and White's formula (Proffit and Sutherland, 1983), a modified form of Engelund and Hansen's formula with Wu, Wang, and Jia's (2000) hiding and exposure correction factor (Wu and Vieira, 2002), and the SEDTRA module (Garbrecht, Kuhnle, and Alonso, 1995). As was expected, the Ackers and White equation did not function for the sediment sizes that were evaluated (Table 4-1), since the majority of the sediment load produced by the WEPP-H model is very fine sediments (e.g., less than 0.04 mm).

Since it was expected that the sediment transport capacity equations would produce results with high variability, a total of 74 runoff events were used in this analysis. As expected, the remaining sediment transport capacity equations produced dramatically different sediment transport rates (Table 5-16, Figure 5-16). Both the Wu, Wang, and Jia (2000) and Engelund and Hansen (1967) equations produced peak sediment transport rates that were entirely within the range of observed values for the 74 events (Table 5-16). All three equations produced peak sediment transport rates that were significantly greater than observed, with the Wu, Wang, and Jia equation producing results that were closest to observed (Table 5-17). The SEDTRA equations predicted sediment transport rates that were the most divergent from observed values (Table 5-17).

Table 5-16. Average, maximum, and minimum percent difference from original peak total sediment concentration for selected sediment transport equation options, for 74 selected runoff events at South Fork Caspar Creek, CA.

Sediment Transport Capacity Equation	Peak Sediment Concentration (mg/L)		
	Average	Maximum	Minimum
Observed	289	3,117	3.1
Wu, Wang, Jia (2000)	468	2,014	1.0
SEDTRA (1995)	864	5,633	1.0
Engelund and Hansen (1967)	772	2,547	1.0
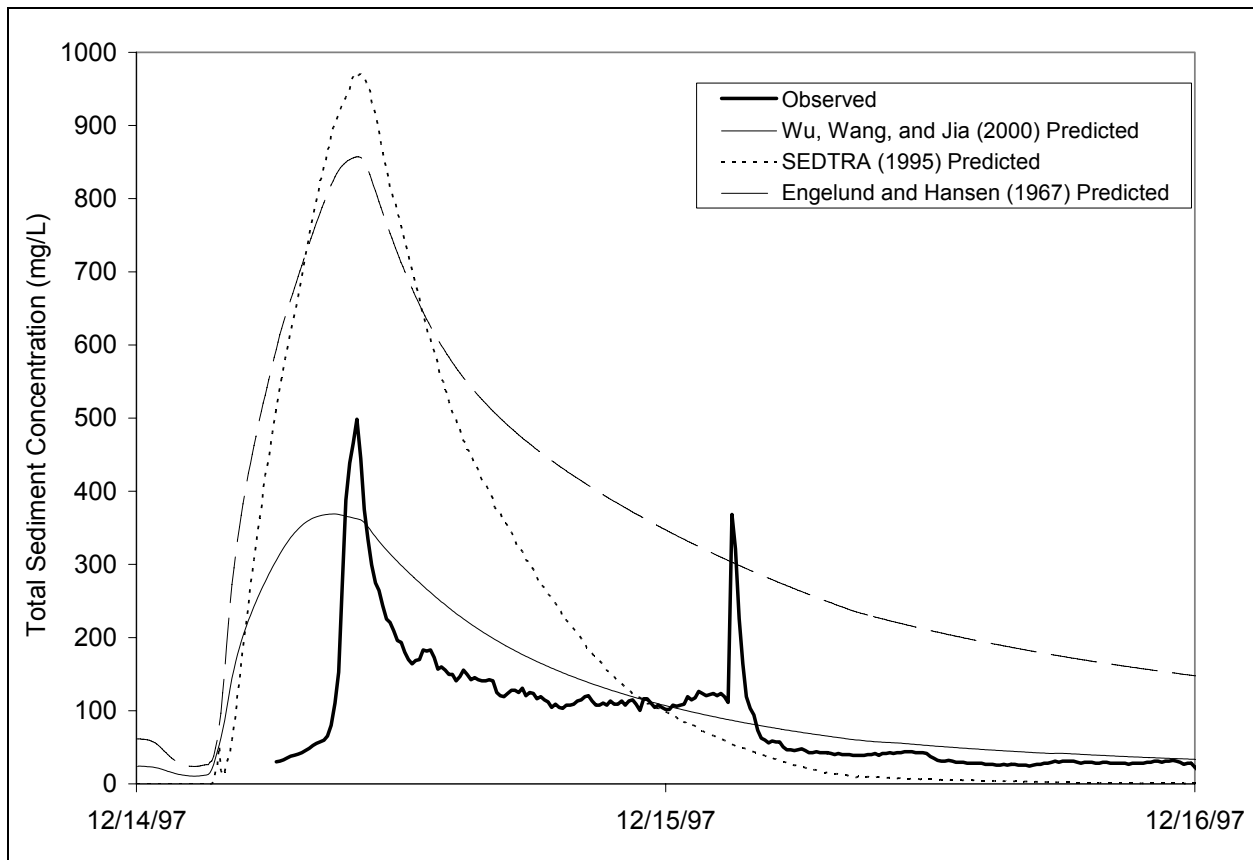
Figure 5-16. Example differences in sediment graphs for three sediment transport capacity equation options available in CCHE1D, for a selected runoff event in South Fork Caspar Creek, CA.

Table 5-17. Average, maximum, and minimum percent difference from observed peak total sediment concentration for selected sediment transport equation options, for 74 selected runoff events at South Fork Caspar Creek, CA.

Sediment Transport Capacity Equation	Percent Difference From Observed Peak Total Sediment Concentration			Nash Sutcliffe Coefficient
	Average	Maximum	Minimum	
Wu, Wang, Jia (2000)	622	18,363	13.3	-0.37
SEDTRA (1995)	1,667	72,053	3.6	-4.5
Engelund and Hansen (1967)	1,113	28,505	2.8	-1.4

It was determined in Chapter Four that the differences between predicted and observed sediment transport rates were largely due to over-predicted sediment loads by the WEPP-H model. As such, it was expected that the CCHE1D model would over-predict sediment loads, regardless of which sediment transport capacity equation was used. What this analysis has demonstrated is that under the conditions modeled, the Wu, Wang, and Jia sediment transport capacity equation consistently produces results that are closer to observed values when compared to the other options available in the CCHE1D model. The SEDTRA and Engelund and Hansen equations produce sediment transport rates that are consistently higher than the Wu, Wang, and Jia equation. Although it is unknown how each of these equations would perform when the upland erosion rates are simulated accurately, it is expected that the Wu, Wang, and Jia equation would produce sediment transport rates that are closer to observed values under the conditions simulated.

SOIL SATURATED HYDRAULIC CONDUCTIVITY

For the Caspar Creek Experimental watershed, soil surveys indicate that soil permeability (i.e., the term used in soil surveys to measure effective saturated hydraulic conductivity (Brady, 1990)) ranges between 15 and 150 mm/hr. To assess the changes in water discharge and

sediment load due to changes in soil saturated hydraulic conductivity (KSAT), erosion simulations were conducted with the following values of KSAT within the observed range: 15, 20, 25, 50, 100, and 150 mm/hr. Two additional simulations were conducted with KSAT values of 5 and 10 mm/hr to assess erosion characteristics of soils that were artificially compacted (e.g., roads, skid trails, landings). Results of each scenario were compared to the scenario with a KSAT value of 50 mm/hr; the approximate value used in the calibration phase of this research.

Changes in KSAT produce significant changes in peak discharge rate, such that increases in KSAT produce decreases in peak discharge rate (Table 5-18). For the storms analyzed, there was a threshold of 25 mm/hr that produced significant changes in peak discharge rate (Figure 5-17). For KSAT values between 25 and 150 mm/hr, the peak discharge changes little with changes in KSAT, with an average change of 3 percent for the entire range (Table 5-19). For KSAT values below 25 mm/hr, the change in peak discharge increases nearly exponentially with a linear change in KSAT (Figure 5-17).

Table 5-18. Average, maximum, and minimum peak discharge rates for changes in soil saturated hydraulic conductivity, for 89 selected runoff events at South Fork Caspar Creek, CA.

Soil Saturated Hydraulic Conductivity (mm/hr)	Peak Discharge Rate (cms)		
	Average	Maximum	Minimum
5	1.74	8.39	0.04
10	1.65	8.27	0.04
15	1.60	8.24	0.04
20	1.57	7.21	0.04
25	1.56	7.20	0.04
50	1.55	7.19	0.04
100	1.55	7.17	0.04
150	1.54	7.16	0.04
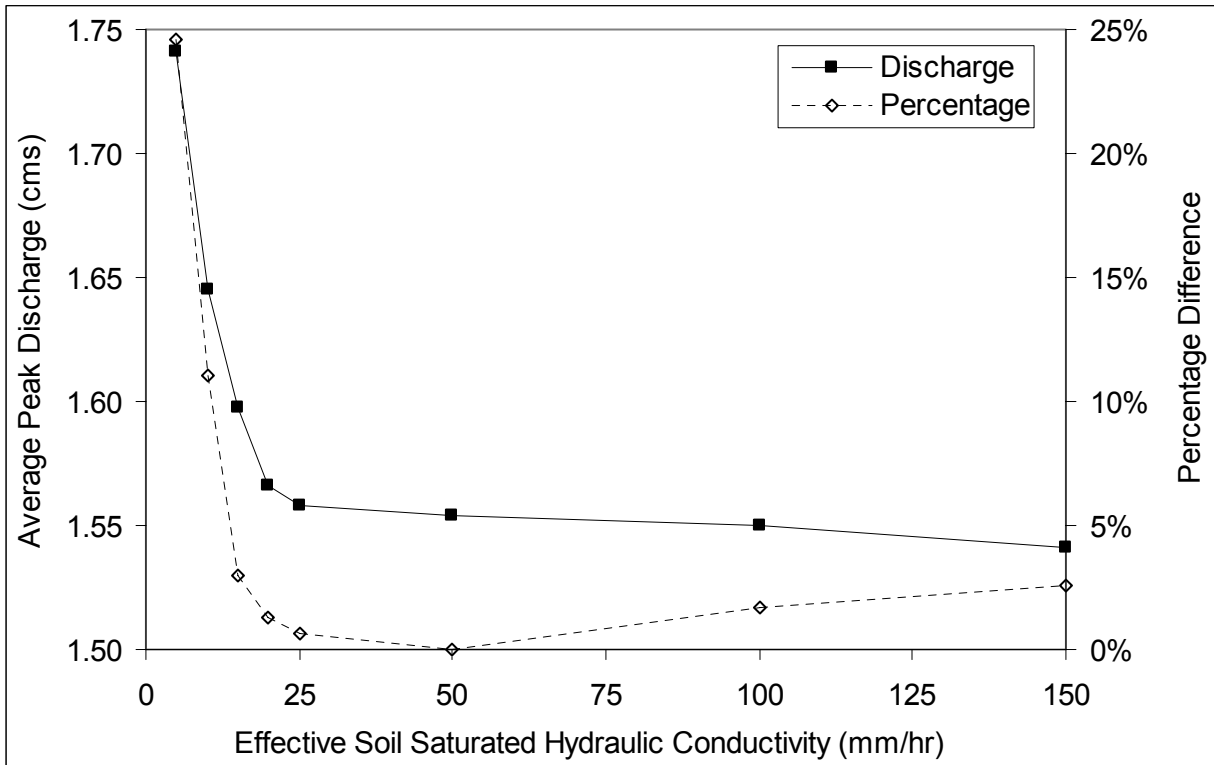
Figure 5-17. Differences in discharge rates for changes in soil saturated hydraulic conductivity

at South Fork Caspar Creek, CA.

Table 5-19. Average, maximum, and minimum percent difference from original peak discharge rates for changes in soil saturated hydraulic conductivity (original KSAT = 50 mm/hr), for 89 selected runoff events at South Fork Caspar Creek, CA.

Soil Saturated Hydraulic Conductivity (mm/hr)	Percent Difference From Original Peak Discharge Rate		
	Average	Maximum	Minimum
5	25	162	0.1
10	11	143	0.0
15	3.0	40	0.0
20	1.3	28	0.0
25	0.7	7.4	0.0
50	0.0	0.0	0.0
100	1.7	18	0.0
150	2.6	34	0.0
Between 5 and 25	24	160	0.0
Between 25 and 150	3.0	39	0.0

The percentage change in peak discharge rate also varied with increasing peak discharge rate. The lowest discharge rates had the highest relative changes, and the highest discharge rates had the lowest changes, with the percentage change in peak discharge rate decreasing exponentially as peak discharge rate increased (Figure 5-18). Since changes in KSAT significantly affect the volume of runoff, in the form of saturated overland flow, changes in runoff volume produce a commensurate effect on sediment erosion. As with discharge, total sediment concentration is increased when KSAT is decreased (Table 5-20). Similar to discharge, the differences in total sediment concentration are dramatically different (for given changes in KSAT) above and below 25 mm/hr (Figure 5-19). Above 25 mm/hr (KSAT), the differences in total sediment concentration are small, and are approximately 3.1 percent different between 25 and 150 mm/hr (Table 5-21). Below 25 mm/hr (KSAT), the differences in total sediment concentration are nearly exponential (Figure 5-19), and are approximately ten times the differences in discharge rate.
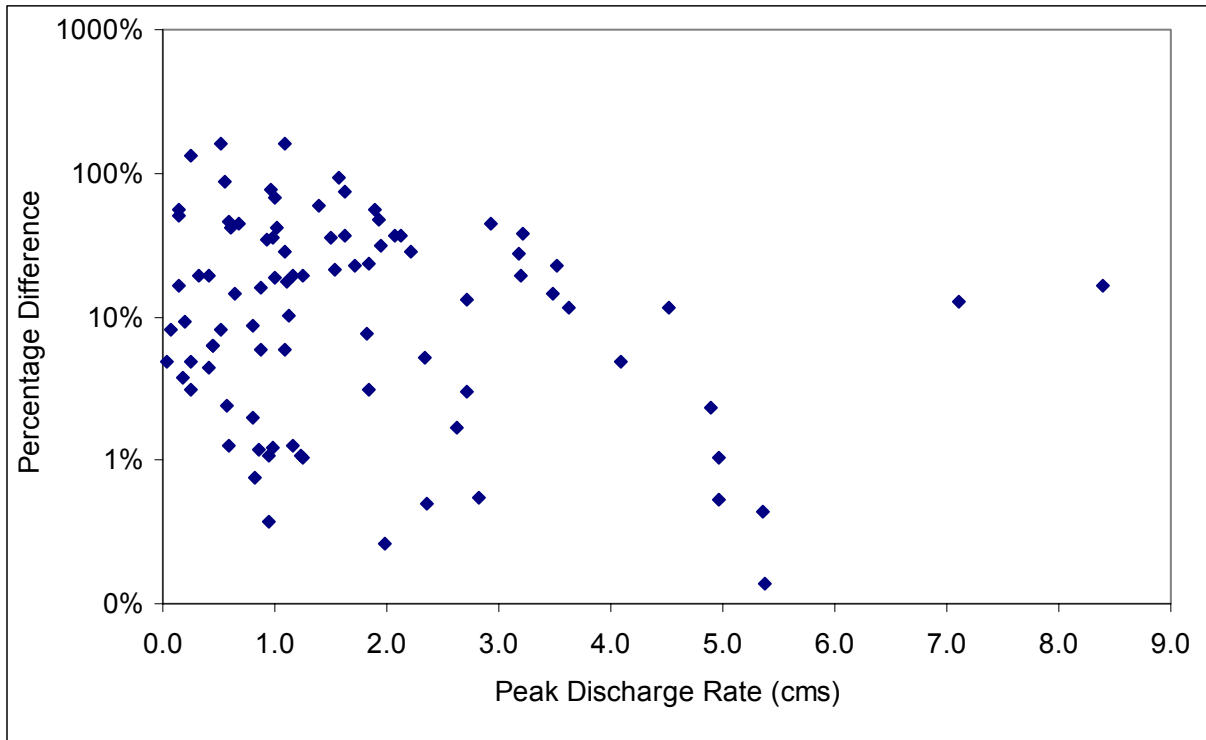
Figure 5-18. Percentage change in peak discharge rate for given peak discharge rates at South

Fork Caspar Creek, CA.

Table 5-20. Average, maximum, and minimum peak sediment concentration for changes in soil

saturated hydraulic conductivity, for 89 selected runoff events at South Fork Caspar Creek, CA.

Soil Saturated Hydraulic Conductivity (mm/hr)	Peak Sediment Concentration (mg/L)		
	Average	Maximum	Minimum
5	719	2,633	62
10	610	2,655	36
15	476	2,671	23
20	403	2,554	12
25	385	2,013	9
50	383	2,014	9
100	382	2,015	10
150	379	2,017	10
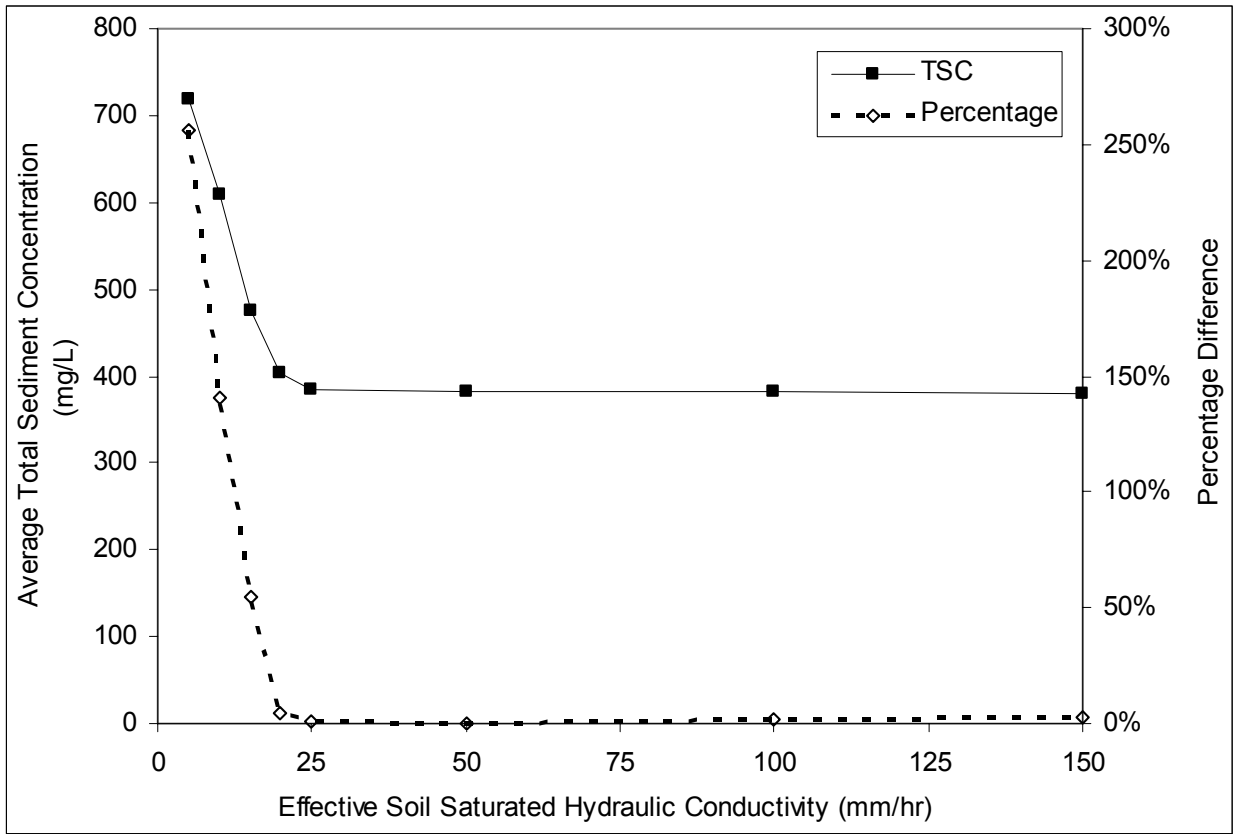
Figure 5-19. Differences in total sediment concentration for changes in soil saturated hydraulic

conductivity at South Fork Caspar Creek, CA.

Table 5-21. Average, maximum, and minimum percent difference from original peak sediment concentration for changes in soil saturated hydraulic conductivity (original KSAT = 50 mm/hr), for 89 selected runoff events at South Fork Caspar Creek, CA.

Soil Saturated Hydraulic Conductivity (mm/hr)	Percent Difference From Original Peak Discharge Rate		
	Average	Maximum	Minimum
5	256	2,816	0.1
10	141	891	0.0
15	55	727	0.0
20	4.7	85	0.0
25	0.8	4.8	0.0
50	0.0	0.0	0.0
100	2.1	18.9	0.0
150	2.6	29.6	0.0
Between 5 and 25	254	2,802	0.1
Between 25 and 150	3.1	33	0.0

The 'threshold' of 25 mm/hr is a site-specific value that is primarily a function of the precipitation volume and intensity for the selected events. None of the events assessed had its maximum inter-storm precipitation intensity greater than 25 mm/hr (Table 5-22). Of the 15 events, only three were less than 5 mm/hr (the lowest KSAT value assessed). The GAML model explicitly accounts for total incoming precipitation and incremental precipitation intensity when computing total water infiltration (Stone et al., 1995). Whenever the precipitation intensity is equal to or greater than the KSAT, a greater proportion of incoming precipitation becomes runoff. As such, the WEPP-H model is most sensitive when precipitation intensity is greater than or equal to the soil KSAT, and least sensitive when KSAT greatly exceeds precipitation intensity.

Table 5-22. Total precipitation, and average and maximum precipitation intensity for 15 selected events at South Fork Caspar Creek, CA.

Event Date	Precipitation (mm)	Average Precipitation Intensity (mm/hr)	Maximum Precipitation Intensity (mm/hr)
12/29/1995	123.7	3.4	17.9
12/30/1995	27.0	2.0	2.3
1/15/1996	50.5	3.5	7.4
1/16/1996	29.5	2.0	4.2
1/18/1996	33.7	6.3	14.4
1/19/1996	14.7	7.6	5.2
1/20/1996	27.7	3.8	5.8
1/23/1996	23.0	3.1	3.1
1/24/1996	51.4	3.6	9.5
1/27/1996	32.7	5.5	9.1
11/26/1997	114.2	3.6	22.6
11/29/1997	34.3	1.4	7.9
12/7/1997	34.1	6.0	8.9
12/8/1997	18.5	4.5	6.1
12/14/1997	49.2	6.5	16.3

SOIL DEPTH

For the Caspar Creek Experimental watershed, soil surveys indicate that depths to bedrock range between 500 and 1,525 mm. For these experiments, soil depths were varied in 250 mm increments through the observed range. For soil depths between 500 and 1,525 mm, the peak discharge rates (Table 5-23, Figure 5-20) and the peak sediment concentrations (Table 5-24, Figure 5-21) both decreased with increasing soil depth. As with soil saturated hydraulic conductivity, the percentage difference in peak discharge rate decreased exponentially with increasing discharge rate (Figure 5-22) suggesting that physiographic characteristics become less important in determining changes in discharge as the magnitude of discharge increases.

Table 5-23. Average, maximum, and minimum peak discharge for selected soil depths, for 89 selected runoff events at South Fork Caspar Creek, CA.

Soil Depth (mm)	Percent Difference From Original Peak Total Sediment Concentration		
	Average	Maximum	Minimum
1525	1.55	7.19	0.04
1250	1.69	7.19	0.04
1000	1.77	7.19	0.04
750	1.89	7.20	0.13
500	2.03	7.78	0.23
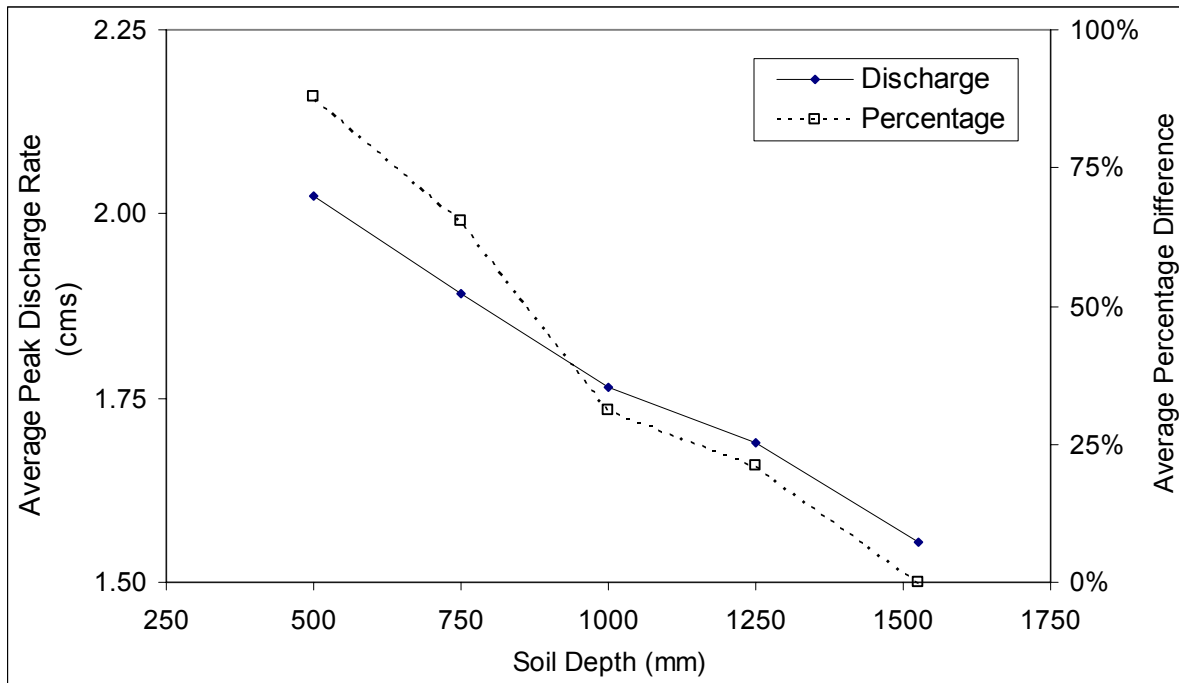
Figure 5-20. Percent difference in peak discharge rate for changes in soil depth in South Fork Caspar Creek, CA.

Table 5-24. Average, maximum, and minimum peak total sediment concentration for selected

soil depths, for 89 selected runoff events at South Fork Caspar Creek, CA.

Soil Depth (mm)	Percent Difference From Original Peak Total Sediment Concentration		
	Average	Maximum	Minimum
1525	383	2,014	9
1250	443	2,004	10
1000	479	2,009	10
750	611	2,222	30
500	652	2,252	37
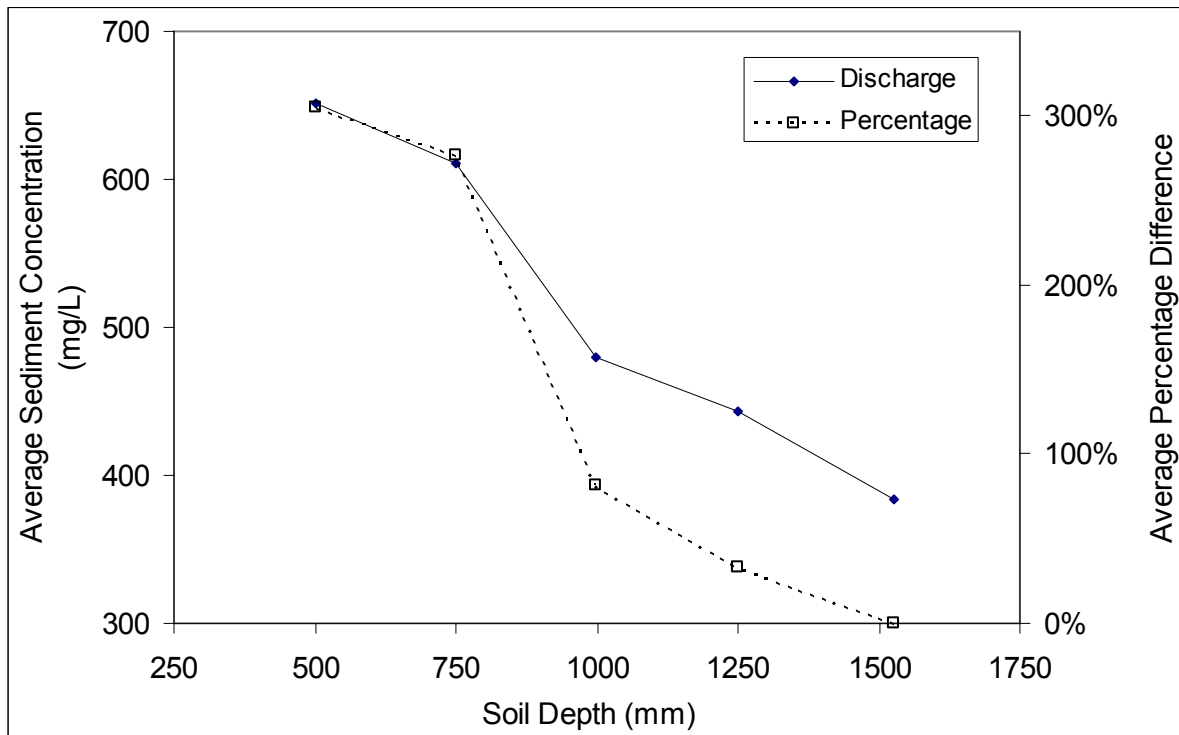
Figure 5-21. Percentage difference in total sediment concentration for changes in soil depth in

South Fork Caspar Creek, CA.
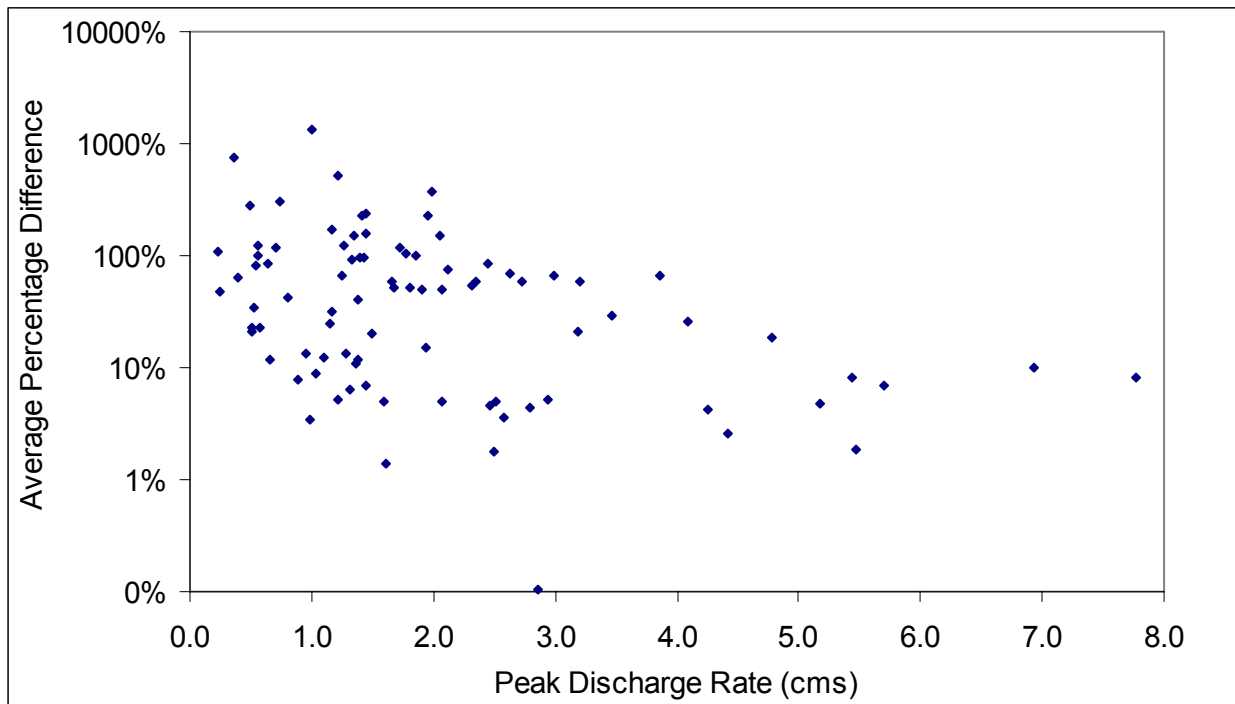
Figure 5-22. Percent difference in peak discharge rate by peak discharge rate for South Fork
Caspar Creek, CA.

Change in soil depth that resulted in differences in peak discharge also resulted in changes in peak sediment concentration (Table 5-24). When soil depths were decreased from 1,525 to 500 mm, the percentage increase in sediment concentration increased nearly linearly (Figure 5-21), with the average sediment concentration nearly doubling with a decrease in soil depth from 1,525 to 500 mm (Table 5-24). The percentage difference in sediment concentration, however, increases nearly exponentially with decreasing soil depth (Figure 5-21), with the largest change in sediment concentration occurring when soil depth is decreased below 1,000 mm.

These results suggest that runoff and sediment erosion are conditionally sensitive changes in soil depth. For the area assessed, when soil depths were greater than or equal to 1,000 mm there were minimal changes in either peak runoff rate or total sediment concentration.

146

However, when soil depths were reduced below 1,000 mm, both peak runoff rate and total sediment concentration increased dramatically. The GAML infiltration model computes the cumulative volume of incoming precipitation that infiltrates into the soil, with the remainder becoming saturated overland flow. By reducing the soil depth, the available water holding capacity of the soil profile is reduced. When the water holding capacity of the soil is reduced, the soil profile can become saturated sooner; resulting in a greater proportion of the incoming precipitation becoming saturated overland flow.

SOIL COVER

Soil surface cover percent was varied from completely bare (5%) to completely covered (100%) in increments of 25% to evaluate the changes in surface erosion and runoff. Changing soil surface cover had an observable, but not statistically significant ($p<0.80$, $\alpha = 0.05$), effect on peak discharge rate. Although the average peak discharge rate changes very little as cover percent is changed (Table 5-25), the percentage increase in peak discharge rate increases with decreasing ground cover (Figure 5-23). The greatest rate of change occurs when ground cover percent is decreased below 25 percent (Figure 5-23). As with analyses of soil depth and soil saturated hydraulic conductivity, changes in soil cover produce a nonlinear effect on peak discharge rate with increasing discharge rate (Figure 5-24). The greatest percentage change in peak discharge rate occurs for the smallest runoff events, with the effect decreasing exponentially as peak discharge rate increases (Figure 5-24).

Table 5-25. Average, maximum, and minimum peak discharge for selected ground cover

percentages, for 89 selected runoff events at South Fork Caspar Creek, CA.

Ground Cover (%)	Peak Discharge Rate (m^3/s)		
	Average	Maximum	Minimum
100	1.55	7.19	0.04
75	1.57	7.14	0.04
50	1.58	7.14	0.04
25	1.57	7.11	0.04
5	1.82	7.12	0.03
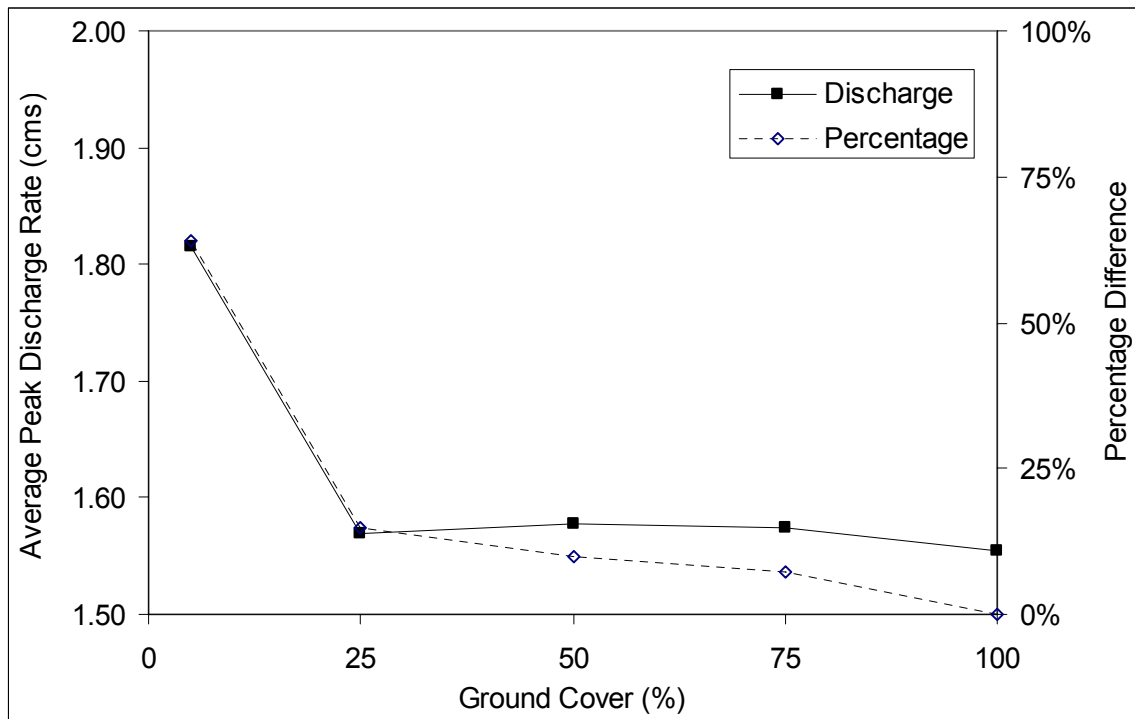
Figure 5-23. Percentage difference in average peak discharge rate (with percentage difference

from 100% cover) for changes in percentage ground cover from 100% cover, simulated at South

Fork Caspar Creek, CA.
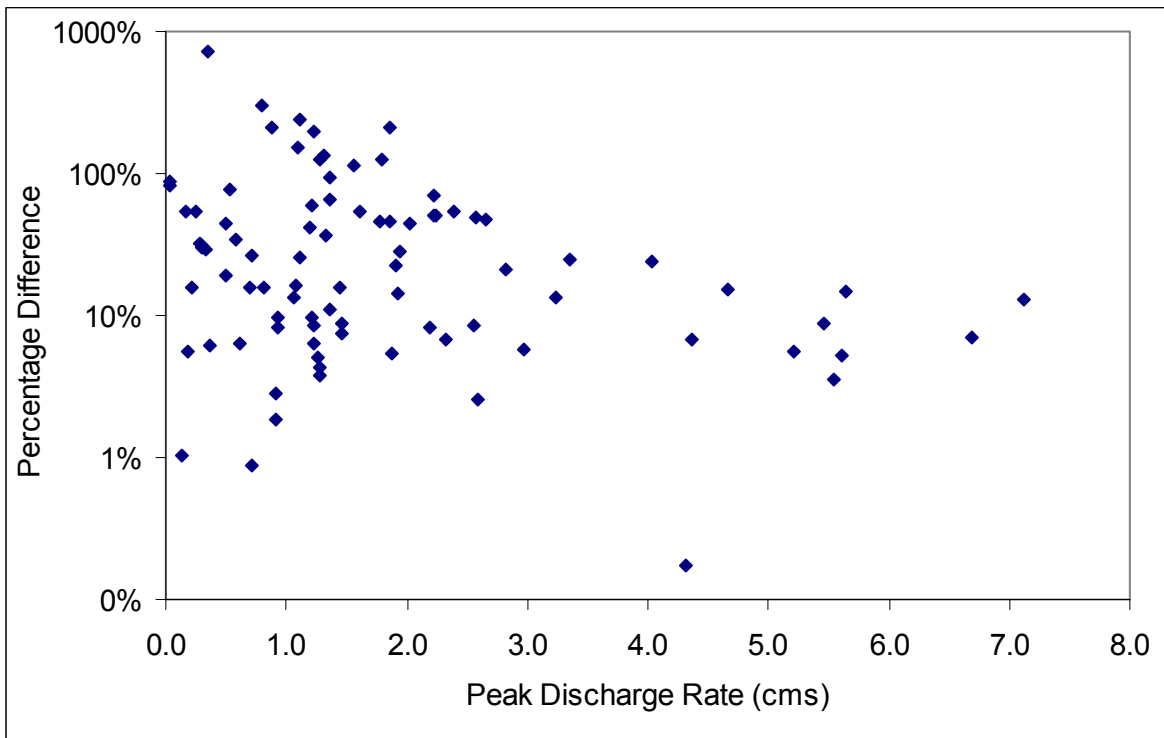
Figure 5-24. Percentage difference in predicted peak discharge rate for given peak discharge rates at South Fork Caspar Creek, CA.

As ground cover and live vegetation are removed, the rates of soil evaporation and vegetation evapotranspiration are altered. Removing soil cover increases soil evaporation by increasing soil temperatures, thereby increasing the vapor flux rate. Removing live vegetation decreases the rate of evapotranspiration, thereby increasing the volume of water in the surface soil. This results in soil saturation occurring sooner, and a greater volume of incoming precipitation becoming runoff. Since there is an observable increase peak discharge rate, it is likely that the changes in evapotranspiration rates (decreased) are significantly greater than the changes in soil evaporation rates (increased). These changes, however, are statistically insignificant.

As with most other analyses discussed in this chapter, small, linear changes in peak discharge rate produce large (i.e., two orders of magnitude) changes in total sediment concentration. Decreasing ground cover percent linearly produces exponentially increasing sediment concentration (Figure 5-25). A decrease in ground cover from 100 to 25 percent produced an average increase in sediment concentration of a factor of ten; and decreasing ground cover from 25 to 5 percent increased sediment concentration another factor of ten (Table 5-26).
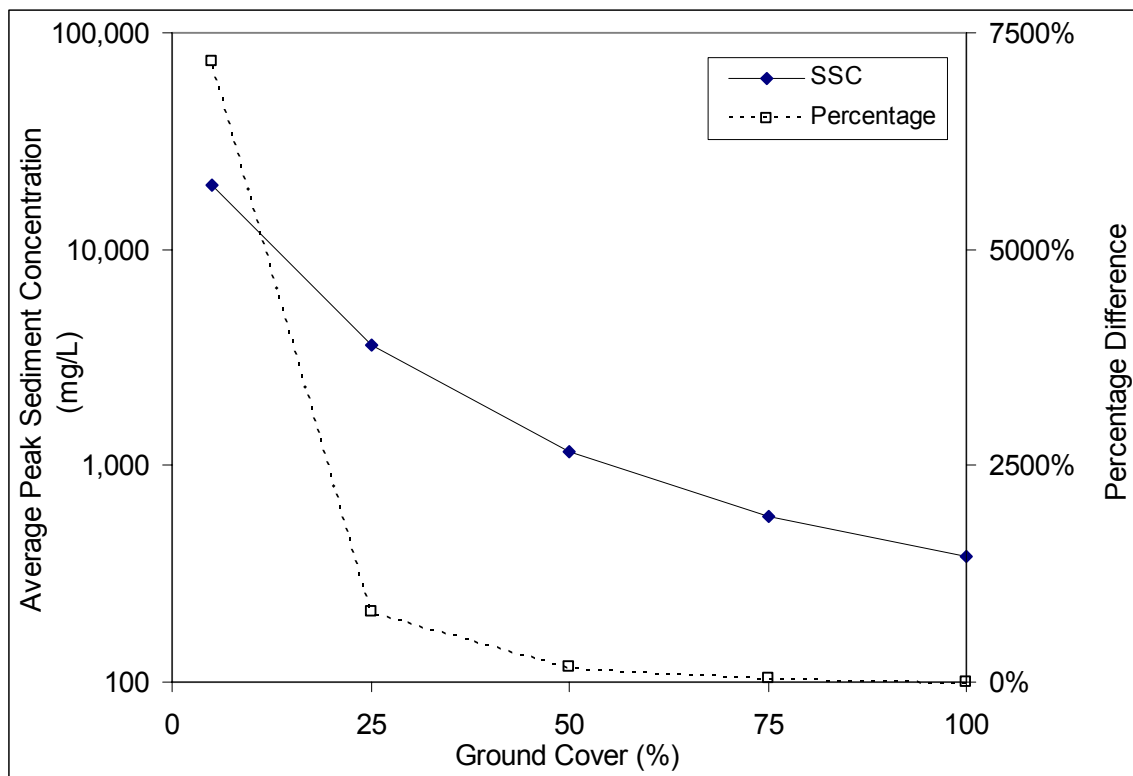
Figure 5-25. Changes in average peak sediment concentration (with percentage difference from 100% cover) for changes in percentage ground cover, simulated at South Fork Caspar Creek, CA.

Table 5-26. Average, maximum, and minimum peak total sediment concentration for selected ground cover percentages, for 89 selected runoff events at South Fork Caspar Creek, CA.

Ground Cover (%)	Peak Total Sediment Concentration (mg/L)		
	Average	Maximum	Minimum
100	383	2,014	9
75	577	3,267	14
50	1,169	7,485	15
25	3,635	20,883	18
5	19,796	137,173	115

Results of this analysis suggest that upland erosion rates are very sensitive to changes in ground cover, even though peak discharge rates are minimally affected by comparable changes in ground cover. Removing soil surface cover exposes mineral soil to the erosive forces of both incoming rainfall (i.e., splash erosion) and flowing water (i.e., hydraulic erosion); which dislodges soil particles. Since there is a greater volume of water moving over the soil surface, the dislodged particles can be transported down slope. With a decrease in cover, there is a decrease in surface roughness, leading to greater amounts of sediment particles remaining in suspension. The overall effect is to increase sediment detachment, transport, and delivery when soil surface cover is decreased; with the greatest effect occurring when the soil surface is nearly devoid of cover.

CONCLUSION

In this chapter, sensitivity to changes in input variables and run-time options specific to CCHE1D and WEPP-H were explored. For the CCHE1D model, three variables (i.e., channel geometry, Manning's roughness coefficient, bed material porosity) and two run-time options were explored (i.e., St. Venant equation solution, and sediment transport capacity equation). For the WEPP-H model, three input variables (i.e., saturated hydraulic conductivity, soil depth, ground surface cover) and no run-time options were explored. For the WEPP-H model, there are no run-time options that affect the results of simulations, since the user can only alter the input data or choose the data reports generated by the model. Based on inspection of the governing equations, it was expected that there would be minimal effects on discharge rates, but significant effects on sediment transport rates (Table 5-27).

Table 5-27. Expected rate of change in peak discharge rate and total sediment concentration for changes in CCHE1D-specific variables and run-time options.

Parameter Changed	Expected Rate of Change in Peak Discharge	Expected Rate of Change in Sediment Concentration
Channel Depth	None to Negligible	Nonlinear
Channel Width	None to Negligible	Nonlinear
Manning's N	None to Negligible	Nonlinear
Bed Material Porosity	Not Evaluated	Linear
St. Venant Equation Solution	None to Negligible	None to Negligible
Sediment Transport Capacity Equation	Not Evaluated	Nonlinear

Peak discharge rates are insensitive to any changes in CCHE1D-specific variables and run-time options (Table 5-28). In the range of discharge rates evaluated, peak discharge rates change less than one percent for all options explored. This result was expected for variables like channel geometry and bed roughness, but somewhat unexpected for the run-time option of St. Venant equation solution. Since discharge rates are supplied to CCHE1D as input boundary conditions, these values should not change appreciably just by changing channel conditions. Since the continuity equation cannot be violated (and still produce a valid solution), discharge should not change appreciably. The cross-sectional flow area and flow velocity may change significantly, but not the discharge rate.

However, using a different solution to the St. Venant equation was expected to give markedly different results since the diffusive wave solution ignores the inertial terms of the momentum equation. Since the channel network evaluated had several tributary junctions, it was expected that there would be significant changes in inertia. Since this effect was not observed, it is likely that the inertial terms are insignificant in comparison to the gravitational and pressure terms. This is likely true since the channel network has relatively steep channels (greater than 4.5%) and the flood waves analyzed had long durations (24 to 72 hours). For these conditions, the flood waves would be primarily kinematic, with negligible inertial effects.

Unlike peak discharge rates, sediment concentration is generally sensitive to changes in CCHE1D-specific variables and run-time options (Table 5-28). Sediment concentration is linearly sensitive to changes in channel geometry, bed roughness, and bed material porosity. The sediment transport capacity equation options, however, result in widely divergent sediment concentration results. For the conditions evaluated in Caspar Creek, the Wu, Wang, and Jia (2000) equation produces results that are closest to observed values; with a large portion of the error due to over-predicted sediment loads by WEPP-H. All sediment transport capacity equation options yielded results that were significantly greater (on the average) than observed

values; but the SEDTRA and Engelund and Hansen equations were approximately an order of magnitude greater than the Wu, Wang, and Jia (2000) equation.

Table 5-28. Sensitivity of peak discharge rate and total sediment concentration to changes in CCHE1D-specific variables and run-time options.

Variable or Option	Range of Values Or Options Available	Peak Discharge Rate Sensitivity	Sediment Concentration Sensitivity
Channel Depth	-50% to +100%	1. Insensitive; 2. Discharge decreases for both increase and decrease in channel width; 3. 0 to -0.16%	1. Linearly Sensitive; 2. Sediment concentration increases with increasing average depth; 3. 0 to 16%
Channel Width	-50% to +100%	1. Insensitive; 2. Discharge decreases for both increase and decrease in channel width; 3. 0 to -0.21%	1. Linearly Sensitive; 2. Sediment concentration decreases with increasing width; 3. 0 to 12%
Manning's N	-50% to +100%	1. Insensitive; 2. Increasing roughness decreases peaks; 3. Increasing roughness increases time to peak; 4. +0.6% to -0.7%	1. Linearly Sensitive; 2. Increasing roughness decreases sediment concentration; 3. +11% to -17%
Bed Material Porosity	1) Komura and Simons (1967); 2) Han and Wang (1981); 3) Constant: 0.10 to 0.40	Not Evaluated	1. Linearly Sensitive; 2. Increasing porosity decreases sediment concentration; 3. 0 to 20%
St. Venant Equation Solution	Dynamic Wave; Diffusive Wave	1. Insensitive; 2. 0.0014% difference	1. Insensitive; 2. 0.11% difference
Sediment Transport Capacity Equation	1) Wu, Wang, and Jia (2000); 2) SEDTRA (1995); 3) Engelund and Hansen (1967)	Not Evaluated	1. Very Sensitive; 2. 622 to 1,667% different from observed

Since predicted sediment concentration is linearly sensitive to most of the CCHE1D-specific variables, reasonable care should be given when estimating the values used in the model. For example, using regional hydraulic geometry relations to estimate channel dimensions provides an efficient and reasonably accurate method for generating needed data at unmeasured channel locations. These data may be in error by up to a factor of two for any cross-section location. Since sediment concentration is linearly sensitive to changes in channel geometry, knowing the error in cross-section geometry dimensions provides the bounds in the potential error in sediment concentration. If an increase in accuracy is desired, measured cross-section data can be used in conjunction with regional hydraulic geometry to reduce the error associated with these measurements.

In general, the governing equations defining flow rates and sediment erosion in WEPP-H are nonlinear, and it is expected that changes to any of the variables in these equations would produce nonlinear changes in both peak flow rates and sediment concentration (Table 5-29). However, due to the interdependence of variables in these equations it is not possible to predict the precise changes mathematically.

Table 5-29. Expected rate of change in peak discharge rate and total sediment concentration due to changes in WEPP H-specific variables and run-time options.

Variable	Expected Rate of Change in Peak Discharge	Expected Rate of Change in Sediment Concentration
Soil Saturated Hydraulic Conductivity	Nonlinear	Nonlinear
Soil Depth	Nonlinear	Nonlinear
Soil Cover	Nonlinear	Nonlinear

Peak discharge rates are conditionally sensitive to changes in WEPP H-specific soil property variables. In general, changes in saturated hydraulic conductivity, soil depth, and soil cover produce linear changes in peak discharge rates (Table 5-30). Decreases in any one of these variables results in increases in peak discharge rates. For the climatic conditions evaluated at Caspar Creek, decreases in saturated hydraulic conductivity below 25 mm/hr or decreases in soil cover below 25% both result in exponential increases in peak discharge rates. For saturated hydraulic conductivity, the threshold of 25 mm/hr was significant because of intensity of precipitation in the coastal, northern California region (which was less than 25 mm/hr for all storms evaluated). For soil cover, the threshold of 25% was significant because the effects of vegetation removal (i.e., decreased evapotranspiration reducing total soil water) begin to overwhelm the effects of reduced cover (i.e., increased soil evaporation in the surface horizon).

Sediment concentration is extremely sensitive to changes in WEPP H-specific soil property variables (Table 5-30). In general, changes in saturated hydraulic conductivity, soil depth, and soil cover produce exponential changes in sediment concentration (Table 5-30). Decreases in any one of these variables will result in significant increases in sediment concentration. Where changes in these variables produced peak discharge differences of less than 100 percent, sediment concentrations can be increased up to two orders of magnitude. The most sensitive of these variables is soil cover, which is the primary change that occurs during typically forest management activities.

The sensitivity of WEPP H-specific variables provides a useful method for calibrating the model to observed results, and for developing alternative management scenarios to evaluate. For example, at very low values of saturated hydraulic conductivity, soil depth, and soil cover, both peak discharge rate and sediment concentration increase rapidly. As such, shallow soils with low saturated hydraulic conductivity and no surface cover (e.g., roads and landings) would

have the most erosion. In these areas, it would be more important to have accurate values for

the input variables than it would be in areas that have not been mechanically compacted.

Table 5-30. Sensitivity of peak discharge rate and total sediment concentration to changes in
WEPP H-specific variables and run-time options.

Variable	Range of Values	Peak Discharge Rate Sensitivity	Sediment Concentration Sensitivity
Soil Saturated Hydraulic Conductivity	5 to 150 mm/hr	1. Conditionally Sensitive; 2. Linear increase above threshold (0 to 3% increase); 3. Exponential increase below threshold (0 to 25% increase); 4. Threshold is related to maximum incoming precipitation intensity	1. Conditionally Sensitive; 2. Linear increase above threshold (0 to 3% increase); 3. Exponential increase below threshold (0 to 250% increase); 4. Threshold is related to maximum incoming precipitation intensity
Soil Depth	500 to 1525 mm	1. Linearly sensitive; 2. Decreasing soil depth increases peak runoff rate; 3. 0 to 90%	1. Very Sensitive; 2. Decreasing soil depth increases sediment concentration exponentially; 3. 0 to 300%
Soil Cover	5% to 100%	1. Conditionally Sensitive; 2. Decreased soil cover increases peak runoff rate; 3. Linear increase above threshold (0 to 15% increase); 4. Exponential increase below threshold (15 to 65% increase); 5. Threshold is 25% ground cover	1. Very Sensitive; 2. Decreased soil cover increases sediment concentration exponentially; 3. 7,200 to 0%

The analyses completed in this chapter provided useful information for selecting run-time options to be used when modeling watershed hydrodynamics with CCHE1D. In addition, these analyses provide useful information for determining which variables are most important to determine more accurately with measured data. In general, peak discharge rates are much less sensitive to changes in variables and run-time options than sediment concentration; and both peak discharge rate and sediment concentration are more sensitive to changes in WEPP H-specific variables than CCHE1D-specific variables. As such, accurate determination of soil properties (i.e., KSAT, depth, cover) is more important than accurate determination of channel properties (i.e., depth, width, roughness, porosity) in achieving accurately modeled results.

CHAPTER SIX

SPATIAL SCALES FOR ASSESSING FOREST MANAGEMENT RELATED EROSION

ABSTRACT

It was found that the results of WEPP Hillslope erosion simulations became more divergent from actual values as the critical source area for first order channels increases. Critical source areas (CSAs) between 5 and 10 ha yield runoff rates that are not significantly different from observed values. As the CSA is increased, runoff rates and sediment loads become exponentially divergent from observed values. This finding addresses a fundamental question of watershed hydrologic modeling: At what assessment scale do hillslope-scale runoff and erosion processes give way to more dominant watershed-scale open channel flow and sediment transport processes? Although there is no definitive answer to this question, it was apparent from this research that the governing equations used to represent hillslope-scale erosion processes in the WEPP Hillslope model begin to break down for assessment areas greater than 10 ha. This area, therefore, represents the upper limit on CSA that can be used to define hillslope planes with the WEPP model.

To demonstrate the utility of the WEPP-2-CCHE modeling framework, it was used to evaluate the changes in runoff and sediment load that could be expected when a forested area has undergone a series of timber harvests (as might be done for a sediment TMDL analysis). It was found that timber harvesting can increase the peak rate and volume of runoff, but the effects are only significant for flow rates that occur several times per year. Sediment loads, however, were significantly increased for all flow rates, regardless of recurrence interval.

INTRODUCTION

The Water Erosion Prediction Project (WEPP) model is one of the few erosion simulation models (e.g., KINEROS2, EUROSEM) that simulates the physical processes of sediment erosion along the entire length of a hillslope. Sediment erosion processes are evaluated as a continuum from the ridge-top to the channel, using local physiographic information to simulate movement of water and sediment down the hillslope. Most erosion simulation models, (e.g., SHE, AGNPS, TOPMODEL, DHSVM, and SWAT), divide hillslope areas into uniform grid cells, using kinematic waves or transfer functions to simulate the movement of water and sediment between adjacent cells as they are moving down the hillslope. Both types of models are known to be sensitive to analytical scale (Singh and Woolhiser, 2002). That is, both runoff and erosion can vary significantly with small changes in grid size (e.g., (Vazquez et al., 2002)) or length of the runoff plane (e.g., (Baffaut et al., 1997)) used to represent individual hillslope elements.

The WEPP Watershed model and the WEPP-2-CCHE modeling system (developed for this research) both use a distributed-parameter, piecewise-aggregation procedure to simulate sediment transport from individual hillslope elements to the outlet of a pre-defined watershed. In this procedure, a watershed area is divided into unique hillslope elements and channel segments; erosion simulations are conducted separately (and independently) for each hillslope; water and sediment are delivered from the hillslope elements to the channel segments; and water and sediment are then transported through the channel network to the watershed outlet. In this type of modeling procedure there are two assumptions regarding physical processes and analytical scale: 1) the aggregation procedure appropriately represents the physical processes at the watershed scale, and 2) hillslopes are discretized such that all analytical areas are of the appropriate size to be analyzed by the hillslope erosion simulator.

The piecewise-aggregation procedure used here is the most common method for distributed-parameter watershed modeling (Singh and Woolhiser, 2002). This method is used by both hydrologic (e.g., SHE, DHSVM, CASC2D) and erosion simulation (e.g., KINEROS, AGNPS, SWAT, WEPP, TOPMODEL) models. It is assumed that if the individual hillslope elements are accurately simulated, that the response at the outlet will be a function of the sum of the individual parts. Since this is a generally accepted modeling procedure, it is not explored further, and the first issue is then the focus of this chapter.

What is the appropriate analytical scale for the WEPP-H model, such that the assumptions and basis of its' governing equations are not violated? When does the dominance of hillslope-scale processes (i.e., overland and rill flow) give way to the dominance of watershed-scale processes (i.e., open channel flow). These questions have no discrete answer, but are fundamental to modeling watershed hydrology (Singh and Woolhiser, 2002; Sivapalan, 2003b). The developers of the WEPP-H model and its interfaces only allude to these questions by giving general rules of thumb:

- "The erosion prediction procedure from this project is to apply to 'field-sized' areas or conservation treatment units. Although the size of a particular field to which the procedure applies will vary with degree of complexity within a field, the maximum size 'field' is about a section (640 acres)" (National Soil Erosion Research Laboratory, 2004).

- "The appropriate scales for application [of the WEPP model] are tens of meters for hillslope profiles, and up to hundreds of meters for small watersheds. For scales greater than 100 meters, a watershed representation is necessary to prevent erosion predictions from becoming excessively large" (Flanagan et al., 1995).

- "TOPAZ requires a critical source area (CSA) and a minimum source channel length (MSCL) to derive a channel network. The delineation of the channel network, as well

as the watershed boundary and sub-catchments, can be repeated until it matches the conditions in the user's area of interest" (Renschler, 2003).

With these 'guidelines', it is essentially up to the modeler to use 'professional judgment' to determine the appropriate analytical scale to use the WEPP-H model (or any other upland erosion model). This is clearly problematic, especially when a modeler wishes to evaluate an ungaged watershed with sparse or no monitoring data. As such, the objective of this analysis is to provide appropriate boundaries for the analytical scale to be used when using the WEPP-H model.

As was previously described, the WEPP-H model uses the TOPAZ program to define the hillslope and channel elements within a watershed to be analyzed. TOPAZ requires the user to define the minimum allowable area above the head of a first order channel (Garbrecht and Martz, 1995). This area, called the critical source area (CSA), is the basis for defining limits on the analytical scale (i.e., the length and width of hillslope elements). In practice, the CSA is set equal to the size of management units (or mapped sub-watersheds), or the CSA is changed until the derived channel network visually matches the observed channel network (Cochrane and Flanagan, 1999). For example, in Chapter Three (of this dissertation) a CSA of 25 ha yielded a derived channel network that matched the observed channel network.

Varying the CSA has several direct and indirect effects. Increasing the CSA directly generally decreases the number of hillslope and channel elements, and increases the average length and width of hillslope elements. By decreasing the number of hillslope and channel elements, the analytical complexity is reduced, thereby decreasing processing and computational time. Indirectly, when the CSA is greater than the size of management units, several management units with possibly disparate properties may be combined into one analytical unit. When this occurs, an empirical method of averaging spatial properties is

required to represent the combined area; which can over-simplify the spatial heterogeneity of physical properties.

However, the most significant effect of changing the CSA is altering the relative importance between hillslope-scale and watershed-scale processes. By increasing the CSA, the hillslope area (both length and width) is increased and the stream channel drainage density is decreased, thereby placing more emphasis on hillslope-scale runoff processes over watershed-scale channel processes. For larger hillslope areas, the length of rills is increased. Under these conditions, because rill lengths are longer and the source area adjacent to rills is greater, there is a greater accumulation of runoff volume in the down-slope direction; and rill erosion is markedly increased. Concomitantly, lateral subsurface flow becomes less important as a mechanism for generating stormflow in stream channels because subsurface flow is typically much slower than surface flow.

For example, in Chapter Three it was determined that the South Fork Caspar Creek (SFCC), an unmanaged watershed with minimal exposed surface soils, was known to have significant lateral subsurface flow and minimal saturated overland flow (Keppeler and Brown, 1998). To calibrate the modeled flow to observed runoff peak rates and volumes, the modeling domain CSA was set to 25 ha, because using CSA levels less than 25 ha produced peak runoff rates and flow volumes that were significantly less than observed. This CSA produced a channel network that matched the mapped network, but produced large hillslope areas drained by long rills. This resulted in accurate runoff volumes, but produced sediment loads that were too high because flow was calibrated first.

Decreasing the CSA has the opposite effect. Shorter hillslopes yield shorter rills, which produces lower rill-flow volumes since there is insufficient source area to generate concentrated surface flow areas. In this situation, lateral subsurface flow becomes a much more important mechanism for generating stormflow in stream channels since the stream channel drainage

density is greatly increased and flow paths from hillslopes to channels is greatly reduced. However, the current version of WEPP is known to produce extremely low lateral subsurface flow volumes (W. Elliot, U.S. Forest Service, Rocky Mountain Research Station, *personal communication*, January 10, 2005), resulting in inaccurate flow volumes and sediment loads. This limitation would affect analyses conducted in any area that has significant runoff volumes from lateral subsurface flow, subsurface pipe flow, or exfiltration. It is expected that this limitation in WEPP is more problematic for unmanaged areas with minimal saturated overland flow and exposed mineral soil areas than it is for managed areas with significant exposed soil subject to concentrated rill-flow.

Since it is unreasonable to assume that a watershed could be modeled as either a large hillslope composed of a series of rills (i.e., ignoring channel flow) or very dense channel network composed of very small hillslope elements (i.e., ignoring rill flow), it is necessary to determine the most appropriate hillslope analytical scale that can then be aggregated to the watershed scale. In doing so, the analytical scale for which the WEPP-H model accurately represents runoff and erosion processes can be determined.

OBJECTIVES

The purpose of this chapter is to determine the hillslope analytical scale (i.e., critical source area) that most accurately represents the hillslope erosion processes, when groups of hillslopes are aggregated to a single watershed. A second objective is to validate the coupled WEPP-2-CCHE model for a series of forest management scenarios. Using the validated modeling results, a potential use of the model is explored: assessing the primary impacts of forest management on runoff and sediment load by comparing the validated model results to results from the same area assuming that the area had not been managed.

METHODS

CRITICAL SOURCE AREA

For this analysis, the CSA was set at 5, 10, 15, 20, 25, and 50 ha to create six unique modeling domains. For each domain, soil properties were assigned the same values as in previous simulations (Table 3-2, in Chapter 3). The North Fork of Caspar Creek Experimental Watershed had several management units harvested between 1986 and 1991 (Figure 6-1). The management units were all clear cut, leaving partially-cut, forested buffers adjacent to the watercourses. Based on the assessment of bare mineral soil and tree retention in Henry (1998), the harvested units were given a variable amount of ground surface cover and canopy cover (Table 6-1) for the years following harvesting operations. A climate file was generated using observed climatic data for the period of 1986 thru 1995 (Table 6-2) to match the harvesting period.

Table 6-1. Ground cover, canopy cover, leaf area index, and biomass conversion ratio values used for WEPP-H erosion simulations on North Fork Caspar Creek, CA, 1986-1995 management scenario.

Years After Harvest	Ground Cover (%)	Canopy Cover (%)	Leaf Area Index	Biomass Conversion Ratio
Pre-harvest	100	100	30	300
Post-harvest	75	75	7.5	20
1	75	75	7.5	20
2	85	85	15	50
3	95	95	25	150
4	100	100	30	300

The WEPP-2-CCHE modeling framework was used as previously described in Chapters Three and Four, using the same run-time options (Table 4-2, in Chapter 4). Peak runoff rate, total daily runoff volume, and peak suspended sediment concentration were modeled and compared to measured values. Nash-Sutcliffe ratios were computed for each variable for each CSA evaluated to determine which value of CSA most accurately modeled observed values.
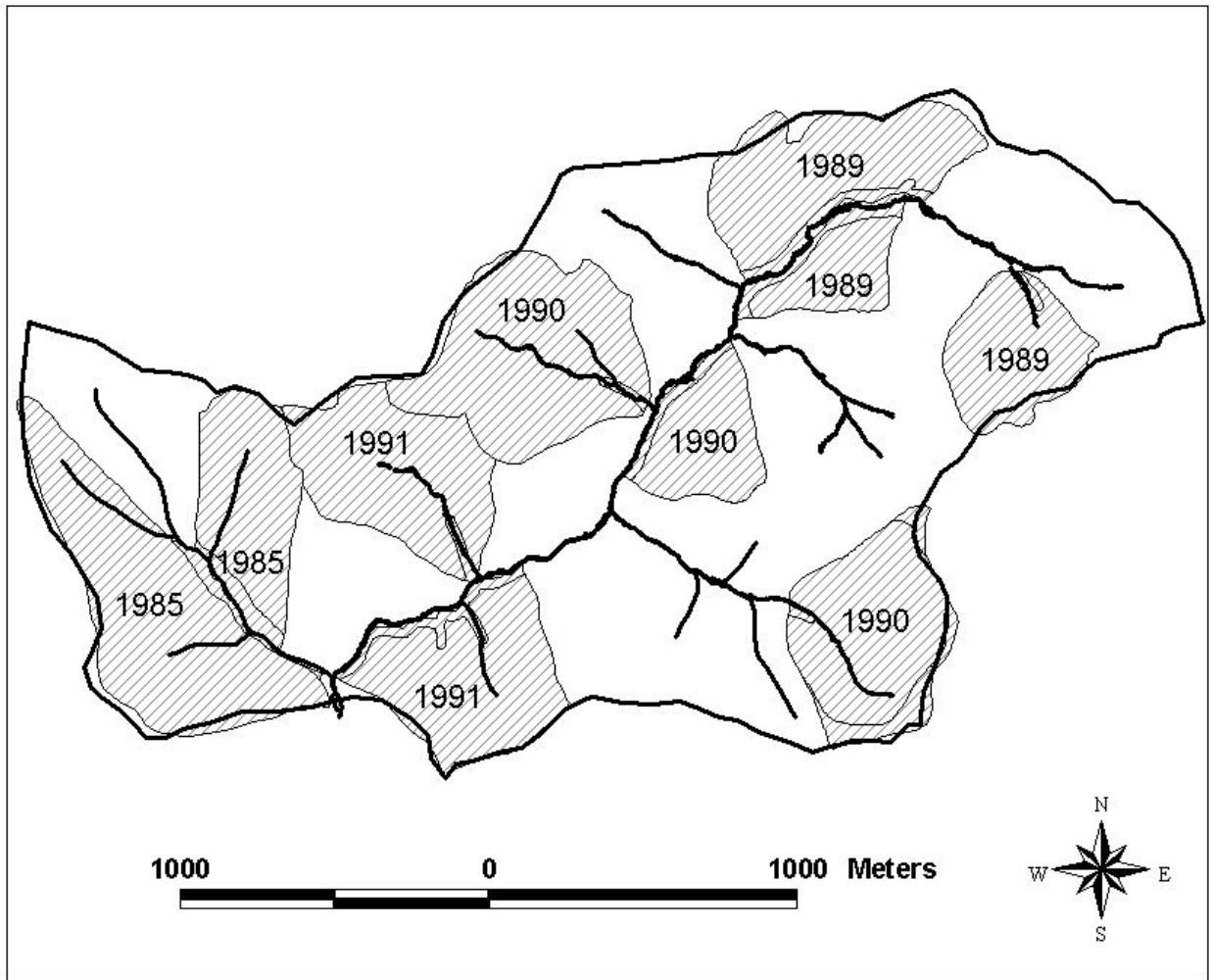
Figure 6-1. Timber harvest units by year for North Fork Caspar Creek, CA.

Table 6-2. Observed Monthly Average Climate Parameters for Caspar Creek, CA (1986-1995), used in WEPP Hillslope simulations.

Month	Maximum Temperature (C)	Minimum Temperature (C)	Solar Radiation (Langleys)	Total Rainfall (mm)
Jan	10.6	6.5	119	203
Feb	10.8	7.5	196	112
Mar	12.0	8.5	283	186
Apr	13.4	8.1	408	71
May	15.0	9.2	483	63
Jun	16.8	10.6	550	19
Jul	17.8	11.3	593	2
Aug	17.5	11.5	502	2
Sep	16.0	10.9	434	6
Oct	14.2	9.8	305	45
Nov	11.4	7.3	188	96
Dec	9.7	6.0	123	205

The WEPP-H model was run with the updated management file, climatic data, and the same soils as for the South Fork Caspar Creek. The CCHE1D model was run with the same settings as for previous analyses (Table 4-2). Modeled peak suspended sediment concentration, peak discharge rate, and total daily volume were compared to observed values for the analysis period (1986-1995). An ANOVA using a Tukey's multiple comparison test (Dean and Voss, 1999) was used to test for significant differences between modeled and observed results.

MANAGEMENT SCENARIO EVALUATION

To evaluate varying management scenarios with the WEPP-2-CCHE modeling framework, one only needs to alter the vegetation management for selected management units and re-run the WEPP-H model to produce new runoff and sediment load estimates for each hillslope. These results are then used to generate a new boundary condition file to run the CCHE1D model. The modeling domains remain the same and no changes to run-time options are necessary.

RESULTS AND DISCUSSION

CRITICAL SOURCE AREA

In the calibration phase of this project, the CSA was set to 25 ha for the SFCC watershed, since this CSA best defined the channel network (when comparing derived channels to mapped channels). The NFCC, however, has variably sized management units, the smallest being 10 ha and the largest being 77 ha (Henry, 1998). As such, to capture the individual properties of each management area, the CSA could be set anywhere in this range. To capture both the management units and the channel network, the CSA for the NFCC simulations were varied between 5 and 50 ha.

The derived channel network for the NFCC matched the mapped channel network when the critical source area was 5 ha (Table 6-3), and became less representative as the source area was increased (Figure 6-2). As expected, as critical source area was increased, the average hillslope area of delineated hillslope elements increased (Table 6-4), the average hillslope length increased (Table 6-5), and the average hillslope width increased (Table 6-6). The increase in both hillslope width and length is approximately linear as CSA increases (Figure 6-3), with hillslope length increasing by a factor of two and hillslope width increasing by a factor of three as CSA is increased from 5 to 50 ha.

Table 6-3. Number of delineated hillslopes and channel segments for selected

critical source areas in North Fork Caspar Creek, CA.

Critical Source Area (ha)	Number of Hillslopes	Number of Channels
5	88	35
10	53	21
15	33	13
20	33	13
25	28	11
50	13	5
Mapped	89	35
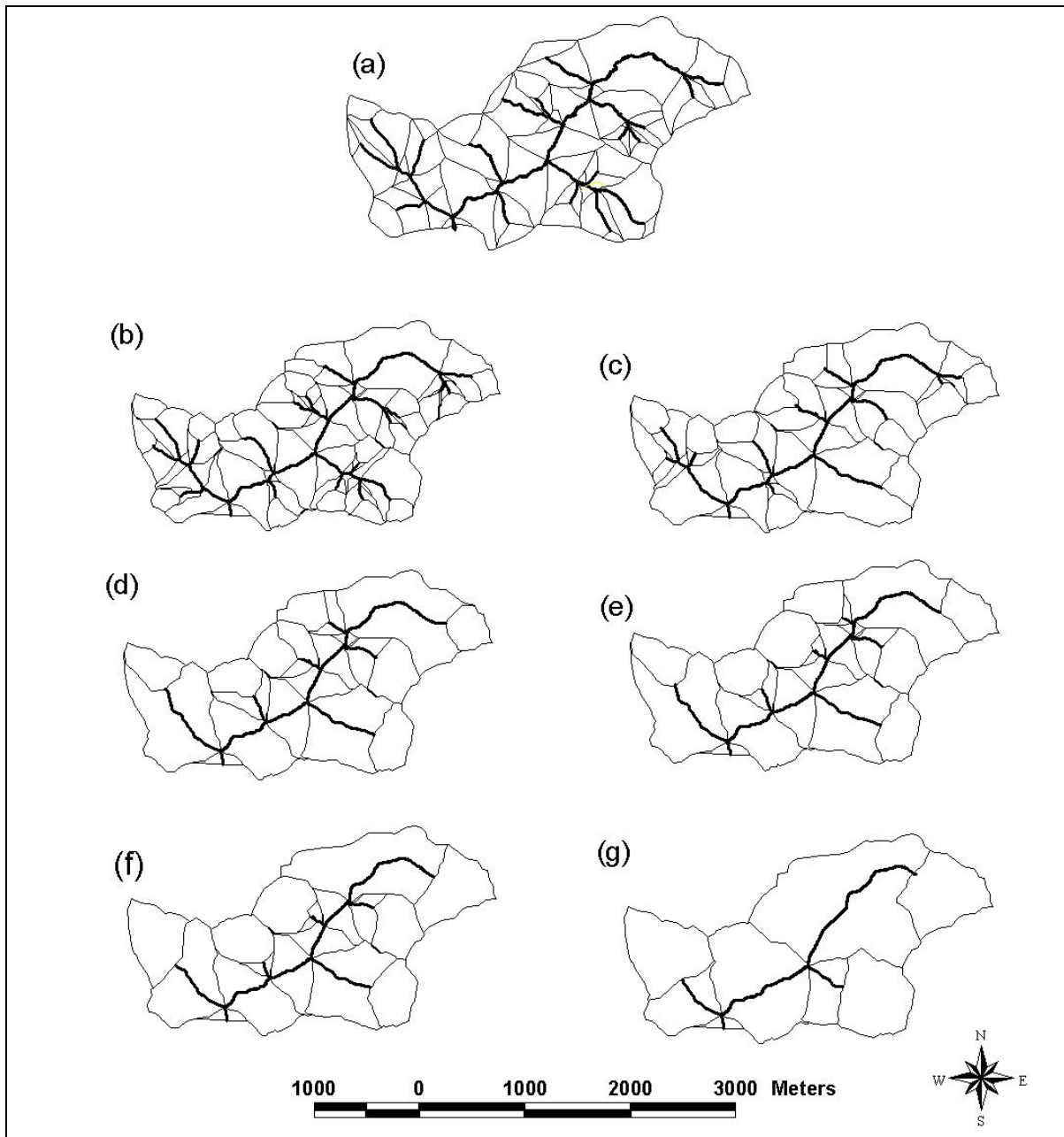
Figure 6-2. Delineated channel network and hillslope elements for varying critical source area, a) mapped network, b) 5 ha, c) 10 ha, d) 15 ha, e) 20 ha, f) 25 ha, g) 50 ha; in North Fork Caspar Creek, CA.

Table 6-4. Hillslope area for derived hillslope elements in North Fork Caspar Creek, CA, for varying critical source areas.

Critical Source Area (ha)	Hillslope Area (ha)		
	Average (standard deviation)	Maximum	Minimum
5	5.4 (6)	37	0.3
10	9.0 (8)	39	0.3
15	14.5 (12)	41	0.9
20	14.5 (12)	44	0.9
25	17.1 (15)	61	1.2
50	37.0 (30)	100	1.7

Table 6-5. Hillslope lengths for derived hillslope elements in North Fork Caspar Creek, CA, for varying critical source areas.

Critical Source Area (ha)	Hillslope Length (m)		
	Average (standard deviation)	Maximum	Minimum
5	174 (104)	429	22
10	216 (115)	451	20
15	253 (143)	486	58
20	263 (123)	442	60
25	278 (156)	564	58
50	379 (203)	674	113

Table 6-6. Hillslope widths for derived hillslope elements in North Fork Caspar Creek, CA, for varying critical source areas.

Critical Source Area (ha)	Hillslope Width (m)		
	Average (standard deviation)	Maximum	Minimum
5	281 (179)	1125	94
10	365 (231)	1125	119
15	480 (288)	1169	145
20	491 (306)	1303	147
25	525 (296)	1277	147
50	838 (532)	1805	147
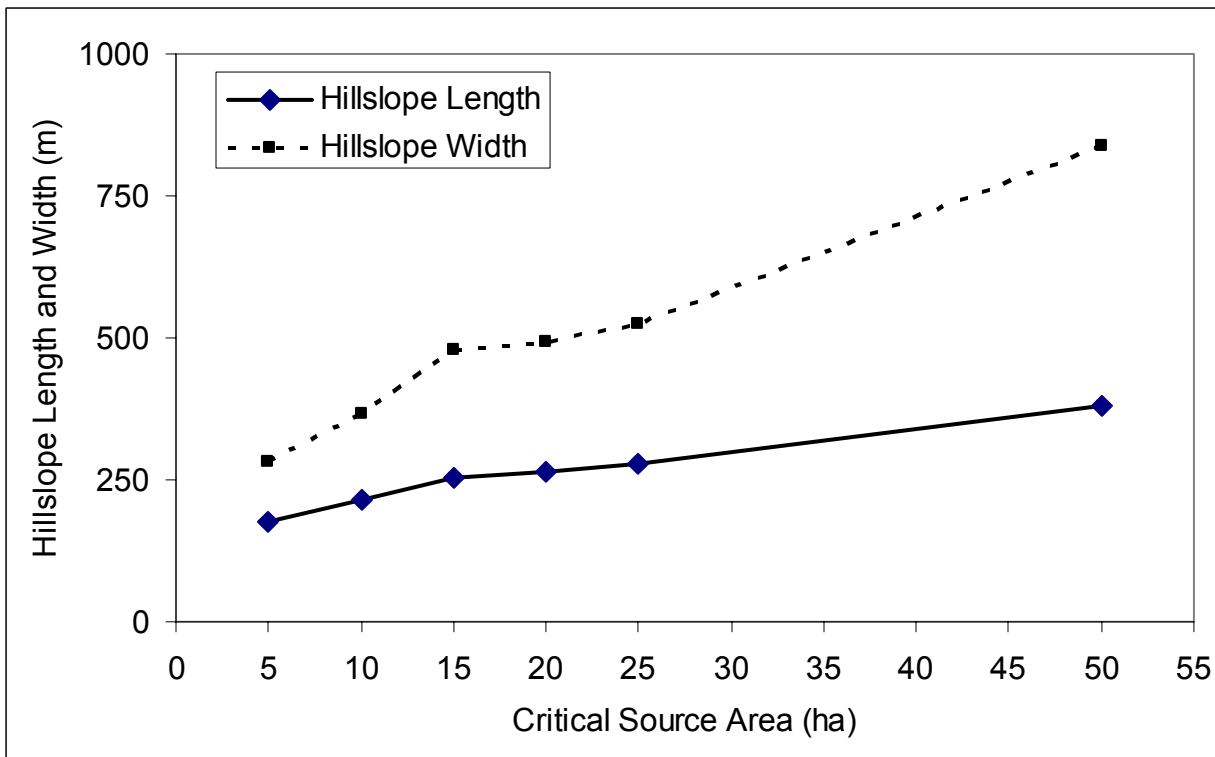
Figure 6-3. Hillslope length and width for varying critical source areas.

Changing the critical source area has a significant effect on modeled peak flow rate, total flow volume, and suspended sediment concentration. As the CSA is increased, modeled results for all three variables become more divergent from observed values. Peak flow rates were not significantly different from observed values when the CSA was either 5 or 10 ha, but were significantly greater for all CSAs above 10 ha (Table 6-7). For all CSAs evaluated, total daily flow volumes were within the same range as observed and had similar Nash-Sutcliffe coefficients, but only the 10 ha domain was not significantly different from observed values (Table 6-8). Although the 5 ha domain resulted in flow volumes that were significantly different from observed values, the 5 ha domain was not significantly different from the 10 ha domain, with each having nearly identical Nash-Sutcliffe model efficiencies. All CSAs evaluated had peak suspended sediment concentrations that were significantly different from observed values (Table 6-9). The 5 and 10 ha CSAs were the closest to observed values, with an average that was twice the observed average, the highest Nash-Sutcliffe coefficients (NS=-1.4), and ranges of values that were comparable to the observed range (Table 6-9).

Table 6-7. Modeled peak flow rates for varying critical source areas in North Fork Caspar Creek, CA.

Critical Source Area (ha)	Peak Discharge Rate (cms)			Nash-Sutcliffe Coefficient
	Average[*] (standard deviation)	Maximum	Minimum	
5	0.51 (0.9)	7.07	0.042	0.49
10	0.53 (0.9)	6.99	0.035	0.46
15	0.58** (1.1)	8.12	0.010	0.24
20	0.56** (1.1)	7.96	0.010	0.28
25	0.50** (1.0)	7.29	0.005	0.41
50	0.48** (0.9)	7.13	0.006	0.44
Observed	0.50 (0.7)	6.66	0.004	--

**Indicates value is significantly different from observed value (α=0.05).
*Sample size: n=502.

Table 6-8. Modeled total daily volume for varying critical source areas in North Fork Caspar Creek, CA.

Critical Source Area (ha)	Total Daily Volume (m³)				Nash-Sutcliffe Coefficient
	Average[*] (standard deviation)		Maximum	Minimum	
5	26,197**	(41,847)	306,512	3,611	0.48
10	27,208	(43,602)	303,392	2,999	0.49
15	28,911**	(50,631)	349,757	811	0.37
20	27,743**	(49,041)	340,370	808	0.39
25	24,330**	(44,086)	314,040	430	0.44
50	23,202**	(42,896)	304,091	529	0.45
Observed	30,234	(41,352)	356,911	358	--

**Indicates value is significantly different from observed value (α=0.05).
*Sample size: n=502.

Table 6-9. Modeled peak suspended sediment concentration for varying critical source areas in North Fork Caspar Creek, CA.

Critical Source Area (ha)	Peak Suspended Sediment Concentration (mg/L)				Nash-Sutcliffe Coefficient
	Average[*] (standard deviation)		Maximum	Minimum	
5	220**	(404)	2,816	13.76	-1.4
10	205**	(411)	2,860	3.09	-1.4
15	256**	(500)	3,398	1.70	-2.5
20	277**	(535)	3,594	1.70	-3.0
25	674**	(3,314)	44,539	0.84	-170
50	1,018**	(4,588)	44,573	0.05	-328
Observed	98	(256)	2,720	2.11	--

**Indicates value is significantly different from observed value (α=0.05).
*Sample size: n=237.

These results were not unexpected. The dominant mechanism that the WEPP-H model uses for sediment transport on hillslopes is rill flow (Foster et al., 1995), with one rill per unit width of hillslope. Sediment is transported from interrill areas via splash and sheet erosion, and is then transported downslope within the rills. In this conceptualization of hillslope erosion processes, as CSA is increased, the hillslope length is increased, the rill length is increased, and the rill density is increased (i.e., stream channels are represented as rills, increasing the total rill length per unit area). These effects have two direct effects: 1) flow volume in rills and sediment load delivered to rills are both increased due to the greater contribution area adjacent to any given rill, and 2) rill erosion is increased due to greater flow volumes producing greater shear stress.

These results also provide additional insight into the results obtained in Chapters Three and Four. The calibration phase of this project was completed using data from the SFCC watershed, the unmanaged watershed pair to NFCC. Flow volume was calibrated first (Chapter 3), followed by sediment load (Chapter 4). A CSA of 25 ha was first used to match the derived channel network to the mapped channel network. Using this CSA, accurate flow volumes in SFCC were modeled; noting that CSAs below 25 ha yielded flow volumes that were significantly lower than observed. This resulted in sediment loads that were approximately twice those observed, because rill erosion was predicted where subsurface flow actually occurred.

The problem with the calibration was that the mechanism for delivering the water to the channels was incorrect. In forested areas of coastal, northern California, the dominant source of flow from hillslopes to channels is lateral subsurface flow (Keppeler and Brown, 1998) and not saturated overland flow. By setting the CSA too high, the flow volumes were correct, but the sediment loads were too high. This illustrates a significant problem with the current WEPP-H model, and the necessity for correctly identifying the dominant hydrologic processes occurring in a watershed such that the appropriate hydrologic model is applied.

The WEPP-H model primarily delivers runoff from hillslopes to channels via surface flow processes (i.e., rill and sheet flow). The model does include lateral subsurface flow in its water balance computations, but the current algorithm is known to produce inaccurate results and is currently being re-coded (W. Elliot, U.S. Forest Service, Rocky Mountain Research Station, Moscow, ID, *personal communication*, January 10, 2005). Until this problem is corrected, using the WEPP-H model in areas where lateral subsurface flow dominates will: 1) dramatically under-predict flow if the CSA is set too low, and 2) dramatically over-predict sediment loads if the CSA is set too high.

MANAGEMENT SCENARIO EVALUATION

To demonstrate the potential uses of the WEPP-2-CCHE modeling framework, the vegetation management regime for NFCC was altered from the known management regime to a scenario where the entire watershed was given the characteristics of an uncut forest (see Chapter 3 for description). The 10 ha CSA modeling domain was chosen for this analysis since it produced the most accurate results for peak load (Figure 6-4), total volume (Figure 6-5), and suspended sediment concentration (Figure 6-6). For the 502 events predicted in the 10-year period, predicted peak discharge rates were reasonably correlated with observed values (NS = 0.46, r^2 = 0.65) and predicted daily runoff volumes were reasonably correlated with observed values (NS = 0.49, r^2 = 0.58). Predicted peak total sediment concentrations, however, were not well correlated with observed values (NS = -1.4, r^2 = 0.06). Since these predicted values were closest to observed values, when compared to all of the other CSA modeling domains, these values were used to represent the sediment load for the management scenario.

a)

b)
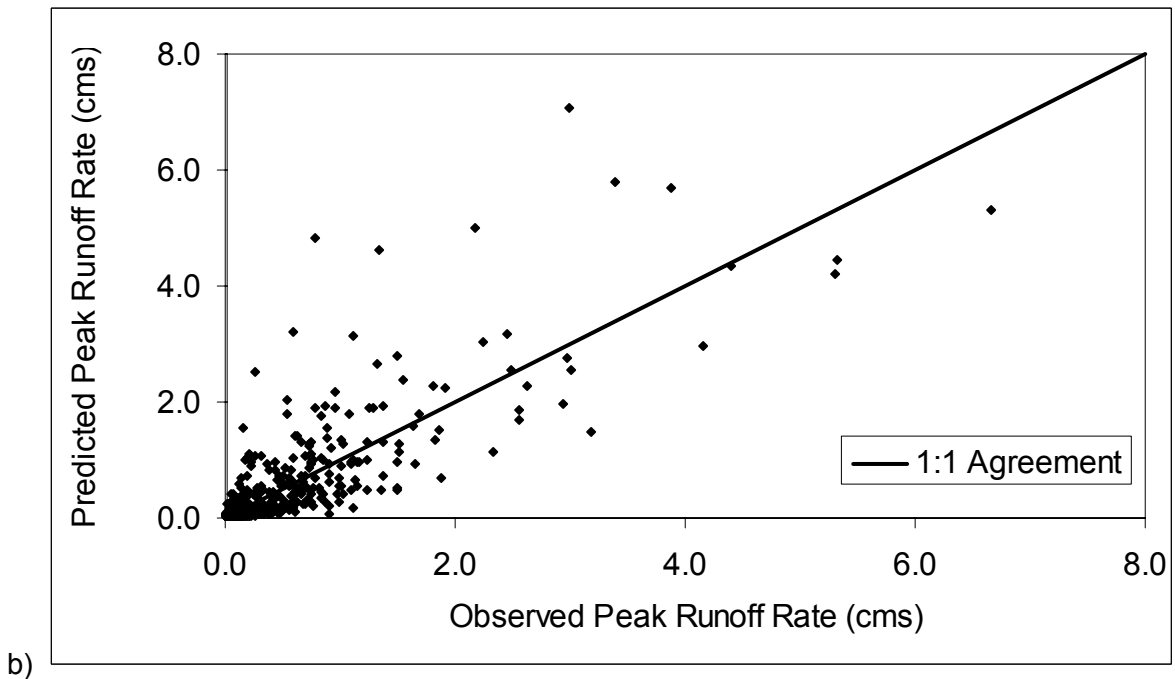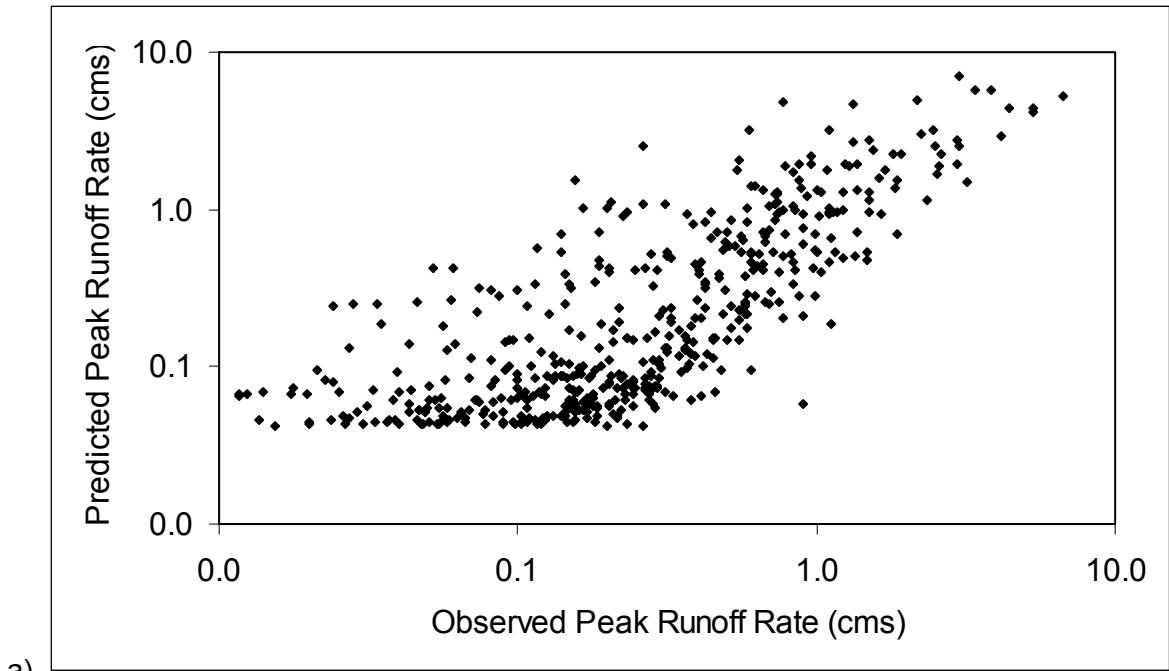
Figure 6-4. Observed vs. predicted peak runoff rates for North Fork Caspar Creek (1986-1995), a) logarithmic axes, b) arithmetic axes.
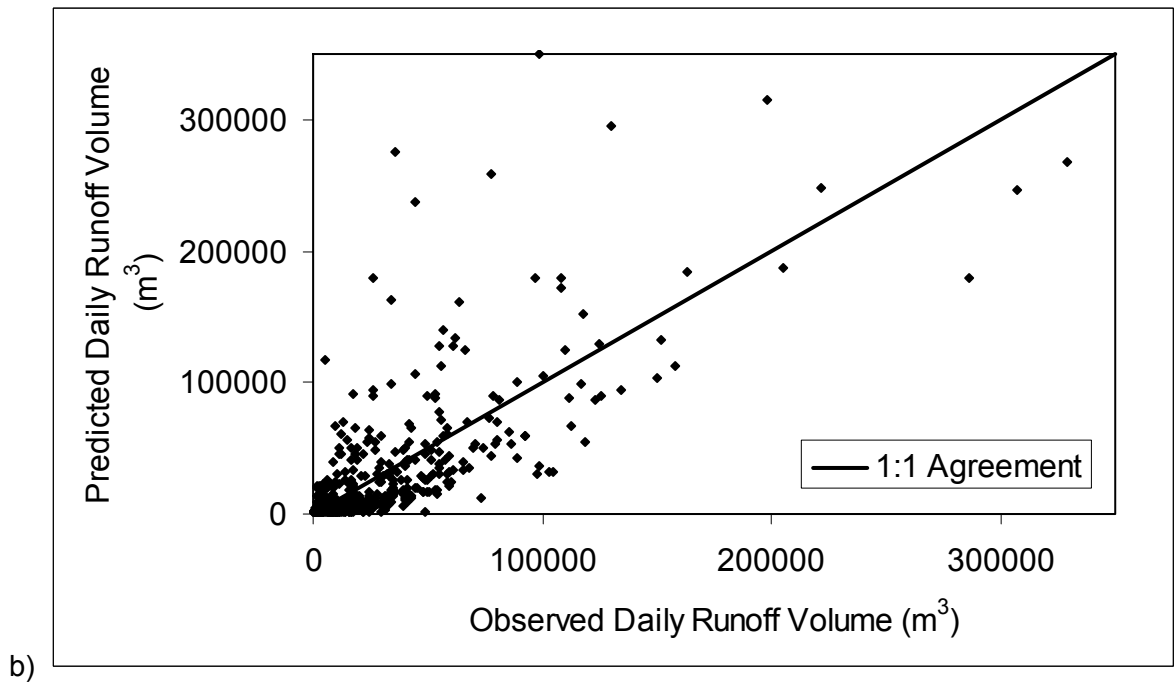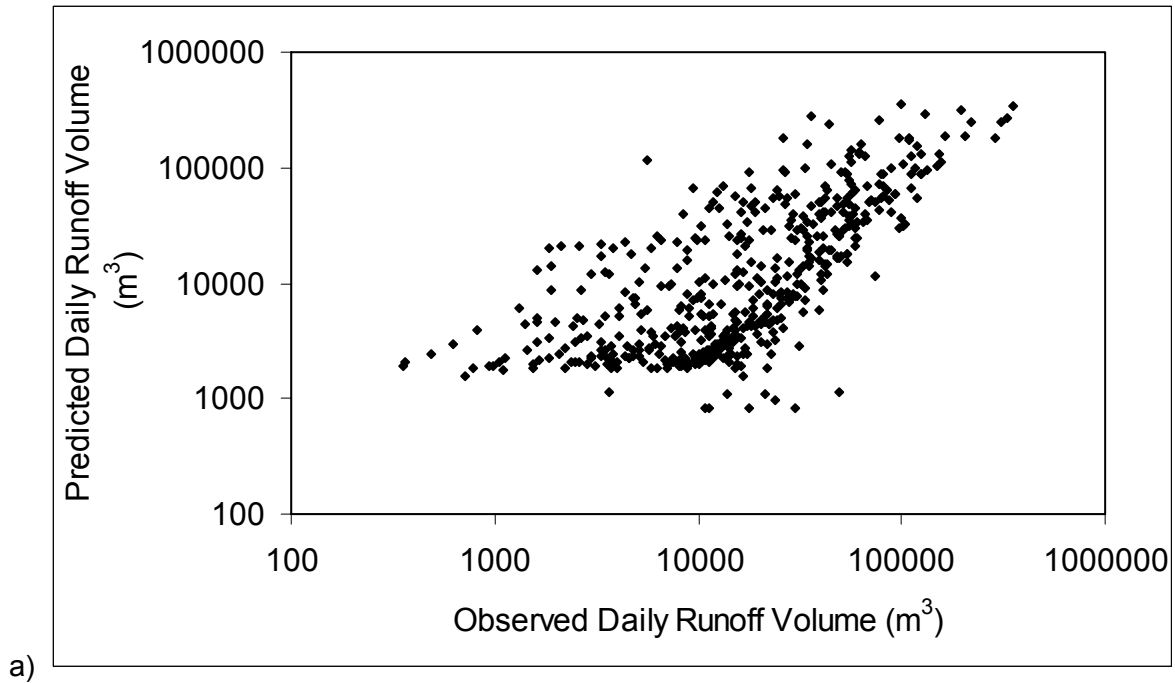
Figure 6-5. Observed vs. predicted daily runoff volumes for North Fork Caspar Creek (1986-1995), a) logarithmic axes, b) arithmetic axes.
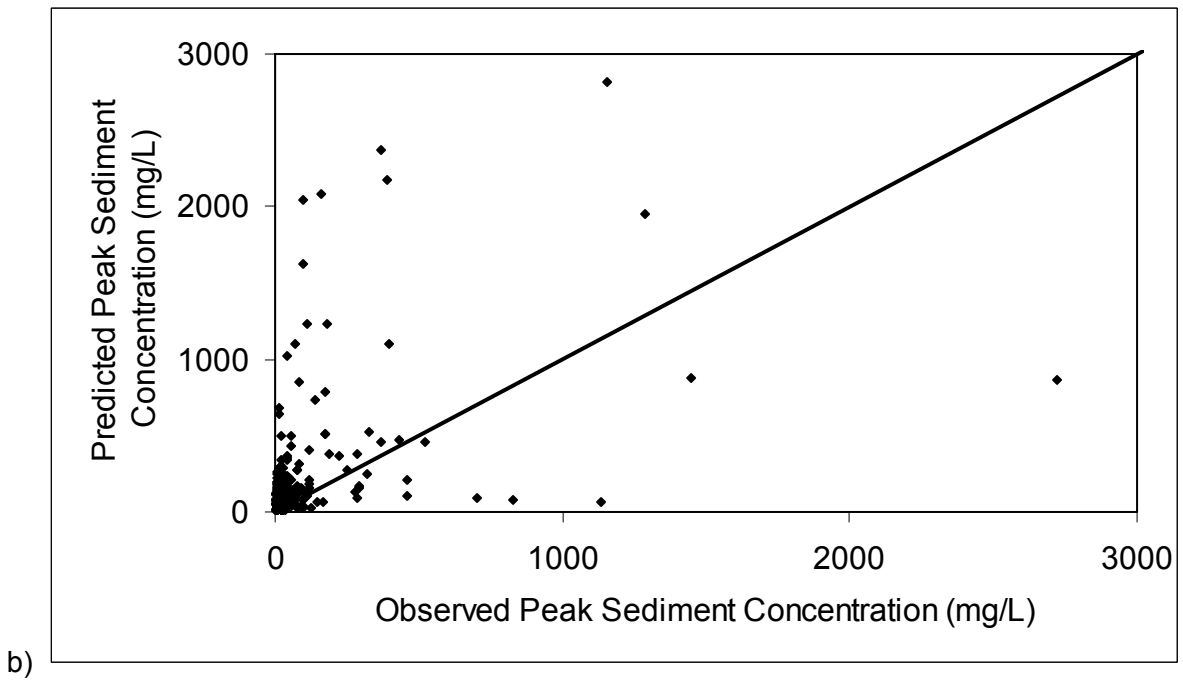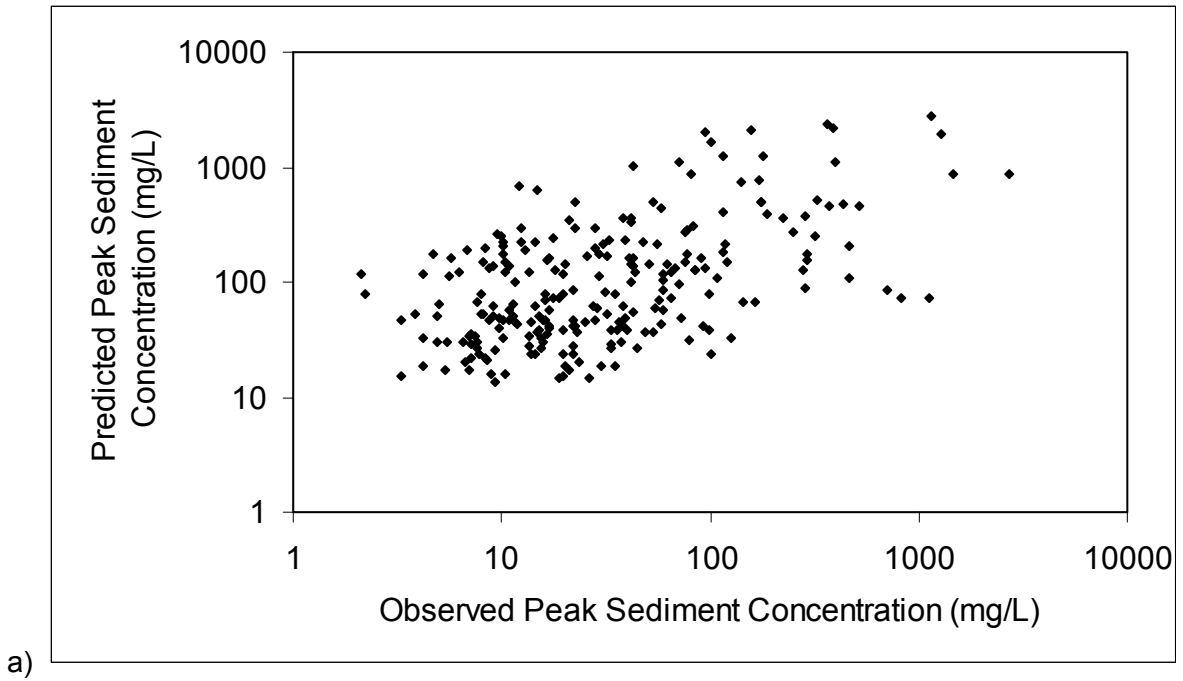
Figure 6-6. Observed vs. predicted peak sediment concentration for North Fork Caspar Creek (1986-1995), a) logarithmic axes, b) arithmetic axes.

The entire erosion-sediment transport scenario was re-run using vegetation cover values of 100 percent (i.e., no management or vegetation removal) for each hillslope during the entire simulation period. The modeled results for the validation procedure (described above) are compared to a 'no management' scenario. These results are only used for illustration purposes, since it was observed above that runoff rates and volumes modeled with low CSAs (i.e., less than 25 ha) can be significantly under-predicted for unmanaged areas dominated by subsurface rather than surface runoff.

Using the un-cut scenario as a baseline condition, the expected changes with management activities are assumed to be the validated values determined above. When the area was harvested, the peak flow rate increased for nearly all discharge events modeled (Figure 6-7). The greatest changes occur for the lowest flows, with the magnitude of change decreasing asymptotically as peak flow rate increases. For the lowest flows, changes of 100 percent in peak discharge rate could occur (Figure 6-8). The effect decreases exponentially as peak discharge rate increases, such that for the largest modeled flow the expected increase in peak discharge rate was less than 0.5 percent (Figure 6-8). For flows that were greater than bankfull (3.1 cms; 1.5 year recurrence interval (Lisle, 1995)), the percentage increase in peak flow was between 0.3 and 0.5 percent (Figure 6-8). These results are consistent with previous research in Caspar Creek by Lewis et al. (2001), who concluded that "the greatest effect of logging on streamflow peaks is to increase the size of the smallest peaks occurring during the driest antecedent conditions, with that effect declining as storm size and watershed wetness increases" (Lewis et al., 2001).

A similar result is observed for daily flow volume. When the area was harvested, the flow volume increased for nearly all discharge events modeled (Figure 6-9). The greatest changes occur for the lowest flows, with the magnitude of change decreasing asymptotically as flow volume increases. For the lowest flows, changes of 100 percent in flow volume could occur

(Figure 6-10), but the effect decreases exponentially as peak discharge rate increases, such that for the largest modeled flow the expected increase in peak discharge rate was less than one percent (Figure 6-10). For flows that were greater than bankfull, the percentage increase in peak flow was between 0.5 and 0.7 percent (Figure 6-8).
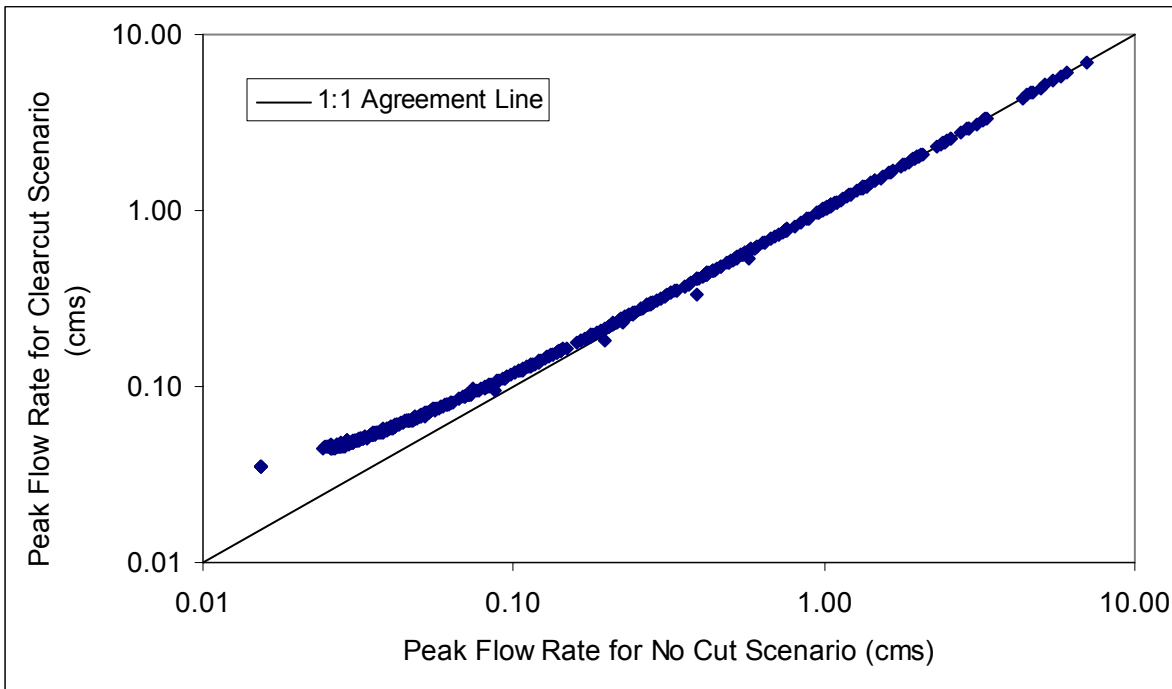
Figure 6-7. Modeled changes in peak flow rate for harvested vs. un-harvested forest management scenarios in North Fork Caspar Creek, CA.
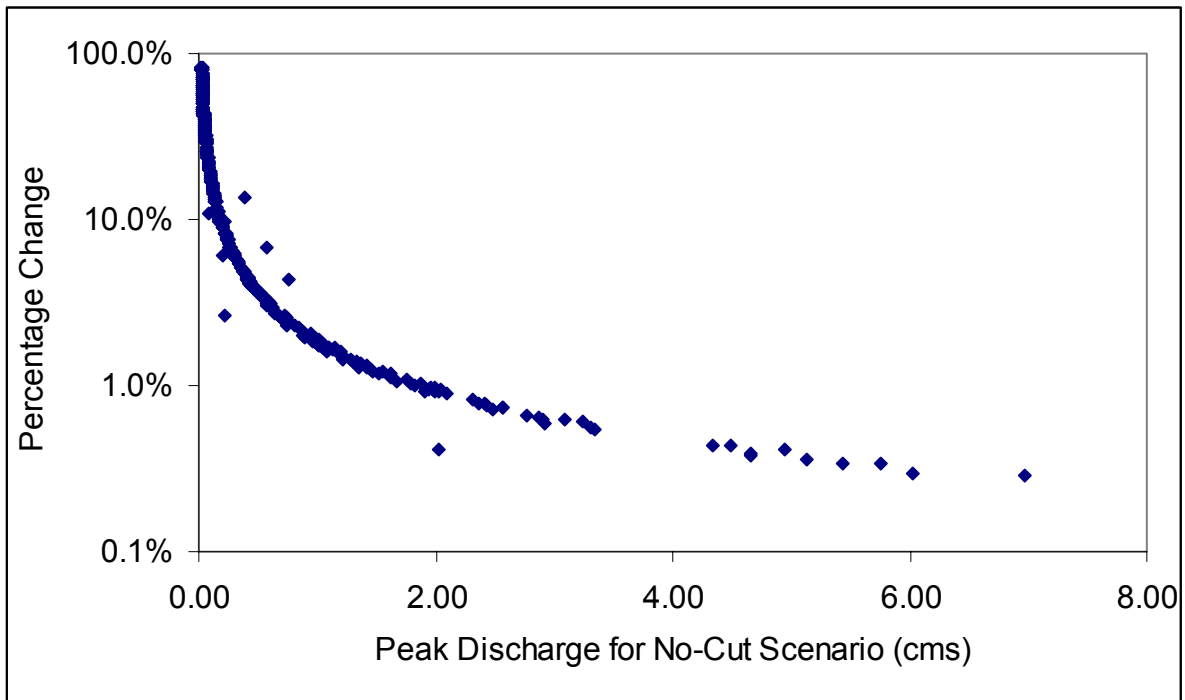
Figure 6-8. Modeled percentage change in peak discharge rate for harvested vs. un-harvested

scenarios in North Fork Caspar Creek, CA.
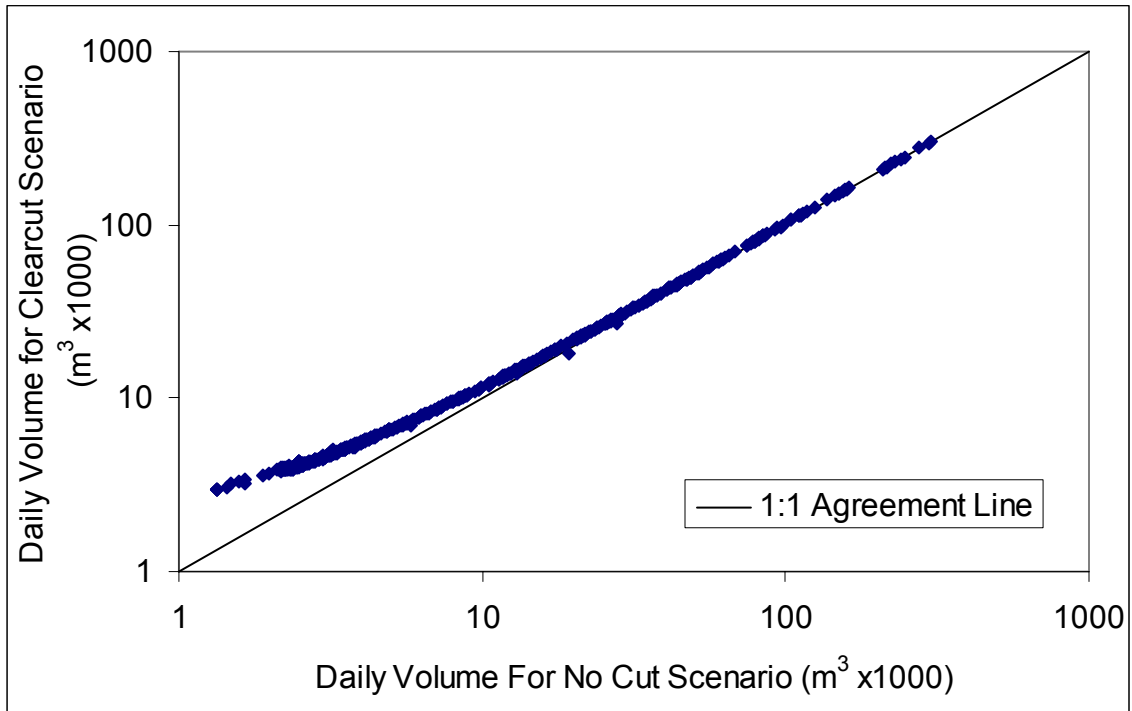
Figure 6-9. Modeled changes in daily flow volume for harvested vs. un-harvested forest

management scenarios in North Fork Caspar Creek, CA.
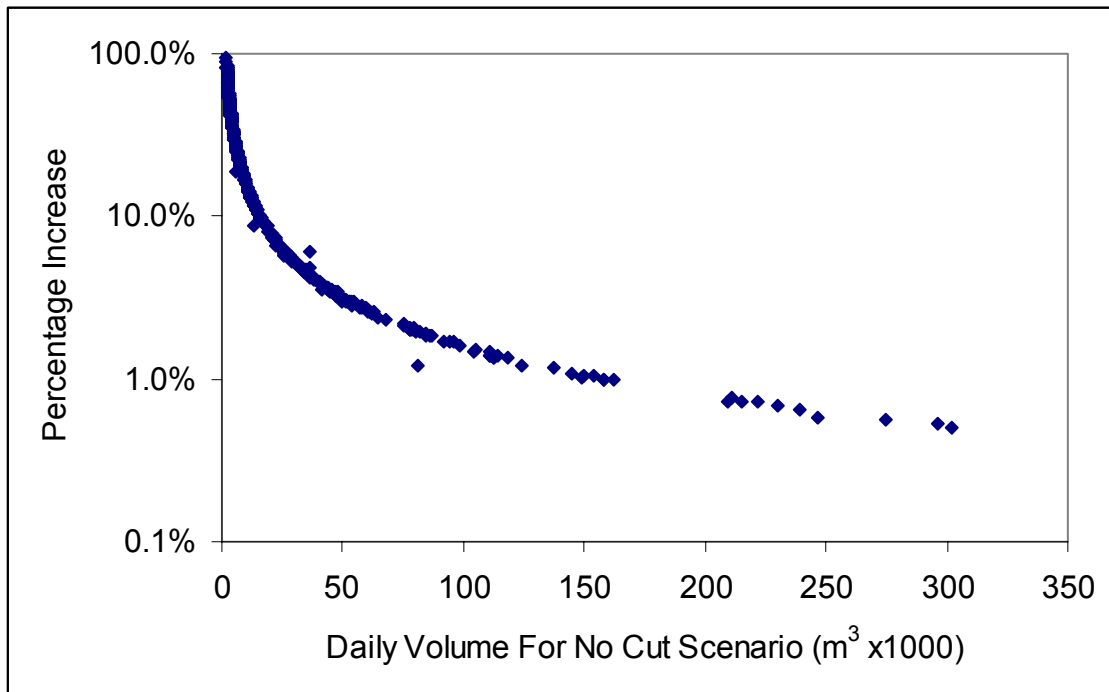
Figure 6-10. Modeled percentage change in peak discharge rate for harvested vs. un-harvested scenarios in North Fork Caspar Creek, CA.

The effect that timber harvesting has on sediment loads is much more pronounced than for flow rates and volumes. Suspended sediment concentration generally increases for the harvested scenario, with several of the events significantly greater than the no-harvest scenario (indicated by the group of diamonds above the 1:1 agreement line on Figure 6-11). Following timber harvesting, suspended sediment concentrations were predicted to be up to 450 percent greater (Figure 6-12). For the same period, Lewis et al. (2001) found that sediment loads in the tributaries increased 123 to 269 percent following timber harvesting, and that the increase in sediment load persisted as long as increased peak flow rates due to timber harvesting persisted. Prior to the 1990 water year, the increases in sediment concentration were at most 30 percent. However, following the 1990 water year, the increases in sediment concentration were very high for two years, then significantly declined, but not to pre-1990 levels.
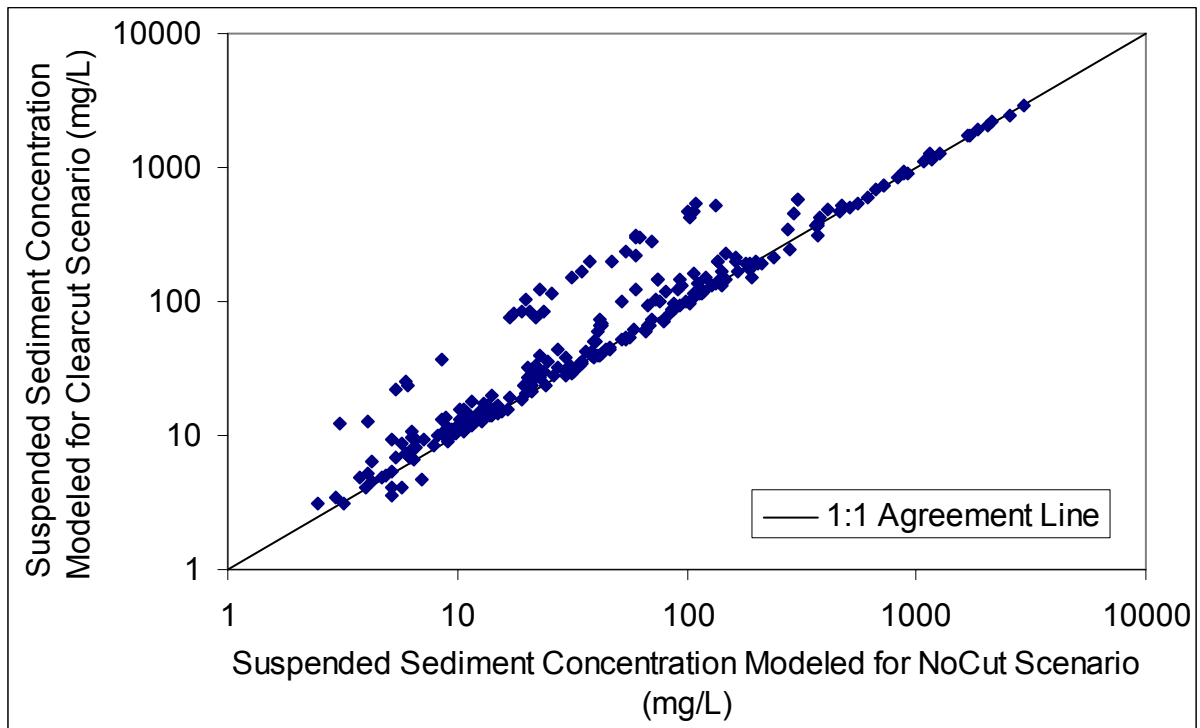
Figure 6-11. Modeled changes in daily flow volume for harvested vs. un-harvested forest management scenarios in North Fork Caspar Creek, CA.

There are two reasons why these results occurred. First, the timing of increases in suspended sediment concentration was coincident with increases in timber harvesting. The majority of timber harvesting occurred between 1989 and 1991; with less than 25 percent of the total harvested area harvested in 1986 (Henry, 1998). Therefore, it was expected that sediment loads would increase more in the period of greater harvesting intensity. Second, the peak flow rates during 1990 and 1991 were much lower than the rest of the period during a drought (Cafferata and Spittler, 1998). Because the units for comparing sediment load were mg/L, load is divided by discharge rate. So, when the load is increased significantly but the discharge rate is not, the change in sediment concentration becomes even greater than would be expected.
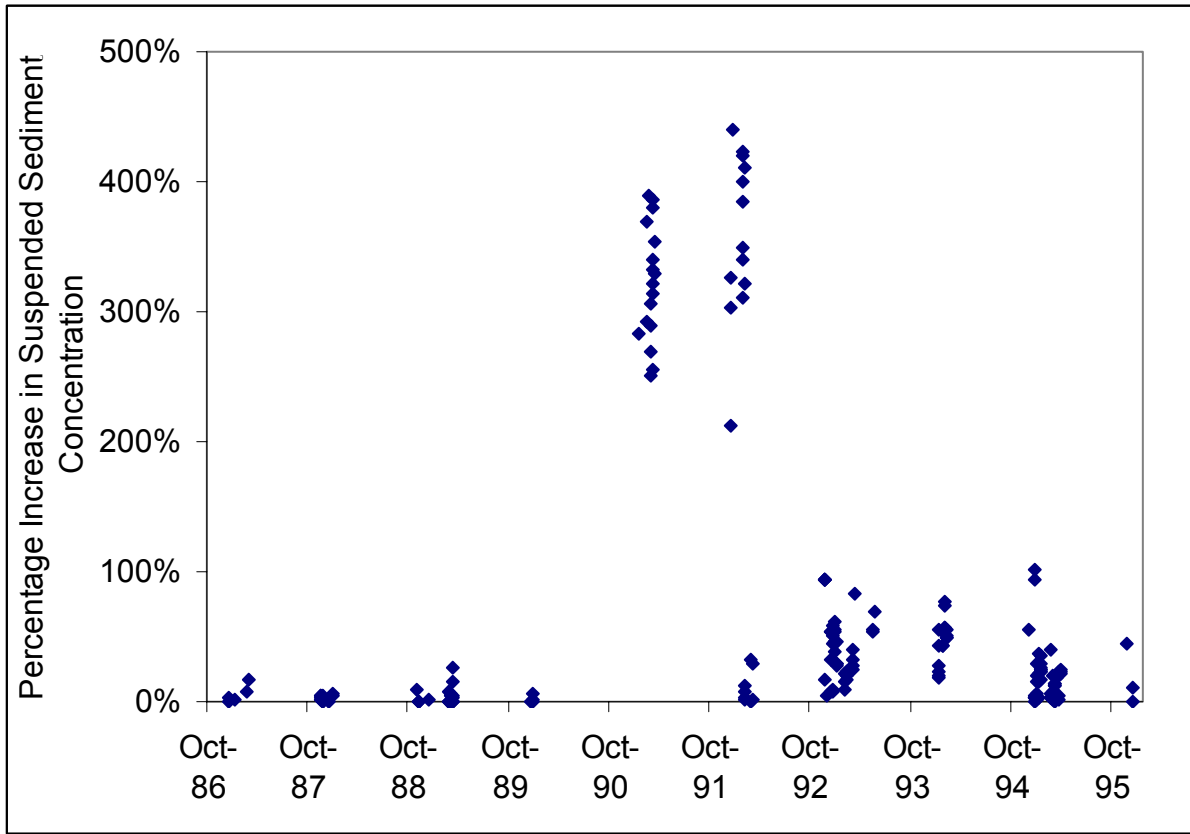
Figure 6-12. Percentage change in suspended sediment concentration between harvested and

un-harvested scenarios, for North Fork Caspar Creek, CA (1986-1995).

CONCLUSION

An extremely difficult problem in modeling is choosing the appropriate analytical scale to represent the physical processes accurately. The WEPP model, by design, is a hillslope-scale runoff and erosion simulator. The model developers, however, have not given clear criteria for the analytical scale for which their model is valid. Without knowledge of this limitation, the model could be (and probably has been) applied to assessment areas that are outside of the valid limits. Although the demarcation line between where hillslope-scale processes are dominant over watershed-scale processes is not clear, it can be inferred from modeled results where representing watershed-scale processes with hillslope-scale equations becomes invalid. For this research, when predicted values for runoff and sediment load deviated significantly from observed values, it was inferred that the physical processes being modeled were not representative of actual conditions.

The critical source area (CSA) above a source channel was used as the criterion for delineating hillslope and channel elements within an assessment area. Modeling domains for the North Fork Caspar Creek were defined with CSAs ranging between 5 and 50 ha. The known management scenario from 1986 to 1995 was defined for each domain. Peak flow rate, total flow volume, and suspended sediment concentration were computed for a series of rain storms and were compared to observed values.

The results of the management scenario indicate that the WEPP-2-CCHE modeling framework can correctly predict significant increases in peak flow rates, total flow volume, and suspended sediment concentration following periods of timber harvesting, and is capable of detecting the persistence of those changes with time. The smallest two CSAs, 5 and 10 ha, produced peak flow rates and total flow volumes that were not significantly different from observed values for the period assessed; thereby validating the modeling framework for these

187

variables under the conditions assessed. Predicted suspended sediment concentrations were significantly different from observed values, were approximately twice those observed, but were within the same range of values as observed.

Changing the critical source area has a significant effect on modeled peak flow rate, total flow volume, and suspended sediment concentration. As the CSA is increased, modeled results for all three variables become more divergent from observed values. As the CSA is increased, the representation of hillslope and channel elements becomes more divergent from observed/mapped elements. The number of hillslope and channel elements decreases with increasing CSA, thereby forcing the WEPP model to apply hillslope-scale process evaluations to increasingly larger hillslope areas (for which it was not designed).

As such, it is inferred that when using the WEPP model for rain-dominated, forested watersheds, the hillslope-scale erosion processes modeled are only valid when the analytical scale is less than 10 ha; which was the limit for the NFCC. It is expected that this analytical scale would not be universally applicable to all climatic and physiographic conditions. Since runoff and erosion processes are highly dependent upon physiographic (e.g., hillslope gradient, soil properties) and climatic (e.g., precipitation depth, duration, form, intensity, and frequency), it would be prudent to determine the appropriate analytical scale for the given conditions based on historic data and field observations.

CHAPTER SEVEN

SYNTHESIS AND GENERAL CONCLUSIONS

Three of the most elusive problems for watershed hydrology are: 1) the prediction of runoff and sediment transport in ungaged watersheds, 2) the fate of transport of sediments as they are moved from their sources to and through watershed channel networks, and 3) the determination of when the dominance of hillslope-scale processes (i.e., overland and rill flow) give way to the dominance of watershed-scale processes (i.e., open channel flow). The results of this research present a step forward in solving these problems. The main goal of this research project was to develop a modeling framework for assessing forest management-related erosion at its sources, and tracking the sediment load as it moves through a channel network to a watershed outlet.

To accomplish this goal, the Water Erosion Prediction Project (WEPP) model was chosen to evaluate hillslope-scale surface erosion processes. The WEPP model is a physically-based upland erosion model commonly used to evaluate agricultural, forest management, and wildfire effects on surface sediment erosion processes. The WEPP model is unique among erosion models in that it explicitly evaluates water balance and surface erosion processes from the ridge top to the channel bottom of a hillslope plane.

Since the WEPP model is not a watershed-scale model, it was coupled with the National Center for Computational Hydrodynamics and Engineering One-Dimensional (CCHE1D) hydrodynamic-sediment transport model. The CCHE1D model is unique among hydrodynamic models in that it explicitly evaluates the full equations of motion (i.e., St. Venant equations) and sediment continuity equation (i.e., Exner Equation) for large channel networks. The successful coupling of these two models was the first time (to date) that a physically-based hillslope erosion simulator was coupled with a watershed-scale hydrodynamic model that uses the dynamic wave solution of the St. Venant equations.

The coupled model was calibrated and validated with observed flow and sediment load data from Caspar Creek Experimental Watershed in coastal, northern California. The coupled model predicts peak flow rates, total flow volume, and sediment loads significantly better than the empirical watershed methods used by the WEPP Watershed model. The coupled model predicted flow rates that were not significantly different from observed values, and sediment loads that were within typical ranges for sediment transport equations.

To demonstrate the utility of the modeling framework, it was used to evaluate the changes in runoff and sediment load that could be expected when a forested area has undergone a series of timber harvests. It was found that, as expected, timber harvesting can increase the magnitude and volume of runoff, but the effects are only significant for flow rates that occur several times per year (on average). Sediment loads, however, were significantly increased for all flow rates, regardless of recurrence interval. This demonstration shows that this tool would be useful for sediment TMDL (total maximum daily load) evaluations, or for cumulative watershed effects components of federal EIR/EIS documents.

In the process of completing this research project, two additional contributions to hydrologic modeling were made. First, a stand-alone computer program was written to generate stream channel cross-section data necessary to run a hydrodynamic model. The procedure uses a combination of regional hydraulic geometry and sparsely measured local data to generate a composite, trapezoidal channel cross-section for every computational node in a watershed channel network. The composite channel is given a floodplain, a main channel, and a flow depth sufficient to carry the 50-100 year recurrence interval flood. Since it is important to have accurate cross-sectional geometry for sediment transport calculation, this method provides an efficient, cost-effective, and accurate means for generating sufficient data to conduct complex hydrodynamic analyses in ungaged watersheds.

The most significant finding of this research project was the upper limit to the assessment area that can be used to validly model surface erosion processes with the WEPP Hillslope model. For the region that was assessed, tt was found that the results of WEPP Hillslope erosion simulations became more divergent from actual values as the hillslope assessment area (i.e., critical source area for first order channels) increases. Critical source areas (CSAs) between 5 and 10 ha yield runoff rates that are not significantly different from observed values. As the CSA is increased, runoff rates and sediment loads become exponentially divergent from observed values.

This finding addresses a fundamental question of watershed hydrologic modeling: At what assessment scale do hillslope-scale runoff and erosion processes give way to more dominant watershed-scale open channel flow and sediment transport processes? Although there is no definitive answer to this question, it was apparent from this research that the governing equations used to represent hillslope-scale erosion processes in the WEPP Hillslope model begin to break down for assessment areas greater than 10 ha. This area, therefore, represents the upper limit on CSA that can be used to define hillslope planes with the WEPP model. This upper limit is only applicable to the physiographic region used for this research; necessitating an evaluation of appropriate CSAs for other physiographic and climatic regimes.

ACCOMPLISHMENTS OF THE RESEARCH PROJECT

There were five significant accomplishments of this research project that will contribute to the body of knowledge regarding watershed-scale erosion, hydrodynamic, and sediment transport modeling.

1. A proof-of-concept was demonstrated for coupling hillslope-scale upland erosion models with watershed-scale channel network hydrodynamic-sediment transport models.

2. The coupled model was calibrated and validated for peak flow, daily runoff volume, and peak suspended sediment concentration for a rainfall-dominated managed and unmanaged watershed.

3. A management scenario was compared to an unmanaged scenario to determine the potential primary effects of forest timber management on runoff and sediment loads at a watershed-scale.

4. Development of clear criteria for the appropriate critical source area that demonstrates the demarcation of where hillslope-scale erosion processes (i.e., rill flow and splash erosion) become less dominant over watershed-scale sediment transport processes (i.e., open channel flow, channel aggradation/degradation) when using the WEPP Hillslope erosion simulator.

5. Development of a procedure for generating cross-sectional geometry data necessary for running complex hydrodynamic models.

LIMITATIONS OF THE RESEARCH

Using this modeling framework requires voluminous spatiotemporal data, which are often sparse in remote areas. Detailed soils data are needed for the WEPP-H model; especially particle size distribution, soil depth, and saturated hydraulic conductivity. Regional hydraulic geometry data are needed, especially for ungaged basins, to run the hydrodynamic model. The algorithm used to generate cross-sectional geometry works best when it has been calibrated with local data. If sediment transport or channel adjustment analyses are to be conducted, it is necessary to have detailed bed material composition information from at least the downstream reach of the watershed.

Although it is believed by the author that the modeling framework can be used for any climatic or physiographic region (because the component models are physically-based and not specific to any region), this assumption was not tested in this research. This research used

192

information from a small, rain-dominated, steep-terrain, forested watershed with generally high gradient stream channels. As such, it cannot be directly inferred that the modeling framework would be applicable in large watersheds (e.g., greater than 100 km^2), watersheds with low gradient channels, or regions that experience significant snowfall or frozen soils. However, the component models, WEPP and CCHE1D, were chosen for this research because other authors have used them for research in areas with these conditions.

The CCHE1D model currently has two limitations: 1) the model has restrictions on the number of hillslopes, channel segments, and computational nodes that can be used for any one modeling domain; thereby restricting the size of the watershed that the model can be applied, and 2) the model currently does not allow for channels that may go dry seasonally; requiring that only higher order channels be analyzed or requiring a constant, minimum baseflow level; and thereby overstating the flow in the channels.

RECOMMENDATIONS FOR FUTURE WORK AND RESEARCH

The modeling framework demonstrated in this research project could be developed into a very useful modeling system. Although not an easy task, a graphical user interface needs to be developed to link the component models, CCHE1D, TOPAZ, and WEPP; and to manage the relational databases needed for each of the models. To do so, several issues with the component models need to be addressed first. The WEPP-H model needs: 1) to allow access to sub-daily time step computations of runoff and sediment loads, 2) remove the WEPP Watershed component that is out-dated, and 3) to improve the lateral subsurface flow and deep percolation subroutines. The CCHE1D model needs: 1) to remove the restrictions on number of computational elements, 2) to allow the user to supply more accurate baseflow information for each channel segment, and 3) develop a routine to allow channel segments to go seasonally dry without causing computational instability.

The applications of this modeling framework are potentially limitless. However, it would be extremely beneficial to determine the applicability of the model in regions with either significant snow cover or frozen soils. Potential applications not explored in this research include: assessing the cumulative impact of varying management systems on a small and large watershed-scales, and assessing the aggradation/degradation potential in specific channel reaches for varying management scenarios.

REFERENCES CITED

A.S.C.E. 1993. Criteria for evaluation of watershed models (ASCE Task Committee on Definition of Criteria for Evaluation of Watershed Models of the Watershed Management Committee Irrigation and Drainage Division). *Journal of Irrigation and Drainage Engineering* 119(3): 429-442.

Abbott, M. B., J. C. Bathurst, J. A. Cunge, P. E. O'Connell, and J. Rasmussen. 1986. An introduction to the European Hydrological System--Systeme Hydrologique Europeen (SHE). *Journal of Hydrology* 87(1-2): 61-77.

Aberle, J. and G. M. Smart. 2003. The influence of roughness structure on flow resistance on steep slopes. *Journal of Hydraulic Research* 41(3): 259-269.

Ackers, P. and W. R. White. 1973. Sediment Transport: A new approach and analysis. *Journal of the Hydraulics Division, American Society of Civil Engineers* 99(11): 2041-2060.

Alonso, C. V., W. H. Neibling, and G. R. Foster. 1981. Estimating sediment transport capacity in watershed modeling. *Transactions of the ASAE* 24: 1211-1220, 1226.

Anderson, H. W., M. D. Hoover, and K. G. Reinhart. 1976. Forests and Water: Effects of Forest Management on Floods, Sedimentation, and Water Supply. USDA Forest Service, General Technical Report PSW-18. Berkeley, CA: USDA Forest Service, Pacific Southwest Forest and Range Experimentation Station.

Angermann, T., W. W. Wallender, B. W. Wilson, I. Werner, D. E. Hinton, M. N. Oliver, F. G. Zalom, J. D. Henderson, G. H. Oliveira, L. A. Deanovic, P. Osterli, and W. Krueger. 2002. Runoff from orchard floors--micro-plot field experiments and modeling. *Journal of Hydrology* 265(1-4): 178-194.

Arnold, J. G., M. A. Weltz, E. E. Alberts, and D. C. Flanagan. 1995. Plant Growth Component (Chapter 8). NSERL Report No. 10. West Lafayette, IN: USDA-ARS National Soil Erosion Research Laboratory.

Ascough, J. C., C. Baffaut, M. A. Nearing, and D. C. Flanagan. 1995. Chapter 13: Watershed Model Channel Hydrology and Erosion Processes. In D. C. Flanagan and M. A. Nearing (eds.). *Technical Documentation: USDA-Water Erosion Prediction Project (WEPP)*, West Lafayette, IN. USDA-ARS National Soil Erosion Research Laboratory.

Baffaut, C., M. A. Nearing, J. C. Ascough, and B. Liu. 1997. The WEPP Watershed Model: II. Sensitivity analysis and discretization on small watersheds. *Transactions of the ASAE* 40(4): 935-943.

Bajracharya, K. and D. A. Barry. 1997. Accuracy criteria for linearized diffusion wave flood routing. *Journal of Hydrology* 195(1-4): 200-217.

Bdour, A. N. 2004. The coupling of a two-dimensional hydrodynamic/sediment routing model with an upland watershed erosion model in a mountain watershed, Red River, Idaho. Unpublished Ph.D. Dissertation. Pullman, WA: Washington State University, Dept. of Civil and Environmental Engineering.

Beck, M. B. 1987. Water quality modelling: a review of uncertainty. *Water Resources Research* 23(8): 1393-1442.

Beven, K. J. 2001. *Rainfall-Runoff Modelling: The Primer.* West Sussex, England. John Wiley & Sons, Ltd.

Bicknell, B., J. C. Imhoff, J. L. Kittle, A. S. Donigan, and R. C. Johanson. 1997. Hydrological Simulation Program - FORTRAN: User's Manual for Version 11. EPA/600/R-97/080, PB97-193114. Research Triangle Park, NC: U.S. Environmental Protection Agency.

Binkley, B. and T. C. Brown. 1993. Forest practices a non-point sources of pollution in North America. *Water Resources Bulletin* 29: 729-740.

Bonta, J. V. 2002. Framework for estimating TMDLs with minimal data. In *Proceedings of the American Society of Agricultural Engineers Conference: Total Maximum Daily Load (TMDL) Environmental Regulations; Fort Worth, Texas, March 11-13, 2002*, pp. 6-12. St. Joseph, MI. American Society of Agricultural Engineers.

Borah, D. K. and M. Bera. 2003. Watershed-scale hydrologic and nonpoint-source pollution models: Review of mathematical bases. *Transactions of the ASAE* 46(6): 1553-1566.

Bouraoui, F. and T. A. Dillaha. 1996. ANSWERS-2000: Runoff and sediment transport model. *Journal of Environmental Engineering* 122(6): 493-502.

Brady, N. C. 1990. *The nature and properties of soils.* New York, NY. Macmillan Publishing Company.

Bravo-Espinosa, M., W. R. Osterkamp, and V. L. Lopes. 2003. Bedload transport in alluvial channels. *Journal of Hydraulic Engineering* 129(10): 783-795.

Brooks, E. S., J. Boll, and P. A. McDaniel. 2004. A hillslope-scale experiment to measure lateral saturated hydraulic conductivity. *Water Resources Research* 40(4): 1-10.

Bryan, R. B. 2000. Soil erodibility and processes of water erosion on hillslope. *Geomorphology* 32(3-4): 385-415.

Bunte, K. and S. R. Abt. 2001. Sampling Surface and Subsurface Particle-Size Distributions in Wadable Gravel- and Cobble-Bed Streams for Analyses in Sediment Transport, Hydraulics, and Streambed Monitoring. General Technical Report RMRS-GTR-74. Fort Collins, CO: U.S. Department of Agriculture, Forest Service, Rocky Mountain Research Station.

Burden, R. L. and J. D. Faires. 2001. *Numerical Analysis, Seventh Edition*. Pacific Grove, CA. Brooks/Cole, Publishing.

Cafferata, P. H. L. 1983. *The Effects of Compaction on the Hydrologic Properties of Forest Soils in the Sierra Nevada*. Series #7. Earth Resources Monograph. USDA, Forest Service.

Cafferata, P. H. L. and T. E. Spittler. 1998. Logging impacts of the 1970's vs. the 1990's in the Caspar Creek Watershed. In R. R. Ziemer (ed.). *Proceedings of the Conference on Coastal Watersheds: The Caspar Creek Story (May 6, 1998: Ukiah, CA)*, pp. 103-115. Albany, CA. Pacific Southwest Research Station, U.S. Dept. of Agriculture, Forest Service.

Castro, J. M. and P. L. Jackson. 2001. Bankfull Discharge Recurrence Intervals and Regional Hydraulic Geometry Relationships: Patterns in the Pacific Northwest, USA. *Journal of the American Water Resources Association* 37(5): 1249-1262.

Chamberlin, T. W., R. D. Harr, and F. H. Everest. 1991. Timber harvesting, silviculture, and watershed processes. In W. R. Meehan (ed.). *Influences of Forest and Rangeland Management on Salmonid Fishes and Their Habitat: Special Publication 19*, Chapter: 6, pp. 181-206. Bethesda, MD. American Fisheries Society.

Chaudhry, M. H. 1993. *Open-Channel Flow*. Englewood Cliffs, NJ. Prentice Hall.

Chikita, K. A., R. Kemnitz, and R. Kumai. 2002. Characteristics of sediment discharge in the subarctic Yukon River, Alaska. *Catena* 48(4): 235-253.

Ciampalini, R. and D. Torri. 1998. Detachment of soil particles by shallow flow: Sampling methodology and observations. *Catena* 32(1): 37-53.

Cochrane, T. A. and D. C. Flanagan. 1999. Assessing water erosion in small watersheds using WEPP with GIS and digital elevation models. *Journal of Soil and Water Conservation* 54(4): 678-685.

Conroy, W. J. 2001. Regional Bankfull Relations for Coastal Northern California Rivers and Streams. *Unpublished* Technical Report TR-2001-0601. Scotia, CA: The Pacific Lumber Company.

Conway, S. 1976. *Logging practices: Principles of timber harvesting systems.* San Francisco, CA. Miller Freeman Publications, Inc.

Cornish, P. M. 2001. The effects of roading, harvesting and forest regeneration on stream-water turbidity levels in a moist eucalypt forest. *Forest Ecology and Management* 152(1-3): 293-312.

Croke, J., P. Hairsine, and P. Fogarty. 2001. Soil recovery from track construction and harvesting changes in surface infiltration, erosion, and delivery rates with time. *Forest Ecology and Management* 143(1-3): 3-12.

Cullen, S. J., C. Montagne, and H. Ferguson. 1991. Timber harvest trafficking and soil compaction in western Montana. *Soil Science Society of America Journal* 55(6): 1416-1421.

Cunge, J. A., F. M. Holly, and A. Verwey. 1980. *Practical aspects of computational river hydraulics.* London, England. Pitman Publishing Limited.

De Roo, A. P. J., C. G. Wesseling, N. H. D. T. Cremers, R. J. E. Offermans, C. J. Ritsema, and K. van Oostindie. 1994. LISEM: a new physically-based hydrological and soil erosion model in a GIS-environment: Theory and implementation. In *IAHS Publication No. 224 (Proceedings of the Canberra Conference),* pp. 439-448. U.K. IAHS Press.

Dean, A. and D. Voss. 1999. *Design and Analysis of Experiments.* New York, NY. Springer.

DeLong, L. L., D. B. Thompson, and J. K. Lee. 1997. The Computer Program FourPT (Version 95.01): A Model for Simulating One-Dimensional, Unsteady, Open-Channel Flow. Water-Resources Investigations Report 97-4016. Bay St. Louis, MS: U.S. Geological Survey.

Douglass, J. E. 1966. Effects of species and arrangement of forests on evapotranspiration. In *International Symposium on Forest Hydrology*, pp. 451-461. W. E. Sopper and H. W. Lull, eds. New York, NY. Pergamon Press.

Downer, C. W., F. L. Ogden, W. D. Martin, and R. S. Harmon. 2002. Theory, development, and applicability of the surface water hydrologic model CASC2D. *Hydrological Processes* 16(2): 255-275.

Dunne, T. and L. B. Leopold. 1978. *Water in Environmental Planning*. New York, NY. W.H. Freeman and Company.

Edeso, J. M., A. Merino, M. J. Gonzalez, and P. Marauri. 1999. Soil erosion under different harvesting managements in steep forestlands from northern Spain. *Land Degradation & Development* 10(1): 79-88.

Engelund, F. and E. Hansen. 1967. *A monograph on sediment transport in alluvial streams*. Copenhagen, Denmark. Teknisk.

Ferro, V. 1998. Evaluating overland flow sediment transport capacity. *Hydrological Processes* 12(12): 1895-1910.

Finkner, S. C., M. A. Nearing, G. R. Foster, and J. E. Gilley. 1989. A simplified equation for modeling sediment transport capacity. *Transactions of the ASAE* 32: 1545-1550.

Flanagan, D. C., J. C. Ascough, A. D. Nicks, M. A. Nearing, and J. M. Laflen. 1995. Overview of the WEPP erosion prediction model. In D. C. Flanagan and M. A. Nearing (eds.). *Technical Documentation: USDA-Water Erosion Prediction Project (WEPP)*, Chapter: 1, West Lafayette, IN. USDA-ARS National Soil Erosion Research Laboratory.

Foltz, R. B. and W. J. Elliot. 1999. Forest erosion probability analysis with the WEPP model. In *ASAE/CSAE-SCGR Annual International Meeting*, St. Joseph, MI. American Society of Agricultural Engineers.

Foster, G. R., D. C. Flanagan, M. A. Nearing, L. J. Lane, L. M. Risse, and S. C. Finkner. 1995. Hillslope Erosion Component. In D. C. Flanagan and M. A. Nearing (eds.). *Technical Documentation: USDA-Water Erosion Prediction Project (WEPP)*, Chapter: 11, West Lafayette, IN. USDA-ARS National Soil Erosion Research Laboratory.

Franz, D. D. and C. S. Melching. 1997. Full Equations (FEQ) Model for the Solution of the Full, Dynamic Equations of Motion for 1-D Unsteady Flow in Open Channels and Through

Control Structures. U.S.G.S. Water-Resources Investigation Report 96-4240. Washington, D.C.: U.S. Geological Survey.

Fread, D. L. 2003. Flow Routing. In T. D. Potter and B. R. Colman (eds.). *Handbook of Weather, Climate, and Water: Atmospheric Chemistry, Hydrology, and Societal Impacts*, Chapter: 30, pp. 543-586. Hoboken, NJ. Wiley-Interscience, John-Wiley & Sons, Inc.

Furniss, M. J., T. D. Roelofs, and C. S. Yee. 1991. Road Construction and Maintenance. In W. R. Meehan (ed.). *Influences of Forest and Rangeland Management on Salmonid Fishes and Their Habitat: Special Publication 19*, Chapter: 8, pp. 297-324. Bethesda, MD. American Fisheries Society.

Garbrecht, J., R. Kuhnle, and C. V. Alonso. 1995. A sediment transport capacity formulation for application to large channel networks. *Journal of Soil and Water Conservation* 50(5): 527-529.

Garbrecht, J. and L. W. Martz. 1995. An Automated Digital Landscape Analysis Tool for Topographic Evaluation, Drainage Identification, Watershed Segmentation, and Subcatchment Parameterization. USDA ARS Report No. NAWQL-95-1. Durant, OK: U.S. Dept. of Agriculture, Agricultural Research Service, National Agricultural Water Quality Laboratory.

Goodrich, D. C., C. L. Unkrich, R. L. Smith, and D. A. Woolhiser. 2002. KINEROS2--A distributed kinematic runoff and erosion model. In *Second Federal Interagency Hydrologic Modeling Conference, Las Vegas, NV*, Boulder, CO. Center for Advanced Decision Support for Water and Environmental Systems, University of Colorado at Boulder.

Green, T. R., S. G. Beavis, C. R. Dietrich, and A. J. Jakeman. 1999. Relating stream-bank erosion to in-stream transport of suspended sediment. *Hydrological Processes* 13(5): 777-787.

Harr, R. D. 1982. Fog drip in the Bull Run Municipal Watershed, Oregon. *Water Resources Bulletin* 18: 785-789.

Harr, R. D., A. Levno, and R. Mersereau. 1982. Streamflow changes after logging 130-year-old Douglas-fir in two small watersheds. *Water Resources Research* 18(3): 637-644.

Henry, N. 1998. Overview of the Caspar Creek Watershed Study. In R. R. Ziemer (ed.). *Proceedings of the Conference on Coastal Watersheds: The Caspar Creek Story (May 6, 1998: Ukiah, CA)*, pp. 1-10. Albany, CA. Pacific Southwest Research Station, U.S. Dept. of Agriculture, Forest Service.

Hicks, B. J., R. L. Beschta, and R. D. Harr. 1991. Long-term changes in streamflow following logging in western Oregon and associated fisheries implications. *Water Resources Bulletin* 27(2): 217-226.

Huang, J., S. T. Lacey, and P. J. Ryan. 1996. Impact of forest harvesting on the hydraulic properties of surface soil. *Soil Science* 161(2): 79-86.

Jackson, C. R., C. A. Sturm, and J. M. Ward. 2001. Timber harvest impacts on small headwater stream channels in the coast ranges of Washington. *Journal of the American Water Resources Association* 37(6): 1533-1549.

Jain, S. C. 2001. *Open-Channel Flow*. New York, NY. John Wiley & Sons, Inc.

Jetten, V. 2002. LISEM: Limburg Soil Erosion Model, User Manual, Version 2.x. The Netherlands: Utrecht Centre for Environment and Landscape Dynamics, Utrecht University.

Jetten, V., G. Govers, and R. Hessel. 2003. Erosion models: quality of spatial predictions. *Hydrological Processes* 17(5): 887-900.

Jha, R., S. Herath, and K. Musiake. 2000. River network solution for a distributed hydrological model and applications. *Hydrological Processes* 14(3): 575-592.

Johnson, B. E., P. Y. Julien, D. K. Molnar, and C. C. Watson. 2000. The two-dimensional upland erosion model CASC2D-SED. *Journal of the American Water Resources Association* 36(1): 31-42.

Johnson, M. G. and R. L. Beschta. 1980. Logging, infiltration capacity, and surface erodibility in western Oregon. *Journal of Forestry* 78(6): 334-337.

Jones, J. A. and G. E. Grant. 1996. Peak flow responses to clear-cutting and roads in small and large basins, western Cascades, Oregon. *Water Resources Research* 32(4): 959-974.

Keim, R. F. and S. H. Shoenholtz. 1999. Functions and effectiveness of silvicultural streamside management zones in loessial bluff forests. *Forest Ecology and Management* 118(3): 197-209.

Keppeler, E. 1998. The summer flow and water yield response to timber harvest. In R. R. Ziemer (ed.). *Proceedings of the Conference on Coastal Watersheds: The Caspar Creek Story (May 6, 1998: Ukiah, CA)*, pp. 35-43. Albany, CA. Pacific Southwest Research Station, U.S. Dept. of Agriculture, Forest Service.

Keppeler, E. and D. Brown. 1998. Subsurface drainage processes and management impacts. In R. R. Ziemer (ed.). *Proceedings of the Conference on Coastal Watersheds: The Caspar Creek Story (May 6, 1998: Ukiah, CA)*, pp. 25-34. Albany, CA. Pacific Southwest Research Station, U.S. Dept. of Agriculture, Forest Service.

Knighton, D. 1984. *Fluvial Forms and Processes*. London, UK. Edward Arnold Publishing.

Komura, S. and D. B. Simons. 1967. River-bed degradation below dams. *Journal of the Hydraulics Division, ASCE* 93(4): 1-13.

Laffan, M., G. Jordan, and N. Duhig. 2001. Impacts on soils from cable-logging steep slopes in northeastern Tasmania, Australia. *Forest Ecology and Management* 144(1-3): 91-99.

Lane, L. J., E. D. Shirley, and V. Singh. 1988. Modelling erosion on hillslopes. In M. G. Anderson (ed.). *Modelling Geomorphological Systems*, Chapter: 10, pp. 287-308. John Wiley & Sons, Ltd.

Lane, P. N. J. and G. J. Sheridan. 2002. Impact of an unsealed forest road stream crossing: water quality and sediment sources. *Hydrological Processes* 16(13): 2599-2612.

Laursen, E. 1958. The total sediment load of streams. *Journal of the Hydraulics Division, American Society of Civil Engineers* 54(1): 1-36.

Leavesley, G. H., R. W. Lichty, B. M. Troutman, and L. G. Saindon. 1983. Precipitation-Runoff Modeling System: User's Manual. U.S.G.S. Water Resources Investigations 83-4238. Denver, CO: U.S. Geological Survey.

Leopold, L. B., M. G. Wolman, and J. P. Miller. 1964. *Fluvial processes in geomorphology*. San Francisco, CA. W.H. Freeman and Company.

Lewis, J., S. R. Mori, E. Keppeler, and R. R. Ziemer. 2001. Impacts of logging on storm peak flows, flow volumes, and suspended sediment loads in Caspar Creek, California. In M. S. Wigmosta and S. J. Burges (eds.). *Land Use and Watersheds: Human Influence on Hydrology and Geomorphology in Urban and Forest Areas*, pp. 85-125. Washington, D.C. American Geophysical Union.

Lindquist, J. and M. N. Palley. 1967. Prediction of Stand Growth of Young Redwood. Bulletin 831. Berkeley, CA: University of California, Division of Agricultural Sciences, California Agricultural Experiment Station.

Line, D. E., D. L. Osmond, S. W. Coffey, R. A. McLaughlin, G. D. Jennings, J. A. Gale, and J. Spooner. 1997. Nonpoint sources. *Water Environment Research* 69(4): 844-860.

Lisle, T. E. 1995. Particle size variations between bed load and bed material in natural gravel bed rivers. *Water Resources Research* 31(4): 1107-1118.

Lisle, T. E. and M. B. Napolitano. 1988. Effects of recent logging on the main channel of North Fork Caspar Creek. In R. R. Ziemer (ed.). *Proceedings of the Conference on Coastal Watersheds: The Caspar Creek Story (May 6, 1998: Ukiah, CA)*, pp. 81-85. Albany, CA. Pacific Southwest Research Station, U.S. Dept. of Agriculture, Forest Service.

Luce, C. H. 1997. Effectiveness of road ripping in restoring infiltration capacity of forest roads. *Restoration Ecology* 5(3): 265-270.

Lyn, D. A. and M. Altinakar. 2002. St. Venant - Exner equations for near-critical and transcritical flows. *Journal of Hydraulic Engineering* 128(6): 579-587.

Lyons, J. K. and R. L. Beschta. 1983. Land use, floods, and channel changes: Upper Middle Fork Willamette River, Oregon (1936-1980). *Water Resources Research* 19(2): 463-471.

McArdle, R. E., W. H. Meyer, and D. Bruce. 1961. The Yield of Douglas-Fir in the Pacific Northwest. Technical Bulletin No. 201. Washington, D.C.: U.S. Department of Agriculture, Forest Service.

McCuen, R. H. 1998. *Hydrologic Analysis and Design, Second Edition.* Upper Saddle River, New Jersey. Prentice-Hall, Inc.

Megahan, W. F. 1972. Subsurface flow interception by a logging road in mountains of central Idaho. In *National Symposium on Watersheds in Transition*, pp. 350-356.

Megahan, W. F. and G. L. Ketcheson. 1996. Predicting downslope travel of granitic sediments form forest roads in Idaho. *Water Resources Bulletin* 32(2): 371-382.

Mein, R. G. and C. L. Larson. 1973. Modeling infiltration during a steady rain. *Water Resources Research* 9(2): 384-394.

Merritt, W. S., R. A. Letcher, and A. J. Jakeman. 2003. A review of erosion and sediment transport models. *Environmental Modelling and Software* 18(8-9): 761-799.

Messina, M. G., S. H. Schoenholtz, M. W. Lowe, Z. Wang, D. K. Gunter, and A. J. Londo. 1997. Initial responses of woody vegetation, water quality, and soils to harvesting intensity in a Texas bottomland hardwood ecosystem. *Forest Ecology and Management* 90(2-3): 201-215.

Meyer-Peter, E. and R. Mueller. 1948. Formulas for Bed-Load Transport. Report on the 2nd Meeting of IAHR. Stockholm, Sweden: International Association of Hydraulic Research.

Montgomery, D. R. 1994. Road surface drainage, channel initiation, and slope instability. *Water Resources Research* 30(6): 1925-1932.

Moramarco, T., Y. Fan, and R. L. Bras. 1999. Analytical Solution For Channel Routing With Uniform Lateral Inflow. *Journal of Hydraulic Engineering* 125(7): 707-713.

Moussa, R. and C. Bocquillon. 2001. Fractional-Step Method Solution of Diffusive Wave Equation. *Journal of Hydrologic Engineering* 6(1): 11-19.

Murakami, S., Y. Tsuboyama, T. Shimizu, M. Fujieda, and S. Noguchi. 2000. Variation of evapotranspiration with stand age and climate in a small Japanese forested catchment. *Journal of Hydrology* 227(1-4): 114-127.

N.C.A.S.I. 1992. The Effectiveness of Buffer Strips for Ameliorating Offsite Transport of Sediment, Nutrients, and Pesticides Form Silvicultural Operation. Technical Bulletin No. 631. Research Triangle Park, NC: National Council of the Paper Industry for Air and Stream Improvement, Inc.

N.C.A.S.I. 1994. Forests As Nonpoint Sources of Pollution, and Effectiveness of Best Management Practices. Technical Bulletin No. 672. Research Triangle Park, NC: National Council of the Paper Industry for Air and Stream Improvement, Inc.

N.C.A.S.I. 1999. Scale Considerations and the Detectability of Sedimentary Cumulative Watershed Effects. Technical Bulletin No. 776. Research Triangle Park, NC: National Council of the Paper Industry for Air and Stream Improvement, Inc.

N.C.A.S.I. 2001. Forestry Operations and Water Quality in the Northeastern States: Overview of Impacts and Assessment of State Implementation of Nonpoint Source Programs Under the Federal Clean Water Act. Technical Bulletin No. 820. Research Triangle Park, NC: National Council for Air and Stream Improvement, Inc.

Nash, J. E. and J. V. Sutcliffe. 1970. River flow forecasting through conceptual models, Part I-A, discussion of principles. *Journal of Hydrology* 10(3): 282-290.

National Soil Erosion Research Laboratory. 2004. WEPP Software - Water Erosion Prediction Project. URL: *http://topsoil.nserl.purdue.edu/nserlweb/weppmain/wepp.html*. Accessed: 9-2-2005.

Nearing, M. A., L. D. Norton, D. A. Bulgakov, G. A. Larionov, L. T. West, and K. M. Dontsova. 1997. Hydraulics and erosion in eroding rills. *Water Resources Research* 33(4): 865-876.

Neitsch, S. L., J. G. Arnold, J. R. Kiniry, and J. R. Williams. 2001. Soil and Water Assessment Tool: Theoretical Documentation, Version 2000. Temple, TX: Grassland, Soil and Water Research Laboratory, Agricultural Research Service.

Nisbet, T. R. 2001. The role of forest management in controlling diffuse pollution in UK forestry. *Forest Ecology and Management* 143(1-3): 215-226.

Parker, G., C. Paola, and S. Leclair. 2000. Probabilistic Exner sediment continuity equation for mixtures with no active layer. *Journal of Hydraulic Engineering* 126(11): 818-826.

Pereira, L. S., A. Perrier, R. G. Allen, and I. Alves. 1999. Evapotranspiration: Concepts and Future Trends. *Journal of Irrigation and Drainage Engineering* 125(2): 45-51.

Ping, F. and R. Xiaofang. 1999. Method of flood routing for multibranched rivers. *Journal of Hydraulic Engineering* 125(3): 271-276.

Ponce, V. M. and A. Lugo. 2001. Modeling Looped Ratings in Muskingum-Cunge Routing. *Journal of Hydrologic Engineering* 6(2): 119-124.

Proffit, G. T. and A. J. Sutherland. 1983. Transport of nonuniform sediment. *Journal of Hydraulic Research* 21(1): 33-43.

Rashin, E., C. Clishe, A. Loch, and J. Bell. 1999. Effectiveness of Forest Road and Timber Harvest Best Management Practices With Respect to Sediment-Related Water Quality Impacts. Publication No. 99-317. Olympia, WA: Washington State Department of Ecology, Environmental Assessment Program.

Renard, K. G., J. M. Laflen, G. R. Foster, and D. K. McCool. 1994. The revised universal soil loss equation. In R. Lad (ed.). *Soil Erosion: Research Methods*, pp. 105-126.

Renschler, C. S. 2003. Designing geo-spatial interfaces to scale process models: the GeoWEPP approach. *Hydrological Processes* 17(5): 1005-1017.

Robichaud, P. R. and T. A. Waldrop. 1994. A comparison of surface runoff and sediment yields from low- and high-severity site preparation burns. *Water Resources Bulletin* 30(1): 27-34.

Rutter, A. J. and A. J. Morton. 1977. A predictive model of rainfall interception in forests. *Journal of Applied Ecology* 14: 567-588.

Savabi, M. R. and J. R. Williams. 1995. Water balance and percolation. In D. C. Flanagan and M. A. Nearing (eds.). *Technical Documentation: USDA-Water Erosion Prediction Project (WEPP)*, Chapter: 5, West Lafayette, IN. USDA-ARS National Soil Erosion Research Laboratory.

Schaffranek, R. W., R. A. Baltzer, and D. E. Goldberg. 1981. A Model for Simulation of Flow in Singular and Interconnected Channels. U.S.G.S. Techniques of Water-Resources Investigations, Book 7, Chapter 3. Washington, D.C.: U.S. Geological Survey.

Sen, D. J. and N. K. Garg. 2002. Efficient algorithm for gradually varied flows in channel networks. *Journal of Irrigation and Drainage Engineering* 128(6): 351-357.

Shen, H. W. 1971. *River Mechanics, Volume I.* Fort Collins, CO. Colorado State University.

Sidle, R. C. and D. M. Drlica. 1981. Soil compaction from logging with a low-ground pressure skidder in the Oregon coast ranges. *Soil Science Society of America Journal* 45(6): 1219-1224.

Singh, V. P. 1988. *Hydrologic Systems: Rainfall-Runoff Modeling.* Englewood Cliffs, NJ. Prentice Hall.

Singh, V. P. 1995. *Computer Models of Watershed Hydrology.* Highlands Ranch, CO. Water Resources Publications.

Singh, V. P. and D. A. Woolhiser. 2002. Mathematical modeling of watershed hydrology. *Journal of Hydrologic Engineering* 7(4): 270-292.

Sivapalan, M. 2003a. Prediction in ungauged basins: a grand challenge for theoretical hydrology. *Hydrological Processes* 17(15): 3163-3170.

Sivapalan, M. 2003b. Process complexity at hillslope scale, process simplicity at the watershed scale: is there a connection? *Hydrological Processes* 17(5): 1037-1041.

Smith, D. M. 1986. *The Practice of Silviculture*. New York, NY. John Wiley & Sons.

Snyder, N. P., K. X. Whipple, G. E. Tucker, and D. J. Merritts. 2003. Channel response to tectonic forcing: field analysis of stream morphology and hydrology in the Mendocino triple junction region, northern California. *Geomorphology* 53(1): 97-127.

Soil Conservation Service, U. S. D. A. 1991. National Engineering Handbook, Section 4: Hydrology. Washington, D.C.: U.S. Government Printing Office.

Startsev, A. D. and D. H. McNabb. 2000. Effects of skidding on forest soil infiltration in west-central Alberta. *Canadian Journal of Soil Science* 80: 617-624.

Stone, J. J., L. J. Lane, E. D. Shirley, and M. Hernandez. 1995. Hillslope Surface Hydrology. In D. C. Flanagan and M. A. Nearing (eds.). *Technical Documentation: USDA-Water Erosion Prediction Project (WEPP)*, Chapter: 4, West Lafayette, IN. USDA-ARS National Soil Erosion Research Laboratory.

Storck, P., L. Bowling, P. Wetherbee, and D. P. Lettenmaier. 1998. Application of a GIS-based distributed hydrology model for prediction of forest harvest effects on peak stream flow in the Pacific Northwest. *Hydrological Processes* 12(6): 889-904.

Swanston, D. N. 1991. Natural Processes. In W. R. Meehan (ed.). *Influences of Forest and Rangeland Management on Salmonid Fishes and Their Habitat: Special Publication 19*, Chapter: 5, pp. 139-180. Bethesda, MD. American Fisheries Society.

Taylor, J. R. 1982. *An introduction to error analysis: The study of uncertainties in physical measurements*. Mill Valley, CA. University Science Books, Oxford University Press.

Thomas, R. B. and W. F. Megahan. 1998. Peak flow responses to clear-cutting and roads in small and large basins, western Cascades, Oregon: A second opinion. *Water Resources Research* 34(12): 3393-3403.

Toffaleti, F. B. 1968. A Procedure for Computation of the Total River Sand Discharge and Detailed Distribution, Bed to Surface. Technical Report No. 5. Vicksburg, MS: U.S. Army Corps of Engineers.

U.S.A.C.E. 1993. River Hydraulics. EM 1110-2-1416. Davis, CA: U.S. Army Corps of Engineer, Hydraulic Engineering Center.

U.S.A.C.E. 1994. Flood-Runoff Analysis. EM 1110-2-1417. Davis, CA: U.S. Army Corps of Engineers, Hydraulic Engineering Center.

U.S.A.C.E. 2000. Hydrologic Modeling System HEC-HMS: Technical Reference Manual. CPD-74B. Davis, CA: U.S. Army Corps of Engineers, Hydrologic Engineering Center.

U.S.E.P.A. 1990. National Water Quality Inventory: 1988 Report to Congress. EPA 440-4-90-003. Washington, D.C.: Office of Water (4503-F), United States Environmental Protection Agency.

U.S.E.P.A. 1999. Protocol for Developing Sediment TMDLs: First Edition. EPA 841-B-99-004. Washington, D.C.: U.S. Environmental Protection Agency.

U.S.E.P.A. 2000. Atlas of America's Polluted Waters. EPA 840-B00-002. Washington, D.C.: Office of Water (4503-F), United States Environmental Protection Agency.

U.S.E.P.A. 2002. The Twenty Needs Report: How Research Can Improve the TMDL Program. EPA 841-B-02-002. Washington, D.C.: Office of Water, United States Environmental Protection Agency.

U.S.E.P.A. 2005. National Section 303(d) List Fact Sheet. URL: *http://oaspub.epa.gov/waters/national_rept.control* . Accessed: 5-4-2004.

Vazquez, R. F., L. Feyen, J. Feyen, and J. C. Refsgaard. 2002. Effect of grid size on effective parameters and model performance of the MIKE-SHE code. *Hydrological Processes* 16(2): 355-372.

Venutelli, M. 2002. Stability and accuracy of weighted four-point implicit finite difference schemes for open channel flow. *Journal of Hydraulic Engineering* 128(3): 281-288.

Vieira, D. A. and W. Wu. 2002a. One-Dimensional Channel Network Model CCHE1D Version 3.0: User's Manual. Technical Report No. NCCHE-TR-2002-02. University, MS: National Center for Computational Hydroscience and Engineering.

Vieira, D. A. and W. Wu. 2002b. CCHE1D Version 3.0 -- Model Capabilities and Applications. Technical Report No. NCCHE-TR-2002-05. University, MS: National Center for Computational Hydroscience and Engineering.

Wallace, J. S. 1997. Evaporation and radiation interception by neighbouring plants. *Quarterly Journal of the Royal Meteorological Society* 123: 1885-1905.

Wang, G., S. Chen, J. Boll, and V. Singh. 2003. Nonlinear Convection-Diffusion Equation with Mixing-Cell Method for Channel Flood Routing. *Journal of Hydrologic Engineering* 8(5): 259-265.

Wang, G.-T., S. Chen, and J. Boll. 2003. A semianalytical solution of the Saint-Venant equations for channel flood routing. *Water Resources Research* 39(4): 1076-1086.

Wang, S. Y., W. Wu, H.-M. Hsia, and C.-C. Cheng. 2002. Simulation of Flood and Sediment Routing in the Pa-Chang River and the Pu-Tze River of Taiwan using CCHE1D Model. In *5th International Conference on Hydro-Science and -Engineering (ICHE-2002) September 18-21, 2002; Warsaw, Poland*, International Association Of Hydraulic Engineering And Research.

Western, A. W., B. L. Finlayson, T. A. McMahon, and I. C. O'Neill. 1997. A method for characterizing longitudinal irregularity in river channels. *Geomorphology* 21(1): 39-51.

Wicks, J. M. and J. C. Bathurst. 1996. SHESED: a physically based, distributed erosion and sediment yield component for the SHE hydrological modelling system. *Journal of Hydrology* 175(1-4): 213-238.

Wigmosta, M. S. and D. P. Lettenmaier. 1999. A comparison of simplified methods for routing topographically driven subsurface flow. *Water Resources Research* 35(1): 255-264.

Wilson, C. J. 1999. Effects of logging and fire on runoff and erosion on highly erodible granitic soils in Tasmania. *Water Resources Research* 35(11): 3531-3546.

Wischmeier, W. H. and D. D. Smith. 1978. Predicting Soil Erosion Losses: A Guide to Conservation Planning. USDA Agricultural Handbook No. 537. Washington, D.C.: U.S. Government Printing Office.

Woolhiser, D. A., R. L. Smith, and D. C. Goodrich. 1990. KINEROS, A Kinematic Runoff and Erosion Model: Documentation and User Manual. U .S . Dept. of Agriculture, Agricultural Research Service, ARS -77. U .S . Dept. of Agriculture, Agricultural Research Service.

Wright, K. A., K. H. Sendek, R. M. Rice, and R. B. Thomas. 1990. Logging effects on streamflow: Storm runoff at Caspar Creek in northwestern California. *Water Resources Research* 26(7): 1657-1667.

Wu, J., Y. Liu, and D. E. Jelinski. 2000. Effects of leaf area profiles and canopy stratification on simulated energy fluxes: the problem of vertical spatial scale. *Ecological Modelling* 134(2-3): 283-297.

Wu, W., D. A. Vieira, and S. Y. Wang. 2004. One-Dimensional Numerical Model for Nonuniform Sediment Transport under Unsteady Flows in Channel Networks. *Journal of Hydraulic Engineering* 130(9): 914-923.

Wu, W. and D. A. Vieira. 2002. One-Dimensional Channel Network Model CCHE1D Version 3.0: Technical Manual. Technical Report No. NCCHE-TR-2002-1. University, MS: National Center for Computational Hydroscience and Engineering.

Wu, W., S. Y. Wang, and Y. Jia. 2000. Nonuniform sediment transport in alluvial rivers. *Journal of Hydraulic Research* 38(6): 427-434.

Wynn, T. M., S. Mostaghimi, J. W. Frazee, P. W. McClellan, R. M. Shaffer, and W. M. Aust. 2000. Effects of forest harvesting best management practices on surface water quality in the Virginia coastal plain. *Transactions of the ASAE* 43(4): 927-936.

Yalin, M. S. 1963. An expression for bed-load transportation. *Journal of the Hydraulics Division, American Society of Civil Engineers* 89(3): 221-250.

Yan, J. and J. Zhang. 2001. Evaluation of the MIKE-SHE Modeling System. Southern Cooperative Series Bulleting # 398.

Yang, C. T. 1973. Incipient motion and sediment transport. *Journal of the Hydraulics Division, American Society of Civil Engineers* 99(10): 1679-1704.

Yang, C. T. 1996. *Sediment Transport: Theory and Practice*. New York, NY. The McGraw-Hill Companies, Inc.

Yen, B. C. and C. Tsai. 2001. Short Communication: On noninertia wave versus diffusion wave in flood routing. *Journal of Hydrology* 244(1-2): 97-104.

Young, R. A., C. A. Onstad, D. D. Bosch, and W. P. Anderson. 1989. AGNPS: A nonpoint-source pollution model for evaluating agricultural watersheds. *Journal of Soil and Water Conservation* 44(2): 4522-4561.

Zhang, X. C., M. A. Nearing, L. M. Risse, and K. C. McGregor. 2003. Evaluation of WEPP runoff and soil loss predictions using natural runoff plot data. *Transactions of the ASAE* 39(3): 855-863.

Ziegler, C. K. and W. Lick. 1986. A Numerical Model of the Resuspension, Deposition, and Transport of Fine-Grained Sediments in Shallow Water. UCSB Report ME-86-3. Santa Barbara, CA: University of California at Santa Barbara.

Ziemer, R. R. 1979. Evaporation and transpiration. *Reviews of Geophysics and Space Physics* 17(6): 1175-1186.